UNIVERSITY OF CALIFORNIA
Santa Barbara

Temporal dynamics and regulation of coastal Antarctic phytoplankton communities: Spring/Summer 1991-1994

A Dissertation submitted in partial satisfaction
of the requirements for the degree of

Doctor of Philosophy

in

Biology

by

Mark Alan Moline

Committee in charge:

Professor Barbara B. Prézelin, Chairperson
Professor Mark Brzezinski
Doctor Hervé Claustre
Professor Eileen Hofmann
Professor Roger Nisbet

1996

The dissertation of Mark Alan Moline is approved

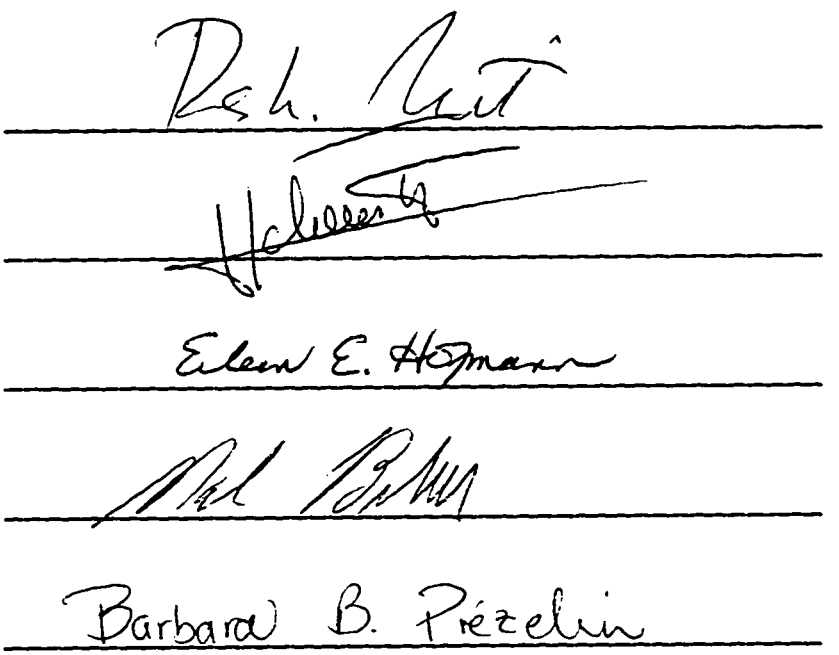

Committee Chairperson

June 1996

TABLE OF CONTENTS

CHAPTER 5

PREFACE

This dissertation consists of an introduction and five related chapters. Each chapter has been written for various scientific journals and review volumes and, as a result, there are some differences in style between chapters. Each chapter is self-contained and includes an introduction, and methods, results and discussion sections. A separate list of literature cited accompanies each chapter along with the appropriate tables and figures.

ACKNOWLEDGMENTS

A combination of a wild trip to the 'Big Easy', recommendations from Mary Putt and John Melack, and a phone call to the Amazon floodplain began my six-year adventure at UCSB. This thesis is the result of the interaction with and continual support of Barbara Prézelin over that period. Beginning with a brief lecture on the R/V Polar Duke in 1990, she has taught me much and contributed significantly both to my understanding of science and in providing tools necessary for future scientific pursuits. I thank her for the wonderful opportunity and guidance.

I would also like to thank the other members of my committee, Mark Brzezinski, Hervé Claustre, Eileen Hofmann, and Roger Nisbet for their support and instruction. Mark Brzezinski always made the time for productive discussions and comments. Roger Nisbet opened up the world of ecological modeling to me, and although I still consider myself an embryo in the field, I hope to pursue this discipline in the future. I cannot begin to comment on the positive influences that Hervé Claustre had on this work and me personally as a scientist. Our daily discussions will always be remembered. I would also like to thank Barbara Prézelin for the foresight and encouragement

of Dr. Claustre's sabbatical. Although not on my committee, Alice Alldredge was a significant part of my experience here at UCSB. She was always there for discussion, advice and recommendations. Both she and Barry Tanowitz greatly improved my abilities as an instructor and for that I am grateful.

Words do not express my feelings for the truly great atmosphere that existed between the students in Dr. Prézelin's lab. The blend of good science and good humor was unique. To everyone in the lab, my deepest appreciation for the many good years together. Nic Boucher, T. J. Evens, Tom Frazer (honorary member), Gier Johnsen, Raffael Jovine, Bernd Kroon, Allen Matlick, Norm Nelson and Oscar Schofield will be life-long friends.

My deep thanks go to the undergraduates who were with me in the field; S. Roll, K. Scheppe, K. Seydel and Elise Stephens. Without their fun interaction and endless hours of hard labor at Palmer Station, this unique dataset would not have been possible. I also thank the National Science Foundation for the support for these students through the Research Experience for Undergraduates (REU) program. This is truly a wonderful program in every respect.

Thanks to the 'Shaving Team' (D. Divins, T. Frazer, K. Haberman, K. Seydel, E. Stephens) for honoring a promise.

Thanks to the 'Blood Club' veterans (N. Boucher, T. Diem, T. Frazer, S. Haddock, O. Schofield, B. Seibel, T. Westerberry) for the many hours under the hoop and for removing my cornea when it got in the way.

I want to express my appreciation to Melvin George for his thoughts and unending strong support from a distance all these years. He helped keep me focused, motivated and always provided the larger context in which to view my graduate experience.

Special thanks to William Krebs, who did a similar study at Palmer 25 years ago. The notes and data from his thesis work, which he generously made available to me, helped in numerous ways.

Many others also assisted with this work in the field and in Santa Barbara. Thanks go to R. Bidigare, B. Bozcar, B. Golden, P. Handley, J. Jones, D. Menzies, T. Newberger, M. Ondrusek, R. Petty, L. Quetin, R. Ross, D. Siegel, R. Smith, S. Stammerjohn, J. Standish, B. Sullivan, L. Washburn, , the ASA personnel at Palmer Station & Punta Arenas, the crew of the R/V Polar Duke, and the staff of MSI and EEMB.

Thanks and love to my family and extended family for always being supportive. Family support is often overlooked and taken for granted. It is the underlying force that got me to where I am and will get me to where I'm going.

Finally, I would like to thank Nicole Desaulniers for her support during the final years of this work. Her continual listening, advice and love, was always needed and welcomed.

VITA

Born - July 9, 1964, Seattle, Washington, USA

EDUCATION

1996	Ph.D., Aquatic Biology, University of California, Santa Barbara
1987	B.A., Biology, Saint Olaf College

PROFESSIONAL EXPERIENCE

1991-96	University of California, Santa Barbara - Research Assistant/Teaching Assistant
1992-93	Curator of UCSB Algal Culture Collection
1990	University of California, Santa Barbara - Lab Analyst I
1988-90	University of Maryland, Horn Point, Cambridge - Research Associate
1987-88	McMurdo Station, Antarctica - Science Administrative Coodinator, National Science Foundation/ITT

1987	University of Maryland, Horn Point, Cambridge - Research Associate
1986	US Fish and Wildlife, Marion, Alabama - Research Associate
1986	University of Maryland, Horn Point, Cambridge - Research Technician
1986	Australian Institute of Marine Science, Townsville - Field Assistant
1985-86	University of Maryland, Horn Point, Cambridge - Research Technician
1984	Cornell University, Isle of Shoals, Maine - Assistant Research Diver

FIELD RESEARCH EXPERIENCE

1993	R/V Polar Duke, Bellingshausen Sea B. B. Prézelin & R. C. Smith - Chief Scientists
1993	R/V Polar Duke, Bellingshausen Sea L. B. Quetin - Chief Scientist
1991-93	Palmer Station, Antarctica Long Term Ecological Research Program
1991	R/V Polar Duke, Bellingshausen Sea

L. B. Quetin- Chief Scientist

1990 R/V Polar Duke, Bellingshausen Sea

R. C. Smith & B. B. Prézelin - Chief Scientists

1988-90 Lake Calado, Amazon River Basin, Brazil

T. R. Fisher & J. M. Melack - Chief Scientists

1986 Lizard Island Research Station, Australia

1985-86 McMurdo Sound, Antarctica

R. B. Rivkin - Chief Scientist

1985 R/V Cape Hatteras, Sargasso Sea

R. B. Rivkin - Chief Scientist

1985 R/V Warfield, Chesapeake Bay

R. B. Rivkin - Chief Scientist

HONORS/AWARDS

1995 1996 Regents Dissertation Fellowship, UCSB

1995 Graduate Travel Grant, UCSB

1995 Instructional Improvement Grant, UCSB

1994 Instructional Improvement Grant, UCSB

1992 University Research SCUBA Certification, UCSB

1990 Brazilian Research (EMBRAPA) Fellowship, Manaus, Brazil

1987 Departmental Distinction, Biology, St. Olaf College

1986 Antarctic Service Medal

1985 Sea Grant Undergraduate Research Fellowship, University of Maryland

1982 Natural Resource and Conservation Award, Town of N. Easton, Massachusettes

SOCIETY MEMBERSHIPS

1990-pres. American Society of Limnology and Oceanography

1992-pres. Oceanography Society

1996-pres. Phycological Society of America

PUBLICATIONS

Putt M, Rivkin RB, Moline MA (1986) Diel periodicities of photosynthesis in Antarctic phytoplankton: species specific response. Antarctic Journal of the United States 21(5): 185-186

Fisher WS, Chintala MM, Moline MA (1989) Annual variation of estuarine and oceanic oyster *Crassostrea virginica* Gmelin hemocyte capacity. J Exp Mar Bio Ecol 127: 105-

Harell RM, Moline MA (1992) Comparative stress dynamics of brood stock striped bass *Marone saxatillis* associated with two capture techniques. J W Aqu Soc 23(1): 58-62

Fisher TR, Moline MA (1992) Seasonal plant cover on the Amazon River Floodplain determined with aerial videography and image analysis. In: Blazquez CH (ed.) Color Aerial Photography in the Plant Sciences and Related Fields. American Society for Photometry and Remote Sensing. pp. 207-216

Prezelin BB, Moline MA, Seydel K, Scheppe K (1992) Palmer LTER: Temporal variabilityin HPLC pigmentation and inorganic nutrient distribution in surface waters adjacent to Palmer Station, December 1991-February 1992. Antarctic Journal of the United States 27(5): 245-248.

Prezelin BB, Boucher NP, Moline MA, Stephens E, Seydel K, Scheppe K (1992) Palmer LTER: Spatial variability in phytoplankton distribution and surface photosynthetic potential within the farfield grid, November 1991. Antarctic Journal of the United States 27(5): 242-245.

Moline MA, Prezelin BB (1994) Palmer LTER: Impact of a large diatom bloom on macro nutrient distribution in

Arthur Harbor during austral summer 1991-1992. Antarctic Journal of the United States 29(5): 217-219

Boucher NB, Prézelin BB, Evens T, Jovine R, Kroon B, Moline MA, Schofield O (1994) Icecolors '93: Biological weighting function for the UV inihibtion of carbon fixation in a natural Antarctic phytoplankton community. Antarctic Journal of the United States 29(5): 272-275

Schofield O, Moline MA, Prézelin BB (1994) Palmer LTER: Photoadaptation in a coastal phytoplankton bloom and impact on the radiation utilization efficiency for carbon fixation. Antarctic Journal of the United States 29(5): 214-216

Moline MA, Schofield O, Prezelin BB (in press) Statistical analyses of environmental predictors for phytoplankton photosynthetic parameters and productivity in an Antarctic time-series database. Antarctic Journal of the United States.

Schofield O, Moline MA, Prézelin BB (in press) Palmer LTER: Photoadaptation in a coastal phytoplankton bloom. Antarctic Journal of the United States.

Moline MA, Prézelin BB, Schofield O, Smith RC (in press) Temporal dynamics of coastal Antarctic phytoplankton:

Environmental driving forces and impact of a 1991-1992 summer diatom bloom on the nutrient and light regimes. In: Battaglia B, Valencia J, Walton DWH (eds.) Antarctic Communities. Cambridge University Press. Invited.

Moline MA, Prézelin BB (in press) High resolution time series data for *in situ* carbon fixation at a Palmer LTER site and its implications for modeling primary production in the Southern Ocean. Polar Biology.

Claustre H, Moline MA, Prézelin BB (in press) Sources of variability in the column photosynthetic cross section for Antarctic coastal water. J Geophys Res.

Moline MA, Prézelin BB (in press) Palmer LTER 1991-1994: Long-term monitoring and analyses of physical factors regulating variability in coastal Antarctic phytoplankton biomass, *in situ* productivity and taxonomic composition over subseasonal, seasonal and interannual time scales. Mar Ecol Prog Ser.

Schofield, O., M. A. Moline and B. B. Prézelin (submitted) Variability in the quantum yields for carbon fixation in coastal Antarctic phytoplankton and the impact on bio-optical productivity models. Limnol Oceanogr.

Moline MA (submitted) Photoadaptive response during the

development of a coastal Antarctic diatom bloom and relationship to water column stability. Limnol Oceanogr.

Prézelin BB, Moline MA, Matlick HA (submitted) Icecolors'93: Spectral UV radiation effects on Antarctic frazil ice algae. In: Lizotte MP, Arrigo KR (eds.) Antarctic Sea Ice: Biological Processes. Antarctic Research Series. American Geophysical Union. Washington D.C. Invited.

FIELDS OF STUDY

Major Field: Aquatic Biology

Studies in Phytoplankton Ecology

Drs. B.B. Prézelin, M.A. Brzezinski, H. Claustre, R. Nisbet, E.E. Hofmann

Studies in Adaptive Physiology

Drs. B.B. Prézelin, H. Claustre

Studies in Biological Oceanography

Drs. B.B. Prézelin, E.E. Hofmann, M.A. Brzezinski, H. Claustre

Studies in Theoretical Ecology

Drs. E.E. Hofmann, R. Nisbet

ABSTRACT

Temporal dynamics and regulation of coastal Antarctic phytoplankton communities: Spring/Summer 1991-1994

by

Mark Alan Moline

Previous studies in the Southern Ocean have documented the large spatial variability in phytoplankton biomass productivity with generally higher concentrations and rates associated with coastal regions and ice edge zones. The relatively low productivity, compared to lower latitudes, in the nutrient rich pelagic waters is thought to be a result of either light limitation through deep vertical mixing, decreased temperatures, and/or micronutrient limitation, however, the processes controlling phytoplankton dynamics are a subject of continual debate. The goals of this thesis are 1) to identify and quantify major factors regulating phytoplankton dynamics in an Antarctic coastal region and 2) to discern the shifting balance of these regulatory factors that determine the variability in phytoplankton biomass, productivity and taxonomic composition. Unlike most studies undertaken in the

Southern Ocean that are logistically restricted to spatial approaches, this work examines at the temporal dynamics in phytoplankton processes related to the physical, biological and chemical environments on time scales of hours to years.

As part of the Palmer Long-Term Ecological Research (PAL-LTER) program, this study attempts to define and quantify the processes that underlie the natural variability in the phytoplankton community. In examining this question, it is expected that these results will help the larger LTER objective of defining ecological processes linking the extent of pack ice with different trophic levels within Antarctic marine communities.

In Chapter 1, is a case study of the interactions between physical forcing and nutrient fields and biological responses, which were magnified during the development of a large diatom bloom. Subseasonal fluctuations in sea ice coverage, mixing depths, wind stress and advective processes were found to be the major driving forces affecting the timing, duration and demise of local phytoplankton blooms. During the bloom, macronutrients were depleted to detection limits and significant shifts in nutrient ratios were observed. Phytoplankton populations were light-limited below ~ 5 m during the bloom resulting from self-shading.

Chapter 2 examines a photophysiological response during the development of the bloom detailed in Chapter 1. An index, using photoprotective xanthophyll pigments, is identified and found to significantly track fluctuations in the incident solar irradiance and the in situ light field over a 3 orders of magnitude change in the water column biomass. Diel studies independently confirm the response time of this index to the ambient light field. In combination with physical data, this index has the potential of assessing the degree of water column stability, which is identified throughout this work to be a major prerequisite for increased phytoplankton biomass and productivity.

The calculation of in situ primary productivity for the study is detailed in Chapter 3. Significant variation in daily integrated rates of primary productivity occurred generally on time scales less than a week. Peak timing and magnitude of daytime periodicities in photosynthesis varied widely over the season, closely coupled to changes in phytoplankton community composition. Primary production estimates, if uncorrected or improperly corrected for daytime periodicities in carbon fixation, are shown to be unreliable predictors of production on longer time scales even if the water column was sampled every few days. High frequency sampling and consideration of diel

periodicity may be requirements when attempting to discern differences between short time-scale variability and long-term trends in Antarctic primary production.

Variability in biomass, primary productivity and taxonomic composition on subseasonal to interannual time scales are detailed in Chapter 4. Interannual variability in biomass and associated in situ productivity in this coastal environment was comparable to variability within years. Despite this variability, the replacement sequence of one dominate phytoplankton group by another was very similar on subseasonal time scales for all 3 years. Results suggest that monitoring changes in phytoplankton successional patterns may be a more sensitive marker for detecting long-term trended changes in Southern Ocean ecosystems than either biomass or productivity indices.

Chapter 5 examines the temporal distribution of inorganic nutrients and utilization by phytoplankton. Macronutrient concentrations during bloom events decreased markedly. Seasonal mean N:P:Si ratios agreed well with previous studies, however, at times over the sampling seasons, ratios indicated disproportionate uptake by phytoplankton and were found to partially depend on the taxonomic composition in the water column. Primary production determined by nutrient depletion

in the water column corresponds well to measure in situ primary productivity for the large 1991-92 bloom, however, this approach can deviate from measured results by an order of magnitude during times of high meltwater input. Ambient nutrient concentrations set the maximum potential for photosynthesis per unit Chl a, however, daily in situ growth rates remained high, suggesting nutrients during this study were non-limiting.

INTRODUCTION

BACKGROUND

Phytoplankton Research in the Southern Ocean

In the past 30 years, phytoplankton distribution and productivity have been documented in the Southern Ocean (Burkholder and Mandelli 1965; Mandelli and Burkholder 1966, El-Sayed 1971; Holm-Hansen et al. 1977; El-Sayed 1984, Smith and Nelson 1985; Bodungen et al. 1986; Sakshaug 1989; Holm-Hansen and Mitchell 1991; Smetacek et al. 1992; El-Sayed and Fryxell 1993). The majority of the Southern Ocean (~30 million km^2) is believed to have low plant biomass averaging 0.4 mg Chl a m^{-3} (Sakshaug et al. 1991). The exceptions to low standing stock areas are coastal regions and the marginal ice zones, the latter of which advance and retreat annually over an area of 16 million km^2 (Gloersen et al. 1992). While these two areas are characterized by higher average biomass, plant distributions are heterogeneous with periodic blooms occurring on small time and space scales. Phytoplankton biomass associated with receding ice edges have been found to be as high as 190 mg Chl a m^{-3} (El-Sayed 1971) but spring/summer maximums more commonly average 5 to 10 mg Chl a m^{-3} (see Smith and Nelson 1986). The importance of such large, but episodic, bloom phenomena in the Southern Ocean is at least fourfold. (1) Phytoplankton blooms can play a

major role in biogeochemical cycling and in particular the global silica cycling (Smith and Nelson 1986; Nelson and Smith 1986; Treguer and Bennekorn 1991). (2) While debatable, blooms are estimated to be responsible for at least half of the Southern Ocean's annual productivity (Smith et al. 1988). (3) Antarctic prymnesiophyte blooms have been found to be an important source of dimethylsulfide (DMS) production (Gibson et al. 1988), which are linked to cloud formation effecting global weather patterns (Bates et al. 1987). (4) Blooms are also a major carbon source for upper trophic levels (Weber and El-Sayed 1985), supporting large populations of krill (*Euphausia superba*), birds, seals, and whales found in the Southern Ocean.

Recent studies [AMERIEZ, BIOMASS, CEMP (CCAMLR), EPOS, ICECOLORS, RACER, Ross Sea, SO-JGOFS, among others] have integrated physical, chemical, optical, and biological data in an attempt to understand the mechanisms and factors controlling phytoplankton standing stock and productivity in Antarctica (Sullivan et al. 1988; Smith and Sakshaug 1990; Mitchell and Holm-Hansen 1991; Sakshaug et al. 1991; Smetacek et al. 1992). Theories and empirical models derived from these studies generally point to resource limitation, temperature, and/or water column stability as the major factors governing phytoplankton bloom dynamics. However, like most field studies conducted in the Southern Ocean, they

were conducted shipboard in pelagic regions, and as a result, were restricted to describing phytoplankton distribution, abundance, productivity, and physiology in a spatial context. Very few have had the opportunity to examine the temporal variations in bloom dynamics (however see work by Krebs 1983; Whitaker 1982; Fukuchi et al. 1985; Perrin et al. 1987; Domanov and Lipski 1990; Mitchell and Holm-Hansen 1991) and those that have are based on a limited parameters of interest (eg. chlorophyll dynamics) usually with a short monitoring period and/or not intensely sampled.

By examining the temporal variations in phytoplankton distribution (vertical), abundance, productivity, growth and community structure of phytoplankton collected from 1991 to 1994 in relation to the physical and chemical environments on time scale of days, it is the goal of this thesis to advance the understanding of the processes regulating phytoplankton dynamics and the time scales of those regulatory processes during the spring/summer seasons in a coastal region near Anvers Island, Antarctica.

The Palmer Long-Term Ecological Research Program

The objectives of this thesis are a part of the Palmer Long-Term Ecological Research (LTER) program, designed to define ecological processes linking the extent of annual pack ice with

different trophic levels within Antarctic marine communities (Ross and Quetin 1991). The annual advance and retreat of sea ice covers an area of ~ 16 million km^{-2}, about half the area of the Southern Ocean. This cycle of ice coverage provides conditions that are distinct from the non-polar oceans and is thought to be a major physical determinant for the temporal and spatial variability in the structure of the Antarctic food web (Smith and Sakshaug 1990. Moreover, the cycles of ice coverage in any particular region of the Southern Ocean are variable from year to year (Zwally et al. 1983), particularly within the LTER region (Stammerjohn 1993). As a consequence, effects of sea ice on the Antarctic marine food web are also likely to be variable. Therefore, it is the goal of the LTER to define the variability in both sea ice dynamics and key components of the food web in order to link ecosystem processes to physical environmental variables, with the future goal of predicting impacts of sea ice changes on the ecosystem dynamics. However, it is clear that before impacts of sea ice on the Antarctic biota can be discerned, the processes that underlie the natural variation in representative populations need to be identified and quantified.

A series of nearshore stations was established adjacent to Palmer Station, Antarctica, (Waters and Smith 1992; see Fig. 1) to define linkages between representative populations within

the bird foraging area during the spring/summer transition. As a component of the LTER, this thesis addresses the controlling processes and natural subseasonal/seasonal/ interannual variation of primary producers within this nearshore grid during the dynamic period of increasing photoperiod, ice melt, and increased animal fecundity.

Previous Phytoplankton Studies in the Vicinity of Palmer Station

A number of previous phytoplankton-related studies have been conducted in the nearshore grid area adjacent to Palmer Station (Shabica et al. 1977; Krebs 1983; Krebs et al. 1987; Holm-Hansen et al. 1989). Shabica et al. (1977) conducted a study from 1970-1971, examining changes in dissolved O_2, pH, salinity and temperature. Meteorological and hydrographic surface samples taken daily off of Palmer Station showed a sharp increase in both pH (to 8.8) and dissolved O_2 (to 120% saturation) in mid December associated with an increase in phytoplankton biomass. Also interesting was the rapid drop in salinity (from 34 ppt to 25 ppt) at the end of November, which lasted for only 3 weeks. Wind speed data collected over the same period showed an annual cycle of high wind speeds (15-20 m s^{-1}) from May to November and lower wind speeds (< 10 m s^{-1}) measured from December to April.

An extensive temporal study from 1971-1974 was conducted by Krebs (1983) and Krebs et al. (1987) in Arthur Harbor. The sampling location was midway between stations A and B of this study (Fig. 1). Hydrographic and meteorological measurements as well as determination of chlorophyll biomass and cell counts were made throughout the water column. Temporal dynamics of pH, O_2, salinity, temperature and wind speed were similar to results by Shabica et al. (1977), however, depth profiles show the decrease in salinity from 34 to 25 ppt was isolated to the upper 3 meters with only a two week duration. Spring, summer and fall blooms were documented with maximum chlorophyll biomass of ~26 mg m^{-3}. The trimodal nature of the standing crop was show to be dependent on low wind stress and glacial meltwater which stabilized the water column. Cell counts revealed that nearly all of the biomass over the three years was diatoms with *Porosira glacialis*, *Nitzschia* spp., *Chaetoceros* spp. and *Rhizosolenia* spp. the dominant species. This study also demonstrated that ice algae served as an inoculum for later water column blooms.

Brief studies by Holm-Hansen et al. (1989) in January of 1985 and 1987 documented the occurrence of large phytoplankton blooms (20 mg Chl a m^{-3} and 25 mg Chl a m^{-3}, respectively) in the LTER nearshore grid area. These blooms were dominated by large diatoms (*Rhizosolenia* and *Odentella*

spp.) with 25% of the chlorophyll biomass associated with the prymnesiophyte *Phaeocystis pouchetii.* Inorganic and particulate nutrient data suggested possible nutrient limitation during this summer period of high biomass. Low assimilation numbers during these blooms were attributed to light limitation by self-shading. Over half of the water column biomass was below the 1% light level.

These studies provide additional information on the physical, chemical and biological dynamics of the area and a historical context in which to interpret results of this study. Given that comparatively little work has been done in the Southern Ocean, historical data from this region may be helpful when attempting to identify and quantify long-term trends.

OVERVIEW OF STUDY

Objectives

This study had the following objectives:

1. Identify and quantify the major factors regulating phytoplankton dynamics in a defined Antarctic coastal environment on subseasonal and seasonal timescales.
2. Identify the time scales of these processes regulating phytoplankton dynamics.

3. Discern the shifting balance of such regulatory factors that might determine the interannual variability in summer diatom bloom dynamics observed in a defined Antarctic coastal environment.

In order to discern the factors controlling phytoplankton dynamics, the sampling regimes need to mimic the space and time scales of the processes being studied. Smith and Nelson (1986) stated "Any mechanism proposed to explain the initiation of an ice edge bloom must also explain the bloom's spatial extent", whether it be defined by the density field, decreased wind stress, or release of a 'seed' population from ice algae. Order of magnitude differences in the chlorophyll *a* concentrations have been shown over distances <5km along ice edge zones (Smith and Nelson 1985, Wilson 1986, Estrada and Delagado 1990, Mitchell and Holm-Hansen 1991), therefore, many spatial studies, which sample at 25-50km intervals, may not be able to accurately resolve the spacial extent of phytoplankton distribution. This question of resolution also holds true for temporal work. Areas sampled on time scales of weeks to months have shown seasonal changes in phytoplankton biomass (El-Sayed and Weber 1982, Satoh et al. 1985, Fukuchi et al. 1985, Lipski 1987), species composition (Krebs 1983, Krebs 1987, Perrin et al. 1987), productivity (El-

Sayed 1971, Domanov and Lipski 1990), and some have examined all of these parameters with respect to the physical, chemical, and optical environments (Whitaker 1982, Holm-Hansen and Mitchell 1991). However, phytoplankton species succession photoadaptation, productivity, growth, and biomass changes occur on time scales of hours to days, therefore, sampling over time scales of weeks to months may be limiting when discerning controlling mechanisms.

In this study, the LTER coastal stations near Palmer Station were repetitively sampled on time scales of days during three field seasons from 1991-1994 to quantify the processes controlling phytoplankton productivity and biomass and to better define the time and space scale variability of these processes.

The following sections briefly describe 1) the specific scientific questions addressed in each chapter, 2) the sampling and approach used in each study and 3) a summary of the main results.

Chapter 1 - Temporal Dynamics of coastal Antarctic phytoplankton: Environmental driving forces and impact of a 1991-1992 summer diatom bloom on the nutrient regimes

The objectives of the study were:

1) to detail bloom development and phytoplankton dynamics off the coast of Anvers Island with the highest temporal resolution ever measured for the Southern Ocean.

2) to define the linkages between the biological signals and the physical and chemical environments.

3) to define the time scale variability of these biological responses to the physical and chemical environments over the austral summer.

Within the Palmer Long Term Ecological Research Program, a suite of biological (algal pigmentation, productivity-irradiance curves, macronutrients) and physical (CTD profiles, wind direction/speed, precipitation) parameters were collected from a Mark V Zodiac® every 2-3 days at LTER nearshore station B from November, 1991 through February, 1992. Seasonal changes are presented in the context of phytoplankton community ecology.

Subseasonal fluctuations in sea ice coverage, fresh water inputs, as well as wind driven and advective processes disrupting stratified surface waters, appeared to be the major driving forces affecting the timing, duration and demise of local phytoplankton blooms. During a large diatom-dominated bloom (~30 mg Chl a m^{-3}), macronutrients were depleted to

detection limits (NO_3^- < 0.05 μmol m^{-3}, PO_4^{3-} < 0.03 μmol m^{-3}), an event rarely documented in the Southern Ocean, and significant shifts in nutrient ratios were observed. For the season, a non-linear relationship between the depth of mixing and integrated biomass within the layer was found. This relationship is similar to previous findings from spatial studies (see Mitchell et al., 1991), illustrating that this dependency of biomass on the stratification of the water column is robust over a large range of space and time scales. High biomass accumulation during the bloom was shown to light limit phytoplankton populations below ~5 m by self-shading. The depth of light limitation deepened after the bloom was physically disrupted and removed from the region by strong advective processes. Major changes in phytoplankton biomass and community composition was found to occur on the same time scales (1-2 weeks) of physical disruption of the water column

This study was published as an invited chapter to the Scientific Committee on Antarctic Research (SCAR) volume Antarctic Communities: species, structure and survival, Cambridge University Press in 1996, in press. Parts of this study also appeared in reports in the Antarctic Journal of the United States in 1992 [27(5), 245-248], 1994 [29(5), 214-216; 217-219], and 1995, in press.

Chapter 2 - Photoadaptive response during the development of an Antarctic diatom bloom and relationship to water column stability

The objectives of the study were:

1) to define a photoadaptive index that could be used to assess a photoadaptive response of Antarctic phytoplankton to changing light environments.

2) to assess the temporal dynamics and kinetics of this index on time scales of hours to weeks.

3) to examine the potential use of this index in defining phytoplankton light histories and the vertical stability of the water column.

CTD profiles were collected from a Mark V Zodiac® every 2-3 days at LTER nearshore station B from November, 1991 through February, 1992. In addition to the in-water temporal changes, weekly diel experiments were conducted over the same time period to access shorter time scale (hourly) changes in phytoplankton pigmentation.

The ratio of the xanthophylls, diadinoxanthin (DD) and diatoxanthin (DT), to chlorophyll a [(DD + DT):Chl a] was shown to be a reliable photoadaptive index during the development of a large Antarctic diatom bloom. This index was found to

significantly track fluctuations in the incident solar irradiance and the in situ light field over a 3 orders of magnitude change in the water column biomass. Depth profiles of the [(DD + DT):Chl *a*] ratio show that the upper 'mixed' layer, assessed by physical data, was in fact stable over the course of the first month. Diel experiments conducted over the same period showed a delayed (5-8 hours) saturating response of the (DD + DT) pool to the Q_{par} (400-700 nm) dose. These time-series results illustrated the potential use of light-dependent pigments in assessing phytoplankton 'light histories' and water column stability.

This study was submitted for publication to Limnology and Oceanography in August, 1996.

Chapter 3 - High-resolution time series data for 1991/1992 primary production and related parameters at a Palmer LTER coastal site: Implications for modeling carbon fixation in the Southern Ocean

The objectives of the study were:

1) to determine in situ productivity over a range of seasonal to subseasonal time scales.

2) to identify time scales of significant variability in marine productivity during the peak growing season.

3) to identify environmental, experimental and analytical factors that can significantly impact the accuracy of daily, weekly and seasonal productivity estimates.

4) to integrate our findings with previous studies of Antarctic coastal primary production.

Data was gathered every 2 to 3 days during a three month period in the austral spring/summer of 1991/1992. Photosynthesis-irradiance (P-I) relationships were determined throughout the euphotic zone and P-I parameters, combined with knowledge of the in-water light field, were used to derive instantaneous rates of in situ primary production. Additionally, weekly samples were collected from surface and chlorophyll a maxima for characterization of the patterns of diel periodicity in P-I parameters.

Seven diel patterns were discerned over the season and used to time-correct instantaneous measurements and derive noontime, daily, monthly and seasonally integrated estimates of production. During the season, a large bloom was responsible for some of the highest daily productivity rates reported for the Southern Ocean (0.8 g C m^{-3} d^{-1}, 6.3 g C m^{-2} d^{-1}). Significant variation in daily integrated rates occurred

generally on time scales less than a week. Peak timing and magnitude of daytime periodicities in photosynthesis varied widely over the season, closely coupled to changes in phytoplankton community composition. Instantaneous measurements of primary production, if uncorrected or improperly corrected for daytime periodicities in carbon fixation, were unreliable predictors of production on longer time scales even if the water column was sampled every few days. High frequency sampling and consideration of diel periodicity may be requirements when attempting to discern differences between short time-scale variability and long-term trends in Antarctic primary production.

This study was published in Polar Biology in 1996, in press.

Chapter 4 - Palmer LTER 1991-1994: Long-term monitoring and analyses of physical factors regulating variability in coastal Antarctic phytoplankton biomass, *in situ* productivity and taxonomic composition over subseasonal, seasonal and interannual time scales

The objectives of the study were:

1) to quantify the variability in phytoplankton biomass, in situ productivity and taxonomic composition over subseasonal, seasonal and interannual time scales.

2) to elucidate environmental mechanisms controlling these temporal patterns.

3) to ascertain which phytoplankton markers are most suitable for longer-term (i.e. decadal) trends in phytoplankton dynamic in coastal waters of the Southern Ocean.

This is a compilation of 3 years (1991-1994) of data collected during the austral spring/summer periods from two LTER stations (B and E) adjacent to Palmer Station, Antarctica. Biological (algal pigmentation, productivity-irradiance curves, macronutrients) and physical (CTD profiles, wind direction/ speed, precipitation, air temperature, tidal height) data were collected daily from Palmer Station and/or a Mark V Zodiac®.

The LTER coastal study sites showed high interannual variability in peak phytoplankton biomass (75 - 494 mg Chl a m^{-2}) and integrated primary production (1.08 - 6.58 g C m^{-2} d^{-1}). Seasonal and annual patterns in biomass and productivity were shown to be driven by shorter time scale physical forcing by local wind stress. Low daily wind speeds (< 10 m s^{-1}) were associated with water-column stabilization. However, extended periods (> 1 week) of low wind stress were required for

increased phytoplankton growth and biomass accumulation. Temperature data supports the view that water masses can be replaced on time scales of a less than a day (tidal influences) to a few days in these coastal waters. Despite the high seasonal and interannual variability in biomass and associated in situ productivity in this coastal environment, the replacement sequence of one dominate phytoplankton group by another was very similar on subseasonal time scales for all 3 years. Diatoms were found to dominate during the spring and late summer. However, cryptophytes were found to dominate in the mid summer in response to changes in salinity resulting from glacial meltwater inputs. These results and previous studies suggests that cryptophytes and other phytoflagellates may be more dominant now than in the past, given the recent warming trends and increased glacial melting.

This study suggests that monitoring changes in phytoplankton successional patterns may be a more sensitive marker for detecting long-term trended changes in Southern Ocean ecosystems than either biomass or productivity indices, where short-term variability of the latter is as great or greater than interannual variations documented to date.

This study was accepted for publication to Marine Ecology Progess Series in August, 1996.

Chapter 5 - Variability of inorganic macronutrients in an Antarctic coastal region (1991-1994)

The objectives of the study were:

1) to quantify the distribution of inorganic nutrients.

2) to identify physical and biological processes that alter water column nutrient concentrations and nutrient ratios.

3) to compare productivity estimates derived from nutrient loss with measured in situ primary productivity (Chapter 4).

4) to examine possible impact of changing ambient nutrient concentrations on phytoplankton physiology.

Inorganic nutrients, biomass, and in situ primary productivity were quantified throughout the water column every 2-3 days at five stations within the LTER nearshore grid during the spring/summer from 1991-1994.

During two periods of low wind stress and stratification of the water column resulted in development of large blooms with biomass approaching 30 mg Chl a m^{-3} and maximum integrated concentrations of 494 mg Chl a m^{-2}. Macronutrient during these events rapidly decreased to very low concentrations (18.5 μM Si, 0.72 μM N, 0.04 μM P). Seasonal mean N:P:Si ratios agreed well with previous studies, however, at times over the sampling seasons, ratios indicated

disproportionate uptake by phytoplankton and were found to partially depend on the taxonomic composition in the water column. Primary production determined by nutrient depletion in the water column was found to correspond well to measure in situ primary productivity for the large 1991-92 bloom. However, determining primary production by nutrient loss can deviate from measured results by an order of magnitude during times of high meltwater input. The maximum potential for photosynthesis per unit Chl a decreased with decreasing nutrient, although was highly variable depending location in the water column and the extent of vertical mixing. Increased synthesis of light harvesting pigmentation occurred during low ambient nutrient concentrations in response to increasing biomass and self-shading. Despite the periods of extremely low nutrient conditions, daily in situ growth rates remained high, suggesting phytoplankton during this study were not nutrient limited.

LITERATURE CITED

Bates TS, Charlson RL, Gammon RH (1987) Evidence for the climatic role of marine biogenic sulfur. Nature 329: 319-321

Bodungen B Von, Smetachek V, Tilzer MM, Zeitzschell B (1986) Primary production and sedimentation during spring in the Antarctic Peninsula region. Deep-Sea Res 33: 177-194

Burkholder PR, Mandelli EF (1965) Carbon assimilation of marine phytoplankton in Antarctica. Proc of NAS of the USA 54: 437-444

Domanov MM, Lipski M (1990) Annual cycle of chlorophyll a and primary production of phytoplankton in Admiralty Bay (Antarctica). Pol. Arch. Hydrobiol. 37: 471-478

El-Sayed SZ (1971) Observations of phytoplankton blooms in the Weddell Sea. In: Llano GA, Walker JE (eds) Vol IV of Antactic Research Series. 17: 301-312

El-Sayed SZ (1984) Productivity of Antarctic waters-A reappraisal. In: Holm-Hansen O, Bolis L, Gilles R (eds) Marine Phytoplankton and Productivity. Springer-Verlag, Berlin pp 19-34

El-Sayed SZ, Weber LH (1982) Spatial and temporal variations in phytoplankton biomass and primary production in the Southwest Atlantic and the Scotia Sea. Polar Biology 1: 83-90

El-Sayed SZ, Fryxell GA (1993) Phytoplankton. In: Antarctic Microbiology. Wiley-Liss, Inc. pp 65-122

Estrada M, Delgado M (1990) Summer phytoplankton distributions in the Weddell Sea. Polar Biology 10: 441-449

Fukuchi M, Tanimura A, Ohtsuka H (1985) Marine biological and oceanographical investigations in Lutzow-Holm Bay. In: Siegfried WR, CondyPR, Laws RM (eds) Antarctic Nutrient Cycles and Food Webs. Springer-Verlag, Berlin pp 52-59

Gibson JAE, Garmick RC, Burton HR, Mctaggart AR (1988) Dimethylsulfide concentrations in the ocean close to the antarctic continent. Geomicrobiology J 6:179-184

Gloersen P, Campbell WJ, Cavalieri DJ, Comiso JC, Parkinson CL, Zwally HJ (1992) Arctic and Antarctic sea ice, 1978-1987: Satellite passive microwave observations and analysis. Tech Rep NASA SP-511, National Aeronautics and Space Administration, Washington D.C.

Holm-Hansen O, El-Sayed SZ, Franceschini GA, Cuhel RL (1977) Primary productivity and the factors controlling phytoplankton growth in the Southern Ocean. In: Llano GA (ed) Adaptations within Antarctic Ecosystems. Gulf, Houston pp 11-50

Holm-Hansen O, Mitchell BG, Hewes CD, Karl DM (1989) Phytoplankton Blooms in the Vicinity of Palmer Station, Antarctica. Polar Biology 10: 49-57

Holm-Hansen O, Mitchell BG (1991) Spatial and temporal distribution of phytoplankton and primary production in the western Bransfield Strait region. Deep-Sea Res 38: 961-980

Krebs WN (1983) Ecology of neritic marine diatoms, Arthur Harbor, Antarctica. Micropaleontology 29: 267-297

Krebs WN, Lipps JH, Burckle LH (1987) Ice diatom floras, Arthur Harbor, Antarctica. Polar Biology 7: 163-171

Lipski M (1987) Variations of physical conditions, nutrients and chlorophyll *a* contents in Admiralty Bay (King George Island, South Shetland Islands, 1979). Pol Polar Res 8: 307-332

Mandelli EF, Burkholder PR (1966) Primary productivity in the Gerlache and Bransfield Straits of Antarctica. J of Mar Res 24: 15-27

Mitchell BG, Holm-Hansen O (1991) Observations and modeling of the antarctic phytoplankton crop in relation to mixing depth. Deep-Sea Res 38: 981-1007

Nelson DM, Smith WOJ (1986) Phytoplankton bloom dynamics of the westerm Ross Sea ice-edge. I and II. Deep-Sea Res 33: 1389-1412

Perrin RA, Lu P, Marchant HJ (1987) Seasonal variation in marine phytoplankton in ice algae at a shallow antarctic coastal site. Hydrobiologia 146: 33-46

Ross RM, Quentin LB (1992) Palmer long-term ecological research (LTER): An overview of the 1991-1992 season. Ant J U S 27: 235-236

Sakshaug E (1989) The physiological ecology of polar phytoplankton. In: Rey L and Alexander V (eds) Proc. 6th Conf. Comité Arctique International, 13-15 May 1985. E. J. Brill, Leiden. pp 61-89

Sakshaug E, Slagstad D, Holm-Hansen O (1991) Factors controlling the development of phytoplankton blooms in the Antarctic Ocean-A mathematical model. Mar Chem 35: 259-271

Satoh H, Wantanabe K, Kanda H, Takahashi E (1986) Seasonal changes of chlorophyll a standing stocks and oceanographic conditions under fast ice near Syowa Station, Antarctica 1983/84. Antarc Rec 30: 19-32

Shabica SV, Hedgpeth JW, Park PK (1977) Dissolved oxygen and pH increases by primary production in the surface water of Arthur Harbor, Antarctica, 1970-1971. In: Llano GA (ed) Adaptations Within Antarctic Ecosystems. Gulf, Houston pp 83-97

Smetacek V, Scharek R, Gordon LI, Eicken H, Fahrbach E, Rohardt G, Moore S (1992) Early spring phytoplankton blooms in ice platelet layers of the Southern Weddell Sea, Antarctica. Deep-Sea Res 39: 153-168

Smith WOJ, Nelson DM (1985) Phytoplankton bloom produced by a receding ice edge in the Ross Sea: Spacial coherence with the density field. Science 277: 163-166

Smith WOJ, Nelson DM (1986) The importance of ice-edge phytoplankton productivity in the Southern Ocean. BioScience 36: 251-257

Smith WOJ, Keene NK, Comiso JC (1988) Interannual Variability in estimated primary productivity of the antarctic marginal ice zone. In: Sahrhage D (ed) Antarctic Ocean and Resources Variability. Springer-Verlag, Berlin Heidelberg pp 131-139

Smith WOJ, Sakshaug E (1990) Polar Phytoplankton. In: W. O. Smith (ed) Polar Oceanography: Part A: Physical Science, Part B: Chemistry, Biology, Geology. Academic Press, Inc. San Diego. pp. 477-526

Stammerjohn SE (1993) Spatial and temporal variability in Southern Ocean sea ice coverage. Masters Thesis. University of California, Santa Barbara. pp 111

Sullivan CW, McClain CR, Comiso JC, Smith WOJ (1988) Phytoplankton standing crops within an Antarctic ice edge assessed by satellite remote sensing. J Geo Res 93: 12487-12498

Treguer P, Bennekorn AJ Van (1991) The annual production of biogenic silica in the Antarctic Ocean. Mar Chem 35: 477-487

Waters KJ, Smith RC (1992) Palmer LTER: A sampling grid for the Palmer LTER program. Ant J U S 27: 236-238

Weber LH, El-Sayed SZ (1985) Spatial variability of phytoplankton and the distribution and abundance of krill in the Indian Sector of the Southern Ocean. In: Siegfried WR, CondyPR, Laws RM (eds) Antarctic Nutrient Cycles and Food Webs. Springer-Verlag, Berlin pp 284-293

Whitaker TM (1982) Primary production of phytoplankton off Signy Island, South Orkneys, the Antarctic. Proc R Soc Lond 214: 169-189

Wilson DL, Smith WO, Nelson DM (1986) Phytoplankton bloom dynamics of the western Ross Sea ice edge I: Primary productivity and species specific production. Deep-Sea Res 33: 1375-1387

Zwally HJ, Parkinson CL, Comiso JC (1983) Variability of Antarctic sea ice and changes in carbon dioxide. Science 220: 1005-1012

Figure 1. Location of LTER nearshore sampling stations A-J. Samples collected from stations A-E were used for this study. The distance between stations B and E is ~3 km.

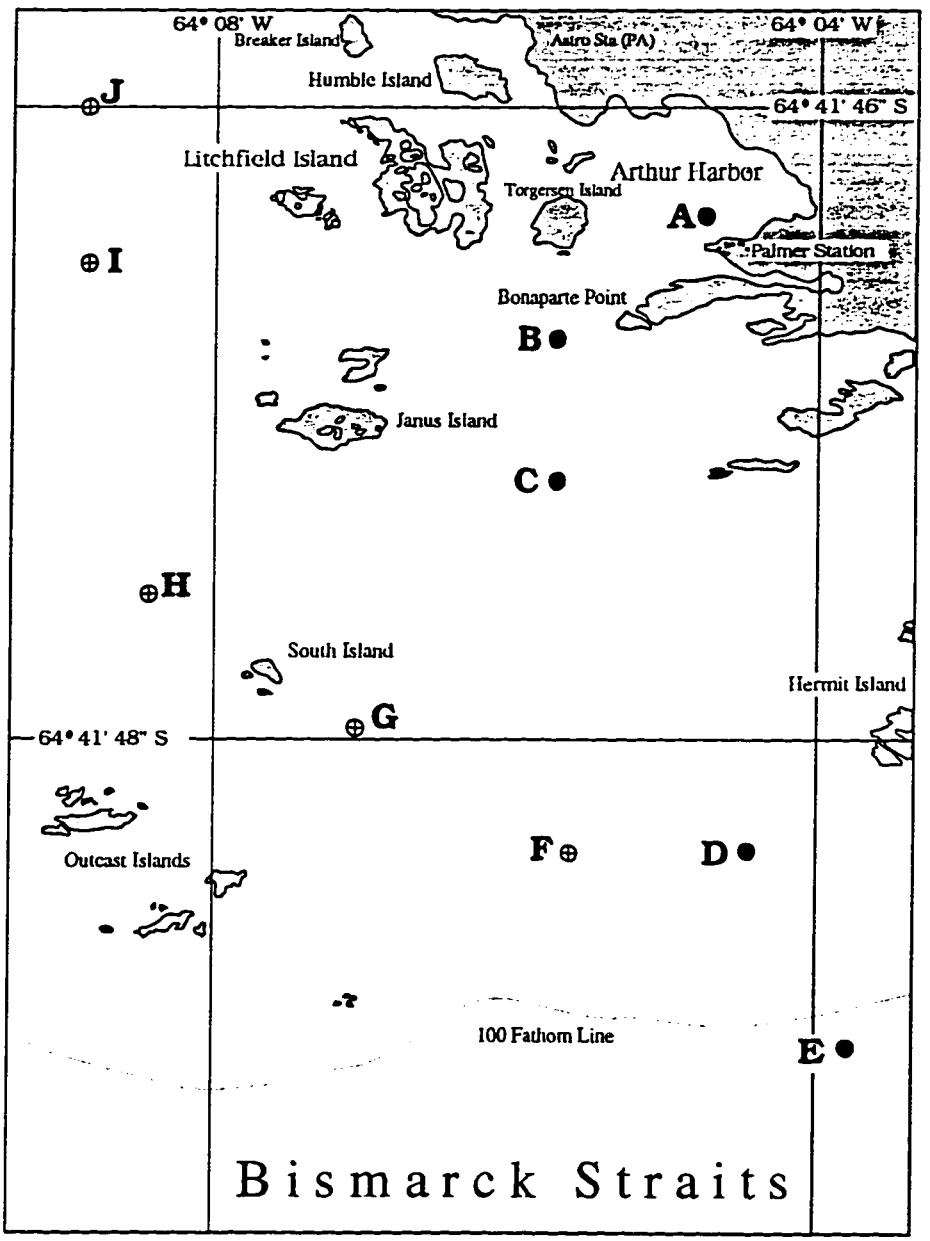
64° 08' W
Breaker Island
Humble Island
Astro Sta (PA)
64° 04' W
64° 41' 46" S
J
Litchfield Island
Arthur Harbor
Torgersen Island
A
I
Palmer Station
Bonaparte Point
B
Janus Island
C
H
South Island
Hermit Island
G
64° 41' 48" S
Outcast Islands
F
D
100 Fathom Line
E
Bismarck Straits

CHAPTER I

Temporal dynamics of coastal Antarctic phytoplankton: Environmental driving forces and impact of a 1991-1992 summer diatom bloom on the nutrient regimes

ABSTRACT

Within the Palmer Long Term Ecological Research Program (PAL-LTER), a suite of environmental data sets were collected at a nearshore station throughout the 1991-1992 austral summer. Seasonal changes are presented in the context of phytoplankton community ecology. Subseasonal fluctations in sea ice coverage, fresh water inputs, as well as wind driven and advective processes disrupting stratified surface waters, appeared to be the major driving forces affecting the timing, duration and demise of local phytoplankton blooms. During a large diatom-dominated bloom (~30 mg Chl *a* m^{-3}), macronutrients were depleted to detection limits (NO_3^- < 0.05 μmol m^{-3}, PO_4^{3-} < 0.03 μmol m^{-3}) and significant shifts in nutrient ratios were observed. Phytoplankton populations were light limited below ~ 5 m during the bloom resulting from self-shading. The depth of light limitation deepened after the bloom was physically disrupted and removed from the region by strong advective processes.

INTRODUCTION

Recent studies have integrated physical, chemical, and biological data in an attempt to understand the mechanisms controlling phytoplankton bloom dynamics in the Southern Ocean (Smith and Sakshaug 1990, Holm-Hansen and Mitchell 1991, Mitchell and Holm-Hansen 1991, Sakshaug et al. 1991). Theories and empirical models derived from such studies suggest that resource limitation and/or water column stability are the major factors governing phytoplankton bloom dynamics. Most studies have been conducted shipboard in pelagic regions and have focused on describing the short term spatial variability of phytoplankton distribution, abundance, productivity, and physiology. Temporal variations in bloom dynamics on the time scale of weeks are less documented (however, see Whitaker 1982, Krebs 1983, Priddle et al. 1986, Mitchell and Holm-Hansen 1991) and are generally based on a limited number of environmental parameters and/or insufficient information to track variations on the time scale of a few days over an entire season. With the PAL-LTER data set from the summer 1991-1992 season, we have just that opportunity. Here, we document the occurrance of a large bloom and present a detailed study of phytoplankton dynamics off the coast of Anvers Island on subseasonal time scales

ranging from days to months within the summer season. By examining these variations on time scales of days, we hope to advance the understanding of the mechanisms regulating phytoplankton productivity and bloom development in Antarctic coastal waters.

METHODS

Between November 1991 and February 1992, a total of 257 discrete water samples were collected repeatedly from Station B (Sta B) in the nearshore waters adjacent to Palmer Station, Antarctica (Fig. 1). Daily precipitation, snow cover and average wind speed and direction measurements were made at Palmer Station during the study period. These measurements were part of a long term database collected by the U. S. National Science Foundation. Prior to sample collection, in-water irradiances of photosynthetically available irradiation (Qpar) were made with a Biospherical® Scalar Irradiance Meter (QSR-170DT) equipped with a QSP-100DT underwater sensor, deployed from a Mark V Zodiac®. Samples were collected in 5L GoFlo® bottle, transferred to dark carboys and immediately returned to Palmer Station for analyses.

Replicate subsamples for nutrient determination were filtered within an hour of collection through a 0.2 mm Nuclepore membrane, and the 20 ml filtrate for each sample was stored in polycarbonate scintillation vials (acid washed) at -70 °C. Samples were later transported at -20°C to the Marine Science Analytical Laboratories, University of California, Santa Barbara for nutrient analyses. Methods for determination of the dissolved inorganic NO_3^-, PO_4^{3-}, and $Si(OH)_4$ concentrations were those of Johnson et al. (1985).

Reverse-phase HPLC procedures of Bidigare et al. (1989) were followed to determine the abundance of 17 phytoplankton pigments. Replicate 1 liter samples were filtered on 0.4 μm nylon 47mm Nuclepore® filters and extracted in 3 ml 90% acetone for 24 hr in the dark (-20 °C). Pigment separation was carried out with a Hitachi® L-6200A liquid chromatograph (436 nm). Peak identities of algal extracts were determined by comparing their retention times with pure pigment standards.

Blue-green photosynthetron methods described by Prézelin et al. (1994) were used to determine photosynthesis-irradiance (P-I) relationships for 77 of the collected samples. Non-linear curve fits for P-I data were calculated using the simplex method of Caceci and Cacheris (1984). Curve fitting provided estimates of P_{max} (the light saturated rate of

photosynthesis), α (the affinity for photosynthesis at light-limited irradiances) and $I_k = P_{max}/ \alpha$ (an estimate of the minimum irradiance required to light saturate photosynthesis).

Physical data were collected with instrumentation on a second Zodiac described by Smith et al. (1992). A total of 21 conductivity and temperature profiles were collected at Sta B using a SeaBird® CTD. Here, we make a preliminary estimate of the upper mixed-layer (UML) based on Sigma-t (σ_t) plots derived from these profiles, using the formulation

$$\max\left|\frac{d\sigma_T}{dz}\right|$$

which assumes the UML depth to be equal to the depth where the gradient in σ_t is maximal. Like Mitchell and Holm-Hansen (1991), we assume if the maximal σ_t gradient was less than 0.05 per meter, then the water column is essentially well mixed to the bottom (ca. 80 m at Sta B).

There were several occassions when a freshwater lens was clearly evident on top of the marine layer. In these instances, an estimate of the mixing depth of the freshwater lens (FW-MLD) was made in addition to the UML depth.

Contour Plots were generated using the Delaunay triangulation method (DeltaGraph® Pro3, DeltaPoint Inc., Monterey, CA, USA).

RESULTS

Until mid-December, the water column at Sta B was routinely covered with ice, buffered from relatively weak local winds, isothermal (-1.3 °C) and mixed to the bottom (Fig. 2). Glacier calving and a major wind event combined to break up and blow out local fast ice in mid-December. Due to solar insolation, ice-free conditions, major snow and glacier melt and precipitation, a freshwater lens (σ_t = 26 - 26.6) developed and persisted throughout the summer season (Fig. 2). In addition to the effects of freshwater, relatively low wind speeds (< 5 m s^{-1}) recorded through the first week in January allowed the water column to stratify and the UML shallowed to 20 m. Surface water temperature within the FW-MLD had warmed to +1.3 °C during this time, while within the UML, below the FW-MLD, the temperature was ca. -0.2 °C (data not shown). Storm activity, beginning the second week of January, produced high precipitation and maintained strong northerly winds (avg. ~15 m s^{-1}) for the following two weeks (Fig. 2). Water stratification broke down and within four days, the UML depth deepened to 55 m. Temperature - salinity relationships over the season indicate a different water mass was advected into

the area during this period (data not shown). With variable winds, the UML depth fluctuated and was not stable until mid February.

Concentrations of chlorophyll a (mg Chl a m^{-3}) at Sta B varied 340-fold over the summer period, ranging from 0.086 to 29.2 mg m^{-3} (Fig. 3). Integrated water column values ranged from 59 to 612 mg Chl a m^{-2}, with up to 70% of the biomass below the UML (Fig. 4). Early summer communities, present under the ice, were dominated by prymnesiophytes (indicated by 19'-hexanoyloxyfucoxanthin), with chrysophytes (19'-butanoyloxyfucoxanthin) (Fig. 3). In mid to late December, coincident with the shallowing of the UML depth to ca. 20 m, a large diatom-dominated (fucoxanthin) bloom developed at Sta B (Fig. 3). For 3 weeks, the bloom intensified with the highest Chl a concentrations observed between 0 and 10 m. Taxonomic identification indicated bloom samples were dominated by a centric diatom, *Coscinodiscus* spp. (D. Karentz, pers. comm.). Within the last week of the bloom, there was a ten-fold increase in the abundance of prymnesiophyte pigmentation and a corresponding decrease in diatom abundance. The presence of single celled *Phaeocystis* spp. was confirmed (D. Karentz, pers. comm.). During the second week of 1992 and corresponding to the advection event described above, Chl a and all other pigments showed a rapid decrease, with the

exception of significant surface concentrations of cryptophytes (alloxanthin) present for a week after the bloom disappearance. Chrysophyte communites were found until the beginning of Feburary when *Phaeocystis* became dominant. As the UML depth began to shallow at the end of the summer monitoring period, diatoms were once again evident.

NO_3^-, PO_4^{3-}, $Si(OH)_4$ concentrations and corresponding molar ratios of $Si(OH)_4$:NO_3^- and NO_3^-:PO_4^{3-} showed dramatic changes over the season (Fig. 5). Associated with the bloom was a depletion of NO_3^- and PO_4^{3-} to detection levels (PO_4^{3-} < 0.03 μmol m^{-3}, NO_3^- < 0.05 μmol m^{-3}). The ratio of NO_3^-:PO_4^{3-} also increased during the bloom and the difference in this ratio between 'nonbloom' ($x = 14.14 \pm 2.99$, n=166) and bloom waters ($x = 48.65 \pm 28.66$, n=51) was found to be significant at $p < 0.01$ (Fig. 6). The large change in the NO_3^-:PO_4^{3-} increase was due to the disproportionatly large uptake of PO_4^{3-} by phytoplankton. After the bloom and coincident with the advection event, PO_4^{3-} and NO_3^- concentrations returned to pre-bloom levels.

The early summer period was characterized by high levels of $Si(OH)_4$ throughout the water column below the ice (Fig. 5) when diatoms were not abundant (Fig. 3). During the diatom bloom, $Si(OH)_4$ concentrations throughout the water column were reduced from >40 μmol m^{-3} to <30 μmol m^{-3}. High

$Si(OH)_4$:NO_3^- ratios during the bloom were primarily due to the large reduction of NO_3^- in the highly stratified UML. Following the bloom and advection of different water masses into the region, $Si(OH)_4$ concentrations thoughout the water column showed a further reduction (Fig. 4). Only in late February did $Si(OH)_4$ concentrations begin to rise.

Figure 7 shows the phytoplankton's photoadaptive state over the season. Phytoplankton were light limited ($Q_{par}/ I_k >$ 1) below 20 m the entire season, however the depth of light limitation shallowed to ~ 5 m during the bloom.

DISCUSSION

Results from this study document phytoplankton dynamics on time scales of days and illustrate the linkages and feedback mechanisms between the biological, physical, and chemical environments. Seasonal freshwater inputs and decreased local winds caused stratification of the water column, which has been found in other studies to be a major controlling factor initiating biomass growth (Whitaker 1982, Smith and Sakshaug 1990, Holm-Hansen and Mitchell 1991, Mitchell and Holm-Hansen 1991, Sakshaug et al. 1991). Water column stability in December allowed the phytoplankton to photoacclimate and

overcome light limitation of growth. Biomass then accumulated in the upper 20 m and resulted in a major diatom bloom. As predicted by Kiefer and Kremer (1981), the zone of maximal growth and biomass shallowed as the bloom progressed. With the increase in biomass and light attenuation, the depth at which the phytoplankton were light limited also shallowed to ~5 m during the bloom (Fig. 7). With the shallowing of the UML, there was a shift in the phytoplankton composition from *Phaeocystis* (~1-3 μm) to a larger diatom species (*Coscinodiscus* spp. ~40-80 μm). Previous studies in the Antarctic have found an identical pattern of transition to larger phytoplankton as water column stability increases (Whitaker 1982, Rivkin 1991).

With the diatom biomass approaching concentrations thought maximal for Antarctic waters (Holm-Hansen et al. 1989), the chemical environment was significantly altered. The relationship between PO_4^{3-} and NO_3^- concentrations before and after the bloom was nearly identical to the Southern Ocean NODC (National Oceanographic Data Center) data given by Kamykowski and Zentara (1989) (Fig. 6). However, during the bloom, a significant shift in the relationship of NO_3^- to PO_4^{3-} showed the preferential uptake of PO_4^{3-}. Without a vertical nutrient flux caused by the strong stratification, this trend continued to detection limits, and therefore, PO_4^{3-} could have become the limiting resource. When PO_4^{3-} concentrations

dropped to detection limits in the upper 10m there was a change in the phytoplankton community from diatoms to *Phaeocystis*. Antarctic diatoms have shown competitive interactions for limiting nutrients, suggesting algal assemblages may vary with limited resources (Sommer 1988, Sommer 1991), but this is the first study to present evidence that a shift in the nutrient field may result in changes in a natural Antarctic phytoplankton population. The change in phytoplankton assemblage may have taken place as a result of PO_4^{3-} limiting the growth of *Coscinodiscus* spp., despite relatively high $Si(OH)_4$ concentrations, and the ability of *Phaeocystis* to utilize low concentrations of both PO_4^{3-} and NO_3^-. The nutrient absorption and storage capacity of the mucilage surrounding *Phaeocystis* colonies has been shown against large gradients of both PO_4^{3-} (Veldhuis et al. 1991) and NO_3^- (Verity et al. 1988), and is a possible mechanism to explain the transition from diatoms to *Phaeocystis* in the low macronutrient environment at Sta B.

The dramatic macronutrient shifts in the water column during the second week of January were due to the advection of a different water mass into the area. The PO_4^{3-} rich, NO_3^- rich, and $Si(OH)_4$ poor water mass observed the later half of this study could have been a result of water with high PO_4^{3-}, NO_3^- and $Si(OH)_4$ concentrations mixing with coastal glacial

meltwater and island runoff with high PO_4^{3-} and NO_3^- concentrations and no $Si(OH)_4$. Such mixing processes would have a diluting affect with $Si(OH)_4$ while not effecting the PO_4^{3-} and NO_3^- concentrations. Supporting evidence for the presence of glacial flour at Sta B is revealed in the σ_t data (Fig. 2) indicating a large freshwater input and high light attenuation in the top 20 meters in the absence of high biomass (data not shown).

The presence of flagellates (cryptophytes (alloxanthin) and chrysophytes (19'-butanoyloxy-fucoxanthin)) during the month following the advection event, may indicate a better adaptability to this period of increased vertical mixing, which has been documented in pelagic regions off the Antarctic Peninsula (Kopczynska, 1992). The final two weeks of the study are of particular interest because it was during this period that a second diatom bloom began to develop. Conditions were very similar to those found earlier in November and December; decreased winds, a shallowing UML, and a transition from *Phaeocystis* to diatoms (fucoxanthin increased from < 0.1 to 0.5 mg m^{-3}). These conditions initiated a second bloom that continued through the third week in March (Haberman, pers. comm.). Krebs (1983) showed that during a sampling period from December 1971 to January 1974 there were major blooms occuring December-January and

secondary less intense blooms during the March-April time period. These findings along with data from this study and Holm-Hansen et al. (1989) suggest that near Palmer Station phytoplankton dynamics and the processes controlling them are similar between years.

Physical factors, thought to partly initiate ice-edge blooms, such as a meltwater lens, also appear to be important in coastal systems, providing the stability needed for biomass accumulation. The depth of the UML, as defined in this study, was found to be an important factor in the development of phytoplankton biomass (Fig. 4). As the UML shallowed (~ 20 m), integrated chlorophyll a within the UML increased an order of magnitude. Mitchell and Holm-Hansen (1991) also showed the same relationship of increasing biomass with shallowing of the UML (Fig. 4). The degree of water column stability appears to also select for certain species; diatoms in a stratified high nutrient condition and *Phaeocystis* and flagellates in a mixed variable nutrient environment prior stabilization.

CONCLUDING REMARKS

Although continued analyses of seasonal and interannual data is needed, results from this study give preliminary indications

that temporal variations in phytoplankton biomass and community structure result from changes in water column stability and in the nutrient regime, and occur on the equivalent time scales as the transitional events (i.e. mixing, advection, stratification) seen in the physical dynamics.

ACKNOWLEDGEMENTS

K. Seydell, K. Scheppe, P. Handley and T. Newberger are thanked for their assistance in sample collection and analyses. I also acknowledge R. Bidigare and M. Ondrusek for providing the HPLC training and pigment standards. Research was supported by the United States National Science Foundation, Office of Polar Programs (grant DPP 90-901127 to B. B. Prézelin). This chapter is Palmer LTER publication number 47.

LITERATURE CITED

Bidigare RR, Schofield O, Prézelin BB (1989) Influence of zeaxanthin on quantum yield of photosynthesis of *Synechococcus* clone WH7803 (DC2). Mar Ecol Prog Ser 56: 177-188

Caceci MS, Cacheris WP (1984) Fitting curves to data. Byte 9: 340-36

Holm-Hansen O, Mitchell BG, Hewes CD, Karl DM (1989) Phytoplankton Blooms in the Vicinity of Palmer Station, Antarctica. Polar Biology 10: 49-57

Holm-Hansen O, Mitchell BG (1991) Spatial and temporal distribution of phytoplankton and primary production in the western Bransfield Strait region. Deep-Sea Res 38(8-9A): 961-980

Johnson KS, Petty RL, Thomsen J (1985) Flow injection analysis for seawater micronutrients. In: A. Zirino (ed) Mapping Strategies in Chemical Oceanography. Advances in Chemistry Series 209: 7-30

Kamykowski D, Zentara S-J (1989) Circumpolar plant nutrient covariation in the Southern Ocean: patterns and processes. Mar Ecol Prog Ser 58: 101-111

Kiefer DA, Kremer JN (1981) Origins of vertical patterns of phytoplankton and nutrients in the temperate, open

ocean: a stratigraphic hypothesis. Deep-Sea Res 28: 1087-1105

Kopczynska EE 1992. Dominance of microflagellates over diatoms in the Antactic areas of deep vertical mixing and krill concentrations. J Plank Res 14: 1031-1054

Krebs WN (1983) Ecology of neritic marine diatoms, Arthur Harbor, Antarctica. Micropaleontology 29(3): 267-297

Mitchell BG, Holm-Hansen O (1991) Observations and modeling of the Antarctic phytoplankton crop in relation to mixing depth. Deep-Sea Res 38(8-9A): 981-1007

Prézelin BB, Boucher NP, Smith RC (1994) Marine primary production under the influence of the Antarctic ozone hole: Icecolors '90. In: Weiler S, Penhale P (eds) Ultraviolet radiation and biological research in Antarctica. Am Geo U 62: 159-186

Priddle J, Heywood RB, Theriot E (1986) Some environmental factors influencing phytoplankton in the Southern Ocean around South Georgia. Polar Biology 5: 65-79

Rivkin RB (1991) Seasonal patterns of planktonic production in McMurdo Sound, Antarctica. Amer Zool 31: 5-16

Sakshaug E, Slagstad D, Holm-Hansen O (1991) Factors controlling the development of phytoplankton blooms in the Antarctic Ocean-A mathematical model. Mar Chem 35: 259-271

Smetacek V, Scharek R, Gordon LI, Eicken H, Fahrbach E, Rohardt G, Moore S (1992) Early spring phytoplankton blooms in ice platelet layers of the southern Weddell Sea, Antarctica. Deep-Sea Res 39: 153-168

Smith RC, Baker KS, Handley P, Newberger T (1992a) Palmer LTER program: Hydrography and optics within the peninsula grid, zodiac sampling grid during the 1991-1992 field season. Ant J U S 27: 253-255

Smith WOJ, Sakshaug E (1990) Polar Phytoplankton. In: W. O. Smith (ed) Polar Oceanography: Part A: Physical Science, Part B: Chemistry, Biology, Geology. Academic Press, Inc. San Diego. pp. 477-526

Sommer U (1988) The species composition of Antarctic phytoplankton interpreted in terms of Tilman's competition theory. Oecologia 77: 464-467

Sommer U (1991) Comparative nutrient status and competitive interactions of two antarctic diatoms (*Corethron criophilum* and *Thalassiosira antarctica*). J Plank Res 13: 61-75

Veldhuis MJW, Colijn F, Admirall W (1991) Phosphate utilization in *Phaeocystis pouchetii* (Haptophyceae). Mar Ecol 12: 53-62

Verity PG, Villareal TA, Smayda TJ (1988) Ecological investigations of blooms of colonial *Phaeocystis pouchetii*.

I. Abundance, biochemical composition, and metabloic rates. J Plank Res 10: 219-248

Waters KJ, Smith RC (1992) Palmer LTER: A sampling grid for the Palmer LTER program. Ant J U S 27: 236-238

Whitaker TM (1982) Primary production of phytoplankton off Signy Island, South Orkneys, the Antarctic. Proc R Soc Lond 214: 169-189

Figure 1. Location of LTER sampling station B (64° 46.45' S, 64° 03.27' W) with respect to Palmer Station and (inset) the Antarctic Peninsula.

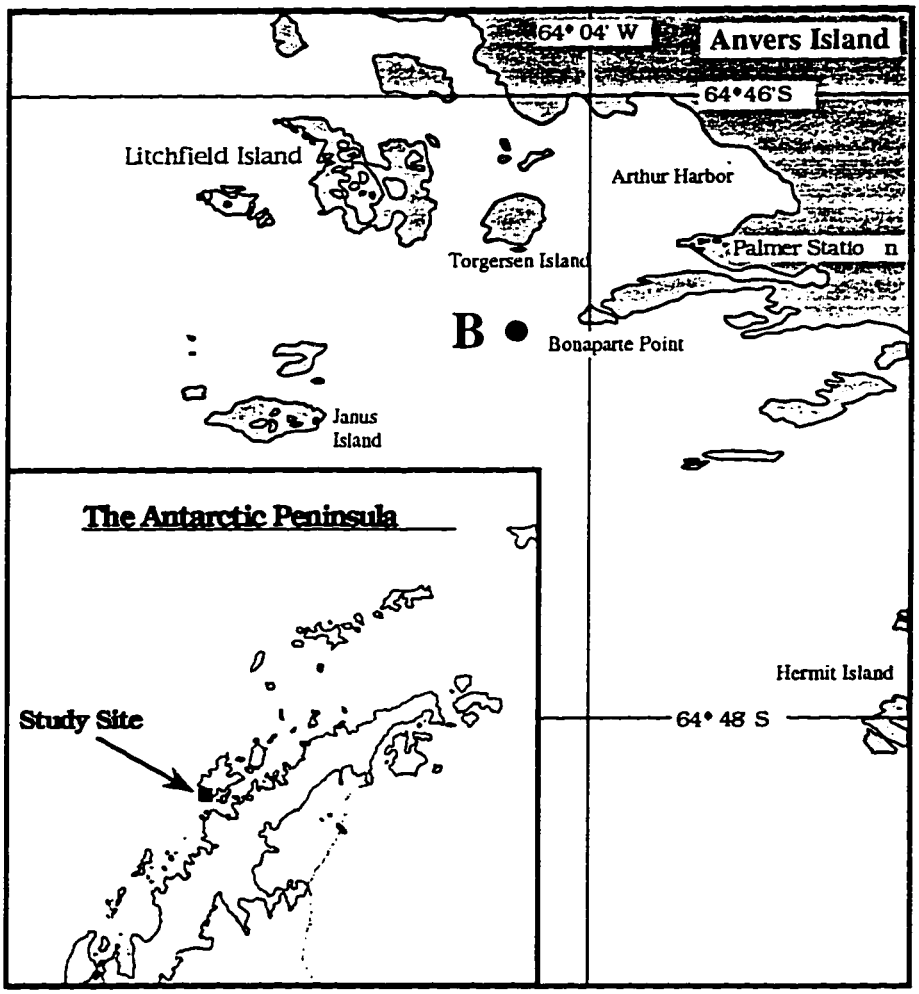
64° 04' W
Anvers Island
64°46'S
Litchfield Island
Arthur Harbor
Palmer Statio n
Torgersen Island
B
Bonaparte Point
Janus
Island
The Antarctic Peninsula
Hermit Island
Study Site
64° 48' S

Figure 2. (upper) Seasonal changes in daily average wind speed (m s^{-1}) and directions at Palmer Station between November 21, 1991 and February 27, 1992. Inserted compass provides direction toward which the wind is blowing. (middle) Seasonal patterns in daily precipitation (mm) (solid line) and relative snow cover (dashed line) at Palmer Station. (lower) Seasonal contour plot of sigma-t (s_t) at Station B. Seasonal changes in the depth of the upper mixed layer (black squares) and the freshwater lens (open diamonds) overlay the s_t contour. Daily presence or absence of pack ice is indicated by hatch bars.

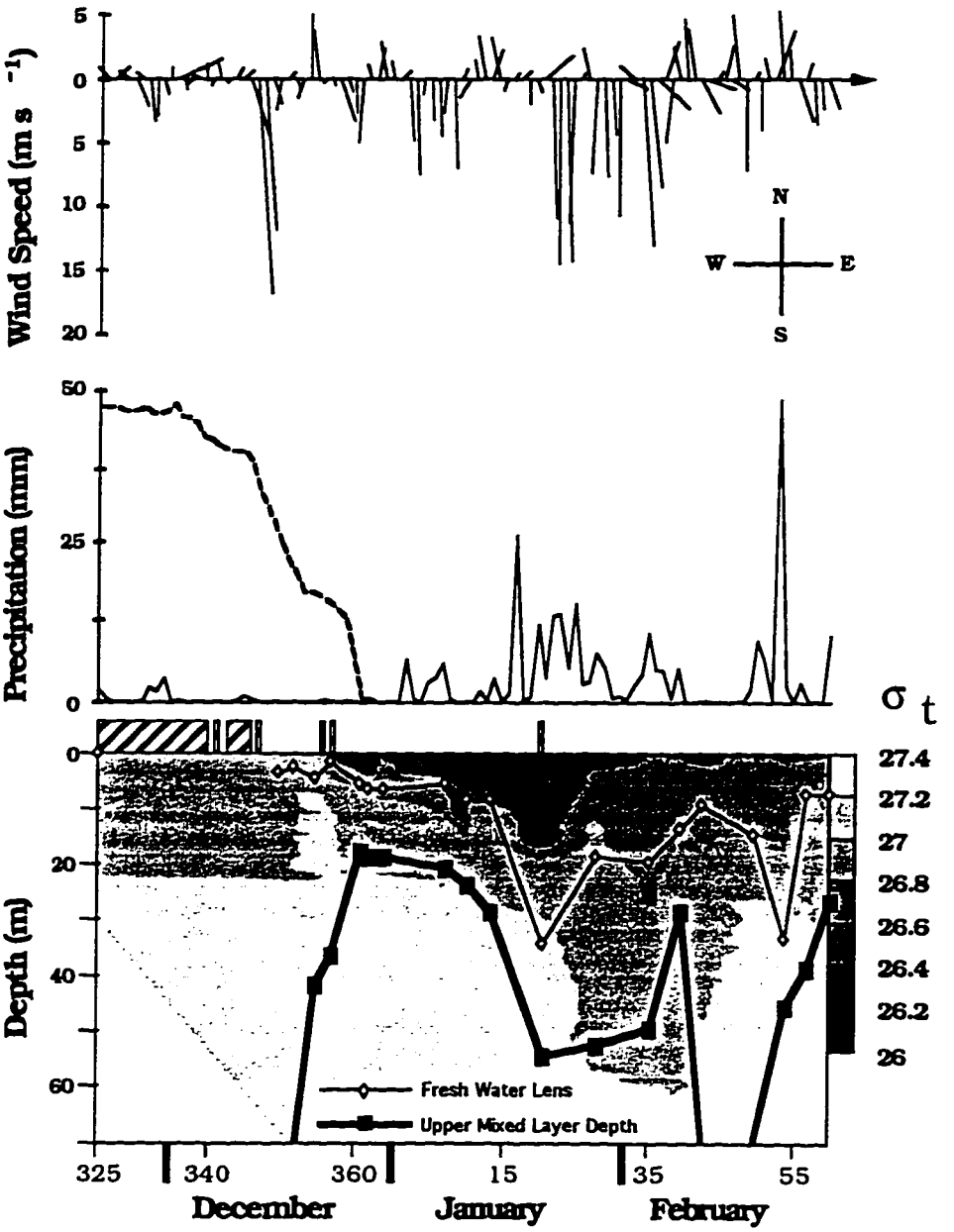
Wind Speed (m s -1)
5
0
5
10
15
20
N
W
E
S
Precipitation (mm)
50
25
0
σ t
Depth (m)
0
20
40
60
27.4
27.2
27
26.8
26.6
26.4
26.2
26
Fresh Water Lens
Upper Mixed Layer Depth
325
340
360
15
35
55
December
January
February

Figure 3. Comparison of the seasonal changes in the depth distribution of key phytoplankton pigments at Station B between November 21, 1991 and February 27, 1992. Pigments shown are indicators for diatoms (fucoxanthin), prymnesiophytes (19'-hexanoyloxyfucoxanthin), chrysophytes (19' butanoyloxyfucoxanthin), and cryptophytes (alloxanthin). Distribution of discrete samples is shown with closed circles. Seasonal changes in the depth of the upper mixed layer (black squares) and the freshwater lens (open diamonds) are shown in the second contour. Daily presence or absence of pack ice is indicated by hatch bars.

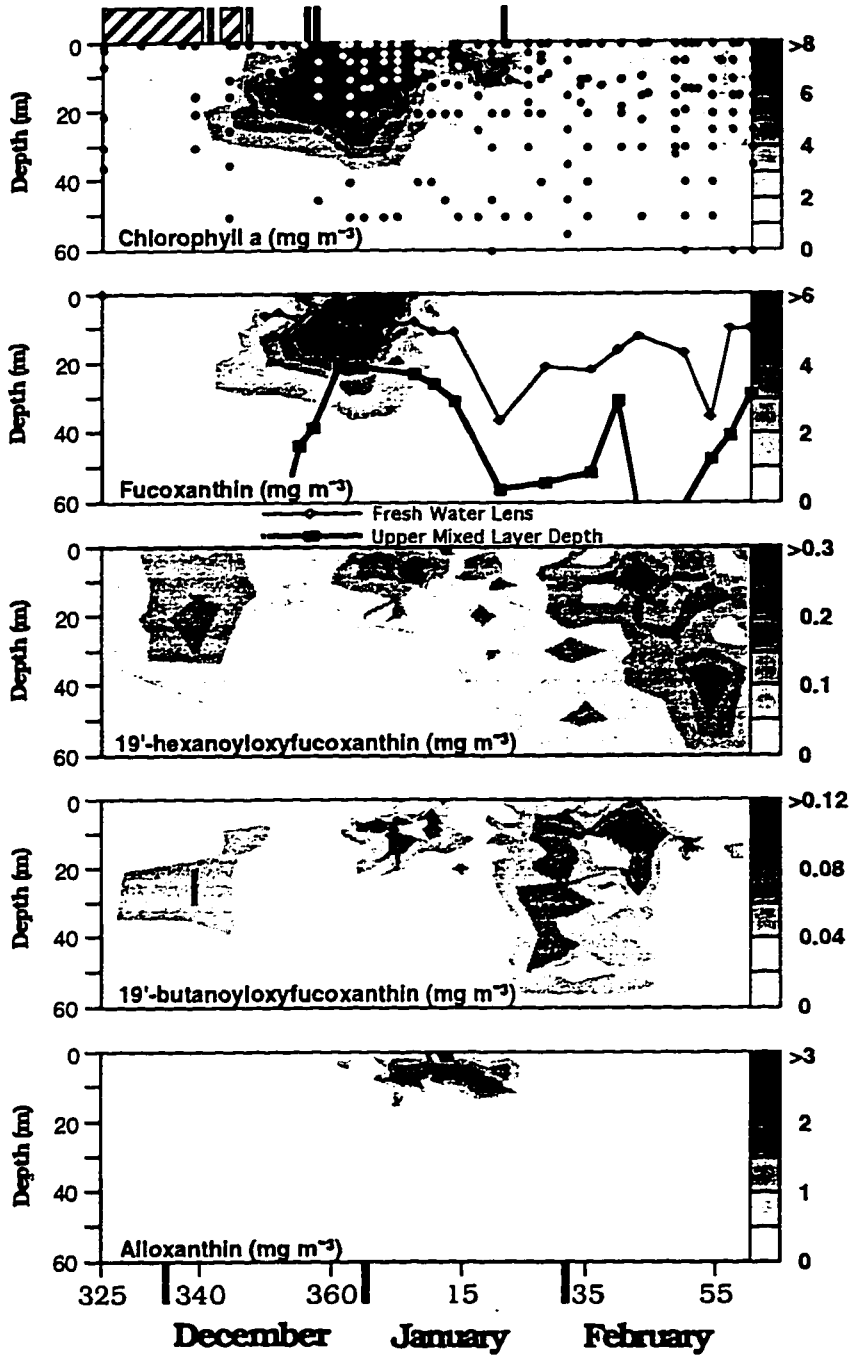
Depth (m)
0
20
40
60
>8
6
4
2
0
Chlorophyll a (mg m⁻³)
>6
4
2
0
Fucoxanthin (mg m⁻³)
Fresh Water Lens
Upper Mixed Layer Depth
>0.3
0.2
0.1
0
19'-hexanoyloxyfucoxanthin (mg m⁻³)
>0.12
0.08
0.04
0
19'-butanoyloxyfucoxanthin (mg m⁻³)
>3
2
1
0
Alloxanthin (mg m⁻³)
325
340
360
15
35
55
December
January
February

Figure 4. Variations in integrated Chl a above the upper mixed layer depth (UML) displayed as a function of time over the austral summer (upper) and UML (lower) for Station B sampled between November 21, 1991 and February 27, 1992. In the lower panel, discrete data points within the PAL-LTER dataset (closed squares) have been differentially labelled to indicate integrated Chl a values present prior to the major shallowing of the UML (closed circles) noted in December, 1991 (Fig. 2) and one value during a major advection event in late January, 1992 (open circle). For comparison, monthly mean values (open triangles), derived from Chl a and s_t profiles collected along the Antarctic Penisula between December 1986 and March 1987, are presented (Mitchell and Holm-Hansen, 1991).

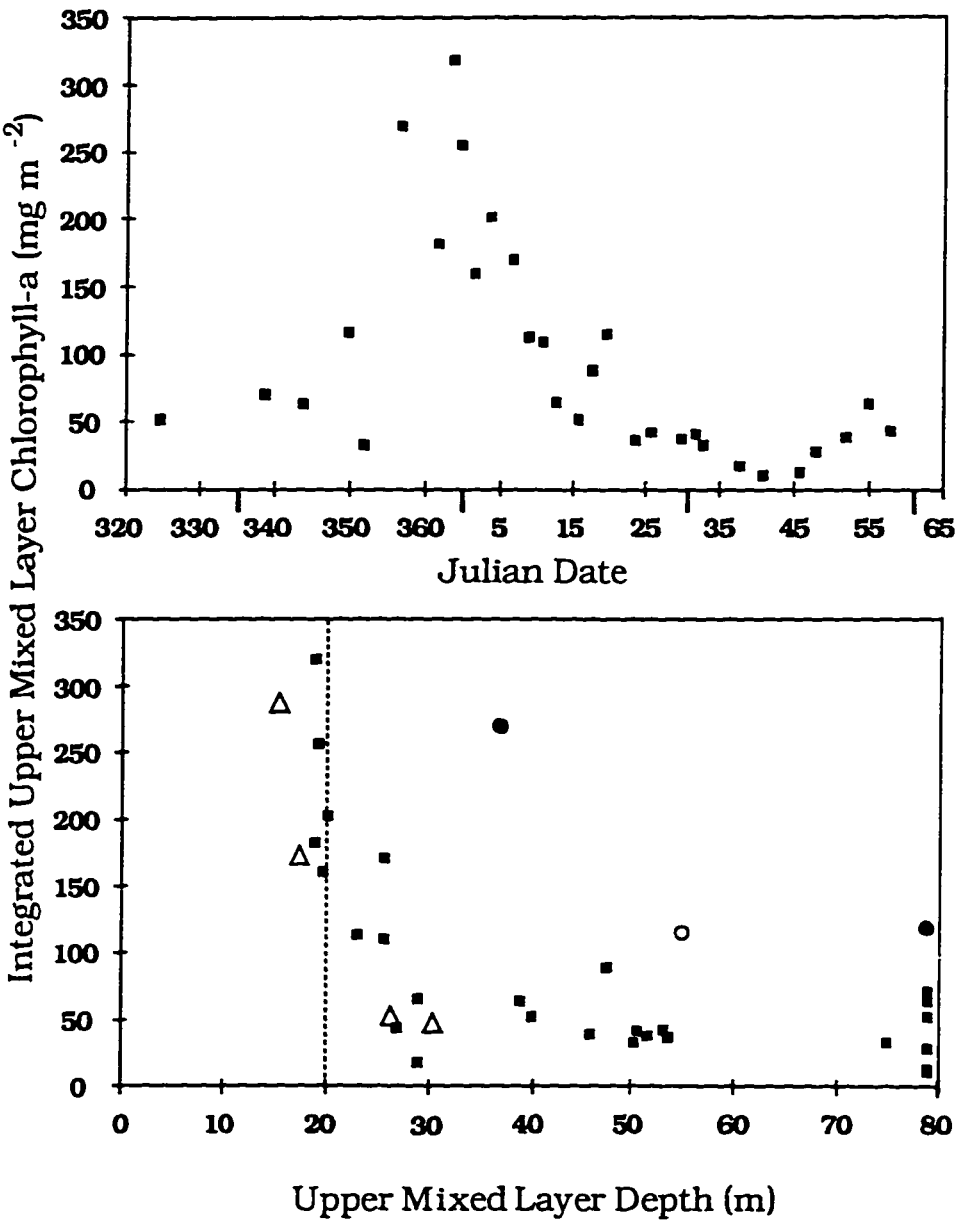
Integrated Upper Mixed Layer Chlorophyll-a (mg m -2)
350
300
250
200
150
100
50
0
320 330 340 350 360 5 15 25 35 45 55 65
Julian Date
350
300
250
200
150
100
50
0
0 10 20 30 40 50 60 70 80
Upper Mixed Layer Depth (m)

Figure 5. Comparison of the seasonal changes in the depth distribution of the major macronutrients NO_3^-, $Si(OH)_4$, PO_4^{3-}, and the derived molar ratios for $Si(OH)_4$:NO_3^- and NO_3^-:PO_4^{3-} determined for discrete samples (closed circles) collected at Station B between November 21, 1991 and February 27, 1992. All concentrations are given in mmol m^{-3}. Seasonal changes in the depth of the upper mixed layer (black squares) and the freshwater lens (open diamonds) are shown in the second contour plot. Daily presence or absence of pack ice is indicated by hatch bars.

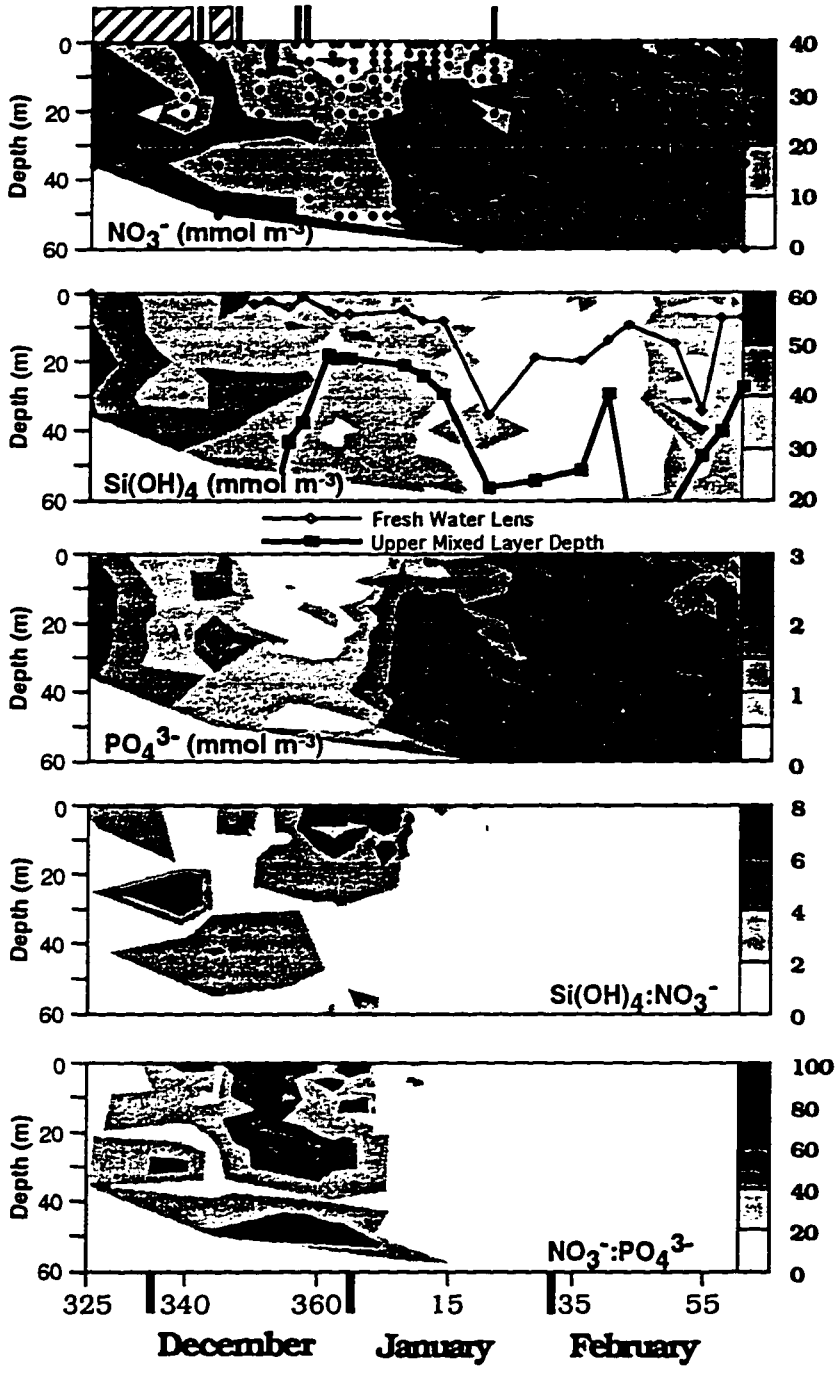
Depth (m)
0
20
40
60
NO_3^- (mmol m^{-3})
40
30
20
10
0
$Si(OH)_4$ (mmol m^{-3})
60
50
40
30
20
Fresh Water Lens
Upper Mixed Layer Depth
PO_4^{3-} (mmol m^{-3})
3
2
1
0
$Si(OH)_4:NO_3^-$
8
6
4
2
0
$NO_3^-:PO_4^{3-}$
100
80
60
40
20
0
325
340
360
15
35
55
December
January
February

Figure 6. Comparison of regression plots for changes in the abundance of inorganic NO_3^- and PO_4^{3-} for all depths sampled at Station B between November 21, 1991 and February 27, 1992. One regression line represents the PO_4^{3-} to NO_3^- relationship (open squares) for both the pre- and post- bloom period. The other regression represents the PO_4^{3-} to NO_3^- relationship (closed squares) during the diatom-dominated bloom occurring between December 10, 1991 to January 9, 1992 (Fig. 3). Shaded areas bordering each regression line represent +/- one standard deviation.

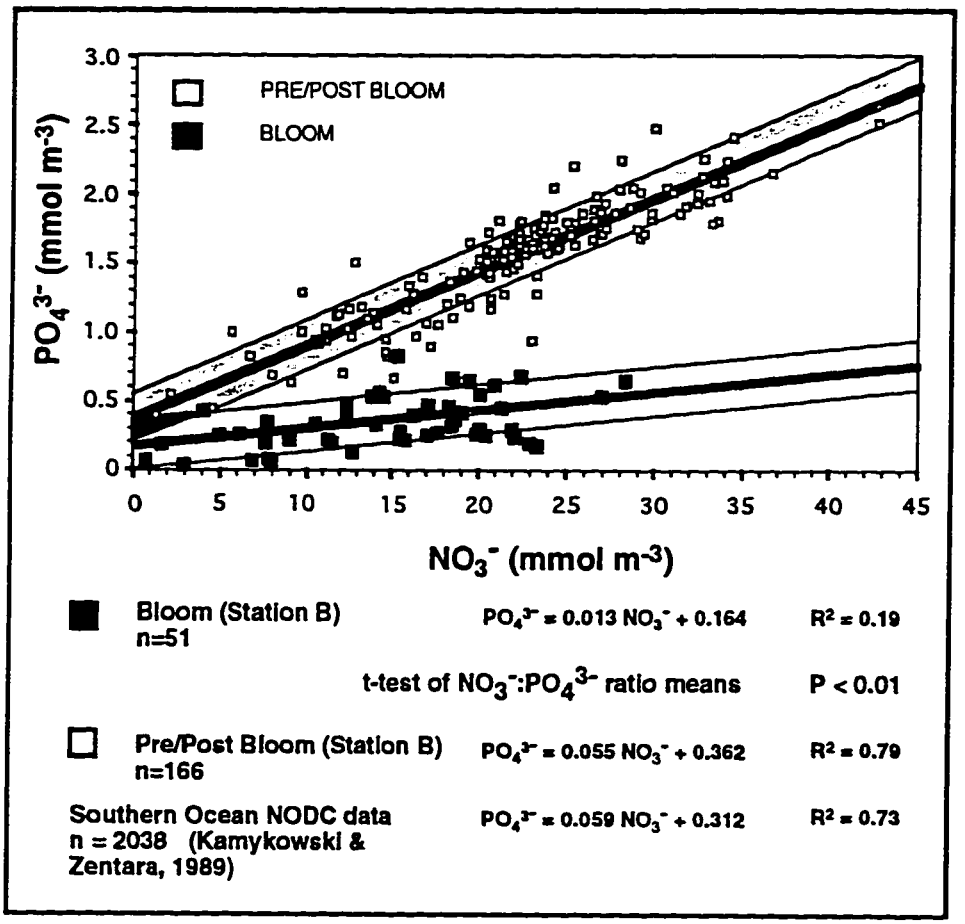
PRE/POST BLOOM
BLOOM
PO_4^{3-} (mmol m^{-3})
NO_3^- (mmol m^{-3})
3.0
2.5
2.0
1.5
1.0
0.5
0
0 5 10 15 20 25 30 35 40 45
Bloom (Station B) n=51
$PO_4^{3-} = 0.013\ NO_3^- + 0.164$
$R^2 = 0.19$
t-test of NO_3^-:PO_4^{3-} ratio means
$P < 0.01$
Pre/Post Bloom (Station B) n=166
$PO_4^{3-} = 0.055\ NO_3^- + 0.362$
$R^2 = 0.79$
Southern Ocean NODC data n = 2038 (Kamykowski & Zentara, 1989)
$PO_4^{3-} = 0.059\ NO_3^- + 0.312$
$R^2 = 0.73$

Figure 7. Depth distribution of the photophysiological parameter Q_{par}/I_k determined for discrete samples collected from Station B between November 27, 1991 and February 27, 1992. Productivity measurements made prior (closed squares), during (closed circles) and after (open diamonds) the major diatom bloom are indicated. Shaded area indicates data where light limitation was evident.

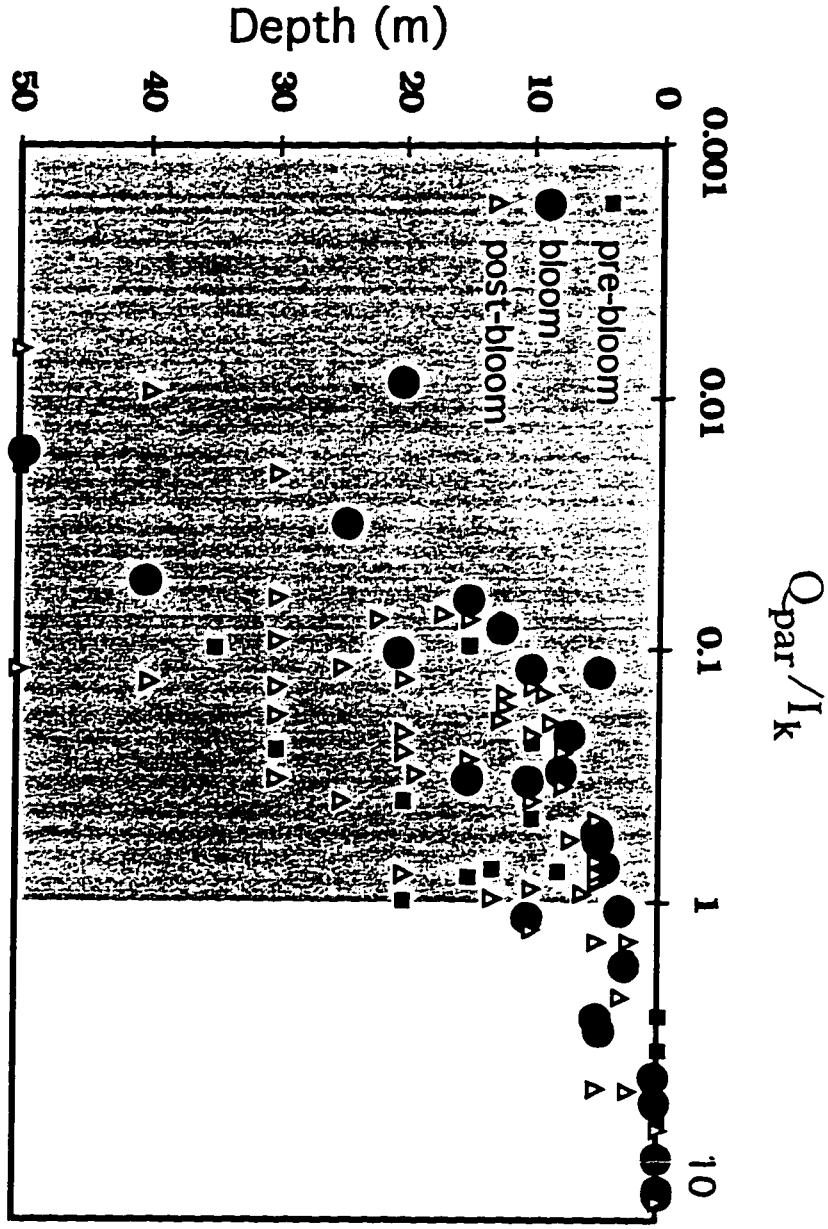
Depth (m)
0
10
20
30
40
50
0.001
0.01
0.1
1
10
Q_{par}/I_k
pre-bloom
bloom
post-bloom

CHAPTER II

Photoadaptive response during the development of a coastal Antarctic diatom bloom and relationship to water column stability

ABSTRACT

The ratio of the xanthophylls, diadinoxanthin and diatoxanthin, to chlorophyll a [(DD + DT):Chl a] was used as a photoadaptive index during the development of a large Antarctic diatom bloom. This index was found to significantly track fluctuations in the incident solar irradiance and the in situ light field over a 3 orders of magnitude change in the water column biomass. Depth profiles of the [(DD + DT):Chl a] ratio show that the upper 'mixed' layer, assessed by physical data, was in fact stable over the course of the month. Diel experiments conducted over the same period showed a delayed (5-8 hrs) saturating response of the (DD + DT) pool to the Q_{par} (400-700 nm) dose. These time-series results illustrate the potential use of xanthophyll pigments in assessing phytoplankton 'light histories' and the degree of water column stability.

INTRODUCTION

The Southern Ocean supports a rich biotic ecosystem and has been recognized as playing an important role in many global processes, such as biogeochemical cycling (Nelson and Smith 1991) and the sequestration of atmospheric CO_2 (Siegenthaler and Sarmiento 1993). These processes are ultimately dependent on autotrophic production by phytoplankton. Although a continued subject of debate (Chisholm and Morel 1991), the primary mechanism controlling phytoplankton production over much of the Southern Ocean is thought to be light-limitation as a result of the deep vertical mixing, characteristic for the region (Mitchell et al. 1991; Nelson and Smith 1991; Sakshaug et al. 1991). This is especially true in neritic and shelf water where potentially limiting micronutrients are replete (de Barr et al. 1995). Accessing the ability of phytoplankton to adapt to changing light fields in these turbulent environments is, therefore, fundamental to improving our mechanistic understanding of the magnitude and distribution patterns of biomass and primary production in the Southern Ocean.

To date, most studies in the Southern Ocean have been conducted shipboard and have focused on describing the spatial variability of phytoplankton abundance, distribution, physiology, and productivity (El-Sayed and Weber 1982; El-

Sayed et al. 1983; Smith and Nelson 1985; Bodungen et al. 1986; Wilson et al. 1986). While spatial studies have shown photoadaptive indices in relation to instantaneous conditions, interpretation of results are either in the context of steady state conditions or an assumed prior condition (Mitchell and Holm-Hansen 1991; Boyd et al. 1995). The ability of phytoplankton to adapt to transient conditions is a dynamic process and warrants investigation over the temporal scales of adaptation. Temporal variability in phytoplankton dynamics have been scarcely documented for the Southern Ocean (Whitaker 1982; Mitchell and Holm-Hansen 1991; Rivkin 1991) and time-series field investigations of photoadaptive processes are rare. Knowledge of the time scales and rates of these processes are critical when attempting to assess the mechanisms controlling primary productivity. Additionally, identification of photoadaptive indices will provide insight on the light histories of phytoplankton and may yield information of the mixing processes operating on similar time scales (Lewis et al. 1984; Cullen and Lewis 1988).

Phytoplankton respond to changes in the light intensity and quality by differentially altering the relative amounts of various pigment concentrations and ratios. Pigments serve two major functions in the cell. Chlorophylls and the majority of the carotenoids function in absorbing light for photosynthesis,

while some carotenoids have been found to function largely as photoprotective pigments (Hagar and Stransky 1970; Stransky and Hagar 1970; Bidigare et al. 1987; Demers et al. 1991; Kerherve 1991; Frank et al. 1994). In diatoms, the carotenoids diadinoxanthin (DD) and diatoxanthin (DT) function as a photoprotective system, undergoing a light regulated de-epoxidation/epoxidation, known as the rapid xanthophyll cycle. These pigments dissipate excess energy by non-photochemical fluorescence quenching, as recently described for marine diatoms (Arsalane et al. 1994; Olaizola et al. 1994) and higher plants (Brugnoli et al. 1994). On time scale of seconds to hours, the (DD + DT) pool has been found to remain constant (Welschmeyer and Hoepffner 1986; Demers et al. 1991; Caron et al. 1992), however, over time scales of hours to days, the pool increases in response to high irradiances (Hagar and Stransky 1970; Stransky and Hagar 1970; Bidigare et al. 1987). Given the changes in in situ light fields in turbulent environments, it has been hypothesized that these pigments could be used as indices of phytoplankton 'light histories' and for potentially determining vertical mixing rates on identical time scales (Lewis et al. 1984; Welschmeyer and Hoepffner 1986; Bidigare et al. 1987). Conceptually, the ratio DT:DD would reflect rapid time scale responses (seconds to hours),

while a measure of the total xanthophyll pool (DD+DT) could assess a photoresponse over time scales of hours to days.

Although DT:DD was found to respond to changes in *in situ* light fields in the Subarctic, it was unreliable for infering mixing rates (Olaizola et al. 1992). This could have resulted from the long handling time of the samples relative to the rate of change between DD and DT and the procedural difficulties in quantifying DT. Recognizing this, Claustre et al. (1994) assessed *in situ* phytoplantkon photoadapation and kinetic rates of photoadaptation in a frontal region in the Mediterranean Sea using DD:Chl *a*. Here, in order to avoid possible influence of short-term fluctuations in the ratio, the biomass-specific xanthophyll pool, (DD + DT):Chl *a*, is quantified as a photophysiological index to assess the photoadaptive response of Antarctic diatoms to changing light environments on time scales of hours to weeks. Accessing these phytoplankton responses may further our understanding of the mechanisms controlling biomass and primary production in the Southern Ocean.

METHODS

From December 5, 1991 until February 27, 1992, a total of 249 discrete water samples were collected at station B (Waters and Smith 1992), as part of the Palmer Long-Term Ecological Research (LTER) program (Ross and Quetin 1992). Sampling was conducted from a Mark V Zodiac® with an effort to sample near solar noon. Prior to collection, vertical profiles of photosynthetically available radiation (400-700 nm, Q_{par}) were measured with a Biospherical® scalar irradiance meter (QSR-170DT) equipped with a QSR-240 reference sensor and a QSP-100DT underwater sensor according to procedures detailed by Moline and Prézelin (1996). Temperature and conductivity data were also collected in conjunction with light measurements from a second Zodiac® detailed in Smith et al. (1992), from which density profiles (σt) were derived (see Moline et al. 1996). The upper mixed layer depths over the season were calculated from the σt profiles according to Mitchell and Holm-Hansen (1991). Whole water samples were collected in cleaned 5 L GoFlo® bottles, transferred to dark acid-washed polypropylene bottles and returned to Palmer Station within 30 min, where samples remained in a cold room (-2 °C) until analyses.

Aliquots of all whole water samples were analyzed at Palmer Station for algal pigments using reverse-phase HPLC procedures described by Bidigare et al. (1989). One liter

samples were filtered under near *in situ* light conditions on 0.4 μm nylon 47 mm Nuclepore® filters and extracted in 3 ml 90% acetone for 24 hr in the dark at -20 °C. Pigment separation was achieved with the aid of a Hitachi L-6200A liquid chromatograph equipped with a Waters Radial-PAK® C^{18} column (8 x 100 mm column; 5 μm particles) and an Hitachi L-4250 UV/VIS Variable Wavelength Detector (436 nm). Peak identities of algal extracts were determined by comparing their retention times with pure pigment provided by R. Bidigare. Quantification of specific pigments from the algal extracts were made by comparing peak areas with those from known amounts of pigment standards.

On 12 occasions over the three month time period, 10 L samples were collected from both the surface and the chlorophyll *a* maximum (Chl *a* max) to examine the diel variations in pigmentation. Each sample was placed in a large Pyrex® carboy and screened with neutral density screening to the *in situ* Q_{par} light level at the depth of collection (surface was screened to 50%). Carboys were incubated outdoors in a seawater tank at ambient temperatures for 24 to 30 hr. Subsamples were retrieved from the carboy at 3-hr intervals for determination of pigmentation using procedures outlined above.

In addition to the Q_{par} sensors on the sampling Zodiac®, a second QSR-240 sensor was positioned at Palmer Station where incident Q_{par} was recorded continuously every 5 min over the 3 month period. A comparison between the two QSR-240 sensors showed that Q_{par} readings differed < 5%. Daily average wind speed/direction measurements were made at Palmer Station during the study period as part of a long term database collected by the U. S. National Science Foundation.

RESULTS AND DISCUSSION

Relatively low wind speeds after the break up of the coastal fast ice resulted in a stable water column during the beginning of December, 1991. This stability was enhanced with freshwater input into the local area from glacial melting and the depth of the upper mixed layer (UML) shallowed to ~ 20 m (Fig. 1A; Moline et al. 1996). With the combination of stability, increased light penetration and the release of concentrated phytoplankton from the ice into the water column, a large bloom developed at station B (Fig. 1A). This near unialgal bloom of Coscinodiscus spp., as confirmed by microscopic examination, persisted for 4 weeks and accounted for more than 95% of the carotenoid pigmentation (as fucoxanthin) at

station B (Moline and Prézelin 1996). Chl a concentrations ranged from 0.3 to ca. 30 mg Chl a m^{-3}. Integrated water column Chl a biomass peaked at 612 mg Chl a m^{-2} the last day of 1991 (Moline et al. 1996).

In January 1992, there was a rapid community transition in the bloom from diatoms to a cryptophyte dominated community (Moline and Prézelin 1996). Unlike diatoms, cryptophytes do not to have a xanthophyll cycle, and pigments which function as photoprotectants in the visible spectrum in this group are not specifically known. Experiments have shown that the primary cryptophyte-specific carotenoid, alloxanthin, functions largely as a photosynthetic pigment, with low transfer efficiency, but also as a photoprotective pigment (G. Johnsen and M. Vernet, pers. comms.). The vertical distribution of alloxanthin:Chl a at station B during January, 1992 showed a subsurface maximum occurring at the 5-10% Q_{par} (0^+) light levels, suggesting a photosynthetic function (data not shown).

Because of the shift in community composition from diatoms to a taxonomic group where the photoprotective pigmentation is uncertain, this study focused on the period from JD 339 (1991) to JD 7 (1992), when diatoms were dominant and the major photoprotective pigments were the xanthophyll pigments, diadinoxanthin (DD) and diatoxanthin (DT). While diatoms are a primary bloom forming

phytoplankton group in the Antarctic, it should be noted that other groups containing xanthophyll pigments, such as prymnesiophytes, also contribute significantly to phytoplankton biomass in the Southern Ocean (El-Sayed and Fryxell, 1993).

Figure 1B shows the photophysiological index, (DD + DT):Chl a, with depth over the study period. First, what is clearly evident is that the ratio decreased with depth for each sampling date, suggesting that the response rate of the photoprotective pigments was always greater than the rates of vertical mixing. Given this, the time evolution of the (DD + DT):Chl a ratio also illustrated the response to changes in the incident light fields and the apparent optical properties of the water column. The 100-fold variation in phytoplankton biomass over the course of the bloom had a measurable effect on the attenuation of Q_{par} in the water column. The 1% Q_{par} light level shallowed from 60 m in early December to ca. 10 m at the peak of the bloom (Fig. 1B). The contours of the (DD + DT):Chl a ratio paralleled the increasing attenuation over the season with 1% Q_{par} depth significantly correlating to an absolute (DD + DT):Chl a ratio between 0.05 and 0.06 ($R^2 = 0.98$), indicating the diatom bloom was potentially light limited from self-shading. Photosynthesis-irradiance data revealed that, in

fact, the depth of light limitation during the peak of the diatom bloom shallowed to ~5 m (data not shown, Moline et al. 1996).

In addition to tracking the increases in attenuation resulting from the bloom, the (DD + DT):Chl a ratio was also significantly correlated ($p < 0.001$) to the light intensity at each depth (Fig. 2) and reflected the general decrease in the incident surface Q_{par} measured over the 33 day period (Moline and Prézelin 1996). This agrees with *in situ* (Claustre et al., 1994) and laboratory studies (Demers et al. 1991; Claustre et al. 1994) showing the xanthophyll pool to be light dependent on daily time scales. Interestingly the most significant correlation was using the Q_{par} integrated 6-8 hrs prior to collection and close to dawn (Fig. 2, inset). Regressions using integrated Q_{par} 6-18 hrs prior to collection did not change much because of the low irradiances during the night. When integrated light from the previous day (18-24 hrs prior to collection) was included, the regressions rapidly decreased (Fig. 2, inset), indicating the photoprotective response was not responding the the light of the previous photoperiod. These results show a 6-8 hour delay in the response of the (DD + DT):Chl a ratio to the *in situ* light field.

The ratio of (DD + DT):Chl a for each depth normalized to the surface values showed a significant linear relationship for light levels between 0.1% and 100% of the Q_{par} (0^-) value (Fig.

3). However, for light levels below 0.1 %, the normalized (DD + DT):Chl a ratio reached minimum values ranging from 15 to 25% of the surface values corresponding to minimum absolute ratios between 0.02 and 0.05. This concurs with profiles take from the Mediterranean Sea showing DD:Chl a decrease exponentially with depth towards a minimum value (Claustre et al. 1994).

The relationship of the photoadaptive index to the in situ light field was further examined by comparing the attenuation coefficients of Q_{par} (Kd) to the 'attenuation coefficient' of the (DD + DT):Chl a ratio (Kr) above the depth of the minimum threshold ratio previously described. With nine profiles, the correlation between the two coefficients was found to be significant ($p < 0.001$), however, the regression line was offset from a 1:1 relationship (Fig. 4). If the relative concentrations of photoprotective pigment pool responded directly to the in situ light field, a 1:1 correspondence between the attenuation coefficients would be expected unless 1) the water column was vertically mixing faster than the photoprotective pigment response rate and/or 2) the surface value approached the minimum threshold values (Fig. 4). The fact that the slope of the regression is near to 1 indicates that the water column was relatively stable for the period of this study. For two sampling

days (JD 350 & 364), however, the coefficients deviated from the 1:1 relationship by more than 50%.

Density profiles collected from JD 344-354 showed no vertical structure (Fig. 1A) and by traditional interpretation, the water column would be considered well mixed. The lack of vertical homogeneity in the photoprotective index over this period suggests little active mixing on the time scale of the photoprotective pigment response. On JD 350, however, there was a discrepancy between Kr and Kd, implying mixing. Because of the interpretive limitations of the in-water physical data, the local wind field was used as a relative index for mixing. Wind forcing in this coastal environment has been shown to be a primary mechanism controlling biomass accumulation (Moline and Prézelin, submitted), a result found in other locations of the Southern Ocean (Lancelot et al. 1993; K. Arrigo, pers. comm.). The average daily wind speeds during this study were significantly below the summer average and only during one period from JD 346 through JD 348 were high wind speeds consistently above the average (Fig. 5). The 53% discrepancy between Kr and Kd measured on JD 350 could be a residual effect of this wind/mixing event not revealed in the density profiles (Fig. 4).

JD 364 also showed a difference between the attenuation of light and the (DD + DT):Chl a ratio, however, wind stress was

low, with the surface (DD + DT):Chl a close to the threshold value. As previously mentioned, an effort was made to sample within an hour of solar noon. This was the case for all profiles with the exception of JD 364, which was sampled ~ 4 hrs prior to solar noon. With evidence for light/dark effects on the concentration of diadinoxathin (Claustre et al. 1994), the diel changes in the chlorophyll a-specific photoprotective pool (DD + DT) were examined as a possible explanation for the deviation of Kr from Kd measured on JD 364.

Results from four weekly diel measurements from JD 339 to JD 7 showed a clear response from both the surface and Chl a max populations to the daily light cycle, illustrating the time of sampling was significant (Fig. 6). It should be mentioned that Chl a concentrations did not change during the diel experiments, therefore, fluctuations in (DD + DT):Chl a were a result of changes in the (DD + DT) pool. It is interesting to note that the magnitude of the daily variation in the surface and Chl a max were not significantly different, illustrating that the cells were responding equally to relative changes in light intensity and not to the spectral light quality.

There was , however, a delay between the peak irradiance and the maximum value of (DD + DT):Chl a at each depth for all diel experiments (Fig. 6). The average delay was ~ 6 hrs with a range from 5.25 to 8.25 hrs. This corresponds well

with the lagged response in the ratio found for the integrated in situ irradiance measurements (Fig. 2) and confirms the response time of the photoprotective pigment pool. This response is significantly slower than that found in kinetic experiments conducted in the Mediterranean Sea, which responded to changes in light intensity within 0.5 hrs (Claustre et al. 1994). In addition to differences in community composition between the two locations, the longer response times for Antarctic phytoplankton in this study may be a function of lower temperatures, slowing enzyme rate kinetics and the de novo synthesis of the xanthophyll pool. Temperature has been found to effect photosynthesis (Tilzer et al. 1986), respiration (Tilzer and Dubinsky 1987), growth rates (Sakshaug and Holm-Hansen 1986), and enzyme activity (Li et al. 1984) in high latitude environments and, therefore, may similarly effect the turnover rates of the xanthophyll pool in natural populations.

The delayed response of the (DD + DT) pool to the in situ light field may have significant implications for primary productivity in this coastal environment. The peak accumulation of the photoprotective pigments occurs significantly later than the peak solar insolation and, therefore, may potentially increase the susceptibility of the cell to photoinhibition during the midday hours. However, over the

experimental days photoinhibition was not detected at high irradiances, saturation irradiances for photosynthesis did not change significantly, and light-saturated photosynthetic potentials were high (3.5-3.6 mg C mg Chl a m^{-3} h^{-1}) with a maximum centered within an hour of solar noon (Moline and Prézelin 1996). Daily minimum values of (DD + DT):Chl a for the diel experiments were 0.15 ± 0.03 for surface samples and 0.07 ± 0.01 for Chl a max samples. These levels of photoprotective pigmentation may have been sufficient to dissipate excess energy in the hours up to and following solar noon, with the synthesis of additional pigmentation (~ 30%) responding to the increasing sensitivity to high light intensities and susceptibility to photoinhibition later in the day (Marra 1978). This mechanism is probable for the diatoms in this study, which were isolated in the stable surface waters at Sta B for more than a month by stratification and exposed to high irradiances. More than 70% of the water column production was light saturated (Claustre et al. 1996) and 85 % of production was light saturated in the upper 5 m (Moline, unpublished data), further evidence suggesting these surface populations were susceptible to high light stress.

When the delays in the photoprotective response for the individual diel experiments were removed, there was a correspondence between the change from the initial (DD +

DT):Chl a value and the Q_{par} dose over each interval (Fig. 7). The response, however, was not linear and showed the change in (DD + DT):Chl a saturating with Q_{par} dose. Above a Q_{par} threshold of 1.66 ± 0.36 Ein m^{-2} for each interval (~ 3 hrs), the change in the (DD + DT):Chl a was stable with a maximum of 0.041 ± 0.004. At Q_{par} doses below 1.66 Ein m^{-2}, there was a significant proportional linear response, with a ratio change of 0.01 for every 0.40 Ein m^{-2} increase in light dose (r^2 = 0.52, n=23).

With (DD + DT):Chl a responding in a predictable manner to the light fields in stable in situ and in vitro conditions, the ratio may be able to provide additional information on the vertical stability of the water column and rates of mixing, given the majority of the phytoplankton contain xanthophyll pigmentation. Traditional interpretation of density profiles provides the depth of 'mixing', however, provides no information on the time scales of the mixing processes. The use of the photoadaptive index, (DD + DT):Chl a, is illustrated in two profiles collected in November, 1991 off the Antarctic Peninsula (Fig. 8). Figure 8A is a protected nearshore coastal station in Dallmann Bay where the mixed layer was ~ 50 m, typical for this area (Mitchell and Holm-Hansen, 1991). Along with homogenous density within this layer, the (DD + DT):Chl a showed uniform distribution, with the ratio within the layer

was higher compared to samples taken at or below the pycnocline. The added physiological response information clearly shows this 'mixed' layer, as defined by physical data, was mixing or had been recently mixing. The high ratio within the layer also indicates exposure to high surface light intensities. For an offshore station ~ 100 km from Anvers Is., the density profile shows a uniform distribution to ~100m with some structure beginning at ~75m (Fig. 8B). Unlike the nearshore station, however, the (DD + DT):Chl a ratio decreases exponentially with depth from the surface 50 m. Results from this study show that the upper water column was in fact stable and had been for at least 2-3 days, given the high ratio and the rate of accumulation of the (DD + DT) pool in figure 6.

While enhanced stratification does increase the overall stability of the water column, as seen during this study as the diatom bloom progressed (Fig. 1), the absence of a pycnocline can not be used to infer mixing. The discrepancies between stratification and stability have been emphasized in previous studies (Ryther 1960; Townsend et al. 1992), however, this point is often overlooked. The degree of stability and the residence time of phytoplankton in the euphotic zone is critical for photoadaptation, growth and productivity (Smetacek and Passow 1990; Nelson and Smith 1991), therefore,

interpretations of these indices within the water column based solely on physical data may be limited.

CONCLUDING REMARKS

The stable conditions during this study allows validation of the photoadaptive index, (DD + DT):Chl a, for interpreting phytoplankton light histories. On scales of hours to weeks, there is a strong coherence of the photoprotective pigment response to the changing light field. While the pool size of DD + DT responded within hours to the instantaneous light field, there is a longer term response to the day to day changes in solar insulation (Fig. 2). With this knowledge, these field results demonstrate the usefulness in (DD + DT):Chl a for improving interpretation of water column stability in diatom dominated waters. With further studies on the rate kinetics of these photoprotective pigments, the use of (DD + DT):Chl a as an index of vertical stability in combination with physical data, much like the recent model by Doney et al. (1995) for photochemical species in the euphotic zone, will provide a better understanding of the effects of high vertical mixing on limiting primary production in the Southern Ocean.

ACKNOWLEDGMENTS

N. Boucher, P. Handley, T. Newberger, K. Seydel, K. Scheppe, and the ASA personnel at Palmer Station are acknowledged for their assistance in data collection during the field season. R. Bidigare and M. Ondrusek for provided HPLC training and pigment standards. Density profiles for figure 8 were generously provided by E. Hofmann. H. Claustre is especially acknowledged for his valuable insights, discussion and comments. Research was supported by the United States National Science Foundation grant DPP 90-901127 to B. B. Prézelin.

LITERATURE CITED

Arsalane W, Rousseau B, Duval J-C (1994) Influence of the pool size of the xanthophyll cycle on the effects of light stress in a diatom: Competition between photoprotection and photoinhibition. Photochem Photobio 60: 237-243

Bidigare RR, Smith RC, Baker KS, Marra J (1987) Oceanic primary production estimates from measurements of spectral irradiance and pigment concentration. Global Biogeochem Cycles 1: 171-186

Bidigare RR, Schofield O, Prézelin BB (1989) Influence of zeaxanthin on quantum yield of photosynthesis of *Synechococcus* clone WH7803 (DC2). Mar Ecol Prog Ser 56: 177-188

Bodungen B Von, Smetachek V, Tilzer MM, Zeitzschell B (1986) Primary production and sedimentation during spring in the Antarctic Peninsula region. Deep-Sea Res 33: 177-194

Boyd PW, Robinson C, Savidge G, Williams PJleB (1995) Water column and sea-ice primary production during Austral spring in the Bellingshausen Sea. Deep-Sea Res 42: 1177-1200

Brugnoli E, Cona A, Lauteri M (1994) Xanthophyll cycle components and capacity for non-radiative energy

dissipation in sun and shade leaves of *Ligustrum ovalifolium* exposed to conditions limiting photosynthesis. Photosynthesis Res 41: 451-463

Caron L, Duval JC, Arsalane W (1992) Comparative efficiency of the violaxanthin-zeaxanthin and diadino-diatoxanthin cycles in PSII photoprotective process. Abstract of Federation of European Societies of Plant Pathology Workshop on the environmental factors affecting photosystem II, Szeged, Hungary

Chisholm SW, Morel FMM (eds) (1991) What controls phytoplankton production in nutrient-rich area of the open ocean. Limnol Oceanogr 36

Claustre H, Kerhervé P, Marty J-C, Prieur L (1994) Phytoplankton photoadaptation related to some frontal physical processes. J Mar Science 5: 251-265

Cullen JJ, Lewis MR (1988) The kinetics of algal photoadaptation in the context of vertical mixing. J Plank Res 10: 1039-1063

De Baar HLW, De Jong JTM, Bakker DCE, Loscher BM, Veth C, Bathmann U, Smetacek V (1995) Importance of iron for phytoplankton blooms and carbon dioxide drawdown in the Southern Ocean. Nature 373: 412-415

Demers S, Roy S, Gagnon R, Vignault C (1991) Rapid light-induced changes in cell fluorescence and in xantophyll-

cycle pigments of *Alexandrium excavatum* (Dinophyceae) and *Thalassiosira pseudonana* (Bacillariophyceae): a photo-protection mechanism. Mar Ecol Prog Ser 76: 185-193

Doney SC, Najjar RG, Stewart S (1995) Photochemistry, mixing and diurnal cycles in the upper ocean. J Mar Res 53: 341-369

El-Sayed SZ, Weber LH (1982) Spatial and temporal variations in phytoplankton biomass and primary production in the Southwest Atlantic and the Scotia Sea. Polar Biology 1: 83-90

El-Sayed SZ, Biggs DC, Holm-Hansen O (1983) Phytoplankton standing crop, primary productivity, and near-surface nitrogenous nutrient fields in the Ross Sea, Antarctica. Deep-Sea Res 30: 871-886

El-Sayed SZ, Fryxell GA (1993) Phytoplankton. In El-Sayed SZ (ed) Antarctic Microbiology. Wiley-Liss, Inc. pp. 65-122

Frank HA, Cue A, Chynwat V, Young A, Gosztola D, Wasielewski MR (1994) Photophysics of the carotenoids associated with the xanthophyll cycle in photosynthesis. Photosynthesis Res 41: 389-395

Hagar A, Stransky H (1970) Das caratinoimuster und die verbeitung des lichtinduzierten xantophyll cyclus in verschiedenen algenklassen. Arch Mikrobiol 73: 77-89

Kerherve P (1991) Résponses photoadaptatives des pigments phytoplanctoniques. Vitesses d'adaptation; photoadaptation et processus hydrodynamiques en zone frontale. DEA Univ. Paris 6

Lancelot C, Billen G, Veth C, Becquevort S, Mathot S (1993) Factors controlling phytoplankton ice-edge blooms in the marginal ice-zone of the northwestern Weddell Sea during seas ice retreat 1988: field observations and mathematical modelling. Polar Biology 13: 377-387

Lewis MR, Cullen JJ, Platt J (1984) Relationship between vertical mixing and photoadaptation of phytoplankton: similarity criteria. Mar Ecol Prog Ser 15: 141-149

Li WKW, Smith JC, Platt T (1984) Temperature response of photosynthesic capacity and carboxylase activity in Arctic marine phytoplankton. Mar Ecol Prog Ser 17: 237-243

Marra J (1978) Effect of short-term variations in light intensity on photosynthesis of a marine phytoplankter: a laboratory simulation study. Mar Bio 46: 191-202

Mitchell BG, Holm-Hansen O (1991) Observations and modeling of the Antarctic phytoplankton crop in relation to mixing depth. Deep-Sea Res 38(8-9A): 981-1007

Mitchell BG, Brody EA, Holm-Hansen O, McClain C, Bishop J (1991) Light limitation of phytoplankton biomass and

macronutrient utilization in the Southern Ocean. Limnol Oceanogr 36: 1650-1661

Moline MA, Prézelin BB (1996) High-resolution time-series data for primary production and related parameters at a Palmer LTER coastal site: Implications for modeling carbon fixation in the Southern Ocean. Polar Biology, in press

Moline MA, Prézelin BB, Schofield O, Smith RC (1996) Temporal dynamics of coastal Antarctic phytoplankton: Environmental driving forces and impact of a 1991-1992 summer diatom bloom on the nutrient regimes. In Battaglia B, Valencia J, Walton DWH (eds) Antarctic Communities. Cambridge University Press. In press

Moline MA, Prézelin BB (submitted) Palmer LTER 1991-1994: Long-term monitoring and analyses of physical factors regulating variability in coastal Antarctic phytoplankton biomass, in situ productivity and taxonomic composition over subseasonal, seasonal and interannual time scales. Mar Ecol Prog Ser

Nelson DM, Smith WOJ (1991) Sverdrup revisited: Critical depths, maximum chlorophyll levels, and the controls of Southern Ocean productivity by the irradiance-mixing regime. Limnol Oceanogr 36: 1650-1661

Olaizola M, Bienfang PK, Ziemann DA (1992) Pigment analysis of phytoplankton during a Subarctic spring bloom: xanthophyll cycling. J Exp Mar Bio Ecol 158: 59-74

Olaizola M, La Roche J, Kolber Z, Falkowski PG (1994) Non-photochemical fluorescence quenching and the diadinoxanthin cycle in a marine diatom. Photosynthesis Res 41: 357-370

Rivkin RB (1991) Seasonal patterns of planktonic production in McMurdo Sound, Antarctica. Amer Zool 31: 5-16

Ross RM, Quentin LB (1992) Palmer long-term ecological research (LTER): An overview of the 1991-1992 season. Ant J U S 27: 235-236

Ryther JH, Hulburt EM (1960) On winter mixing and the vertical distribution of phytoplankton. Limnol Oceanogr 5: 337-338

Sakshaug E, Holm-Hansen O (1986) Photoadaptation in Antarctic phytoplankton: variations in growth rate, chemical composition and P versus I curves. J Plank Res 8: 459-473

Sakshaug E, Slagstad D, Holm-Hansen O (1991) Factors controlling the development of phytoplankton blooms in the Antarctic Ocean-A mathematical model. Mar Chem 35: 259-271

Siegenthaler U, Sarmiento JL (1993) Atmoshperic carbon dioxide and the ocean. Nature 365: 119-125.

Smetacek V, Passow U (1990) Spring Bloom initiation and Sverdrup's critical-depth model. Limnol Oceanogr 35: 228-234

Smith RC, Baker KS, Handley P, Newberger T (1992) Palmer LTER program: Hydrography and optics within the peninsula grid, zodiac sampling grid during the 1991-1992 field season. Ant J U S 27: 253-255

Smith WOJ, Nelson DM (1985) Phytoplankton bloom produced by a receding ice edge in the Ross Sea: Spatial coherence with the density field. Science 277: 163-166

Stransky H, Hagar A (1970) Das caratinoimuster und die verbeitung des lichtinduzierten xantophyll cyclus in verschiedenen algenklassen, II. Arch Mikrobiol 71: 164-190

Tilzer MM, Elbrachter M, Gieskes WW, Beese B (1986) Light-temperature interactions in the control of photosynthesis in Antractic phytoplankton. Polar Biology 5: 105-111

Tilzer MM, Dubinsky Z (1987) Effects of temperature and daylength on the mass balance of Antarctic phytoplankton. Polar Biology 7: 35-42

Townsend DW, Keller MD, Sieracki ME, Ackleson SG (1992) Spring phytoplankton blooms in the absence of vertical water column stratification. Nature 360: 59-62

Waters KJ, Smith RC (1992) Palmer LTER: A sampling grid for the Palmer LTER program. Ant J U S 27(5): 236-238

Welschmeyer NA, Hoepffner N (1986) Rapid xantophyll cycling: an in situ tracer for mixing in the upper ocean. EOS (Trans Am Geophys Union) 67:969

Whitaker TM (1982) Primary production of phytoplankton off Signy Island, South Orkneys, the Antarctic. Proc R Soc Lond 214: 169-189

Wilson DL, Smith WOJ, Nelson DM (1986) Phytoplankton bloom dynamics of the western Ross Sea ice edge I: Primary productivity and species specific production. Deep-Sea Res 33: 1375-1387

Figure 1. A) The seasonal change in the depth distribution of chlorophyll a (mg Chl a m^{-3}) at LTER station B (64° 46.45' S, 64° 03.27' W) from December 5, 1991 to February 27, 1992. Contours of Chl a values in excess of 8 mg m^{-3} are not shown. The distribution of discrete samples collected for HPLC determinations is shown by open circles. The depths of the upper 'mixed'layer were calculated according to Mitchell and Holm-Hansen (1991) and are indicated by open squares. B) The seasonal change in the depth distribution of the (diadinoxanthin + diadinxanthin)/Chlorophyll a ratio [(DD + DT):Chl a] from December 5, 1991 to January 7, 1992 (see text for explaination of this time period). The depths of the 1% surface Q_{par} are indicated by closed circles. Contour plots were generated using the Delaunay triangulation method.

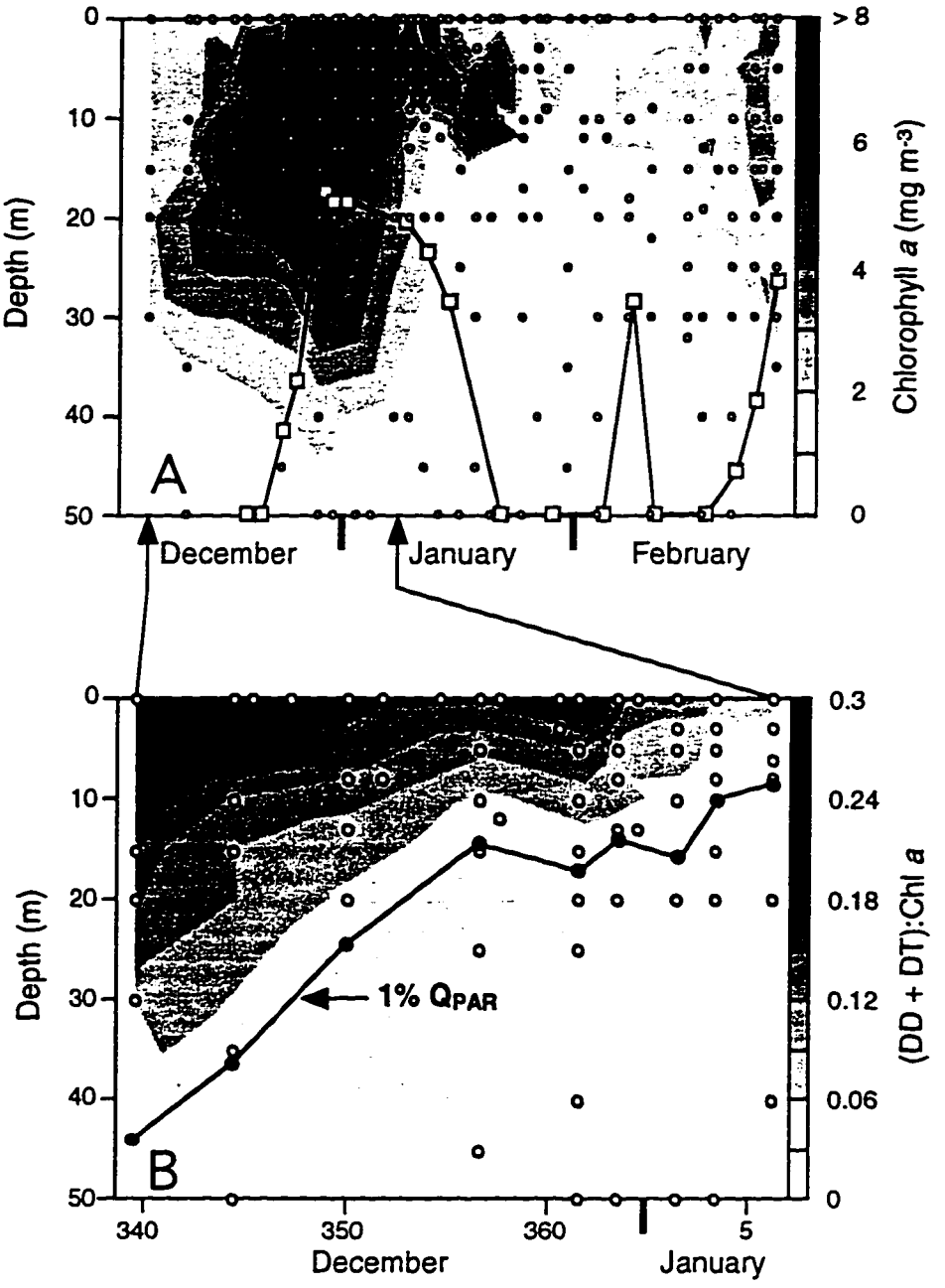
Depth (m)
0
10
20
30
40
50
> 8
6
4
2
0
Chlorophyll a (mg m-3)
A
December
January
February
Depth (m)
0.3
0.24
0.18
0.12
0.06
0
(DD + DT):Chl a
1% QPAR
B
340
350
360
5
December
January

Figure 2. Relationship between integrated Q_{par} irradiance at each sampling depth and the (DD + DT):Chl *a* ratio for collected from December 5, 1991 to January 7, 1992. Q_{par} irradiance for each day was integrated up to 24 hrs prior to collection at one hour steps and at each step regressed against the measured (DD + DT):Chl *a* ratio (inset). The highest significant correlation coefficents were found to be the Q_{par} irradiance integrated 6-8 hrs prior to collection. From 6-18 hrs prior to collection, the sigificance of the correlation does not change because of the minimal contribution of light during the night (horizontal shaded bar). The arrow indicates the seven hour integrated Q_{par} irradiance values that were used in this figure.

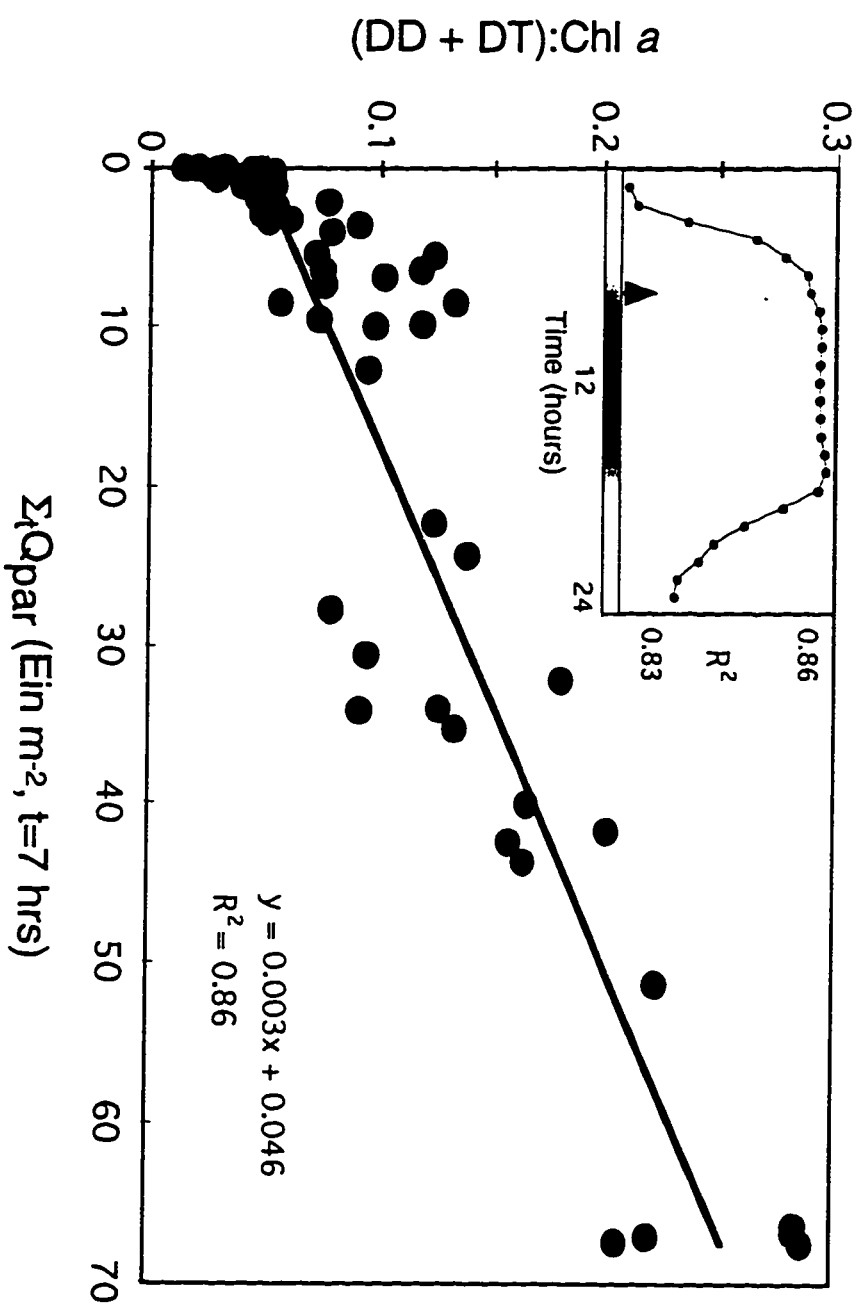
(DD + DT):Chl a
0
0.1
0.2
0.3
0
10
20
30
40
50
60
70
ΣtQpar (Ein m-2, t=7 hrs)
y = 0.003x + 0.046
R2 = 0.86
Time (hours)
12
24
0.83
0.86
R2

Figure 3. The percent of the surface (DD + DT):Chl *a* ratio at each sampling depth compared with the percent of the surface Q_{par} (0^-) at each respective depth for samples collected from December 5, 1991 and January 7, 1992 (n = 65). The power function best defining the data between 0.1 and 100 % surface Q_{par} (0^-) is: % surface [(DD + DT):Chl *a*] = 26.053* [% Q_{par} (0^-)]*exp(0.27); n = 57.

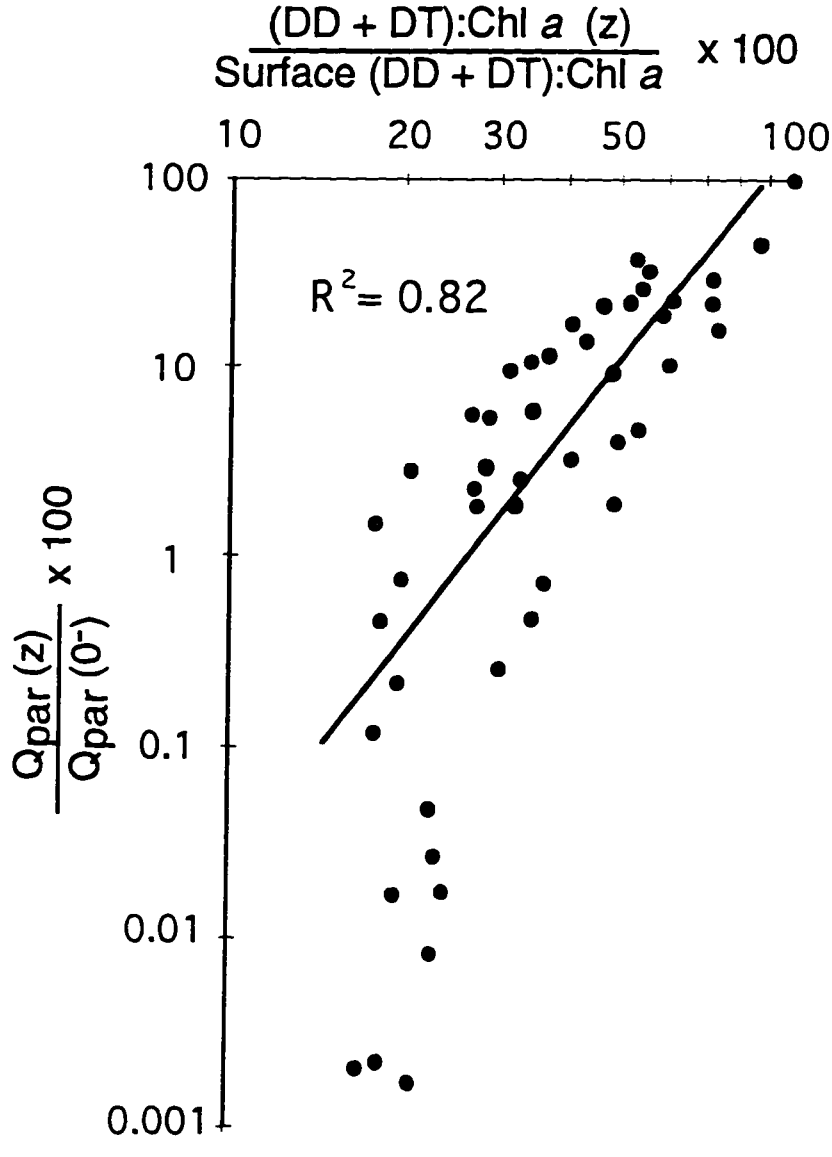
(DD + DT):Chl a (z) / Surface (DD + DT):Chl a x 100
10
20
30
50
100
100
10
1
0.1
0.01
0.001
R² = 0.82
Qpar (z) / Qpar (0⁻) x 100

Figure 4. The relationship between the Q_{par} attenuation coefficent (Kd) and the attenuation coefficent (Kr) calculated from the nine vertical profiles of the (DD + DT):Chl *a* ratio collected over the study period. The regression line is: Kr = .881*Kd - 0.022. The 1:1 relationship is included for comparison.

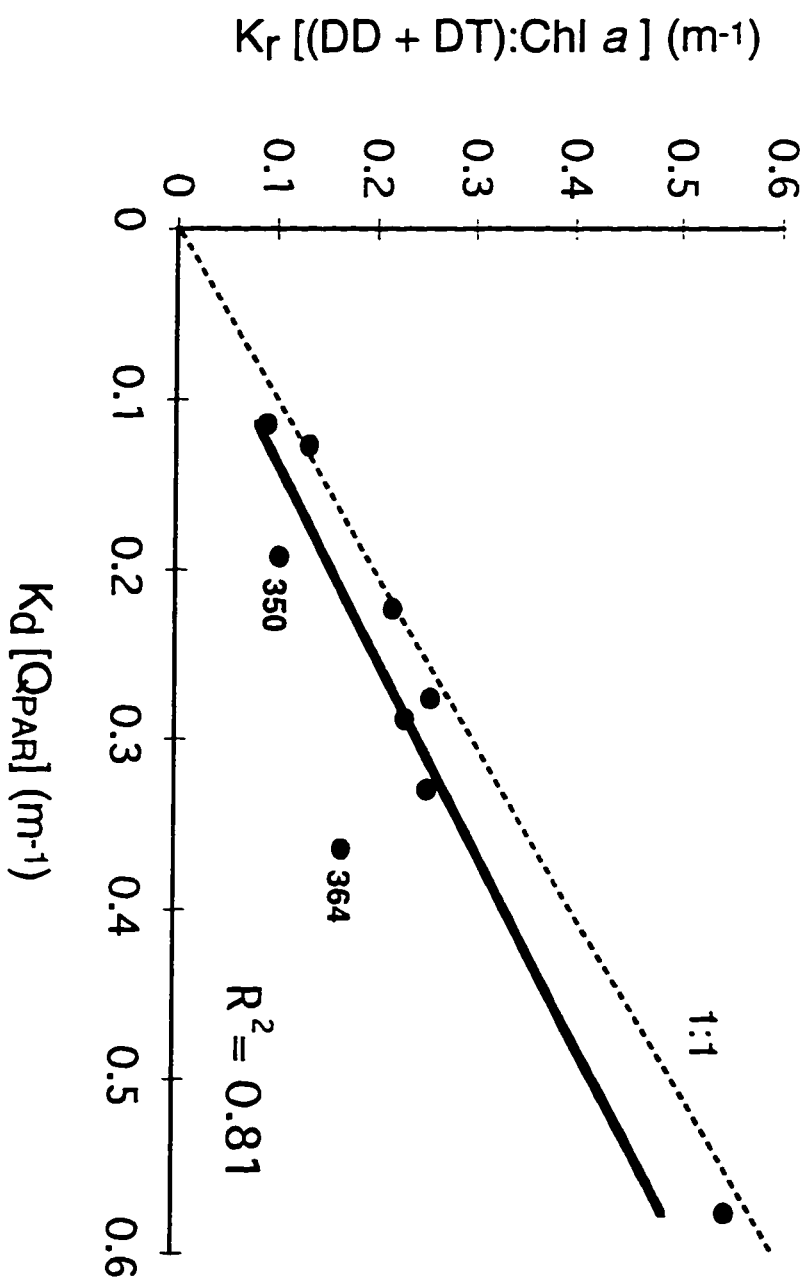
Kr [(DD + DT):Chl a] (m-1)
0
0.1
0.2
0.3
0.4
0.5
0.6
Kd [QPAR] (m-1)
350
364
1:1
R2= 0.81

Figure 5. The average daily wind speed recorded at Palmer Station from December 1, 1991 to January 7, 1992. Profile sampling dates are indicated by black bars. The dotted line is a six year (1989-1995) average daily wind speed for the same period.

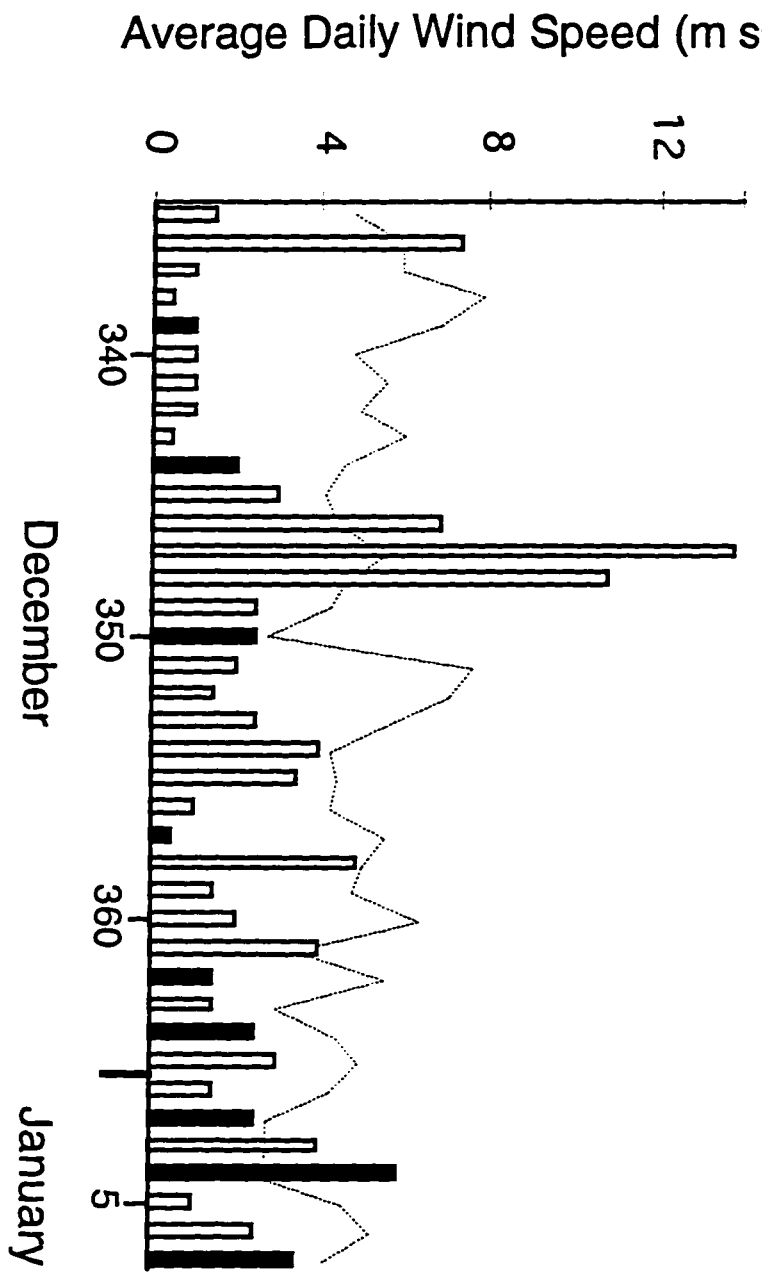
Average Daily Wind Speed (m s-1)
0
4
8
12
340
350
360
5
December
January

Figure 6. Daily change in the (DD + DT):Chl *a* (normalized to the daily maximum) for surface and chlorophyll *a* maximum samples and average incident Q_{par} irradiance on December 16, 23, 30, 1991 and January 7, 1992. A third-order polynomial has been fit to all data to illustrate the average delay (~ 6 hrs) in the response of the normalized (DD + DT):Chl *a* ratio to the average light field.

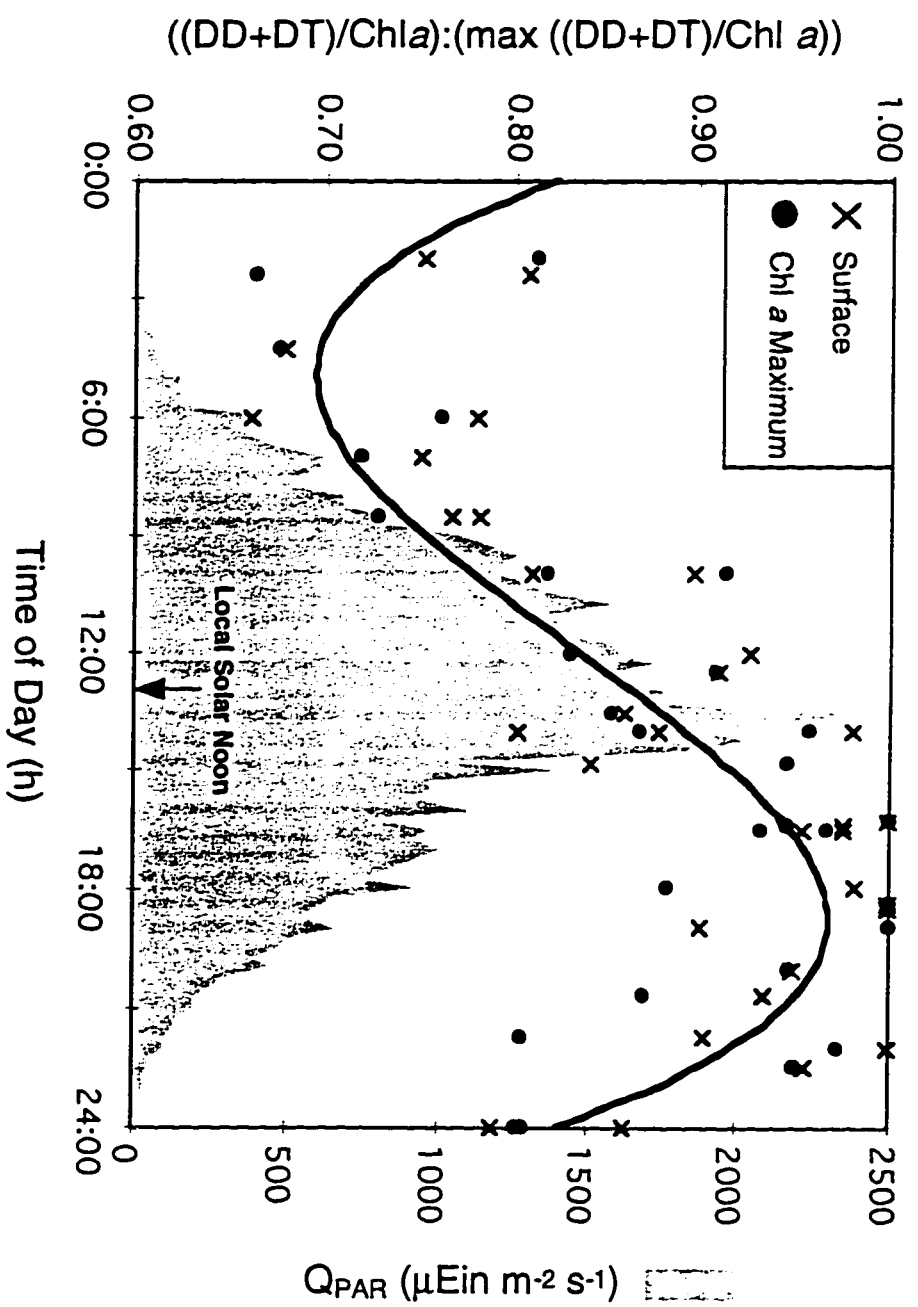
((DD+DT)/Chl*a*):(max ((DD+DT)/Chl *a*))
0.60
0.70
0.80
0.90
1.00
0:00
6:00
12:00
18:00
24:00
Time of Day (h)
Surface
Chl *a* Maximum
Local Solar Noon
0
500
1000
1500
2000
2500
Q_{PAR} (µEin m^{-2} s^{-1})

Figure 7. The absolute change in (DD + DT):Chl *a* from the daily minimum as a function of Q_{par} dose for each time interval over the day for surface and chlorophyll *a* maximum samples taken on December 16, 23, 30, 1991 and January 7, 1992. This response is evaluated after removing the time delay shown in Fig. 6 for each depth and each day (see text).

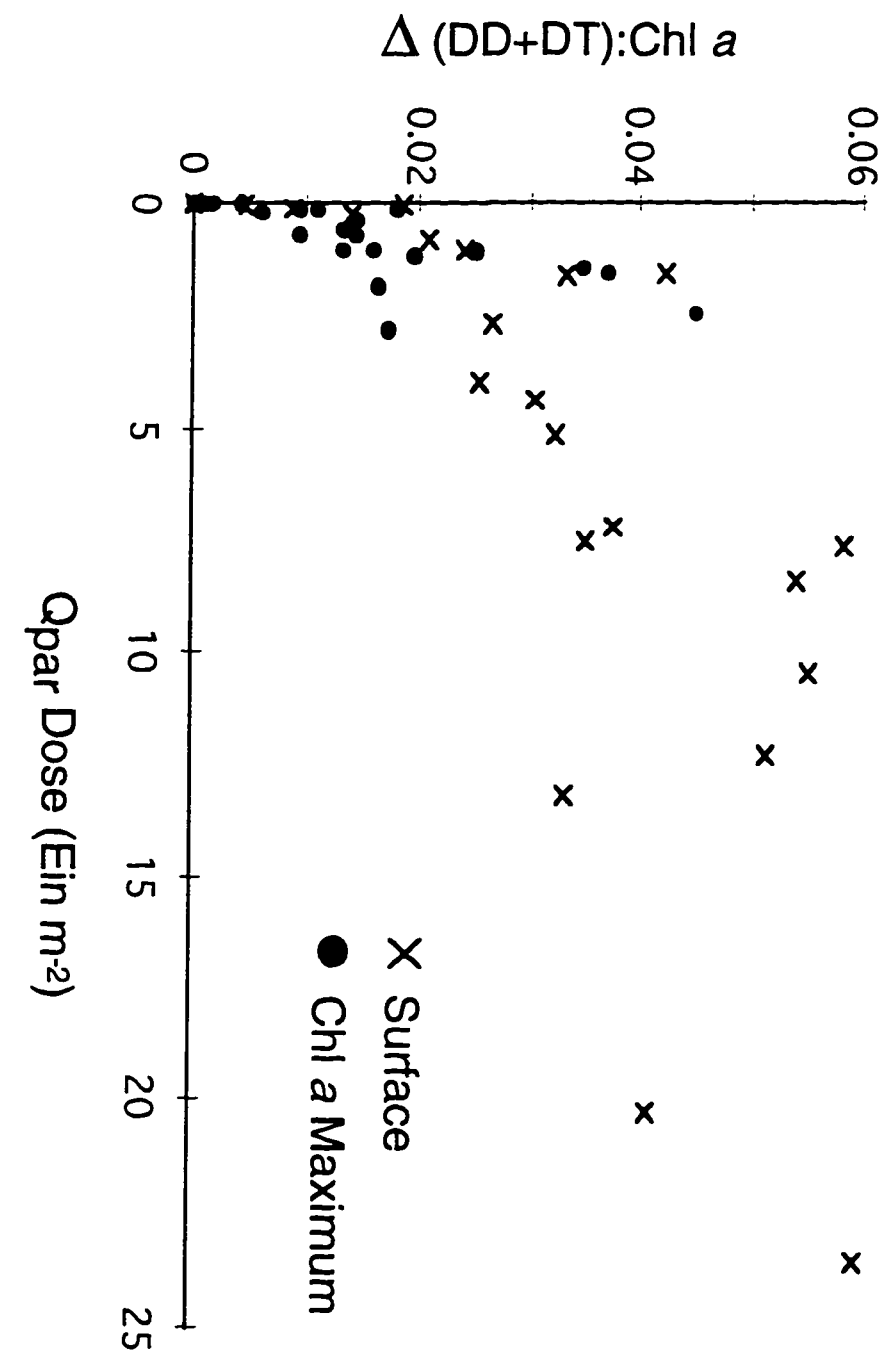
Δ (DD+DT):Chl a
0
0.02
0.04
0.06
0
5
10
15
20
25
Qpar Dose (Ein m-2)
X Surface
● Chl a Maximum

Figure 8. Profiles of the photoadaptive index, (DD + DT):Chl a, in relation to water column density for two LTER stations, A) 700.040; 64° 20.00' S, 65° 57.32' W and B) 600.140; 64° 15.15' S, 63° 02.35' W, taken November, 1991 along the Antarctic Peninsula.

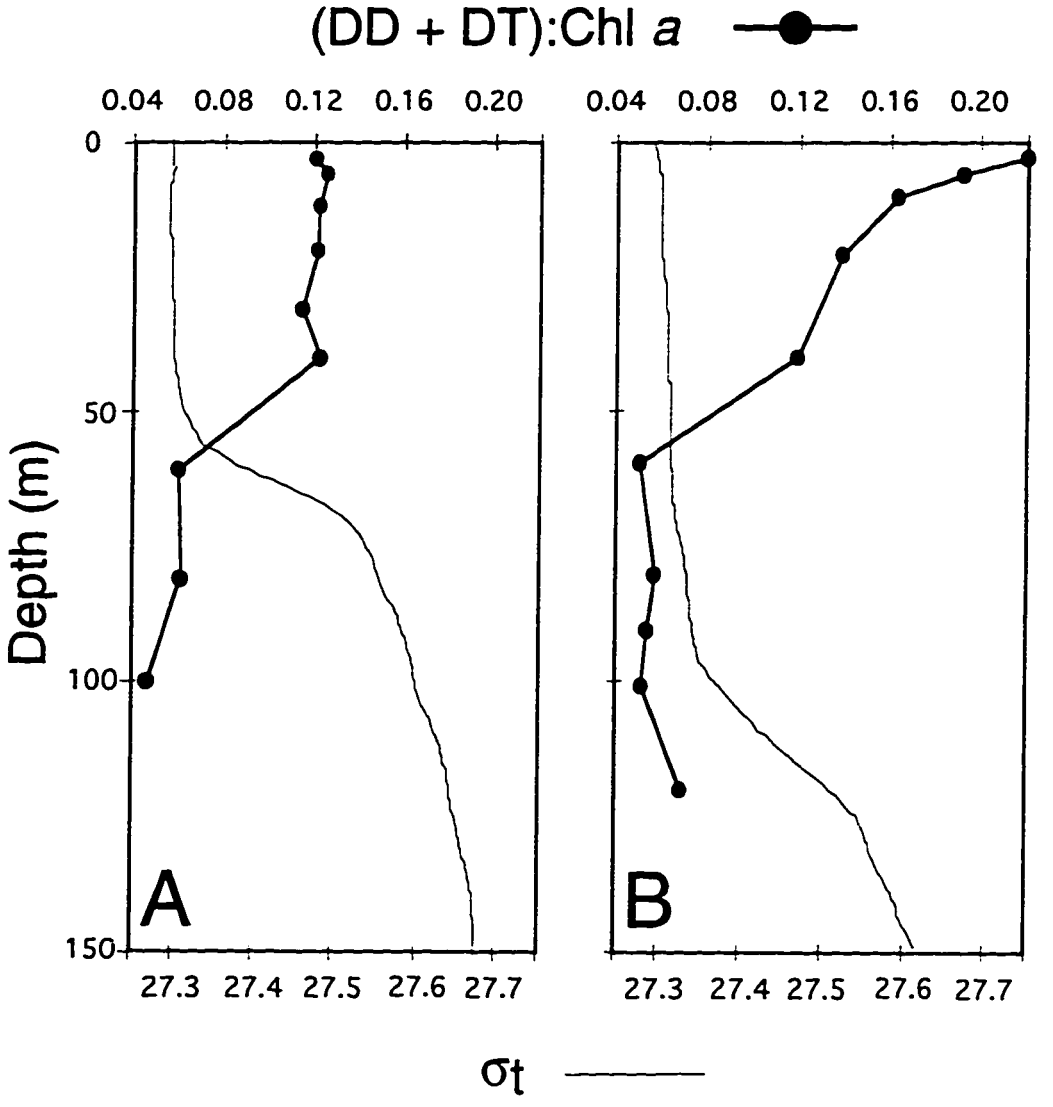
(DD + DT):Chl a
0.04 0.08 0.12 0.16 0.20
0.04 0.08 0.12 0.16 0.20
0
50
100
150
Depth (m)
A
B
27.3 27.4 27.5 27.6 27.7
27.3 27.4 27.5 27.6 27.7
σt

CHAPTER III

High-Resolution Time-Series Data for 1991/1992 Primary Production and Related Parameters at a Palmer LTER Coastal Site: Implications for Modeling Carbon Fixation in the Southern Ocean

ABSTRACT

Our goal was to provide a high-resolution temporal data base for modeling primary production in shelf waters adjacent to Palmer Station, Antarctica. Here, the resulting data base is used to 1) determine in situ productivity over a range of seasonal to subseasonal time scales; 2) identify time scales of significant variability in marine productivity during the peak growing season; 3) identify environmental, experimental and analytical factors that can significantly impact the accuracy of daily, weekly and seasonal productivity estimates; and 4) integrate our findings with previous studies of Antarctic coastal primary production. Data was gathered every 2 to 3 days during a three month period in the austral spring/summer of 1991/1992. Photosynthesis-irradiance (P-I) relationships were determined throughout the euphotic zone and P-I parameters, combined with knowledge of the in-water light field, were used to derive instantaneous rates of in situ primary production. Additionally, weekly samples were collected from surface and chlorophyll a maxima for characterization of the patterns of diel periodicity in P-I parameters. Seven diel patterns were discerned over the season and used to time-correct instantaneous measurements and derive noontime, daily, monthly and seasonally integrated estimates of production.

During the season, a large bloom was responsible for some of the highest daily productivity rates reported for the Southern Ocean (0.8 g C m^{-3} d^{-1}, 6.3 g C m^{-2} d^{-1}). Significant variation in daily integrated rates occurred generally on time scales less than a week. Peak timing and magnitude of daytime periodicities in photosynthesis varied widely over the season, closely coupled to changes in phytoplankton community composition. Instantaneous measurements of primary production, if uncorrected or improperly corrected for daytime periodicities in carbon fixation, were unreliable predictors of production on longer time scales even if the water column was sampled every few days. High frequency sampling and consideration of diel periodicity may be requirements when attempting to discern differences between short time-scale variability and long-term trends in Antarctic primary production.

INTRODUCTION

The Southern Ocean supports a rich biotic ecosystem, ultimately dependent on autotrophic production by phytoplankton. Many previous studies have documented large spatial variations in primary productivity (cf. Holm-Hansen et al. 1977; El-Sayed et al. 1983; Bodungen et al. 1986; Wilson et al. 1986; Holm-Hansen and Mitchell 1991; Helbling et al. 1995). Production associated with marginal ice zones (cf. Smith and Nelson 1985; Holm-Hansen and Mitchell 1991; Prézelin et al. 1994) and coastal shelf regions (cf. El-Sayed and Weber 1982; Holm-Hansen and Mitchell 1991; Prézelin et al. 1992a) is generally higher than offshore waters, which are characteristically oligotrophic (Smith and Sakshaug 1990; Sakshaug et al. 1991). Few studies, however, have examined the temporal variability in primary productivity in any of these regions. Exceptions include Horne et al. (1969), who sampled coastal waters at South Orkney Island every 5-6 days over a period of 1 month; Whitaker (1982) sampled the same sites as Horne et al. (1969) but with a sampling frequency of ca. 20 days over a 2 year period; Holm-Hansen and Mitchell (1991) sampled 4 sites in coastal waters along the Palmer Peninsula at 20 day intervals for a 4 month period; and Rivkin (1991) sampled McMurdo Sound every 5-6 days for a period of

5 months. Recent analyses of sampling frequency effects on error estimates of primary production (Taylor and Howes 1994) suggest, however, that the above sampling regimes may not be sufficient to resolve significant variations in local production which occur on shorter (less than 1 week) times scales. If true, unknown errors would be included in derived production estimates on longer time scales, with ramifications for ecosystem modeling and interpretation of seasonal dynamics in phytoplankton communities of the Southern Ocean.

The Palmer LTER is a multidisciplinary program established in 1990 (Ross and Quetin 1992). It seeks to understand and model predictive interactions between different marine trophic levels and the chemical / optical / physical environment of coastal waters in the Southern Ocean. Work was defined in the context of common goals and philosophy of the U. S. LTER NETWORK, which included requirements for the definition of patterns and control of primary production within the LTER study site along the Palmer Peninsula, as well as spatial and temporal distributions of populations representing different trophic structures. With relatively little background data, starting up a long-term research program required much attention to both field program design and intensive data collection in order to assure the ability to eventually distinguish between natural short-

term variability and long-term trend due to natural cycles (i. e. ice coverage) or unnatural environmental perturbations brought on by global climate change (i. e. global warming, ozone diminution).

Sampling of time-series stations within 5 km of Palmer Station was particularly intense in the first year of the program (1991-1992), as phytoplankton dynamics were thought likely to change significantly over small time and space scales, with serious implications for interpretation of long-term data sets and sampling strategies. To this end, carbon fixation rates were determined on an average of every 2 to 3 days to estimate instantaneous, daily and monthly simulated in situ rates of primary productivity for the three month spring-summer period. Uncertainty of the timing and magnitude of daily changes in production, known to introduce significant errors in estimates of in situ rates of primary production in both temperate (cf. Harding et al. 1982; Prézelin et al. 1987; Smith et al. 1987; Prézelin and Glover 1991) and polar latitudes (Rivkin 1987; Rivkin and Putt 1988), made it also necessary to measure and incorporate diel variation in the rate estimates for the season. The resulting high-resolution time-series data set, collected for a single LTER station, is employed here to 1) determine simulated in situ productivity on time scales and for durations not previously reported for the Antarctic: 2) identify

time scales of significant variability in productivity during the peak growing season in these largely uncharacterized locations, so that perhaps less resolved sampling strategies could be justified in following LTER field seasons: 3) determine and examine factors that may significantly affect daily, weekly and seasonal productivity estimates: and 4) integrate our results with previous studies of Antarctic coastal primary production. These findings would provide insights and advancements in primary production estimates useful to the planning of other multidisciplinary programs (i. e. GLOBEC and JGOFS) which share similar goals of ascertaining the differences between short-term variability and long-term trends in primary production in diverse regions of the Southern Ocean.

METHODS

Sampling

From 3 December, 1991 until 27 February, 1992, a total of 249 discrete water samples were collected at the LTER Station B (Sta B; Fig. 1) for concurrent determinations of physical, optical, biological and chemical parameters related to phytoplankton ecosystem dynamics. Prior to collection, vertical profiles of photosynthetically available radiation (400-700 nm, Q_{par}) and

temperature were measured. In addition, in situ chlorophyll (Chl) fluorescence profiles were measured (Smith et al. 1992a). From the light and fluorescence profiles, subsurface sampling depths were preselected to include the surface, Chl a maximum (Chl a max), the 30%, 12%, 7% and 3% Q_{par} light levels and usually one sample near the bottom (~ 65 m). Sampling was conducted from a Mark V Zodiac® with an effort to sample near solar noon. Whole water samples were collected in cleaned 5 L GoFlo® bottles, transferred to acid-washed dark bottles and returned to Palmer Station within 30 min, where samples remained in a cold room (-2 °C) until analyses.

HPLC Pigment Analysis

Aliquots of all whole water samples were analyzed for the algal pigments using reverse-phase HPLC procedures described by Bidigare et al. (1989). One liter samples were filtered on 0.4 μm nylon 47 mm Nuclepore® filters and extracted in 3 mL 90% acetone for 24 hr in the dark at -20 °C. Pigment separation was achieved with the aid of a Hitachi L-6200A liquid chromatograph equipped with a Waters Radial-PAK® C^{18} column (8 x 100 mm column; 5 μm particles) and an Hitachi L-4250 UV/VIS Variable Wavelength Detector (436 nm). Peak identities of algal extracts were determined by comparing their retention times with pure pigment standards. For the purposes

of the present study, temporal/spatial patterns are presented only for the chemotaxomic marker pigments Chl a (an indicator of total phytoplankton biomass), alloxanthin (a marker for cryptophytes), 19'-hexanoyloxyfucoxanthin (an indicator of prymnesiophytes and in Antarctica a particular marker for *Phaeocystis* spp.) (Bidigare et al. 1995) , 19'-butanoyloxy-fucoxanthin (indicator of chrysophytes), and fucoxanthin (a diatom marker in Antarctica where fucoxanthin is not abundant in the major prymnesiophyte, *Phaeocystis* sp.). For additional details on the seasonal dynamics of algal pigmentation at Sta B, as well as surrounding LTER nearshore transect stations, see Prézelin et al. (1992b) and Moline et al. (1996).

Q_{par} Measurements

Surface and in-water fluxes of Q_{par} (400-700 nm) were measured respectively with a Biospherical® scalar irradiance meter (QSR-170DT) equipped with a QSR-240 reference sensor and a QSP-100DT underwater sensor. A second QSR-240 sensor was positioned next to outdoor incubators at Palmer Station where diel patterns of simulated in situ primary production were determined (see below). Incident Q_{par} was recorded continuously every 5 min over the 3 month period. A comparison between the two QSR-240 sensors showed that

Q_{par} readings differed < 5%. Theoretical clear-sky maxima of daily integrated Q_{par} (E m^{-2}) over the season were calculated from Morel (1991) and D. Antoine (pers. comm.) using an atmospheric correction (350 DU for ozone content and 2 cm precipitable water content). Bio-optical nomenclature used throughout this study is from Prézelin et al. (1993b).

Photosynthesis-Irradiance Relationships

On 39 days over the course of the sampling season, a total of 397 photosynthesis-irradiance (P-I) curves were determined for water-column samples collected from Sta B. Of these, 181 P-I relationships were measured immediately after field collection for determinations of 'instantaneous' rates of primary production. The remaining 216 P-I curves represent the 12 weekly analyses of diel variations in P-I parameters in both surface and Chl *a* max samples (see below).

All P-I measurements were made in blue-green light ($CuSO_4$ filters) Q_{par} photosynthetrons, using established radiolabelled $H^{14}CO_3$ uptake procedures (Prézelin et al. 1989; Prézelin and Glover 1991). Blue-green light fields more closely mimic in-water spectral conditions in clear ocean waters and tend to release cells from artificial white light (or far-red) effects, which can reduce carbon uptake rates and photosynthetic quantum efficiencies (Prézelin et al. 1989; Schofield et al. 1991). Incubation times were kept to 90 min

and incubation temperatures were controlled to within 0.2 °C of in situ temperatures. After incubation, samples were fixed with 20 mL formalin solution, acidified with glacial acetic acid:methanol (1:30), and heat dried (Prézelin and Glover 1991). Dried samples were resuspended in 1 mL of deionized water before National Diagnostics Liquiscint® scintillation fluor was added. Quench-corrected disintegrations per min were determined on a LKB 1217 liquid scintillation counter.

Non-linear curve fits for P-I data were calculated using the Simplex method of Caceci and Cacheris (1984). Curve fitting provided the photosynthetic parameters P_{max} (the light saturated photosynthetic potential), α (the light-limited photosynthetic efficiency), I_k (= P_{max}/α; an estimate of the minimum irradiance required for the onset of light saturated photosynthesis), β (the efficiency of photoinhibition) and I_t (the irradiance threshold for the onset of photoinhibition). Estimates of the standard deviations for the P-I parameters were calculated using the procedures described by Zimmerman et al. (1987).

The derived P-I parameters from the nearly 400 P-I curves formed the data base for bio-optical modeling of in situ primary production in the present time series. To increase the accuracy of our estimates for primary production on different time scales, we eliminated from the data base any P_{max} values

with standard deviation estimates > 25% of the parameter value and any a value with a standard deviation > 30%. This reduced the size of the productivity data base by less than 10%. When Q_{par}-photoinhibition was evident, standard deviations for β and I_t were often large as a result of a limited number of high irradiance data points. However, given that Q_{par}-photoinhibition was rarely predicted at *in situ* irradiances (data not shown), uncertainty in β values would have had little impact on the accuracy of simulated *in situ* productivity estimates in the present study on time scales longer than one day.

Diel Measurements

On 12 occasions over the three month time period, 10 L samples were collected from both the surface and the Chl *a* max to determine the diel variation in the P-I parameters. Samples were placed in large Pyrex® carboys, screened with neutral density screening to the *in situ* Q_{par} light level at the depth of collection (surface was screened to 50% transmission), and incubated outdoors in a seawater tank at ambient temperatures for 24 to 30 hr. Subsamples were retrieved from the carboy at 3-hr intervals for determination of pigmentation and P-I relationships, using procedures outlined above. The day:night variations in P-I parameters were plotted in order to

resolve the time of day when the parameter reached its maximum value (i. e. maxP_{max}) and to quantify the magnitude (i. e. maximum:minimum ratio) of the daytime variation in each P-I parameter. If diel patterns for the absolute variations in a P-I parameter (i. e. P_{max}) were overlaid for different days that were deemed comparable (see below), a similar pattern was found but with different absolute. To compare the timing and magnitude of diel variations on different days, each diel patterns was normalized to its maximum value for that day (i. e. P_{max}: maxP_{max}) (Fig. 2).

It should be noted that since 1/4" Pyrex® does not transmit solar ultraviolet radiation reaching the earth surface (ca. 295-400 nm) at wavelengths less than ca. 324 nm, incubated samples may have been released or possibly recovering from UVB (295-320 nm) inhibition during the diel studies. A previous study of natural communities of *Phaeocystis* spp. under the influence of the 1990 ozone 'hole' indicated that these phytoplankters were immediately released from all UVB inhibition when placed in Q_{par}-only incubators (Prézelin et al. 1994). With respect to UVA radiation (320-400 nm), our studies of Antarctic phytoplankton show it to be generally photoinhibitory and sometimes photosynthetically useful depending upon circumstances (Prézelin et al. 1994). The incorporation of UV inhibition, with consideration of the

mixing regimes and in situ light histories can not yet be adequately addressed in this portion of the LTER field program. We, therefore, take a conservative approach to estimating simulated in situ rates of primary production and assume the diel patterns determined in the outdoor incubators are for Q_{par}-rates of photosynthesis only.

Calculation of Simulated In Situ Primary Productivity

Before the simulated in situ estimates of primary production could be calculated, it was necessary to first evaluate the different diel periodicity patterns of P-I parameters and then to determine which patterns to assign to different instantaneous samples in order to generate time-dependent rates of primary production. The approach was very similar to that developed for time-correcting photosynthetic data to get a near synoptic view of in situ productivity off coastal California (Prézelin et al. 1987; Smith et al. 1987; Smith et al. 1989) and in the Sargasso Sea (Prézelin and Glover, 1991). Diel patterns for each Chl a-specific P-I parameter were sorted based upon shared biological and physical characteristics (i. e. water-mass type, pigment composition, location in water column and temporal occurrence over the season). As a result of this analyses, 7 distinct sets of diel patterns of variations in P_{max} and a were revealed over the season. Each normalized diel

pattern for a P-I parameter (i. e. Fig. 2 for pattern I) was manually fit and then interpolated at 2-hr intervals over the day, thereby allowing any instantaneous determination of any in situ P-I parameter to be extrapolated to an absolute diel pattern with the same 2 hr resolution. I_k was relatively constant for any individual diel measurements over the season, with a patterns always significantly correlated with P_{max} patterns ($p<0.0001$). Daily I_k patterns were therefore considered constant for calculations of simulated in situ productivity. Patterns for β and I_t were also determined for each diel measurement and incorporated in the calculations using the same criteria as for P_{max} and α.

Simulated in situ photosynthetic rates for a given depth and time [P (z, t)] were calculated as a hyperbolic tangent (Neale and Richerson 1987),

$$P(z,t) = P_{max}(z,t) \bullet \tanh\left(\frac{Q_{par}(z,t)}{I_k(z,t)}\right) \qquad \text{Eq. 1}$$

when Q_{par} (z, t), the in situ irradiance, was less than I_t (z, t) and

$$P(z,t) = P_{\max}(z,t) \bullet \tanh\left(\frac{Q_{par}(z,t)}{I_k(z,t)}\right) \bullet \exp\left[-\beta\left(Q_{par}(z,t) - I_t(z,t)\right)\right] \quad \text{Eq. 2}$$

when Q_{par} (z, t) was greater than I_t (z, t). Resulting estimates of hourly in situ primary production, at 2 hr intervals, over the day were then used to determine daily rates by trapezoidal integration at each discrete sampling depth. Trapezoidal integration was also used for calculating depth integrated rates, which were then integrated to estimate weekly, monthly and seasonal rates of primary production. Contour plots in this study were generated using the Delaunay triangulation method (DeltaGraph Pro3®, DeltaPoint Inc., Monterey, CA, USA).

RESULTS

Seasonal Light Field Variation

Under clear sky conditions, it is the progressive changes in daylength and solar zenith angle (Fig. 3A) which determine seasonal changes in daily integrated irradiance (Fig. 3B) reaching at any given location on earth. However, at LTER Sta B from late spring through the summer of 1991/1992, incident Q_{par} was routinely less than the theoretical limit (Fig. 3B). On average, only 73% ± 29% of daily Q_{par} reached the study site

over the course of the monitoring program (Fig. 3C). Fluctuations in daily integrated Q_{par} could vary 2 to 3 fold within one to two days of each other. On the time scales of a few weeks, daily integrated Q_{par} appeared to reflect the somewhat periodic nature of Antarctic storms and their associated increased cloud cover (Fig. 3B). Clearer sky conditions were more prevalent in early summer when the diatom bloom occurred and at the end of the field season in late February, 1992. During a storm event the last week in January, only ca. 28% of daily Q_{par} reached the study site. As in other studies (Holm-Hansen and Mitchell 1991), incident Q_{par} was occasionally higher than the calculated maximum for clear skies and is thought to result from reflection by snow/ice cover.

Attenuation of surface Q_{par} in the water column at LTER Sta B varied greatly over the season, due to the 100-fold variation in phytoplankton biomass (Fig 4). Chl a concentrations ranged from 0.3 to ca. 30 mg Chl a m^{-3} over the late spring/summer season with the 1% Q_{par} light level correspondingly varying between 60 and 10 m. Two to 10-fold fluctuations in phytoplankton standing stock and light attenuation were evident within any given week of sampling (Fig. 4). The rapid short-term fluctuations in daily integrated surface irradiance (Fig. 3B), phytoplankton biomass (Fig. 4A)

and its effect on *in situ* attenuation coefficients for Q_{par} (illustrated by changing percent light depths in Fig. 4B) combined to determine the seasonal pattern of daily integrated in-water Q_{par} at LTER Sta B (Fig. 5A).

Water-column stability, as measured by the depth of the upper mixed layer [UML; Mitchell and Holm-Hansen (1991)], was found to be a major driving force for the accumulation of biomass in the water column at Sta B through the first LTER season (Moline et al. 1996). Further evidence for this conclusion is the significant relationships between changes in the percent light depths and the depth of the UML (Fig. 5B). As phytoplankton biomass increased in response to the shallowing UML depth on time scales of a couple of days, there was a corresponding decrease in the depth of the euphotic zone. Data regarding the photoadaptive responses and optimization of light utilization efficiency for photosynthesis during this period are discussed elsewhere (Schofield et al. 1994, Schofield et al., submitted).

Seasonal Variations in Phytoplankton Community Composition and Diel Patterns of Photosynthesis

Late spring and the initiation of a diatom bloom with a midday peak in productivity. In late November 1991, the water column at Sta B was ice-covered (Fig. 4) and the spring

phytoplankton community was dominated by a mixed assemblage of diatoms (as indicated by the presence of fucoxanthin), prymnesiophytes (19'-hexanoyloxyfucoxanthin; in the Antarctic primarily *Phaeocystis* spp.) and chrysophytes (19'-butanoyloxyfucoxanthin) (Fig. 6). There were also indications of chlorophytes (Chl b) throughout the region (Prézelin et al. 1992b). The combination of relatively clear skies, low solar zenith angles, increasing daylength (Fig. 3) and low phytoplankton biomass (0.83 mg Chl a m^{-3}; Fig. 4) all contributed to the observation that the absolute solar insolation in the water column, even under surface ice, was at or near the highest values measured during the 1991/1992 spring/summer seasons (Fig. 5A). These bright light environments were confined to a fresher meltwater lens (FML) about 5 m deep with relatively low values of daily integrated Q_{par} in the well mixed water below the FML (Fig. 7). Phytoplankton community composition of these two mixing regimes was not significantly different (Fig. 6), suggesting that the pycnocline separating the FML from the UML in the late spring might have been weak, i. e. setting up and breaking down on short time scales. Our observations of deep mixing below the FML in late November are consistent with measurements of high concentrations of inorganic nutrients throughout the water column, i. e. NO_3 in excess of 30 μM;

$Si(OH)_4$ in excess of 40 μM, and PO_4^{3-} greater than 1 μM (Moline and Prézelin1994, Moline et al.1996).

The local fast/pack ice broke up and was blown out of the area in early December 1991 (ca. JD 347) (Fig. 4A). There was a significant increase in the daily integrated in-water Q_{par} (Fig. 4A), even though skies were exceedingly cloudy (Fig. 3B). As incident solar radiation increased during the last two weeks of December (Fig. 3B), the water temperature within the FML increased 2 °C, from -1.3 °C to +1.3 °C. Decreased wind forcing during this period (Moline et al. 1996) shallowed the UML to within 20 m of the surface (Fig. 7). Concentrations of pigment biomarkers for prymnesiophytes and chrysophytes decreased throughout the water column while diatom pigmentation increased several fold (Prézelin et al. 1992b; Moline et al. 1996). A near unialgal bloom of *Coscinodiscus* spp., as confirmed by microscopic examination, persisted for 4 weeks in late spring/early summer (JD 340 to JD 007) and came to account for more than 95% of the carotenoid pigmentation in both the surface and Chl a max at Sta B (Fig. 6).

Chl a concentrations during the *Coscinodiscus* spp. bloom were routinely between 15 and 25 mg Chl a m^{-3} (Fig. 6A). At its peak on the last day of 1991, integrated water column Chl a biomass reached 612 mg Chl a m^{-2} (Moline et al. 1996). The

rate of increase in Chl a biomass over the lifetime of the bloom (i. e. from 0.3 to 30 mg Chl a m^{-3}) was greater than that attributable solely to concentrating phytoplankton to a shallower UML. Preliminary estimates suggest *Coscinodiscus* spp. communities were doubling in biomass about once every 4 days. The impact of increased pigmentation on water clarity was evident during the bloom, with the 1% Q_{par} level reduced to within 10 m of the surface and the 0.1% Q_{par} level at 15 m (Fig. 4B).

It is not surprising that the development of a large diatom bloom also had a major impact on macronutrient distribution within the region (Prézelin et al. 1992b; Moline and Prézelin1994; Moline et al. 1996). In brief, there was a highly significant linear relationship between PO_4^{3-} and NO_3 before and after the diatom bloom, identical to that defined for much of the Southern Ocean (Kamykowski and Zentara, 1989). However, the development and maintenance of this diatom bloom radically altered this linear chemical relationship, which previously had been suggested to be a diagnostic characteristic of the plant/nutrient interactions for Antarctic waters (Kamykowski and Zentara, 1989). During the bloom, PO_4^{3-} and NO_3 levels were depleted to below detection levels and $Si(OH)_4$ levels were significantly reduced. NO_3:PO_4^{3-} ratios tripled and PO_4^{3-} limitation of diatom growth was indicated by the later

stages of the bloom in the first week of January 1992. When PO_4^{3-} and NO_3 levels dropped below detection levels in surface waters, rates of diatom biomass increases slowed (Fig. 6A) and there was a small but detectable increase in *Phaeocystis* spp. concentrations (19'-Hexanoyloxyfucoxanthin biomarker) in the low nutrient FML between JD 355-365 (Fig. 6B).

Primary production measurements at LTER Sta B began on JD 339 (Fig. 7), just prior to the onset of the diatom bloom, and were made about every 3 days. Determinations of the diel periodicities in P-I parameters for bloom populations were measured once a week for surface and Chl a max samples. The normalized diel patterns for daytime variations in P_{max} were very similar for each of the five weekly samples collected during the diatom bloom (Fig. 2). The single representative pattern, resolved from the pooled P_{max} data for surface diatom communities (pattern I, Fig. 2 & 8), was characterized by an approximate 2-fold change in P_{max} over an 20-hr photoperiod with the peak timing of P_{max} (i. e. maxP_{max}) occurring about an hour before solar noon (Fig. 7). I_k values changed little over each day (101 ± 13 $\mu E\ m^{-2}\ s^{-1}$, n=24), indicating a close coupling between the timing and magnitude of diel periodicities in P_{max} (3.66 ± 1.13 mg C mg Chl $a^{-1}\ m^{-3}\ h^{-1}$) and α (0.36 ± 0.15 mg C mg Chl $a^{-1}\ m^{-3}\ h^{-1}/\mu E\ m^{-2}\ s^{-1}$). Such tight coupling has been

documented often for diel periodicities in temperate latitude phytoplankton (Harding et al. 1982; Prézelin 1992), several of which have a biological clock regulating the daytime timing of peak photosynthetic capabilities (Prézelin 1992).

The diel periodicities for Chl a max communities (ca. 15 m) during the diatom bloom (Fig. 8, pattern II) were very similar to those resolved for surface samples (Fig. 8, pattern I). P_{max} changed 2-fold over the day with dawn and dusk values about 55-60% of maxP_{max}. However, unlike surface communities, Chl a max communities displayed their maximum photosynthetic potential in the early afternoon, about 1-to-2 hr after solar noon. Again, α values covaried with P_{max} (3.54 ± 1.54 mg C mg Chl a^{-1} m^{-3} h^{-1}; n=30), but with lower I_k values for these deeper diatoms communities (84 ± 17 μE m^{-2} s^{-1}).

Diel periodicity in carbon fixation were incorporated into final primary production estimates (see below). The monthly primary production estimates for December, representing the bulk of the diatom bloom, was 79 g C m^{-2}. Daily integrated rates were greatest in late December, reaching a value of almost 7 g C m^{-2} d^{-1} (Fig. 10 B), when estimates of radiation utilization efficiencies (Schofield et al. 1994, Schofield et al., submitted) indicated that the phytoplankton within the bloom

were operating at near maximal photosynthetic quantum efficiencies.

Early summer and the demise of a diatom bloom, followed by a near-surface Cryptophyte bloom with an early morning peak in photosynthetic potential. In January 1992, there was a rapid transition from a diatom-dominated bloom to one dominated by cryptophytes (alloxanthin) in both the surface and Chl a max (Fig. 6). The depth of the Chl a max, however, had shallowed from a depth of ca. 15 m within the UML to a depth of ca. 5 m within the FML (Fig. 7) and was almost completely dominated by cryptophytes between JD 10 and 20 (Fig. 6C). The cryptophyte bloom was restricted to the near surface low salinity waters, with the pycnocline between the FML and deeper waters separating it from the remnants of the prior diatom bloom (Moline et al. 1996). The highest Chl a concentration for the entire season (29.2 mg Chl a m^{-3}) was recorded in the shallow Chl a max on January 11, 1992 (Fig. 6A). Light attenuation was particularly high within the cryptophyte bloom, perhaps due to glacial flouring, and appeared to have an effect on the photoadaptive state of the phytoplankton. Surface I_k values were only 68 ± 26 μE m^{-2} s^{-1} (n=8) with I_k values of 46 ± 9 μE m^{-2} s^{-1} (n=9) for the Chl a max.

While surface Chl a concentrations were high, primary production was less during this period than during the previous diatom bloom (Fig. 10, see below). The intense near-surface cryptophyte bloom persisted for approximately two weeks until strong storm-related wind forcing advected the water mass out of the area.

Independent determinations of diel variations in P-I parameters for the surface and Chl a max samples collected on the 14th and 21st of January revealed a single pattern (III) for the cryptophyte-dominated community (Fig. 8). Diel pattern III was remarkably different from those observed for diatom communities a few weeks earlier in the season (Fig. 8). Timing of peak P_{max} during the cryptophyte bloom occurred near dawn, or 7-8 hr before solar noon. In mid-afternoon, when P_{max} values would have been highest for diatom-dominated communities, P_{max} values in the cryptophyte community were at a daily minimum.

A very dilute diatom-dominated community was present below 15 m and the cryptophyte bloom. This community was low-light adapted, with an average I_k of 44 ± 15 $\mu E\ m^{-2}\ s^{-1}$ (n=10), or about half that of diatoms in the Chl a max during the diatom bloom (see above). Direct measurements of diel periodicities of photosynthesis in this deeper remaining diatom

community were not made. For subsequenct daily integrated production estimates, we applied the pattern of diel periodicity in P_{max} and a determined for the Chl a max during the diatom bloom in December, assuming that the two diatom communities had identical diel periodicities. This assumption was based on photophysiological similarities between the deep communities during and just after the diatom bloom (Schofield et al., submitted). If we erred in this assumption, the impact on the primary productivity estimates would be small given the low biomass and low photosynthetic activity at the base of the euphotic zone (Fig. 4).

Mid-summer mixed phytoplankton communities, unstable water columns and shifting diel patterns of photosynthesis. Storm activity from late January through the first week of February 1992 generated strong winds and heavy precipitation, resulting in the advection of the cryptophyte bloom water mass from the region (Moline et al. 1996). The advected water mass was replaced by one slightly warmer, nutrient replete and containing dilute (<0.5 mg Chl a m^{-3}) mixed communities of diatoms, prymnesiophytes and other flagellated chromophytes (Chl c-containing phytoplankton). In particular, there was a significant increase in chrysophytes (19'-butanoyloxyfucoxanthin) (Fig. 6). High attenuation of Q_{par}

continued after the advection of the cryptophyte/diatom bloom from Sta B (Fig. 4B & 5), due largely to the presence of glacial flour in the meltwater of the upper 5-10 m (Smith et al. 1992a; Moline et al. 1996).

Diel pattern IV was resolved for these mixed communities the fourth week of January, and was sufficiently distinctive from other patterns to require separate consideration in seasonal productivity estimates (Fig. 9). A single diel pattern of photosynthesis was resolved for the surface and Chl a max during this period of rapid change with a maxP_{max} late in the afternoon. For pattern IV, represented by JD 28, the I_k values for the surface and Chl a max were 85 ± 18 μE m^{-2} s^{-1} (n=6) and 52 ± 2 μE m^{-2} s^{-1} (n=4) respectively. Once again, I_k values were relatively constant over the day with P_{max} of 1.22 ± 0.8 mg C mg Chl a^{-1} m^{-3} h^{-1} for the surface and 2.46 ± 1.33 mg C mg Chl a^{-1} m^{-3} h^{-1} for the Chl a max.

There was a radically different diel P_{max} pattern the following week. Comparing pattern IV with pattern V (Fig. 9), the timing of maxP_{max} apparently shifted some 12 hr to peak near dawn, much like the earlier cryptophyte bloom. The magnitude of the daytime changes in P_{max} remained at about 2-fold and I_k values determined for the surface and Chl a max were 91 ± 26 μE m^{-2} s^{-1} (n=9) and 76 ± 18 μE m^{-2} s^{-1} (n=6)

respectively. Although there was a slight increase in the relative abundance of prymnesiophytes (Fig. 6), there is no apparent taxonomic, hydrographic (aside from salinity) or photophysiological explanation for the large and real shift in peak timing of maxP_{max} between pattern IV and V.

By the first week in February, major wind events had subsided and there was a temporary decrease in the UML depth (Fig. 7). The mixed phytoplankton community comprised of diatoms, prymnesiophytes, chrysophytes and cryptophytes remained in the water column. However, there was a shift toward increasing dominance by prymnesiophytes at the expense of chrysophytes (Fig. 6). Once again the diel patterns in photosynthesis shifted significantly. Diel Pattern VI resolved the daytime variation in P_{max} for samples collected from the surface and Chl a max on February 4th (JD 35), as well as for the surface sample collected on the February 10th (JD 41). Maximum photosynthetic potential for these communities were at solar noon with a 2-fold variation over the day (Fig. 9).

The Chl a max sample collected below the FML on February 10th (JD 41), like the surface sample collected the same day, also displayed a midday peak in maxP_{max} (pattern VII, Fig. 9). The magnitude of the diel periodicity in P_{max}, however, was dampened compared to all other previous patterns, with P_{max}

varying 25-30% over the day. Diel patterns for samples collected from the surface and Chl a max on February 10th were different despite no significant differences in the community structure between depths (Fig. 5). I_k values were similar for the surface (63 ± 6 μE m^{-2} s^{-1}, n=5) and Chl a max (64 ± 21 μE m^{-2} s^{-1}, n=6), suggesting photoacclimation to similar light fields during the previous period of high wind mixing.

Late summer, restratification and reemergence of diatom dominance with a midday peak in photosynthetic potential. Pattern VII was representative not only of the Chl a max community on February 10th, but also of the diatom-dominated communities that reemerged during the last 10 days of our seasonal monitoring program at LTER station B (Fig. 6). With gradually increasing water-column stability and restratification, integrated Chl a concentrations increased from 35 to 93 mg Chl a m^{-2}. Again, I_k values for the surface (66 ± 7 μE m^{-2} s^{-1}, n=8) and Chl a max (63 ± 14 μE m^{-2} s^{-1}, n=15) were not significantly different.

Simulated In Situ Primary Production Estimates

The seven diel photosynthetic patterns for each P-I parameter were applied to the instantaneous P-I parameters and the in situ Qpar light field measured over the season (Fig. 7). Diel-corrected estimates of simulated in situ daily integrated primary productivity for Sta B were derived according to Equation 1 or 2 and are shown in Figure 10A. Most striking was the elevated production during the bloom. The highest daily production (0.75 g C m^{-3} d^{-1}) occurred at 7.5 m on December 30, 1991 when Chl a concentrations were 25.0 mg m^{-3}. As with the phytoplankton biomass (Fig. 4A), productivity decreased at Sta B in mid-January after the advection of the bloom from the area and increased again at the end of the sampling season with increasing water-column stability (Fig. 7). Depth-integrated productivity estimates for the season were significantly correlated with integrated biomass ($p<0.001$), showing peak values during the bloom (Fig. 10B). Peak integrated productivity was 6.3 g C m^{-2} d^{-1} with a total integrated production for the season of 135 g C m^{-2}. December had the highest calculated integrated monthly productivity (79 g C m^{-2}) with decreased carbon fixation as the season progressed (January = 36 g C m^{-2}; February = 19 g C m^{-2}). An average of 56 ± 13% of the water column productivity was light-saturated over the season, and despite occasionally high

in situ irradiances (Fig. 5A), only 3% of the samples were photoinhibited ($Q_{par} > I_t$).

Diel Effects on Estimates of Daily Integrated Production

When productivity estimates based solely on the instantaneous P-I parameters and the Q_{par} light field were compared to those considering the 7 diel patterns applied at particular depth and time intervals over the season (indicated in Fig. 7), significant differences of ± 30% were apparent throughout the water column (Fig. 11A). This difference was found despite the attempt over the season to center sample collection around solar noon. Water-column productivity was overestimated by instantaneous P-I parameter estimates most of the season, with the significant exception being the period in mid-January when a population of cryptophytes dominated the water column.

Diel-corrected daily productivity estimates for this study were further compared to those based solely on midday P-I parameter values (Fig. 11B). Noon-based estimates simulate synoptic coverage and could be comparable to estimates made from satellite measurements collected on fixed time intervals. Similar to the instantaneous P-I parameter estimates, noon-based productivity overestimated diel-corrected production an

average of ca. 20%. As with the instantaneous estimates, the minimum photosynthetic potential for Pattern III occurred at solar noon and noon-based productivity showed an underestimation of 37% for the near-surface cryptophyte population during January.

Table 1 summarizes results of the diel-corrected productivity compared productivity estimates based on instantaneous P-I parameters and midday values for different time scales over the season at Sta B. Most notable are the high differences between the diel-corrected and the midday productivity estimates over all time intervals (column E). Differences between the diel-corrected and the instantaneous productivity estimates (column C) were lower and tended to increase as the time interval was shortened. Interestingly, diel correction of instantaneous productivity data integrated over the season resulted in only a 7% difference.

DISCUSSION

The high-resolution data derived from our 1991/1992 austral spring/summer monitoring of LTER Station B documents the high variability in primary productivity for this coastal region on time scales ranging from hours to seasons. While previous

studies in the Antarctic have reported diel variation in photosynthesis (Rivkin and Putt 1988) and productivity on longer time scales (Horne et al. 1969; Whitaker 1982; Rivkin 1991), this is one of the first studies to integrate results across these time scales. In doing so, we were able to resolve the significance of hourly, daily, and weekly variations on subseasonal and seasonal primary productivity estimates. Furthermore, we were able to elucidate some of the underlying phytoplankton group-specific photophysiological characteristics that contributed to the observed temporal variability in primary production and associated effects on chemical and optical properties of the water column. Lastly, on time scales of a few days to seasons, we documented the close biological-physical coupling between phytoplankton productivity and water-column stability at this long-term ecosystem monitoring site. The format for data analyses presented here has been repeated for the two subsequent years (1992/93 and 1993/94) in order to test the robustness of our seasonal observations from one year to the next.

Diel periodicity of photosynthesis. Diel periodicity of photosynthesis at LTER Sta B was observed throughout the sampling period, with significant temporal variability in timing of peak photosynthetic potential (maxP_{max}) over the day.

Photosynthetic potentials for phytoplankton at Sta B varied up to 55 % of the maximum over the day and the timing of the maximum ranged between 05:00 to 17:00 LT over the season. Similar results for Antarctic diatoms have been found in McMurdo Sound, with the maximum photosynthetic potential varying up to 80% of the maximum over the day (Rivkin and Putt 1988). The timing of the maximum for the McMurdo diatoms shifted from midday to midnight and was suggested to be dependent on the change in photoperiod during the spring/summer transition. Diel periodicity of photosynthesis at Sta B, however, did not change with photoperiod, but appeared to be mostly consistent with changes in phytoplankton community composition throughout the season. Previous work has shown a species-specific diel response in diatoms isolated from McMurdo Sound (Rivkin and Putt 1988), further suggesting that diel patterns vary with community composition changes.

Temporal dynamics at Sta B showed that the community composition changes were dependent on the water-column stability and water-mass type (Moline et al. 1996). Spatial studies in the Southern Ocean have reported similar findings with single species dominance associated with particular regions and water masses (Sommer 1988; Estrada and Delgado 1990; Mura et al. 1995). The majority of primary productivity

measurements made in the Antarctic are spatial studies crossing many different water types and phytoplankton communities, with sampling occurring at different times of day and without opportunities to determine diel variations in productivity parameters. If, as this study suggests, diel periodicity is shown to be largely dependent on community composition, the absence of these diel measurements in diverse waters may have a very significant impact upon the calculated production estimates and interpretation of the data. The greatest effects would be seen in communities which show a large variation in daily potential photosynthetic response and have a diel maximum that is offset from time of sampling.

Although diel periodicities of photosynthesis in this study were closely coupled to the community composition, there was evidence to indicate that periodicity was also related to the mixing regimes. Diel patterns within a fixed phytoplankton community were subtly different if surface and Chl a max communities were separated by a pycnocline. During the bloom, surface and Chl a max samples were collected from the FML and the UML, respectively, and different diel patterns were found at the two depths (Fig. 7). This was also the case on the 10th of February (JD 41) when the depth of the UML shallowed to ca. 35 m. These differences in periodicity were found with no apparent difference in the community

composition (Fig. 6) and may have been a result of unique physical conditions (i. e. salinity, temperature) existing within the two layers. Over the course of this study, when both the surface and Chl a max samples were taken from the same mixed layer (i. e. FML) the diel periodicities displayed the same patterns.

Knowledge of diel periodicity in carbon fixation significantly increased the accuracy of productivity estimates over time scales ranging from a day to several weeks. The specific timing and diel variation in photosynthetic potential over the season at Sta B was shown to alter production estimates by ± 30% or greater on any given day during the season (Fig. 11, Table 1). The largest effect was seen for cryptophyte populations when the magnitude of photosynthetic potential was high (55%) and the timing of the maximum was furthest from local solar noon. With the effect of diel periodicity on daily estimates as high as ± 30%, there was a potential for a large effect on the time-integrated estimates. For the present study, however, the effect of diel periodicity on weekly, monthly and seasonally integrated productivity was less (ca. 10%) resulting from the combination of over- and underestimates (Table 1). Previously reported potential effects of diel periodicity on productivity measurements for temperate oceans (Harding et al. 1982;

Prézelin et al. 1987; Smith et al. 1987; Prézelin and Glover 1991) and the Southern Ocean (Rivkin 1987) agree well with the range reported here, further emphasizing the importance for diel correction of instantaneous measurements, especially during periods of high productivity.

High sampling frequency provided robust determinations of time-integrated primary productivity. Recently, Taylor and Howes (1994) documented the effect of sampling frequency on seasonal primary productivity estimates for a temperate coastal embayment. They showed that by sampling on intervals of 5 days or less (as in the present study), the sampling-frequency-induced (SFI) error was equivalent to the error limit of the analytical method. However, sampling intervals on the order of 14 to 30 days, as in many Antarctic studies, produced an SFI error of ± 35%. According to Taylor and Howes (1994), studies such as Whitaker (1982) with five samples taken over a 100 day period, would have estimated SFI errors of ca. ± 30%. A study by Horne et al. (1969) at the same location, sampling every 5.2 days, would have an estimated SFI ca. ± 5%. Similarly, error estimates for this study due to sampling frequency would be below 5%. SFI errors, however, are dependent on the variability in the system measured. The above estimates are based on the variability in

the system measured by Taylor and Howes (1994), and therefore, do not necessarily reflect the effect of sampling frequency in Antarctic coastal waters.

Simulated in situ productivity for Sta B was measured on time scales not previously measured in the Antarctic (2 to 3 day intervals) and is adequately resolved to examine the SFI error. In order to estimate the SFI error at Sta B, the measured depth-integrated daily productivity was subsampled at different intervals over the season. The primary productivity measured for this study (135 g C m^{-2}) on 2- to 3-day intervals was considered to be the 'true' productivity and used as the reference for estimates made for the different sampling frequencies. Sampling intervals, ranging from 4 to 20 days, were applied to the measured data, starting from the first day of sampling in December, 1991. The starting time for each subsampling interval was then sequentially moved one day later over a range of fifteen days, resulting in fifteen data subsets. These fifteen data subsets revealed the range of variability in the SFI errors for each sampling interval and accounted for the particular seasonal dynamics at Sta B. Productivity estimates were found to significantly vary based on sampling interval and the time at which the seasonal integration begins (Fig. 12). The percent difference from the measured productivity increased with the sampling interval

ranging from ca. ± 5% for the 4-day sampling interval to ± 50% for the 20-day sampling interval. The major bloom event in late December, 1991, responsible for ca. 65% of the seasonal production at Sta B, occurred on a time scale less than 3 weeks. By sampling on identical intervals (i.e. 20 days), the productivity associated with these events can be entirely missed. At Sta B, had we implemented a sampling interval of 20 days, we could have underestimated seasonal productivity by as much as 50% (Fig. 12). These SFI errors are generally higher than those reported by Taylor and Howes (1994) suggesting that the temporal variability in integrated primary productivity for Antarctic coastal regions may be higher than that for temperate coastal regions.

Incorporation of diel measurements in daily integrated rates of primary productivity, combined with high sampling frequency, provided accurate and reliable seasonal production estimates for coastal waters of the southern ocean. Given the effort and evaluations documented herein, we believe our estimates of primary production to be accurate and reliable for long-term monitoring. Daily rates of primary productivity at LTER Sta B varied consistently with biomass at discrete depths throughout the water column ($p<0.001$), for integrated biomass ($p<0.001$) and incident Q_{par} ($p=0.05$), with peak production occurring

during the massive coastal bloom. Q_{par}-dependent production rates during the bloom (0.75 g C m^{-3} d^{-1} and 6.3 g C m^{-2} d^{-1}) are some of the highest recorded for the Antarctic. Blooms, such as this one, are not uncommon near Anvers Is. (Shabica et al. 1977; Krebs 1983; Holm-Hansen et al. 1989) and in other near-shore environments (Horne et al. 1969; Whitaker 1982). Previous studies have attributed elevated levels of biomass to enhanced water-column stability, low grazing pressure, and micro-element enrichment from land runoff (Holm-Hansen et al. 1989; Mitchell and Holm-Hansen 1991). Although there are no data in the present study to comment on possible micro-element enrichment, water-column stability was found to be a major factor responsible for high biomass and productivity at Sta B (Moline et al. 1996).

Pattern of seasonal change (spring bloom, mid summer low productivity, fall increase) looks remarkably like generalized changes occurring at temperate latitudes. Here, however, the observed changes over the 1991/1992 season were driven by very different patterns of physical/chemical/optical forcing than those described for temperate latitude seasonal succession of phytoplankton (Harris and Piccinin 1980, Harris 1986). As detailed in Moline et al. (1996), the mechanisms for enhanced water-column stability initiating the bloom formation were a combination of ice/snow meltwater lens and decreased wind

speeds. Light and nutrient limitation set the upper limit of biomass accumulation and productivity during the bloom. After the bloom was advected from the region, a period of strong winds and intense mixing kept biomass and production low from mid January until the end of February. Unlike for temperate latitudes, grazing and nutrient limitation during this time were found not to influence the phytoplankton dynamics (Moline et al. 1996). The UML shallowed with decreasing winds in the end of February and resulted in increased productivity and another significant but less intense bloom in March, 1992 (K. Habermann, pers. comm.). This pattern for productivity in the Antarctic has been found previously (Krebs 1983), suggesting not only similar driving forces but also a consistency in the timing of the various driving forces influencing the annual patterns. Interestingly, the seasonal productivity pattern observed in 1991/1992, and reported here, was not seen in preliminary findings from the 1992/1993 and 1993/1994 spring/summer seasons at LTER Sta B (data not shown), indicating the need for further analyses before generalizations can be made about seasonal patterns of productivity for coastal Antarctica.

Monthly and seasonal productivity estimates from Sta B were generally higher compared to other productivity time series data for Antarctic coastal regions (Table 2). Total

integrated productivity for the season was generally higher, but in the range reported by other studies for the same time interval. The trend of decreasing productivity from December through February held for all studies, but was highly variable. Comparing results of these different time-series studies is difficult and depends on methods, location of sampling, frequency of sampling and the materials used. With the exception of this study and Arrigo and McCain (1994), samples for the time-series studies listed in Table 2 were incubated in situ using borosilicate glass bottles. This material does not transmit light below ca. 324 nm, thus, decreasing exposure to ultraviolet radiation (UVR). Recent studies have quantified the effects of UVR on natural Antarctic phytoplankton populations, with emphasis on biologically damaging UVB radiation due to the decrease in stratospheric ozone (O_3) concentrations (Smith et al. 1992b; Prézelin et al. 1993a; Prézelin et al. 1994). Although the effects of decreasing O_3, and associated increases in UVB radiation, on integrated phytoplankton production have been estimated between 6 and 12% (Smith et al. 1992b), the effects of natural background UVR have been estimated to decrease daily surface production by 60-70% (El-Sayed et al. 1987; Prézelin et al. 1994) and integrated production by ca. 23% (Boucher 1994). Inhibition of primary production by UVR is not included for any of the estimates listed in Table 2, and is

beyond the scope of this study. It is, however, potentially important when deriving and comparing seasonal productivity estimates (Boucher and Prézelin, 1996).

CONCLUDING REMARKS

We have quantified the seasonal carbon fixation for an Antarctic coastal site and have documented the large temporal variability associated with these highly productive environments. We have also shown that high-frequency sampling strategies, which include some accommodation for diel photosynthetic periodicity, are prerequisites for accurate determinations of seasonal primary production in the Southern Ocean. It is clear that before long term (i. e. years to several decades) 'signals', which indicate trended changes in primary production, in any region of the ocean brought on by climate change can be irrefutably determined, some knowledge of the 'noise' reflecting significant variations on shorter time scales (days, months, seasons) is required. Addressing sources of potentially large errors, such as diel photosynthetic periodicity and sampling frequency, in productivity estimates, helps to better define the natural variability in the ecosystem, and

provides a baseline for future interpretation of long-term trends in phytoplankton dynamics in the Southern Ocean.

ACKNOWLEDGEMENTS

N. Boucher, P. Handley, T. Newberger, K. Seydel, K. Scheppe, and the ASA personnel at Palmer Station are acknowledged for their assistance in data collection during the field season. I thank R. Bidigare and M. Ondrusek for generously providing HPLC training and pigment standards. N. Boucher and H. A. Matlick provided valuable technical assistance during the analyses of data. Funding was provided by the United States National Science Foundation, Office of Polar Programs (grant DPP 90-901127 to B. B. Prézelin). This chapter is Palmer LTER publication number 48.

LITERATURE CITED

Arrigo KR, McCain CR (1994) Spring phytoplankton production in the Western Ross Sea. Science 266: 261-263

Bidigare RR, Schofield O, Prézelin BB (1989) Influence of zeaxanthin on quantum yield of photosynthesis of *Synechococcus* clone WH7803 (DC2). Mar Ecol Prog Ser 56: 177-188

Bidigare RR, Iriarte JL, Kang S-H, Ondrusek ME, Karentz D, Fryxell GA (1995) Phytoplankton: Quantitative and qualitative assessments. In Ross R, Hofmann E, Quetin L (eds) Foundations for Ecosystem Research in the Western Antarctic Peninsula Region. Antarctic Research Series, American Geophysical Union, Washington, D.C. In press

Bodungen B Von, Smetachek V, Tilzer MM, Zeitzschell B (1986) Primary production and sedimentation during spring in the Antarctic Peninsula region. Deep-Sea Res 33: 177-194

Boucher NP (1994) Antarctic phytoplankton primary production under enhanced flux of ultraviolet radiation: a bio-optical approach. PhD Thesis, U. of California, Santa Barbara

Boucher NP, Prézelin BB (1996) Spectral modeling of UV inhibition of in situ Antarctic primary production using a

newly derived biological weighting function. Photochem Photobio, in press

Caceci MS, Cacheris WP (1984) Fitting curves to data. Byte 9: 340-362

El-Sayed SZ, Weber LH (1982) Spatial and temporal variations in phytoplankton biomass and primary production in the Southwest Atlantic and the Scotia Sea. Polar Biology 1: 83-90

El-Sayed SZ, Biggs DC, Holm-Hansen O (1983) Phytoplankton standing crop, primary productivity, and near-surface nitrogenous nutrient fields in the Ross Sea, Antarctica. Deep-Sea Res 30: 871-886

El-Sayed SZ, Stephens FC, Bidigare RR, Ondrusek ME (1987) Effects of ultraviolet radiation on Antarctic marine phytoplankton. In: Kerry KR, Hempel G (eds) Antarctic Ecosystems. Springer-Verlag, Berlin pp 379-385

Estrada M, Delgado M (1990) Summer phytoplankton distributions in the Weddell Sea. Polar Biology 10: 441-449

Harding LW, Prézelin BB, Sweeney BM, Cox JL (1982) Primary productivity as influenced by diel periodicity of phytoplankton photosynthesis. Mar Biol 61: 95-105

Harris GP (1986) Phytoplankton Ecology: Structure, Function and Fluctuation. Chapman and Hall Ltd., London pp 383

Harris GP, Piccinin BB (1980) Physical variability and phytoplankton communities. IV. Temporal changes in the phytoplankton community of a physically variable lake. Arch Hydrobiol 89: 447-73

Helbling WE, Villafañe VE, Holm-Hansen O. (1995) Variability of phytoplankton distribution and primary production around Elephant Island, Antarctica, during 1990-1993. Polar Biology 15: 233-246

Holm-Hansen O, El-Sayed SZ, Franceschini GA, Cuhel RL (1977) Primary productivity and the factors controlling phytoplankton growth in the Southern Ocean. In: Llano GA (ed) Adaptations Within Antarctic Ecosystems. Gulf, Houston pp 11-50

Holm-Hansen O, Mitchell BG, Hewes CD, Karl DM (1989) Phytoplankton Blooms in the Vicinity of Palmer Station, Antarctica. Polar Biology 10: 49-57

Holm-Hansen O, Mitchell BG (1991) Spatial and temporal distribution of phytoplankton and primary production in the western Bransfield Strait region. Deep-Sea Res 38(8-9A): 961-980

Horne AJ, Fogg GE, Eagle DJ (1969) Studies in situ of the primary production of an area of inshore Antarctic Sea. J Mar Biol Ass UK 49: 393-405

Kamykowski D, Zentara S-J (1989) Circumpolar plant nutrient covariation in the Southern Ocean: patterns and processes. Mar Ecol Prog Ser 58: 101-111

Krebs WN (1983) Ecology of neritic marine diatoms, Arthur Harbor, Antarctica. Micropaleontology 29(3): 267-297

Mitchell BG, Holm-Hansen O (1991) Observations and modeling of the Antarctic phytoplankton crop in relation to mixing depth. Deep-Sea Res 38(8-9A): 981-1007

Moline MA, Prézelin BB (1994) Palmer LTER: Impact of a large diatom bloom on macronutrient distribution in Arthur Harbor during austral summer 1991-1992. Ant J U S. 29(5): 217-219

Moline MA, Prézelin BB, Schofield O, Smith RC (1996) Temporal dynamics of coastal Antarctic phytoplankton: Environmental driving forces and impact of a 1991-1992 summer diatom bloom on the nutrient regimes. In Battaglia B, Valencia J, Walton DWH (eds) Antarctic Communities. Cambridge University Press. In press

Morel A (1991) Light and marine photosynthesis: a spectral model with geochemical and climatological implications. Prog Oceanog 26: 263-306

Mura MP, Satta MP, Agusti S (1995) Water-mass influences on summer Antarctic phytoplankton biomass and community structure. Polar Biology 15: 15-20

Neale PJ, Richerson PJ (1987) Photoinhibition and the diurnal variation of phytoplankton photosynthesis, I, Development of a photosynthesis-irradiance model from studies of in situ responses. J Plankton Res 9: 167-193

Prezelin BB (1992) Diel periodicity in phytoplankton productivity. In Berman T, Gons HJ, Mur LR (eds) The Daily Growth Cycle of Phytoplankton. Kluwer Academic Publishers, Dordrecht. Hydrobiologia 238: 1-35

Prézelin BB, Bidigare RR, Matlick HA, Putt M, VerHoven B (1987) Diurnal patterns of size-fractioned primary productivity across a coastal front. Mar Biol 96: 563-574

Prézelin BB, Glover HE, VerHoven B, Steinberg DK, Matlick HA, Schofield O, Nelson NB, Wyman M, Campbell L (1989) Blue-green light effects on light-limited rates of photosynthesis: relationship to pigmentation and productivity estimates from the Sargasso Sea. Mar Ecol Prog Ser 54: 121-136

Prézelin BB, Glover HE (1991) Variability in time/space estimates of phytoplankton biomass and productivity in the Sargasso Sea. J Plankton Res 13S: 45-67

Prézelin BB, Boucher NP, Moline MA, Stephens E, Seydel K, Scheppe K (1992a) Palmer LTER program: Spatial variability in phytoplankton distribution and surface

photosynthetic potential within the peninsula grid, November 1991. Ant J U S 27(5): 242-245

Prézelin BB, Moline MA, Seydel K, Scheppe K (1992b) Temporal variability in HPLC pigmentation and inorganic nutrient distribution in surface waters adjacent to Palmer Station, December 1991-February 1992. Ant J U S 27(5): 242-245

Prézelin BB, Boucher NP, Smith RC (1993a) Daytime of UV-A and UV-B inhibition of photosynthetic activity in Antarctic surface waters. In: Yamamoto HY, Smith CM (eds) Photosynthetic Responses to the Environment, Current Topics in Plant Physiology. Amer Soc of Plant Physiologists 2: 150-155

Prézelin BB, Nelson NB, Schofield O, Boucher NP, Smith RC, Waters K, Bidigare RR, Lewis MR, Baker KS, Stegmann P (1993b) Bio-optics in U. S. JGOFS: Handbook of bio-optical nomenclature. U. S. JGOFS Planning Report #18. U. S. JGOFS Planning Office, Woods Hole, pp 159-165

Prézelin BB, Boucher NP, Smith RC (1994) Marine primary production under the influence of the Antarctic ozone hole: *Icecolors '90.* In: Weiler S, Penhale P (eds) Ultraviolet Radiation and Biological Research in Antarctica. American Geophysical Union, Washington D. C., 62: 159-186

Rivkin RB (1987) Diel periodicity of photosynthesis in polar phytoplankton: Potential influence on primary production. Science 238: 1285-1288

Rivkin RB (1991) Seasonal patterns of planktonic production in McMurdo Sound, Antarctica. Amer Zool 31: 5-16

Rivkin RB, Putt M (1988) Seasonal pattern of diel periodicity in photosynthesis by polar phytoplankton: Species-specific responses. J Phycol 24: 369-376

Ross RM, Quentin LB (1992) Palmer long-term ecological research (LTER): An overview of the 1991-1992 season. Ant J U S 27: 235-236

Sakshaug E, Slagstad D, Holm-Hansen O (1991) Factors controlling the development of phytoplankton blooms in the Antarctic Ocean-A mathematical model. Mar Chem 35: 259-271

Schofield O, Prézelin BB, Smith RC, Stegmann PM, Nelson NB, Lewis MR, Baker KS (1991) Variability in spectral and nonspectral measurements of photosynthetic light utilization efficiencies. Mar Ecol Prog Ser 78: 253-271

Schofield O, Moline MA, Prézelin BB (1994) Photoadaptation in a coastal phytoplankton bloom and impact on the radiation utilization efficiency for carbon fixation. Ant J U S. 29(5): 214-216

Schofield O, Moline MA, Prézelin BB Variability of the maximum quantum yield for carbon fixation in Antarctic coastal waters. Limnol Oceanogr, submitted

Shabica SV, Hedgpeth JW, Park PK (1977) Dissolved oxygen and pH increases by primary production in the surface water of Arthur Harbor, Antarctica, 1970-1971. In: Llano GA (ed) Adaptations Within Antarctic Ecosystems. Gulf, Houston pp 83-97

Smith RC, Bidigare RR, Prézelin BB, Baker KS, Brooks JM (1987) Optical characterization of primary productivity across a coastal front. Mar Biol 96: 574-591

Smith RC, Prézelin BB, Bidigare RR, Baker KS (1989) Bio-optical modeling of photosynthetic production. Limnol Oceanogr 34: 1526-1546

Smith RC, Baker KS, Handley P, Newberger T (1992a) Palmer LTER program: Hydrography and optics within the peninsula grid, zodiac sampling grid during the 1991-1992 field season. Ant J U S 27: 253-255

Smith RC, Prézelin BB, Baker KS, Bidigare RR, Boucher NP, Coley T, Karentz D, MacIntyre S, Matlick HA, Menzies D, Ondrusek M, Wan Z, Waters KJ (1992b) Ozone depletion: ultraviolet radiation and phytoplankton biology in Antarctic water. Science 255: 952-959

Smith WOJ, Nelson DM (1985) Phytoplankton bloom produced by a receding ice edge in the Ross Sea: Spatial coherence with the density field. Science 277: 163-166

Smith WOJ, Sakshaug E (1990) Polar Phytoplankton. In: Smith WOJ (ed) Polar Oceanography: Part A: Physical Science, Part B: Chemistry, Biology, Geology. Academic Press, Inc. San Diego. pp 477-526

Sommer U (1988) The species composition of Antarctic phytoplankton interpreted in terms of Tilman's competition theory. Oecologia 77: 464-467

Taylor CD, Howes BJ (1994) Effect of sampling frequency on measurements of seasonal primary productivity and oxygen status in near-shore coastal ecosystems. Mar Ecol Prog Ser 108: 193-203

Wilson DL, Smith WO, Nelson DM (1986) Phytoplankton bloom dynamics of the western Ross Sea ice edge I: Primary productivity and species specific production. Deep-Sea Res 33: 1375-1387

Whitaker TM (1982) Primary production of phytoplankton off Signy Island, South Orkneys, the Antarctic. Proc R Soc Lond 214: 169-189

Zimmerman RC, SooHoo JB, Kremer JN, D'Argenio DZ (1987) Evaluation of variance approximation techniques of non-

linear photosynthesis-irradiance models. Mar Biol 95: 209-215

Table 1. Integrated production (g C m^{-2}) at Station B for various time intervals from December 1991 through Feburary 1992. Column A: P-I parameters vary over the day based on diel measurements; Column B: P-I parameters constant over the day at their time of sampling; Column C: percent difference between column A and B; Column D: P-I parameters constant over the day at midday values; Column E: percent difference between column A and D.

Time Interval	A Diel Corrected	B No Correction	C %difference (1-A/B)	D Midday Corrected	E %difference (1-A/D)
Season	134.6	144.8	+7.1	220.4	+38.9
Month					
Dec 91	79.2	88.4	+10.4	134.9	+41.3
Jan 92	36.0	36.4	+1.1	54.1	+32.7
Feb 92	19.3	20.0	+3.4	31.4	+36.3
Week					
21-28 Dec 91	36.0	30.3	+11.4	46.5	+34.8
21-28 Jan 92	1.0	1.1	+13.2	1.6	+32.4
21-28 Feb 92	12.1	12.3	+2.1	17.1	+27.9
Day					
24 Dec 92	2.8	3.1	+11.6	4.7	+41.3
24 Jan 92	0.1	0.1	+28.2	0.2	+47.7
24 Feb 92	2.6	2.6	-1.0	3.7	+29.8

Table 2. Time series data of coastal phytoplankton productivity reported for the Southern Ocean. Integrated productivity and monthly totals are included.

Reference/Location	Time Period From	Time Period To	Sampling Interval (days)	Integrated Total ($gC\ m^{-2}$)	December Total ($gC\ m^{-2}$)	January Total ($gC\ m^{-2}$)	February Total ($gC\ m^{-2}$)
Horne et al.1969 (S.Orkney Is.)	27 Jan 67	27 Feb 67	5.2	50.0	--	--	40.9
Whitaker, 1982	5 Dec 72	23 Feb 73	20.0	219.6	112.5	92.2	26.5
Whitaker, 1982 (S.Orkney Is.)	5 Dec 73	27 Feb 74	21.0	55.4	44.2	9.4	5.8
Rivkin, 1991 (McMurdo Sound)	5 Dec 85	5 Jan 86	5.1	39.7	39.7	--	--
RACER Sta 43† (Gerlache Strait)	22 Dec 86	27 Feb 87	22.3	74.1	--	38.0	19.8
RACER Sta 13† (Low Is.)	27 Dec 86	27 Feb 87	20.6	79.9	--	49.9	22.7
RACER Sta 48† (Bransfield Strait)	19 Dec 86	27 Feb 87	17.5	104.6	--	54.1	16.7
RACER Sta 39† (Livingston Is.)	25 Dec 86	27 Feb 87	21.3	57.4	--	28.6	15.8
Arrigo+McCain, 1994 (Victoria Land)‡	10 Dec 78	19 Feb 79	11.8	141	--	51.5	--
This Study (LTER Sta B)	5 Dec 91	27 Feb 92	**2.3**	**134.6**	**79.2**	**36.0**	**19.3**

†Holm-Hansen & Mitchell, 1991.
‡Modeled production from Coastal Zone Color Scanner (CZCS) imagery.

Figure 1. Location of LTER sampling station B (64° 46.45' S, 64° 03.27' W) with respect to Palmer Station and (inset) the Antarctic Peninsula.

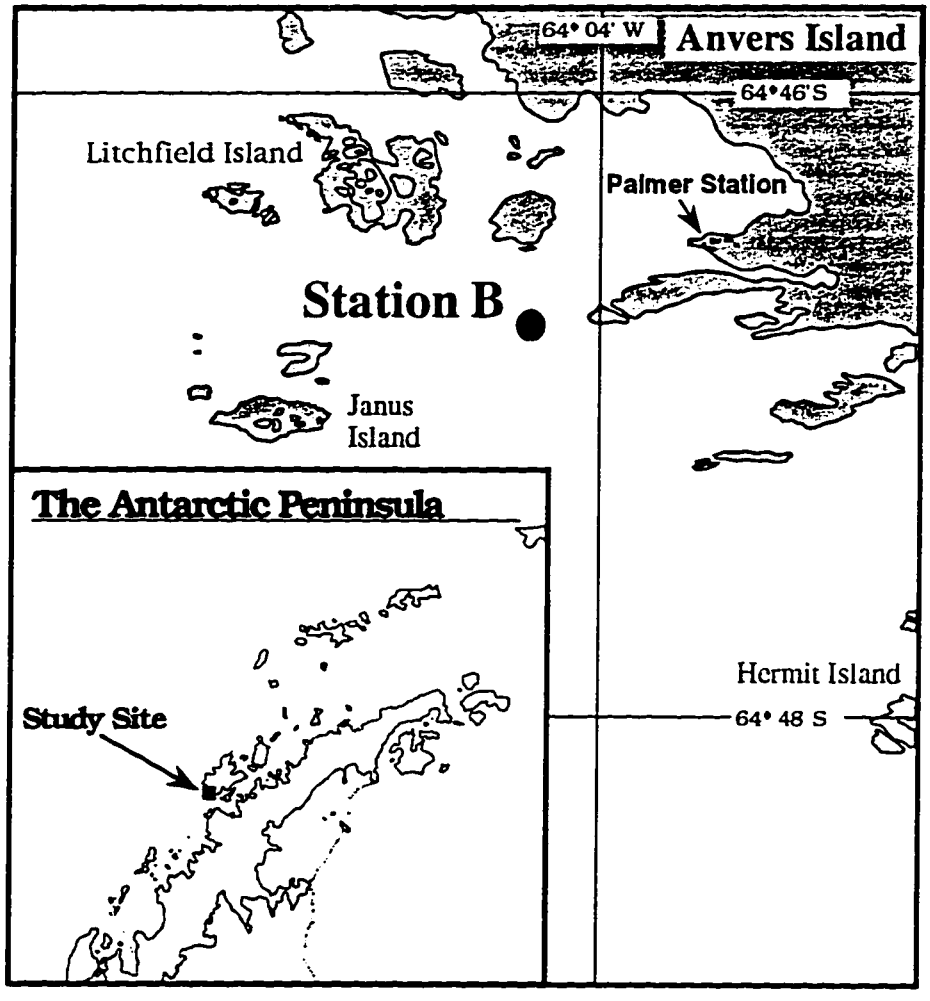
64° 04' W
Anvers Island
64°46'S
Litchfield Island
Palmer Station
Station B
Janus
Island
The Antarctic Peninsula
Hermit Island
Study Site
64° 48 S

Figure 2. Comparison of the normalized patterns for diel measurements of volumetric P_{max} for five dates between December 12, 1991 and January 7, 1992, when a diatom bloom dominated the phytoplankton assemblage at LTER Sta B. Each diel pattern is normalized to the peak value for P_{max} measured on that day, i. e. the daytime variation in the ratio P_{max}:maxP_{max} is plotted and compared for each diel sampling date. The solid line indicates a manual fit for the diel measurements and is used to time correct instantaneous measurements in order to calculate integrated daily rates of primary production (see text for details).

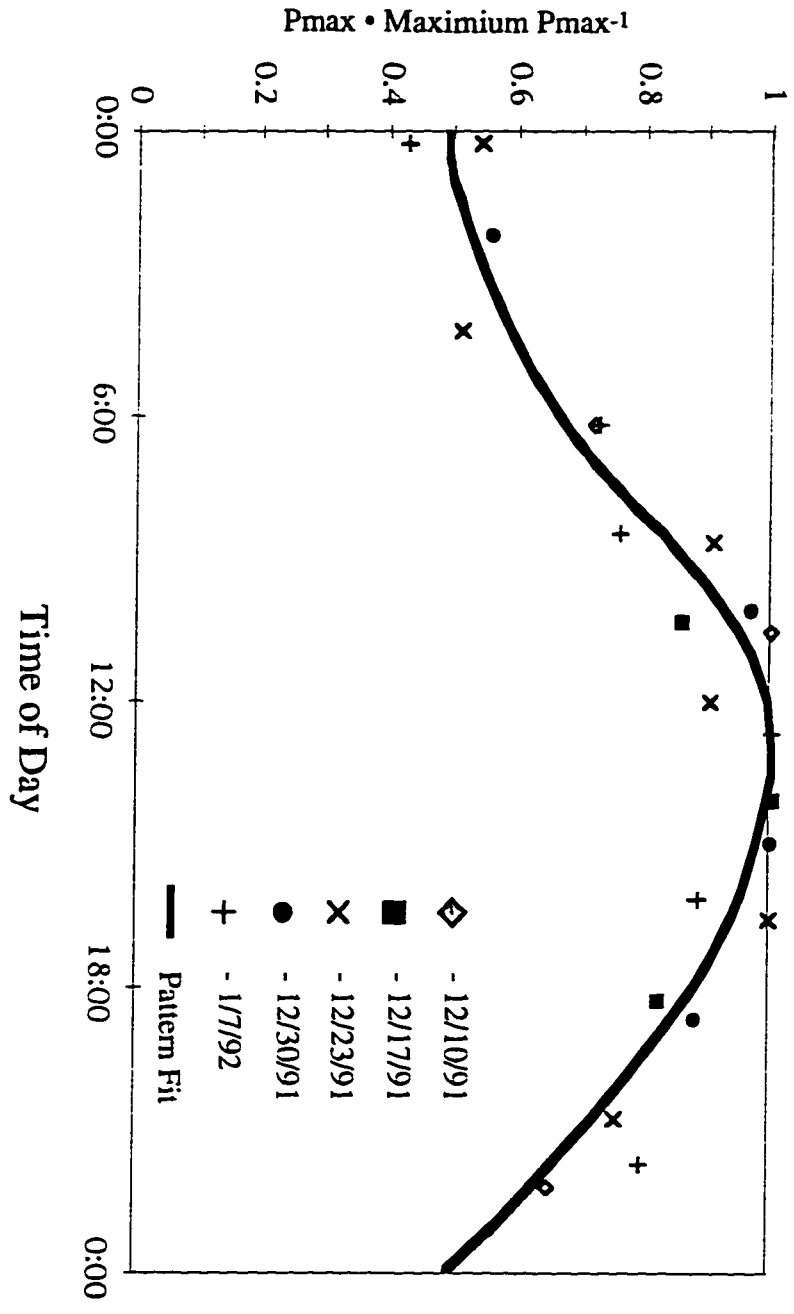
Pmax • Maximium Pmax-1
0
0.2
0.4
0.6
0.8
1
0:00
6:00
12:00
18:00
0:00
Time of Day
Pattern Fit
- 1/7/92
- 12/30/91
- 12/23/91
- 12/17/91
- 12/10/91

Figure 3. A) Seasonal changes in midday solar zenith angle (dashed line) and daylength (solid line) at the latitude (64° S) for Palmer LTER Sta B sampled between November 21, 1991 (JD 325) and February 27, 1992 (JD 058). B) Comparison of the seasonal changes in the measured (shaded area) and theoretical maximum (clear sky, dashed line) daily integrated Q_{par} ($E\ m^{-2}d^{-1}$) for Palmer Station during the late austral spring and summer of 1991/1992. C) Seasonal changes in the above-water ratio of measured:clear-sky flux of daily integrated Q_{par} Palmer LTER Sta B.

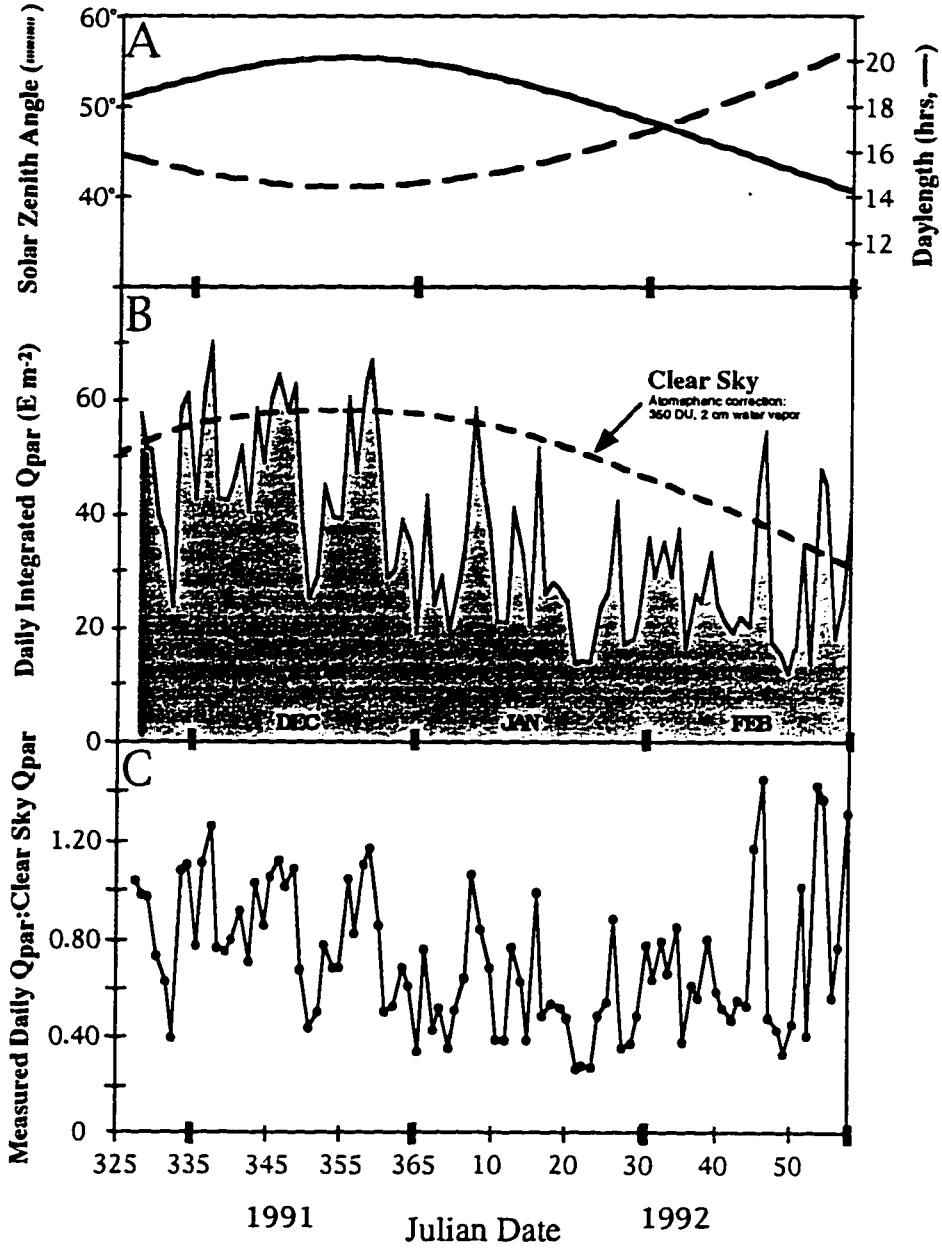
A
B
C
Solar Zenith Angle (——)
Daylength (hrs, —)
60°
50°
40°
20
18
16
14
12
Daily Integrated Qpar (E m-2)
Clear Sky
Atmospheric correction:
350 DU, 2 cm water vapor
60
40
20
0
DEC
JAN
FEB
Measured Daily Qpar:Clear Sky Qpar
1.20
0.80
0.40
0
325
335
345
355
365
10
20
30
40
50
1991
Julian Date
1992

Figure 4. Seasonal change in the depth distribution of (A) chlorophyll a (mg Chl a m^{-3}) and (B) percent Q_{par} (0^{+}) at LTER Sta B from November 21, 1991 to February 27, 1992. The distribution of discrete samples collected for Chl a determinations is shown by filled circles. The presence of significant pack ice (i. e. >50% coverage) is indicated by hatch bars. Note that contours of Chl a values in excess of 8 mg m^{-3} are not shown and that concentrations within the phytoplankton bloom were generally in excess of 20 mg m^{-3} (see text).

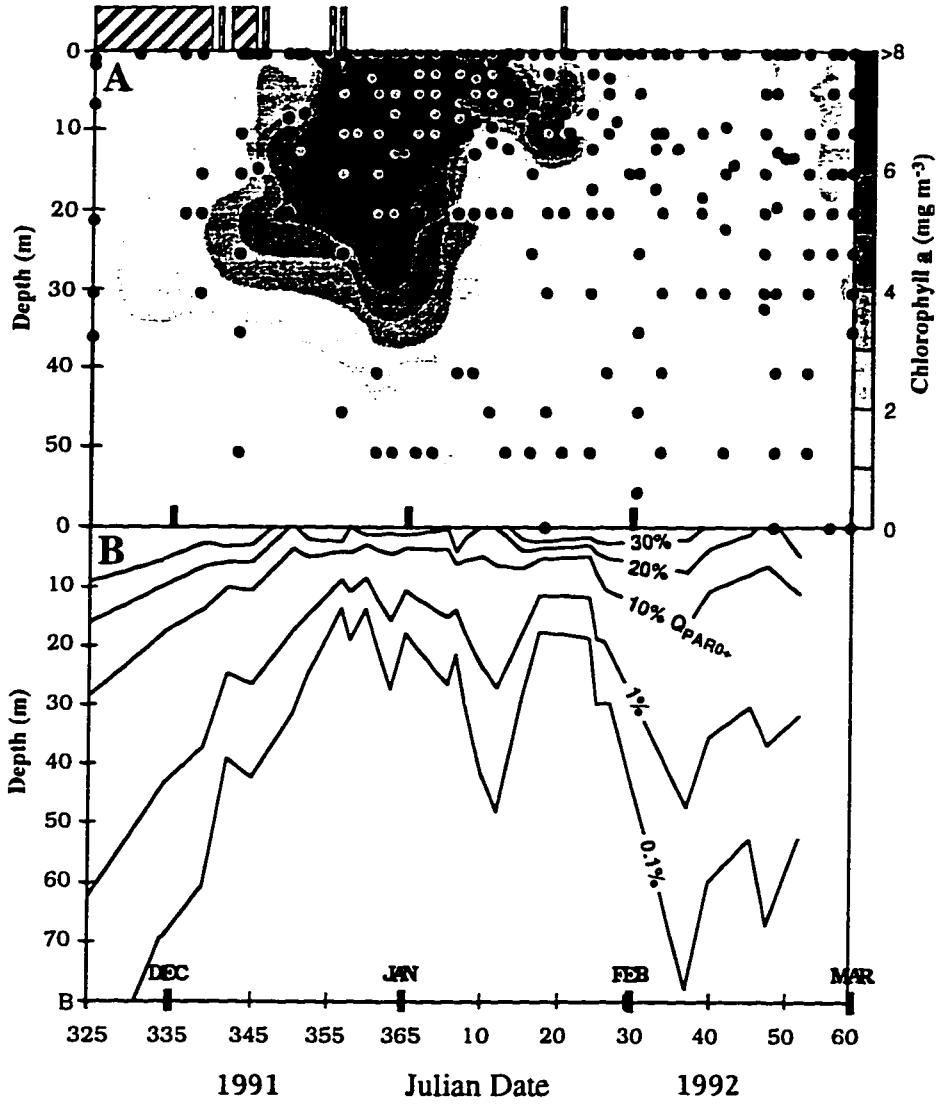
A
B
Depth (m)
Chlorophyll a (mg m-3)
30%
20%
10% QPAR0-
1%
0.1%
DEC
JAN
FEB
MAR
1991
Julian Date
1992

Figure 5. A) Seasonal variation in the in-water daily integrated Q_{par} at Palmer LTER Sta B from November 21, 1991 to February 21, 1992. B) Relationships between the 10% surface Q_{par} (solid squares) and 1% surface Q_{par} (open circles) light depths and the depth of the upper mixed layer (UML) at Palmer LTER Sta B. The UML was calculated using methods described in Mitchell and Holm-Hansen (1991).

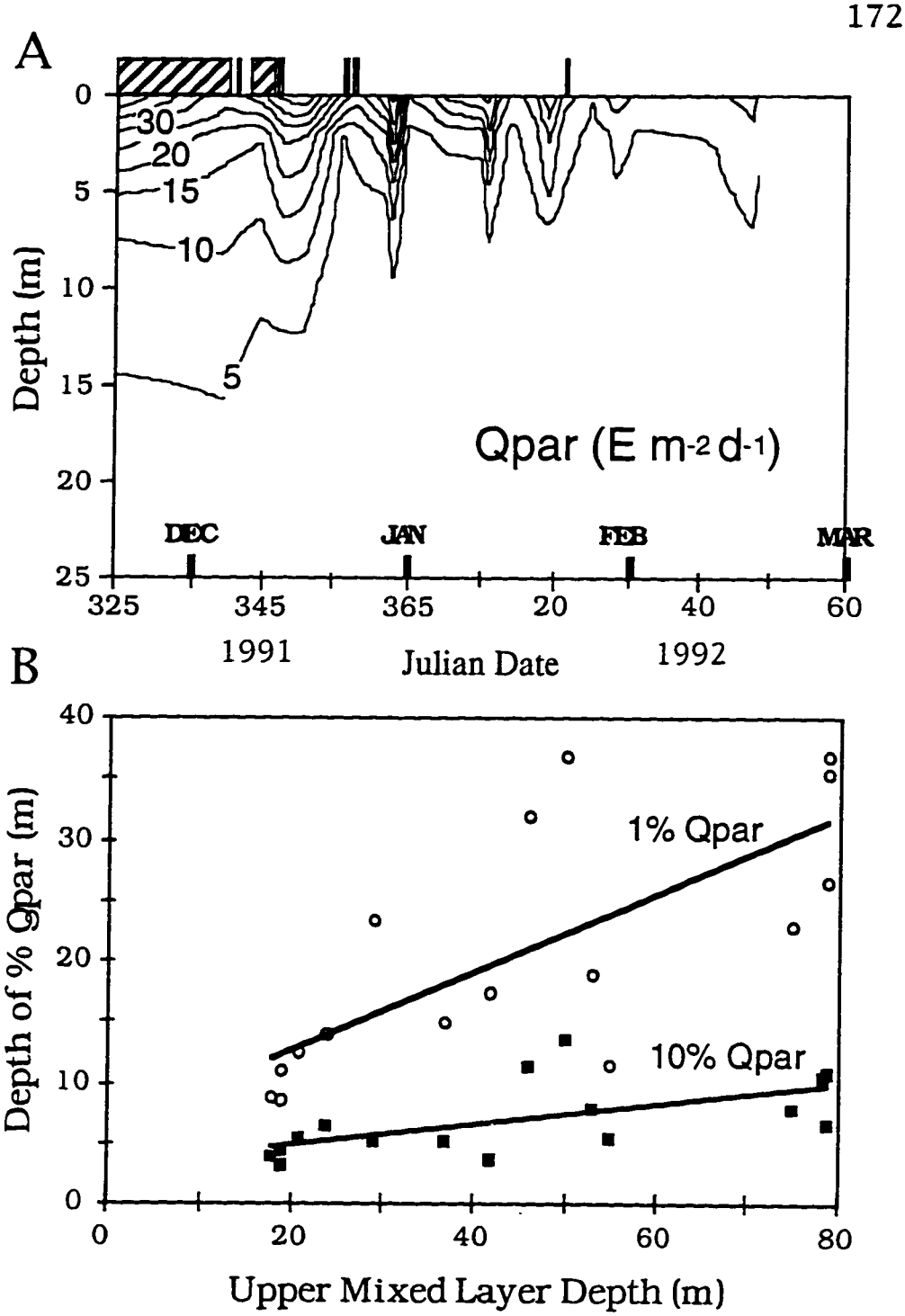
A
Depth (m)
0
5
10
15
20
25
30
20
15
10
5
Qpar (E m-2 d-1)
DEC
JAN
FEB
MAR
325
345
365
20
40
60
1991
Julian Date
1992
B
Depth of % Qpar (m)
40
30
20
10
0
1% Qpar
10% Qpar
0
20
40
60
80
Upper Mixed Layer Depth (m)

Figure 6. Seasonal change in dominant phytoplankton groups in surface and Chl a max communities at Palmer LTER Sta B from November 21, 1991 to February 27, 1992. A) Comparison of the fluctuations in surface and Chl a max phytoplankton biomass. B) Shifts in dominant phytoplankton groups in surface waters at LTER Sta B, as indicated by changing percent contribution of each of 4 chemotaxonomic marker carotenoids to the sum total of the 4 pigments. C) Same as B but for seasonal change in phytoplankton community composition within the Chl a max. Marker pigment include fucoxanthin for diatoms, alloxanthin for cryptophytes, 19'-hexanoylfucoxanthin for prymnesiophytes, and 19'-butanoylfucoxanthin for chrysophytes. Note that while surface samples were always at collected within 0.5 m of the surface, the Chl a max sampling depths varied between 5-20 m over the season (Fig. 7).

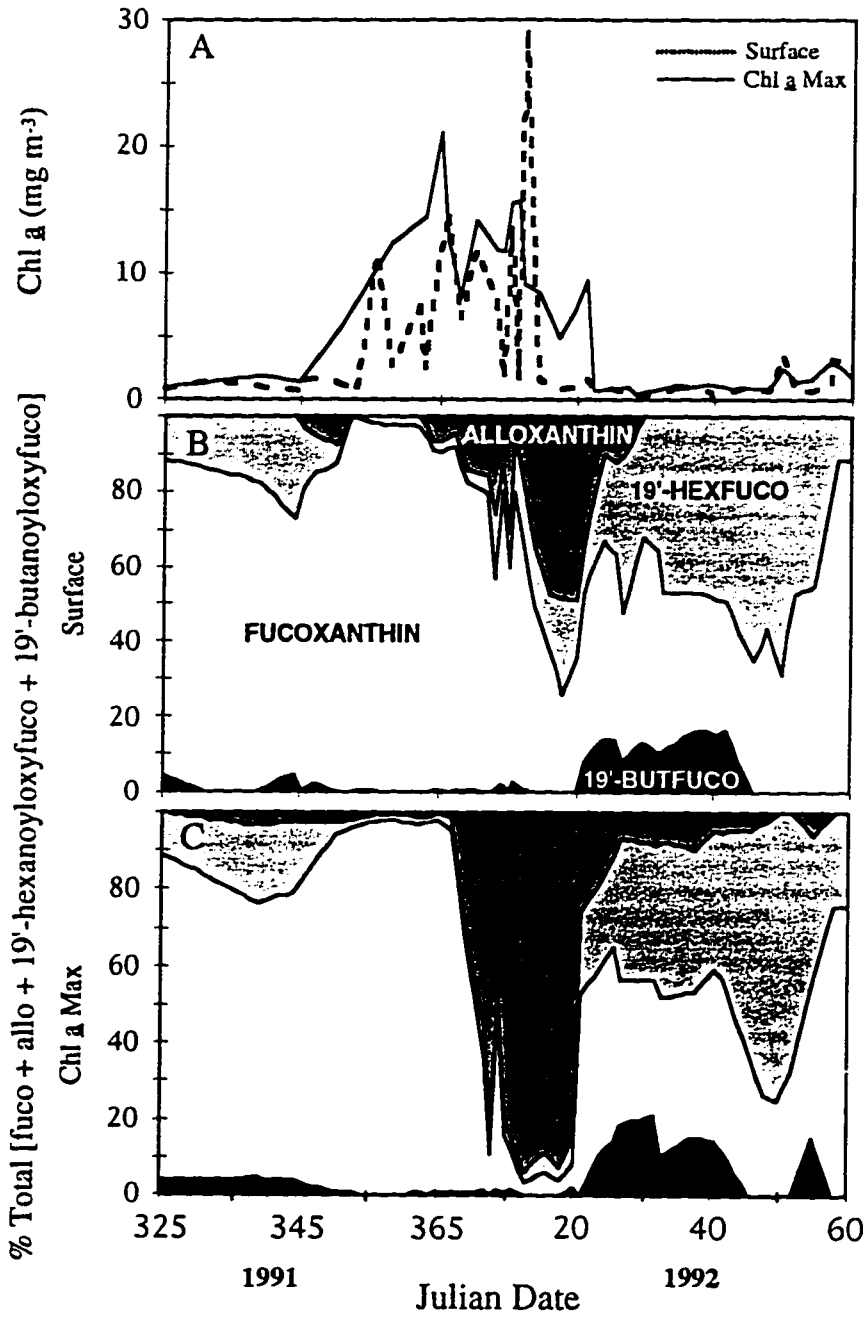
A
Surface
Chl a Max
Chl a (mg m-3)
30
20
10
0
B
ALLOXANTHIN
19'-HEXFUCO
FUCOXANTHIN
19'-BUTFUCO
Surface
80
60
40
20
0
C
Chl a Max
80
60
40
20
0
% Total [fuco + allo + 19'-hexanoyloxyfuco + 19'-butanoyloxyfuco]
325
345
365
20
40
60
1991
1992
Julian Date

Figure 7. Depth distribution of samples (all circles) collected for P-I curve determinations and calculations of simulated in situ productivity from December 5, 1991 to February 27, 1992. Large open circles represent the times and depths of sample collection from surface waters and the Chl a maxima for simulated in situ determinations of diel variations in P-I parameters. Overlaid are the calculated depths of the upper mixed layer (lower solid line) and fresher meltwater lens (upper solid line) (from Moline et al. 1996). Each shaded area indicates a composite of samples where a single diel pattern of variation in P-I parameters was applied to time correct instantaneous measurments to estimate daily integrated rates of primary production. Seven (I-VII) distinct patterns for diel variations in P-I parameters were resolved over the season (Figs. 8 & 9) and are shown here to illustrate which patterns were applied to which discrete samples.

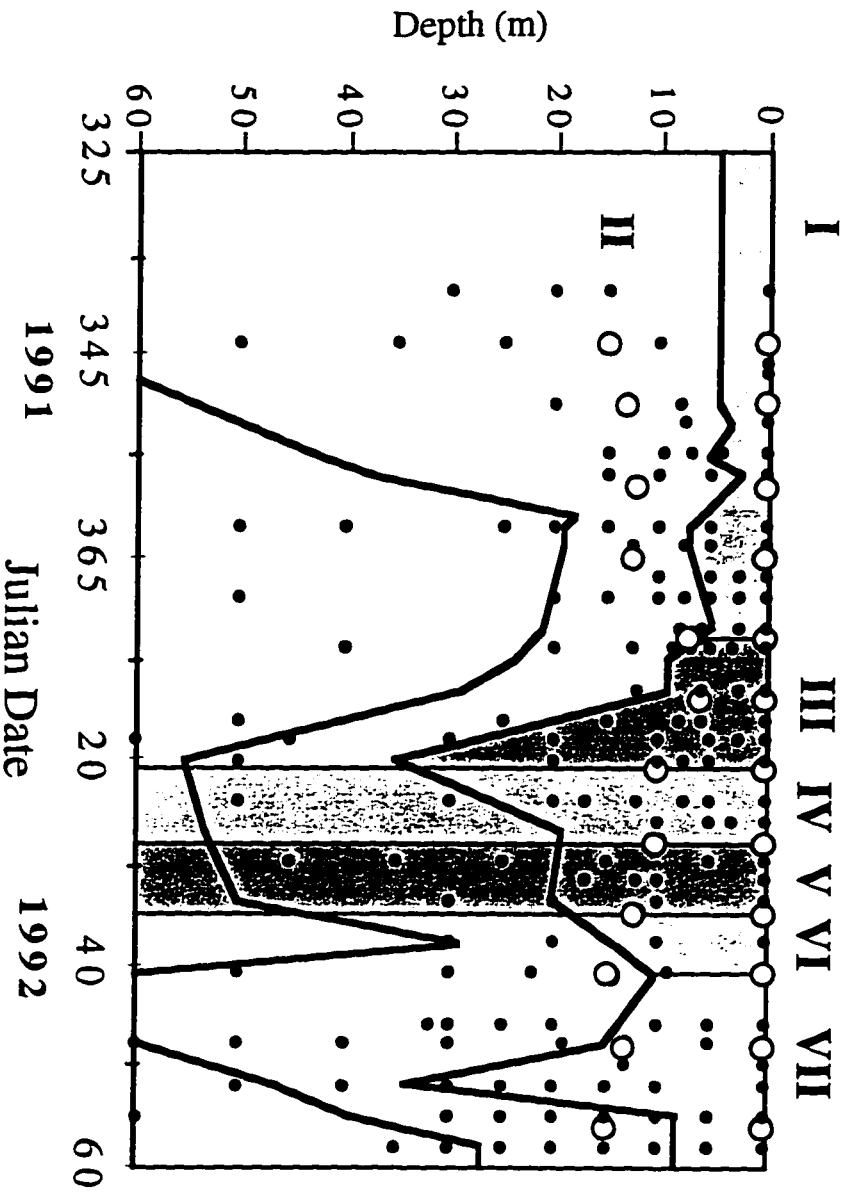
Depth (m)
0
10
20
30
40
50
60
I
II
III
IV
V
VI
VII
325
345
365
20
40
60
1991
Julian Date
1992

Figure 8. Diel patterns determined for P_{max}:maxP_{max} at LTER Sta B from December 10, 1991 though January 21, 1992. Pattern I is representative of early spring and diatom bloom samples collected above the FML. Pattern II is representative of diatom-dominated samples collected below the FML for the first 2 months of sampling. Pattern III is representative of the cryptophyte bloom that occurred within the FML in the middle of January 1992 (see Fig. 7). The mean daylength for each pattern is presented so that the relationship between the peak P_{max} activity and the timing of dawn/dusk and solar noon may be discerned.

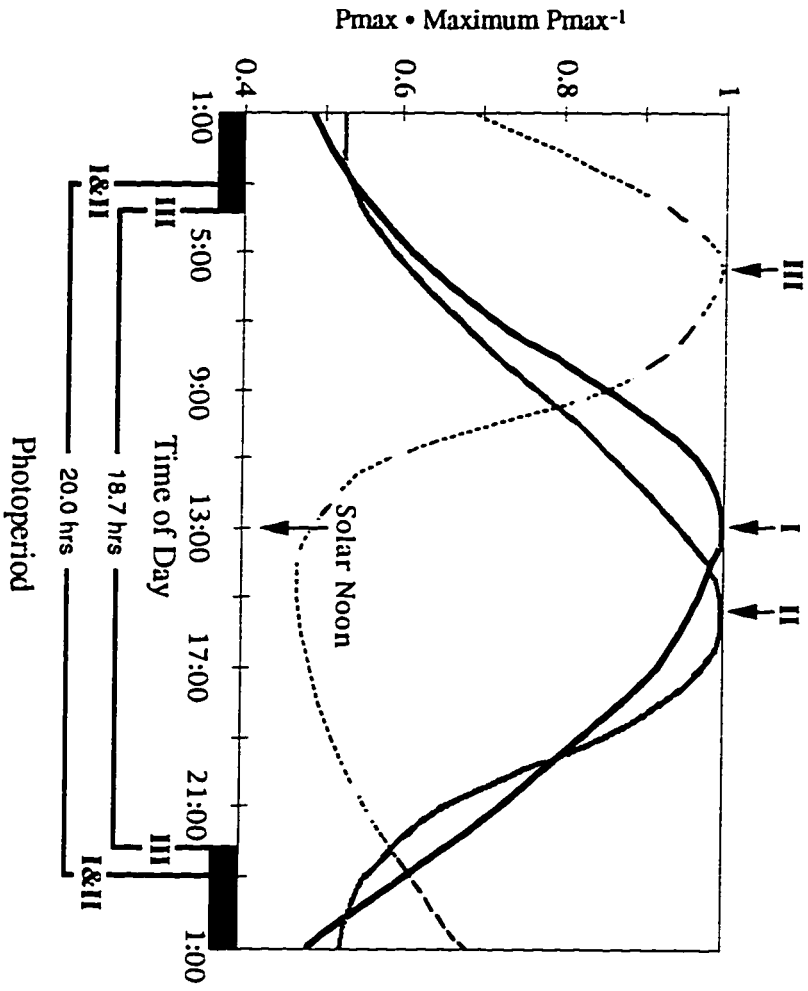
Pmax • Maximum Pmax-1
0.4
0.6
0.8
1
1:00
5:00
9:00
13:00
17:00
21:00
1:00
Time of Day
Solar Noon
I
II
III
III
I&II
18.7 hrs
III
I&II
20.0 hrs
Photoperiod

Figure 9. Diel patterns determined for P_{max}:maxP_{max} at LTER Sta B from January 21, 1992 though February 25, 1992 (see Fig. 7). Patterns IV, V, and VI are representative of mixed phytoplankton communities advected through the region during a strong wind mixing event. Pattern VII is representative of a the reemergence of a diatom-dominated phytoplankton community during late summer restratification of the water column. The mean daylength for each pattern is presented so that the relationship between the peak P_{max} activity and the timing of dawn/dusk and solar noon may be discerned.

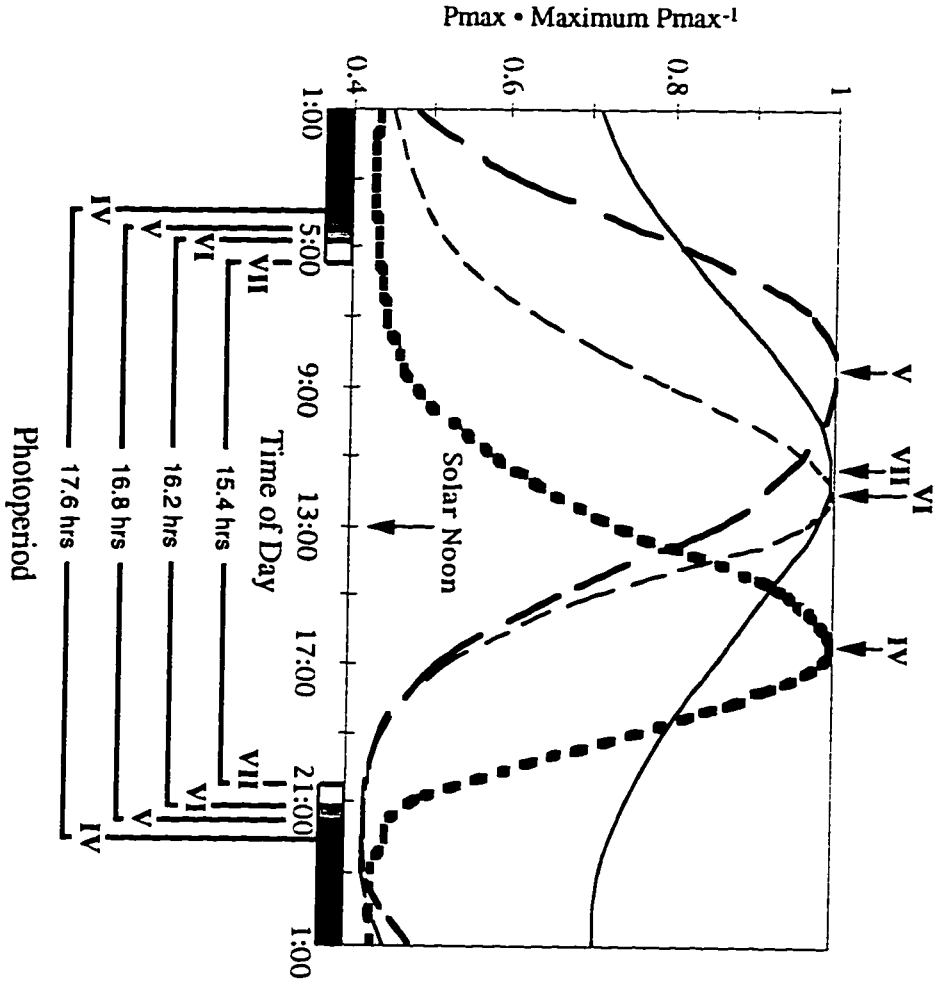
Pmax • Maximum Pmax-1
0.4
0.6
0.8
1
1:00
5:00
9:00
13:00
17:00
21:00
1:00
Time of Day
Solar Noon
V
VII
VI
IV
Photoperiod
IV
V
VI
VII
15.4 hrs
16.2 hrs
16.8 hrs
17.6 hrs
VII
VI
V
IV

Figure 10. A) Depth and time distribution of daily simulated *in situ* Q_{par}-based productivity over the austral summer of 1991-1992 at LTER Sta B. B) Seasonal changes in daily integrated watercolumn productivity, based on Q_{par}-dependent measurements of rates of carbon fixation.

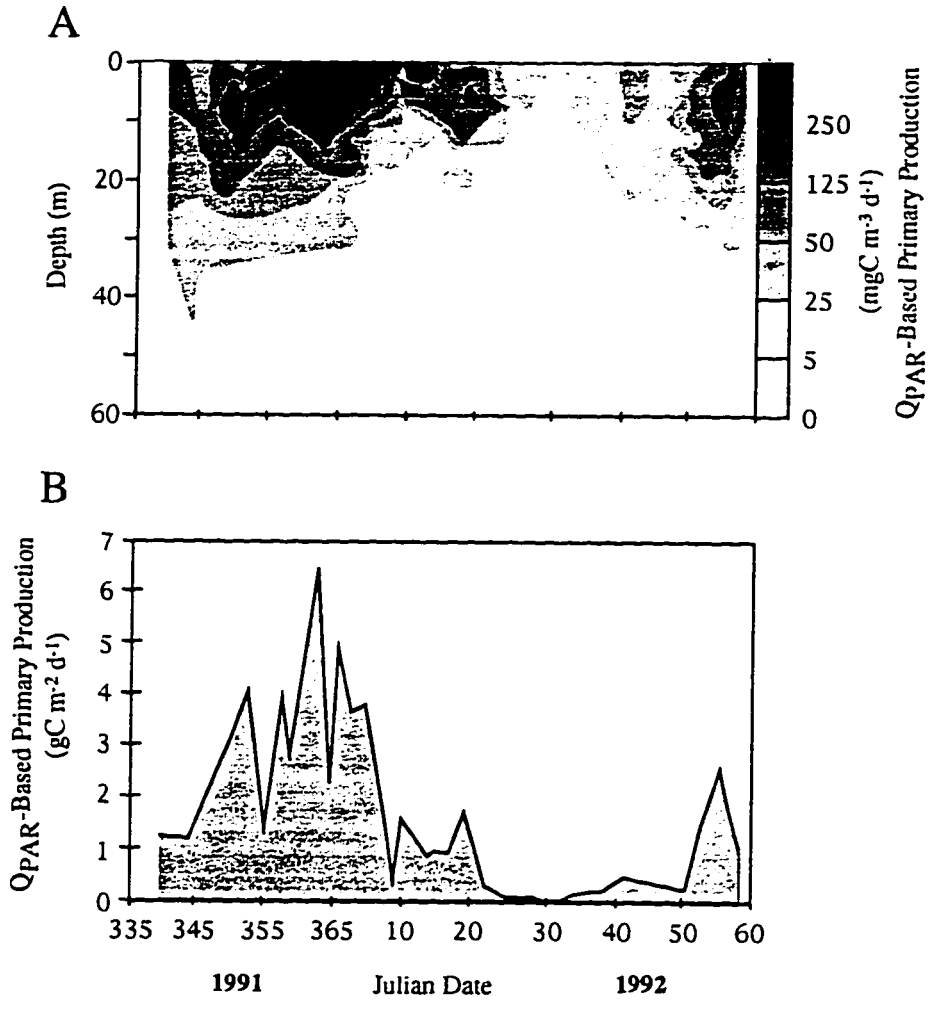
A
0
20
40
60
Depth (m)
250
125
50
25
5
0
(mgC m-3 d-1)
QPAR-Based Primary Production
B
7
6
5
4
3
2
1
0
QPAR-Based Primary Production
(gC m-2 d-1)
335 345 355 365 10 20 30 40 50 60
1991
Julian Date
1992

Figure 11. A) The depth and time distribution at LTER Sta B of the percent difference between estimates of daily primary productivity based solely on the instantaneous measurements *versus* those which have been time corrected for diel periodicity in P-I parameters. Positive values represent times and depths where production estimates based upon a single measurement made sometime between midmorning and late afternoon overestimate those measurements where diel periodicity in photosynthesis has been considered, and *visa versa.* B) Comparison of percent difference between estimates of daily integrated rates of primary production based solely on derived noon-time estimates of P-I parameters which are held constant over the day and those based upon estimates of diel variations in P-I parameters. The percent difference between the two productivity estimates was calculated for each of the seven different diel pattterns (Figs. 8 & 9) of photosynthesis resolved over the season at LTER Sta B.

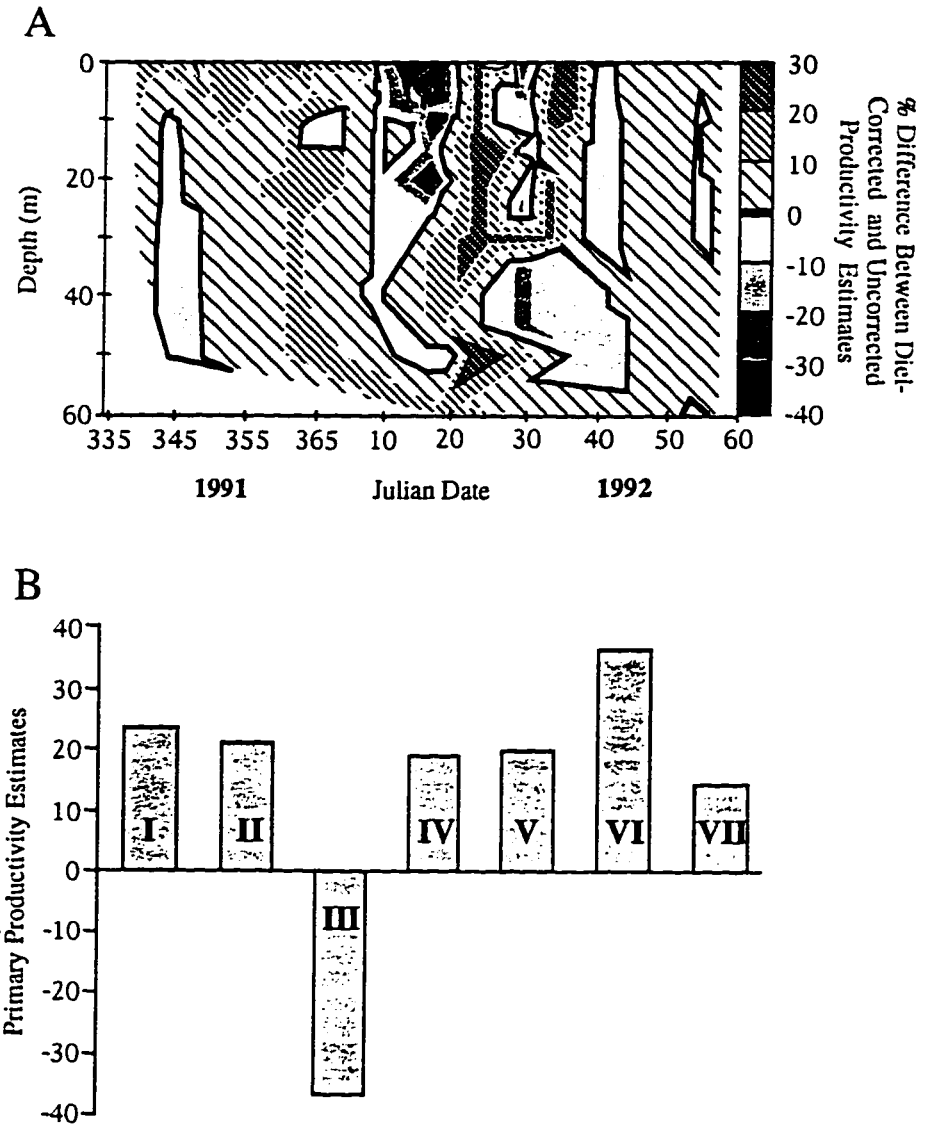
A
0
20
40
60
Depth (m)
335 345 355 365 10 20 30 40 50 60
1991
Julian Date
1992
30
20
10
0
-10
-20
-30
-40
% Difference Between Diel-Corrected and Uncorrected Productivity Estimates
B
40
30
20
10
0
-10
-20
-30
-40
% Discrepancy of Noon vs. Diel-Based Primary Productivity Estimates
I
II
III
IV
V
VI
VII

Figure 12. Examination of the effect of sampling frequency on the accuracy of estimates of primary productivity at LTER Sta B during the austral summer of 1991-1992. The mean (closed circles), standard deviation (open box) and range (vertical lines) of the percent difference from the measured seasonal productivity (135 g C m^{-2}) are shown for sampling intervals ranging from every 2.3 days to every 20 days.

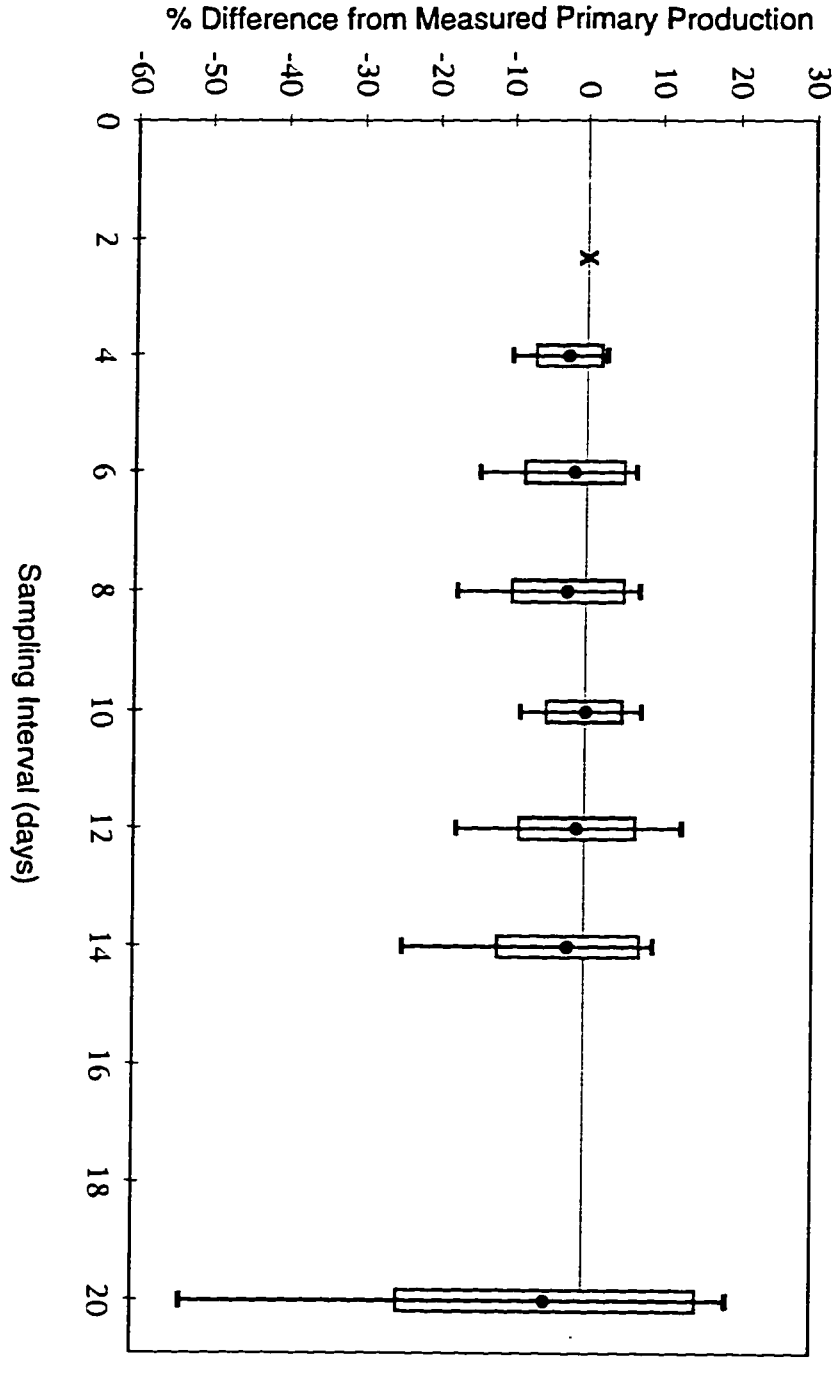
% Difference from Measured Primary Production
-60
-50
-40
-30
-20
-10
0
10
20
30
Sampling Interval (days)
0
2
4
6
8
10
12
14
16
18
20

CHAPTER IV

Palmer LTER 1991-1994: Long-term monitoring and analyses of physical factors regulating variability in coastal Antarctic phytoplankton biomass, *in situ* productivity and taxonomic composition over subseasonal, seasonal and interannual time scales

ABSTRACT

A 3 year high-resolution temporal data base related to phytoplankton dynamics was collected during the austral spring/summer periods of 1991-1994 in shelf waters adjacent to Palmer Station, Antarctica. Here, the data base is used 1) to quantify the variability in phytoplankton biomass, in situ productivity and taxonomic composition over subseasonal, seasonal and interannual time scales; 2) to elucidate environmental mechanisms controlling these temporal patterns; and 3) to ascertain which phytoplankton markers are most suitable for longer-term (i.e. decadal) trends in phytoplankton dynamic in coastal waters of the Southern Ocean. The LTER coastal study sites showed high interannual variability in peak phytoplankton biomass (75 - 494 mg Chl a m^{-2}) and integrated primary production (1.08 - 6.58 g C m^{-2} d^{-1}). Seasonal and annual patterns in biomass and productivity were shown to be driven by shorter time scale physical forcing by local wind stress. Low daily wind speeds (< 10 m s^{-1}) were associated with water-column stabilization. However, extended periods (> 1 week) of low wind stress were required for increased phytoplankton growth and biomass accumulation. Temperature data supports the view that water masses can be

replaced on time scales of a less than a day to a few days in these coastal waters. Such disruptions are associated with abrupt changes in local primary production and may lead to sudden shifts in local phytoplankton community structure. Despite the high seasonal and interannual variability in biomass and associated in situ productivity in this coastal environment, the replacement sequence of one dominate phytoplankton group by another was very similar on subseasonal time scales for all 3 years. Results suggest that monitoring changes in phytoplankton successional patterns may be a more sensitive marker for detecting long-term trended changes in Southern Ocean ecosystems than either biomass or productivity indices, where short term variability of the latter is as great or greater than interannual variations documented to date.

INTRODUCTION

There has been a concerted effort in the past decade to integrated physical, chemical, and biological data in an attempt to understand the mechanisms controlling phytoplankton bloom dynamics in the Southern Ocean (Smith and Nelson 1985; Lancelot et al. 1991ab; Mitchell and Holm-Hansen 1991; Sakshaug et al. 1991; Mathot et al. 1992; Smetacek et al. 1992; Scharek et al. 1994; De Baar et al. 1995; Smith et al. 1995; Turner and Owens 1995). These studies have been conducted shipboard in pelagic regions and have focused on the spatial variability of phytoplankton distribution, abundance, productivity, and physiology related to the respective physical and chemical environments. Enhanced biomass and productivity have been found to be associated with frontal regions, marginal ice edge zones and coastal regions. Theoretical and empirical models derived from such studies suggest that water column stability, grazing and/or resource limitation are the major factors governing phytoplankton bloom dynamics. While these studies have advanced the understanding of the mechanisms controlling phytoplankton dynamics, they have also pointed to the need for better

temporal resolution of these processes (Holm-Hansen et al. 1989; Mitchell and Holm-Hansen 1991).

Few studies have examined the temporal variability in biomass and primary productivity in the Southern Ocean, and those that have (Horne et al. 1969; Bienati and Comes 1971; Whitaker 1982; Krebs 1983; Satoh et al. 1986; Domanov and Lipski 1990; Rivkin 1991) are generally based on a limited number of environmental parameters and/or lack sufficient resolution to track seasonal variations. Recent analyses of sampling frequency effects on error estimates of primary production for coastal Antarctic regions (Moline and Prézelin 1996) show that the above sampling regimes are not sufficient to resolve significant short time scale variations in local primary production and may lead to errors in seasonal estimates as high as 50%. These potential errors have significant ramifications for interpretation of seasonal and interannual dynamics and, more importantly, for identifying and quantifying the mechanisms controlling the seasonal patterns in phytoplankton communities of the Southern Ocean.

A high-resolution temporal data base was collected in shelf waters adjacent to Palmer Station, Antarctica for concurrent determinations of physical, biological and chemical parameters related to phytoplankton ecosystem dynamics

during the austral spring/summer period of 1991-1994. This work was done as part of the Palmer Long-Term Ecological Research (LTER) program, a multidisciplinary program established to understand and model interactions between different marine trophic levels and with the variable chemical/optical/physical environments of the Southern Ocean (Ross and Quetin 1992). Here, this highly resolved nearshore data base is used 1) to quantify the variability in phytoplankton biomass, *in situ* productivity and taxonomic composition over subseasonal, seasonal and interannual time scales, and 2) to elucidate mechanisms controlling these temporal patterns. These findings provide insights and advancements for ascertaining the differences between short-term variability and long-term trends in phytoplankton dynamics for diverse regions of the Southern Ocean.

METHODS

Sampling and Physical Measurements

Over the austral spring/summer period from November, 1991, through January, 1994, a total of 1,140 discrete water samples were collected at the LTER stations B and E (Sta B/E; Fig. 1) for

concurrent determinations of physical, optical, biological and chemical parameters related to phytoplankton ecosystem dynamics. Sta B is a shallow nearshore station (~75 m), while Sta E is a significantly deeper (~280 m) and more exposed station located on the northern edge of the Bismark Strait. The distance between Sta B and E is ca. 3 km. Water column sampling was conducted from a Mark V Zodiac® and, whenever possible, samples were collected with in a few hours of solar noon. Daily air temperature, snow cover and average wind speed/direction measurements were made at Palmer Station during the study period as part of a long term database collected by the U. S. National Science Foundation. Sea ice coverage was assessed by daily observations. A more detailed description of the sampling strategy for the 1991-92 season, which was identical, with one exception, for the following two field seasons, is given by Moline and Prézelin (1996).

The one exception between years is that water column density data is only available for the 1991-1992 season when 38 conductivity and temperature profiles were measured at Sta B and E using a SeaBird® CTD on a second Zodiac® described by Smith et al. (1992). The original reports of the findings are found in Smith et al. (1992) and Moline et al. (1996). The

depth of the upper mixed-layer (UML) based on the sigma-t (σ_t) profiles was estimated using the formulation

$$\max\left|\frac{d\sigma_T}{dz}\right| \qquad \text{Eq. 1}$$

which assumes the UML depth to be equal to the depth where the gradient in σ_t is maximal. Like Mitchell and Holm-Hansen (1991), it was assumed that if the maximal σ_t gradient was less than 0.05 per meter, then the water column is essentially well mixed to the bottom (ca. 80 m at Sta B) or below the sampling depth (100 m for Sta E).

Phytoplankton Pigmentation

Aliquots of all whole water samples were analyzed for the algal pigments using reverse-phase HPLC procedures detailed in Moline and Prézelin (1996) for the 1991-92 season and Wright et al. (1991) for the following two years. One liter samples were filtered on 0.4 μm nylon 47 mm Nuclepore® filters and extracted in 3 ml 90% acetone for 24 hr in the dark at -20 °C. Pigment separation was achieved with the aid of an Hitachi® L-6200A pump and an L-4250 UV/VIS variable wavelength detector (436 nm) equipped with a Waters® Radial-PAK C_{18} column (8 x 100 mm; 5 μm) during the 1991/92 season and a

Waters® Resolve C_{18} column (3. 9 x 300 mm; 5 μm) for the following two seasons. Peak identities of algal extracts were determined by comparing their retention times with pure pigment standards. Calibration studies comparing methods of Bidigare et al. (1989) and Wright et al. (1991), showed no significant quantitative differences for any of the pigments of interest. For the purposes of the present study, temporal/spatial patterns are presented for chlorophyll a (Chl a), an indicator of total phytoplankton biomass, and the phytoplankton group-specific pigments Chlorophyll b (Chl b) for chlorophytes (Jeffrey 1974), fucoxanthin (Fuco) for diatoms (Wright and Jeffery 1987) alloxanthin (Allo) for cryptophytes (Gieskes 1983) and the sum of 19'-hexanoyloxyfucoxanthin (Hex) and 19'-butanoyloxyfucoxanthin (But) as a marker for chromophytes-nanoflagellates (in the Antarctic primarily *Phaeocystis pouchetii*) (Vaulot et al. 1994; Wright and Jeffrey 1987). In order to estimate the respective contribution of each taxonomic groups, multiple regression analyses were performed on the vertically integrated concentrations (surface to 0.1% Q_{par} (400-700nm) light level) of the taxonomic pigments against Chl a (Gieskes et al. 1988; Everitt et al. 1990; Bustillos et al. 1995). The regression analyses for each year yielded the following results:

1991-92: Chl *a* = 2.00 Fuco + 3.15 Allo + 1.99 (Hex + But) + 0.68 Chl *b* (r^2 = 0.99, $p<0.001$)

1992-93: Chl *a* = 1.54 Fuco + 2.92 Allo + 1.91 (Hex + But) + 0.42 Chl *b* (r^2 = 0.94, $p<0.001$)

1993-94: Chl *a* = 1.30 Fuco + 3.49 Allo + 1.45 (Hex + But) + 0.50 Chl *b* (r^2 = 0.71, $p<0.001$)

For additional details and results of the regression analyses, see Claustre et al. (1996).

Surface and In-Water Q_{par} Measurements

Surface and in-water Q_{par} (400-700 nm) measurements made during the 1991-92 season are detailed in Moline and Prézelin (1996). For the 1992-93 and 1993-94 seasons, Q_{par} measurements were performed using an in-water Li-Cor® LI-190SA quantum scalar irradiance sensor and a Li-Cor® LI-190SA reference sensor. In addition to irradiance profiles taken during sampling, incident Q_{par} was recorded continuously every 5 min over the 3 yr period using a Li-Cor® LI-190SA. A comparison between data collected from the sensors at Palmer Station and those collected from the Zodiac® sampling platform showed that Q_{par} readings differed < 5 %.

Intercalibration of the sensors between years showed a difference of < 1 %. In-water and reference light data were used to calculate the percent Q_{par} at each sampling depth, which was assumed not to change over the course of a day. Percent Q_{par} data were interpolated (linear interpolation of log-transformed data) vertically in the water column over one meter intervals for primary production calculations (see below).

Photosynthesis-Irradiance Relationships and Primary Production Calculations

Estimates of in situ primary production rates were derived from photosynthesis-irradiance (P-I) relationships measured for 756 discrete water samples. The P-I procedures, detailed for the 1991-92 season in Moline and Prézelin (1996), were the same methods used for the following two seasons. Freshly collected field samples were incubated in laboratory blue-green light Q_{par} photosynthetrons, using established radiolabelled $H^{14}CO_3$ uptake procedures (Prézelin et al. 1989; Prézelin and Glover 1991). Blue-green light fields more closely mimic in-water spectral conditions in clear ocean waters and tend to release cells from artificial white light (or far-red) effects, which can reduce carbon uptake rates and

photosynthetic quantum efficiencies (Prézelin et al. 1989; Schofield et al. 1991). Incubations times were kept to 90 min and incubation temperatures were controlled to within 0.2 °C of in situ temperatures. It is possible that ultraviolet light (UV) inhibition effects on the in situ primary production, if evident, were removed during the Q_{par} incubation in the absence of UV radiation (Boucher and Prézelin 1996ab). Thus, values reported here should be considered upper limit estimates of in situ rates of primary production in Antarctic coastal waters.

Non-linear curve fits for P-I data were calculated using the Simplex method of Caceci and Cacheris (1984). Curve fitting provided the photosynthetic parameters P_{max} (mg C mg Chl a^{-1} h^{-1}), the light-saturated photosynthetic potential, Ik (μEin m^{-2} s^{-1}), an estimate of the minimum irradiance required to saturate photosynthesis, α [mg C mg Chl a^{-1} h^{-1} (μEin m^{-2} s^{-1})$^{-1}$], the light limited photosynthetic efficiency, β [(mg C mg Chl a^{-1} h^{-1} (μEin m^{-2} s^{-1}) $^{-1}$], the efficiency of photoinhibition and It (μEin m^{-2} s^{-1}), the irradiance threshold for the onset of photoinhibition. Estimates of the standard deviations for the P-I parameters were calculated using the procedures described by Zimmerman et al. (1987). Discrete P-I relationships with estimated standard deviations of > 25 % for P_{max} and/or 30 %

for α were eliminated from this study. The effect was to reduce the size of the productivity data base by less than 10%.

In addition to measuring the 'instantaneous' P-I parameters, weekly determinations of the diel periodicity (3 hr resolution) for each P-I parameter were performed at the surface and Chl a maximum over the 3 yr study in order to time-correct the instantaneous measurements and accurately determine daily rates of in situ primary production. The methods of determining diel periodicities of P-I parameters and integrating these measurements into the daily rate calculations have been thoroughly detailed in Moline and Prézelin (1996). The resulting P-I parameters determined for every 2 hr interval over the day were linearly interpolated at 1 m intervals with depth and combined with Q_{par} for each meter (see above) for calculating primary production.

Interpolating light data and photosynthetic parameters over small depth interval (1 m) improved the accuracy of primary production estimates than would have been achieved by employing more common trapezoidal integration procedures. Trapezoidal integration assumes a linear change of the integrated parameter between two consecutive depths. Such an assumption is reasonable for depth distribution of biological properties (i.e. photosynthetic parameters), but not

for light attenuation which decreases log-linearly with depth. Analyses (not given) show that trapezoidal integration procedures applied to even 5-10 m depth intervals can lead to a significant higher estimation of production than would have been predicted with light fields interpolated for 1 m intervals.

Thus, primary production was calculated at each 1 m interval and then integrated over depth. In situ primary production at each meter for every 2 hr intervals over the day [P (z, t)] was calculated, using the hyperbolic tangent model of Neale and Richerson (1987), such that

$$P(z,t) = P_{max}(z,t) \bullet \tanh\left(\frac{Q_{par}(z,t)}{I_k(z,t)}\right) \qquad \text{Eq. 2}$$

when Q_{par} (z, t), the measured integrated in situ irradiance for each 2 hr interval, was less than I_t (z, t) and

$$P(z,t) = P_{max}(z,t) \bullet \tanh\left(\frac{Q_{par}(z,t)}{I_k(z,t)}\right) \bullet \exp\left[-\beta\left(Q_{par}(z,t) - I_t(z,t)\right)\right] \qquad \text{Eq. 3}$$

when Q_{par} (z, t) was greater than I_t (z, t). Daily rates of production were computed as the sum of the twelve daily 2 hr intervals.

For intervening days where discrete samples were not taken, estimates of parameters used in the primary productivity calculations and pigmentation were derived by interpolation using exponential kriging methods (Spyglass® Transform, Champaign, IL). This method incorporates the measured light field when calculating estimates of primary productivity and does not assume a linear transition between sampling days. The primary assumption of this approach is that significant variability in biological parameters occur on longer time scales than the daily fluctuation in the light field. This is a reasonable assumption given data collected during the 1991-92 season showed a maximum daily variation of 2-fold in biomass and other biological parameters, while the daily Q_{par} light field varied a factor of 4 over the same time interval. Transmission of Q_{par} through ice was held constant at 10%, which was the average measured for the different ice conditions (i.e. pack, brash, or fast ice) observed at Sta B.

RESULTS

Interannual and Subseasonal Variability in Standing Stock and Water Column Dynamics

The 1991-1992, 1992-1993 and 1993-1994 temporal contour plots of Chl *a* biomass distribution, for both LTER stations B and E, are compared in Figures 2A & B. With one exception at Sta E in 1992-1993, the annual peak biomass was observed in December of each year. Accumulated phytoplankton biomass was high in 1991-1992; low in 1992-1993; and moderate in 1993-1994. On subseasonal time scales in each year, there were periods of abrupt changes in water column phytoplankton biomass. In general, the magnitude of variability in Chl a biomass measured within a few day within a given year was as great as the variability in Chl a biomass compared for similar periods between years.

The 1991-1992 field season was characterized by a large phytoplankton bloom immediately following the break-up of the local fast ice at Sta B (Fig. 2A & B, top). At the start of the sampling season, the 'seed' population that gave rise to the bloom was evident below the ice at Sta B (Moline and Prézelin 1996; Moline et al. 1996), unlike the lower Chl a biomass at Sta E which was ice free in early December, 1991. The initiation of

the bloom was coincident with an extended period of low wind stress (Fig. 3) and water column stability in the absence of a pycnocline. Although this has been shown previously for other regions (Ryther 1960; Townsend et al. 1992), the specific importance of low wind stress on stability and the development of blooms is only occasionally emphasized (Sakshaug and Slagstad 1992). Stabilization was enhanced by density stratification resulting from the input of glacial meltwater. The upper mixed layer depth (UML) shallowed from 60 m to 10 m during the first 2 weeks of December (Fig. 2A & B, top), concentrating the developing bloom in the surface waters (Moline et al. 1996). Peak Chl a concentrations reached 29.21 mg Chl a m^{-3} at Sta B and 10.89 mg Chl a m^{-3} at Sta E, with concentrations from 3-5 mg Chl a m^{-3} extended down to a depth of ca. 50 m at both stations. At the peak of the bloom, up to 75% of the total integrated Chl *a* was below the 0.1% Qpar light level, suggestive of high sinking rates.

Although water column biomass was significantly higher at Sta B than at Sta E during the 1991-1992 bloom, there were pulsed events at Sta E when the integrated biomass was comparable between stations (Fig. 2A & B, top). These events occurred periodically on 7-8 day intervals and were found to be coupled to the tidal cycles (Fig. 4). The tides at Palmer

Station during December, 1991 were primarily diurnal with solar (K1) and lunar (O1) constituents, similar to findings by Amos (1993a). The maximum tide differential ranged from ~ 0.4 m during neap tides (JD 349 & 362) to ~ 1.6 m during the spring tide (JD 357) (Fig. 4, middle). Because profiles were made near solar noon each day, the direction of the tidal flushing changed at the time of sampling over the season. From JD's 344-349 and 357-362, the flow was from Sta E to B. Similarly, from JD 349-357 the flow was from Sta B to E. This tidal signal was also seen in the difference in the integrated biomass between stations (Fig. 4, middle). As the flow from B to E reached a maximum on JD 357, the large diatom bloom from Sta B was advected offshore and extended to Sta E with the difference in biomass signals between the stations reaching a minimum. Likewise, when the flow from Sta E to B reach a maximum on JD 362, water was pushed up against the coast and there was a maximum difference in the integrated biomass between stations. The tidal signal was also recorded in the differential in average surface temperatures between stations (Fig. 4, bottom). When the difference in the biomass between Sta E and B was at a minimum, temperatures at both stations converged.

The accumulation of biomass at Sta B increased phytoplankton absorption (Schofield et al. 1994; 1996) and surface waters warmed from -1.2 °C in early December to +2 °C at the peak of the bloom on JD 362 (Fig. 5A, top). With the tidal advection, this relatively warm water periodically extended out to Sta E, increasing temperatures from -0.5 °C to 0.5 °C (Fig. 5B, top). Interestingly to note was that during the period of surface stratification and stability in December, 1991, there were periodic intrusions of warmer high salinity at depth. This may have been a result of tidal forcing and/or current patterns in the Bismark Strait advecting Circumpolar Deep Water (CDW), known to influence regions well inshore of the continental shelf break (Hofmann et al. 1993; Klink et al. 1994), into the study area.

In mid January 1992, the bloom was advected from the area and replaced with a low biomass water column (Moline et al. 1996). The advection event occurred on a time scale shorter than the sampling frequency (every 2-3 days) and, unlike the tidal advection, was too rapid to be detected from the changing biomass signals between Sta B to E. The advection of a new water mass into the area was evident by the rapid warming of the entire water column at stations B and E (Fig. 5A & B). Low biomass (< 0.5 mg Chl a m^{-3}) persisted at both stations until the

end of February when Chl *a* concentrations increased in the presence of enhanced stratification (Fig. 2A & B). Further warming (> 1 °C) of the water column in mid February was coincident with high precipitation and increased runoff from the coast (Moline et al. 1996).

During the 1992-93 field season, the region around the LTER nearshore stations was ice free and had been so for most of the year (Palmer Station Ice Observation Record) with the exception of two days in November at Sta B. In 1992-1993, spring or summer phytoplankton blooms were absent (Fig. 2A & B, middle). Biomass concentrations at were relatively low over the entire season with peak concentrations at Sta B in late December and early February of 2.25 and 2.12 mg Chl a m^{-3}, respectively. Peak standing crop at Sta E occurred in late November and was generally less coupled with Sta B than during the 1991-92 season. Vertical profiles routinely indicated uniform depth distributions of Chl a concentrations at both Sta B and E, suggestive of significant vertical mixing. At the same time, water columns were generally isothermal (Fig. 5A & B, middle) and coincident with average daily wind speeds in excess of 10 m s^{-1} for much of the season (Fig. 3). Similar to the 1991-92 season, there was a seasonal warming of the

water column, however, surface temperatures during 1992-93 were generally warmer than the previous year.

During the 1993-94 season, sampling began in late August when heavy land-fast ice was a dominant feature at Sta B. The presence of the ice had a measurable cooling effect on the water column temperature profiles (Fig. 5A & B, bottom). The gap in ice cover at Sta B in late September 1993 corresponded to a temperature increase in the water column, suggesting that advection of a different watermass was coupled to the ice break-up. During the late winter and early spring, biomass remained low, averaging 0.17 mg Chl a m^{-3} (Fig. 2A & B, bottom). There was an increase in Chl *a* measured at Sta B during the beginning of October that was not recorded at Sta E. It may have been the result of sampling disturbance of the highly concentrated ice algal communities. After the ice break-up in early November, biomass steadily increased at Sta B to a maximum of 4.91 mg Chl a m^{-3} at the end of December. Although high winds, similar to the 1992-93, dominated most of the field season, the development of this small bloom corresponded to 10-day period of low wind speeds in mid December, 1993 (Fig. 3). As during the 1991-92 season, the timing of surface warming was coupled to the increase in biomass (Fig. 5A & B, bottom). Sta E showed similar temporal

biomass distribution to Sta B. However, the overall concentrations at Sta E were lower than at Sta B (Fig. 2A & B, bottom). Like the 1991-92 season, there were periodic fluctuations in the integrated biomass at both stations resulting from tidal forcing.

Daily Primary Production

Figure 6 compares the estimated daily rates of in situ primary production as a function of depth for both Sta B and E during the 3 consecutive field seasons between 1991 and 1994. Not surprising, most of the time variability in in situ rates of daily primary production was closely coupled to variability in phytoplankton biomass (compare Figs. 2 & 6). The highest carbon fixation rates for all 3 field seasons (748 mg C m^{-3} d^{-1}) were associated with the 1991-92 bloom at Sta B. In the following season, maximum daily production was almost 6-fold lower (130 mg C m^{-3} d^{-1}) and observed in near surface waters at Sta E, not B, in mid December. Maximum production at Sta B in the 1992-1993 season (79 mg C m^{-3} d^{-1}) was even lower and evident not in mid December but in mid to late November. In the last field season of 1993-1994, primary production once again peaked in December at both stations with the production at Sta B being higher than that at Sta E. Maximum rates of

primary production, however, only reached 82 mg C m^{-3} d^{-1} in December 1993, a value 9-fold lower than that measured at the very same location at the same time of year but 2 years earlier.

Interesting to note is that the depth of significant production shallowed in response to increased light attenuation. During the 1991-92 bloom, the depth of the 0.1% isolume shallowed to ~8 m and up to 70% of the water column primary production became light limited (Moline and Prézelin 1996). Low light penetration persisted even after the demise of the bloom largely due to the input of highly attenuating particles associated with the runoff of glacial meltwater (Smith et al. 1992) typical for the spring/summer season (Shabika et al., 1977). The initiation of glacial runoff is indicated in all contour plots by arrows and occurred in late December in 1991, in early December of 1992, and in mid November of 1993. The input of glacial meltwater also significantly attenuated in-water light fields during December and January of the 1992-93 season when Chl a biomass was particularly low. Significant production during the late winter months of 1993 was restricted to surface waters largely due to the low daily surface irradiance at that time of the year and attenuation of light by ice cover.

Seasonal variations in integrated water column biomass and areal rates of daily primary production are compared in Figure 7. It is clear that local biomass and primary production can be an order of magnitude higher for bloom years than non bloom years. While light appeared to drive the day to day variation in production, the magnitude of seasonal and interannual production corresponded (only to first order) to the biomass variability. Total integrated biomass (mg Chl a m^{-2}) was significantly correlated to daily integrated primary production (mg C m^{-2} d^{-1}) over all three years (Fig. 8; $p < 0.0001$). Although significant at these scales, the coupling between biomass and productivity has been found to be highly variable in relation to a number of environmental parameters. See Claustre et al.(1996) for a detailed discussion of the robustness of the relationship between Chl a biomass and primary production within this temporal data base. Table 1 summarizes the seasonal and interannual variation in Q_{par}, areal biomass and the calculated in situ primary production on monthly time scales for the 3 year study. Monthly mean biomass and total primary productivity for Sta B and E from 1991-1994 showed increases associated with the seasonal change in the light field.

Phytoplankton Community Structure

Seasonal and interannual variations in phytoplankton community composition is defined here and analyzed as changes in the percent contribution of integrated water column taxon-specific pigments to the total Chl a concentration. Contour plots of the temporal variability in euphotic zone phytoplankton community composition for both Sta B and Sta E for all 3 field seasons are given in Figure 9. Where CTD casts were made available, the average sigma-t was estimated for the water column and plotted its variability over time for the 1991-1992 season. Initially apparent is that the patterns of phytoplankton community change are similar between stations for any given year but that the timing of these changes, which can occur abruptly, differ significantly between years.

Diatoms comprised over 70% of the initial biomass at Sta B for the 1991-92 season (Fig. 9A). This dominance increased with the development of the bloom and peaked at over 95% at the height of the bloom. During the bloom, there was a rapid (one week) transition from this diatom community to one 90% dominated by cryptophytes. Cryptophytes remained at Sta B until the advection event occurred, at which time it was replaced with a mixed community of diatoms and *Phaeocystis pouchettii*, the dominant prymnesiophyte in the Southern

Ocean (Bidigare et al. 1996). A similar pattern was found for Sta E in 1991-92, although the duration of the cryptophyte dominance was longer (Fig. 9B). Chlorophytes were found to contribute little (< 10%) to the overall seasonal biomass.

This seasonal successional pattern was repeated for the 1992-93 and 1993-94 seasons at Sta B and E (Fig. 9A & B), despite the differences in physical forcing and changes in the magnitude of biomass. Late winter periods appeared to have dilute 'seed' population of mixed diatoms and prymnesiophytes, with ca. 5% cryptophytes. For all 3 seasons, cryptophytes increased their dominance to 70-90% during the summer period, followed by a mixed population similar to that at the beginning of the season.

The presence of ice appeared to determine the 'seed' phytoplankton community at the beginning of the growth season. Diatoms communities in late spring/early summer of 1991 and 1993, prior to the succession by cryptophytes, were comprised primarily of *Coscinodiscus* sp., the same genus associated with the ice communities earlier in both seasons (Moline et al. 1996; Schofield et al. 1995). During the 1992-93 season, where there was no significant ice cover over the entire year, the diatom *Corethron criophilum*, known as a pelagic species (Sommer and Stabel 1986; El-Sayed and Fryxell 1993;

Froneman et al. 1995), was dominant. This species was also the dominant diatom in the late summer for all 3 years.

DISCUSSION

The Palmer LTER is a multidisciplinary program which seeks to understand and model predictive interactions between different marine trophic levels and the chemical, optical and physical environments of the Southern Ocean. One area of focus is to define the patterns and control of primary production, especially as related to spatial and temporal distributions of populations representing trophic structures. The 1991-1994 data presented here represents the first 3 field seasons of the time-series studies. Starting up a long-term research program in a remote and environmentally extreme area, with relatively little background data, required much attention to both design of the field program and intensive data collection in order to assure the ability to eventually distinguish between natural short-term variability and long-term trends due to natural cycles (i.e. ice coverage) or unnatural environmental perturbations brought on by global climate change (i.e. global warming, ozone diminution). The

resulting nearshore data base has already been used 1) to document the 1991-1992 variability in surface biological, optical, chemical and physical properties in the region (Moline et al. 1996) ; 2) to illustrate the impact the 1991 bloom had on water column chemistry (Moline and Prézelin 1994); 3) to show that instantaneous measurements of primary production, if uncorrected or improperly corrected for daytime periodicities in carbon fixation, were unreliable predictors of production on longer time scales even if the water column was sampled every few days (Moline and Prézelin 1996); and 4) to quantify the variability, and sources of variability, in the photosynthetic light utilization indexes (Y*) (Claustre et al. 1996) and maximum quantum yield (Schofield et al. 1994; 1996), and the consequences for remote sensing of in situ rates of primary production for coastal waters of the Southern Ocean. Here, the interannual variations in phytoplankton biomass, primary production and phytoplankton community structure, are presented for the first time with an emphasis on illustrating the physical forcing functions underlying the interannual and subseasonal variations. The outcome of the present analyses is a better understanding of phytoplankton community dynamics in Antarctic coastal waters and insights into which

phytoplankton markers might be most suitable for detecting ecological change on times scales longer than a few years.

Interannual variability in phytoplankton biomass and photosynthesis is equivalent to seasonal variability. In Figure 10 is a summary what is known of the seasonal range of variability in integrated water column biomass in Antarctic coastal waters. At any given location, Chl a biomass can vary by more than 2 orders of magnitude on subseasonal time scales, with the South Orkney Islands along the Palmer Peninsula and McMurdo Sound being the more extreme examples (Fig. 10A). The only multiple-year record providing integrated water column biomass, other than the present study, has shown interannual variability (Fig. 10B) to be significantly smaller (only 2.3-fold) than the range of seasonal variability (Fig. 10A) (Whitaker 1982). This result has lead to the notion that a summer phytoplankton blooms are a predictable repeated annual event for Antarctic coastal waters (Smith et al. 1995). While comparatively similar magnitude and variability in the annual standing stock was found for this study (Fig. 10), significantly higher interannual variation was measured for Sta B & E (6.6-fold), suggesting a less predictable yearly pattern. While most of the biomass accumulation and primary

production occurred during the months of maximum solar insulation (Table 1), the difference in the solar insulation between years varied a maximum of only 3.3 % and, therefore, cannot account for the range in peak biomass and primary production signals measured between years for this study.

Close coupling exists between wind stress, water column stability and bloom development.

Water column stability was found to be the primary mechanism controlling the variability in biomass, a result found for other areas of the Southern Ocean (Smith and Nelson 1985; Mitchell and Holm-Hansen 1991; Mitchell et al. 1991). Water column stability, in turn, appeared to be driven by the seasonal variability in wind (Fig. 3), with the input of fresh water and thermal stratification during the summer months enhancing the stability (Moline et al. 1996).

The strong coupling between wind stress, water column stability and biomass accumulation was most evident during the 1991-92 season. Wind stress was low for an extended period during this season, resulting in the shallowing of the UML. The duration (days) of low wind speeds was correlated with the depth of the UML, with the threshold for 'low' wind speeds of < 11 m s^{-1} showing the highest significance ($r^2 = 0.36$,

$p < 0.001$). The shallowing of the UML and stratification maintained phytoplankton in the upper euphotic zone and the major diatom bloom developed. The non-linear relationship between the UML and biomass accumulation for this study (Moline et al. 1996) is in close agreement with previous findings in other regions in the Southern Ocean (Mitchell et al. 1991; Nelson and Smith 1991), illustrating the requirement of stabilization for bloom development. Even when all the physical processes in the water column (stratification, mixing, advection) are ignored for this three year study, there was a significant relationship between the seven-day moving averages of wind and biomass for all three seasons ($r^2 = 0.14$, $p < 0.01$). On a seasonally integrated scale, the influence of wind on the variability in biomass is clear. Seasonal average wind speeds for 1991-92, 1992-93, and 1993-94 seasons were 7.96, 10.58, and 10.52 m s^{-1}, respectively with corresponding average integrated standing stocks of 76.2, 39.23, and 24.32 mg Chl *a* m^{-2}.

The influence of wind on the formation of blooms have also been shown for other regions of the Southern Ocean. For ice-edge blooms in the marginal ice-zone of the northwestern Weddell Sea, after examining the influences of ice meltwater, light, trace metals, and grazing pressures, Lancelot et al. (1993)

concluded that strong wind conditions (> 14 m s^{-1}) were the primary determinant for bloom development even during the summer months of the highest solar insulation. Recent analyses of remotely sensed biomass in the Ross Sea have shown that the large annual spring bloom coincides with typically low wind speeds for the entire area (K. Arrigo, pers. comm.). Additionally, for areas of high sustained winds (i.e. Terra Nova Bay), there was a delay in the development of phytoplankton blooms until the average wind speeds drop below a certain threshold.

Tidal forcing results in high daily variability between stations on space scales of 2-6 km.

There was strong coherency between Sta B and E in the annual and monthly integrated biomass (r^2 = 0.86) and primary production (r^2 = 0.84) (Table 1). This could be considered probable given that both stations are nearshore and influenced by the timing and magnitude of springtime glacial ice melt, which releases large quantities of fresh water into local surface waters and strong episodic wind events that affect the entire Palmer region (Moline et al. 1996; Moline and Prézelin 1996). However, as the period of integration decreased, the correspondence between the stations decreased (Fig. 7). This

may partially due to advection events which occurred on time scales of less than a month. In addition to wind driven advection, advection resulting from the summer flow of fresh water from land, and possible influence of current patterns in the Bismark Strait, there was a strong tidal influence.

Tidal advection of different water masses has been documented for the Palmer Station area (Amos 1993a), however, the influence of this phenomena on temporal patterns of phytoplankton biomass and primary production has not been shown. During the spring tide, where the tide differential is maximum, the sampling time was found to be critical. Given the maximal flushing measured on JD 357, the integrated biomass at Sta E in the most productive upper 20m would range from 33.1 to 165.7 mg Chl *a* m^{-2} over the course of the day, showing characteristics of both the inshore bloom waters and the less productive Bismark Strait waters, at least 3 km on either side of the station. This 5-fold variation in the daily signal also has implications for spatial sampling, which in the Southern Ocean is often on scales larger than the lateral watermass movement due to tidal forcing (Smith and Nelson 1985; Huntley et al. 1991; Waters and Smith 1992).

A consistent annual pattern in the development of cryptophyte-dominated phytoplankton is determined by the timing of the glacial meltwater runoff.

Given the high seasonal and interannual variability in the biomass and productivity responding to the fluctuating meteorological and hydrographic conditions during this study, similar variability for other aspects of phytoplankton dynamics might be expected. This was not the case, however, and a consistent and repeated annual pattern in phytoplankton succession was found. Cryptophyte dominance for all three seasons was found to be timed to the melt of the local snow cover and the initiation of glacial meltwater input into this coastal region (Fig. 9A & B). The percent dominance of cryptophytes was highly correlated to the density change in the water column (r^2=0. 57, $p < 0.001$), further suggesting that the mechanism for this transition was the seasonal change in salinity. This is in good agreement with temperate regions, where this class is often associated with brackish water environments (Prézelin and Bozcar 1986).

A number of other 'low' salinity environments in the Antarctic that have also been shown to be dominated by cryptophytes. Buma et al. (1992) found cryptophytes contributed to over 95% of the total biomass in the low salinity

waters (Tréguer et al. 1991) of a retreating marginal ice zone in the Weddell-Scotia Confluence area. Cryptophytes were also shown to increase with decreasing salinity during the summer months in the confluence of the Bellingshausen and Weddell seas, along the Antarctic Peninsula (Mura et al. 1995). In the Ellis Fjord, McMinn and Hodgson (1993) have documented the dominance of cryptophytes coinciding with the high summer input of freshwater. In the perennially ice-covered lakes of the Dry Valleys, cryptophytes are found to dominate the phytoplankton community (Lizotte and Priscu 1992). These populations, however, are rarely seen below the low salinity surface layer beneath the ice, even though nutrients are often depleted in this layer (M. Lizotte, pers. comm.).

The best marker for longer term changes in ecosystem dynamics may be the timing and pattern of seasonal changes in phytoplankton community composition. Given cryptophytes populations respond to changes in water column salinity, variations in the timing, duration and the quantity of the annual fresh water input may be reflected in the taxonomic changes in the phytoplankton community. Air temperature records showed the day where average temperature exceeded the freezing point was progressively

earlier with each year (JD 333, 316 and 309 for the three years respectively). The number of days that temperatures were above freezing during the summer months were also longer with each year. This is in agreement with the both the timing of the onset of glacial melt and the duration of the cryptophyte dominance for each successive year (Fig. 9A & B). The average timing and magnitude of cryptophyte dominance at Sta B and E in relation to the mean air temperature is summarized for 1991-1994 in Figure 11. The initiation of cryptophyte dominance is timed to the average air temperature exceeding the freezing point and the variability in this dominance is highest in December, where the timing of glacial melting changes from year to year (Fig. 9A & B). The variability in the percent cryptophytes decreased in January, when the populations were established in the region (Fig. 11). By February, water column salinity returned to pre-meltwater conditions (Fig. 9A & B) and cryptophytes showed a marked decrease.

A statistically significant warming trend (2-3 °C) for the mid-Antarctic Peninsula over the past 50 years has been established (King 1994; Stark 1994), with potential effects on both sea-ice dynamics (Weatherly et al. 1992; Murphy et al. 1995) and glacial melting. From these long-term trends and

the results presented here, one may hypothesize that a shift in community composition has been occurring over the past decades with increasing of dominance of cryptophytes in the coastal regions of the Southern Ocean. Although long-term data sets of phytoplankton seasonal successional are scarce, the few that have been collected suggest a trended change in the community composition. A 24-year study (1970-1993) in Paradise Bay has found a significant reduction in the abundance of diatoms and an increase in cryptophytes and other phytoflagellates (Ferreya and Tomo 1979; Ferreya, pers. comm.). A taxonomic study by Krebs (1983) sampling from 1972-1974 near Sta B found only diatoms (unlike this study for 1991-94) and the cell numbers were highly correlated to Chl a concentrations, suggesting low abundances of other phytoplankters. More recently, a four-year study (1990-1993) near the South Shetland Islands found dramatic decreases in the abundance of diatoms and a corresponding increase in cryptophytes and other phytoflagellates (Villafañe et al. 1995). A decrease in the surface salinity was recorded over this time (Amos 1993b), however, authors rejected the notion that these small hydrographic changes could have any significant effect on taxonomic composition. Whether or not these studies and others (Ferraria and Sar 1992; Vernet 1992; Kang and Lee

1995) are taken as evidence for environmental change, they do imply a connection. Long-term trended changes in the community composition, especially during the peak growing season, may have significant influences on other trophic levels in the ecosystem (Bird and Karl 1991), and therefore may be an important consideration for future studies and data interpretation. As monitoring of taxonomic change, as well as meteorological and hydrographic parameters, continues near Palmer Station as part of the LTER program, perhaps a more definitive answer will emerge.

CONCLUDING REMARKS

Our highly resolved 3-year data set quantifies the large seasonal and interannual variability in biomass and primary production for Antarctic coastal waters, and shows a close linkage to physical forcing in the local region. Wind stress, ice coverage, the timing of ice break-up, freshwater input and advection were all found to contribute to the high variability in the magnitude and temporal distribution of phytoplankton in these highly productive environments. Variability appeared to be high whether the time scale of interest was one day or three

years. This apparent time-independent variability illustrates the need to increases the resolution of temporal sampling to better quantify the short-term variability and the mechanisms driving that variability. If the goal is to elucidate long-term environmental change in the Southern Ocean, the use of moorings should perhaps be more seriously considered for future studies, despite the inevitable logistic problems associated with deployment. Notwithstanding the high temporal variability in biomass and associated production, one of the most surprising results of work presented here was the consistent annual successional pattern of the local phytoplankton communities influenced by the presence of sea ice and the seasonal input of meltwater from surrounding glaciers. These findings suggest that seasonal succession may be a better predictor of long-term environmental change than traditional biomass and productivity indices, which are shown here to be highly variable on a sub-seasonal to interannual time scales.

ACKNOWLEDGEMENTS

N. Boucher, B. Bozcar, T. Diem, T. Evens, B. Golden, P. Handley, R. Jovine, H. Matlick, T. Newberger, S. Roll, K. Seydel, K. Scheppe, O. Schofield, J. Standish, B. Sullivan, T. Westerberry and the ASA personnel at Palmer Station are acknowledged for their assistance in data collection during the three field seasons. R. Bidigare and M. Ondrusek are thanked for generously providing HPLC training and pigment standards. D. Karentz is thanked for providing tide data. H. Claustre is especially acknowledged for his assistance in data analyses and valuable insights, discussion and comments. This study was supported by National Science Foundation grant DPP 90-901127 to B. Prézelin. This is Palmer LTER publication number XX.

REFERENCES

Amos AF (1993a) RACER: The tides at Palmer Station. Ant J U S 28: 162-164

Amos AF (1993b) AMLR program: Interannual variability in the Elephant Island surface waters in the austral summer. Ant J U S 28: 201-204

Bidigare RR, Schofield O, Prézelin BB (1989) Influence of zeaxanthin on quantum yield of photosynthesis of *Synechococcus* clone WH7803 (DC2). Mar Ecol Prog Ser 56: 177-188

Bidigare RR, Iriarte JL, Kang S-H, Ondrusek ME, Karentz D, Fryxell GA (1996) Phytoplankton: Quantitative and qualitative assessments. In: Ross R, Hofmann E, Quetin L (eds) Foundations for Ecosystem Research in the Western Antarctic Peninsula Region. Antarctic Research Series, American Geophysical Union, Washington, D. C. In press

Bienati NL, Comes RA (1970) Contribucion del Instituto Antartico Argentio 109: 4-22

Bird DF, Karl DM (1991) Massive prasinophyte bloom in northern Gerlache Strait. Ant J U S 26: 152-154

Boucher NP, Prézelin BB (1996a) An *in situ* biological weighting function for UV inhibition of phytoplankton carbon

fixation in the Southern Ocean. Mar Ecol Prog Ser, in press.

Boucher NP, Prézelin BB (1996b) Spectral modeling of UV inhibition of an in situ Antarctic primary production using a newly derived biological weighting function. Photobio Photochem, in press.

Buma AGJ, Gieskes WWC, Thomsen HA (1992) Abundance of Cryptophyceae and chlorophyll-b containing organisms in the Weddell-Scotia Confluence area in the spring of 1988. Polar Biology 12: 43-52

Bustillos-Guzman J, Claustre H, Marty J-C (1995) Specific phytoplankton signature and their relationship to hydrographic conditions in the coastal northwestern Mediterranean Sea. Mar Ecol Prog Ser 124: 247-258

Caceci MS, Cacheris WP (1984) Fitting curves to data. Byte 9: 340-362

Claustre H, Moline MA, Prézelin BB (submitted) Sources of Variability in the Light Utilization Index for Antarctic Coastal Waters. J Geophys Res

De Baar HJW, Jong JTMde, Bakker DCE, Loescher BM, Veth C, Bathmann U, Smetacek V (1995) Importance of iron for plankton blooms and carbon dioxide drawdown in the Southern Ocean. Nature 373: 412-415

Domanov MM, Lipski M (1990) Annual cycle of chlorophyll a and primary production of phytoplankton in Admiralty Bay (Antarctica). Pol Arch Hydrobio 37: 471-478

El-Sayed SZ, Fryxell GA (1993) Phytoplankton. In: Friedmann IE (ed) Antarctic Microbiology. Wiley-Liss, Inc. pp. 65-122

Everitt DA, Wright SW, Volkman JK, Thomas DP, Lindstrom EJ (1990) Phytoplankton community compositions in the western equatorial Pacific determined from chlorophyll and carotenoid pigment distribution. Deep-Sea Res 37: 975-997

Ferrario ME, Sar E (1992) RACER: phytoplankton populations in the Gerlache Strait. Ant J U S 27: 158-159

Ferreyra GA, Tomo AP (1979) Contribucion del Instituto Antartico Argentio 264: 150-184

Froneman PW, McQuaid CD, Perisssinotto R (1995) Biogeographic structure of the microphytoplankton assemblages of the south Atlantic and Southern Ocean during austral summer. J Plank Res 17: 1791-1802

Gieskes WWC (1983) Dominance of cryptophyceae during the phytoplankton spring bloom in the central North Sea detected by HPLC analysis of pigments. Mar Bio 75: 179-185

Gieskes WWC, Kraay GW, Nontji A, Setiapermana D, Sutomo (1988) Monsoonal alteration of a mised and a layered structure in the phytoplankton of the euphotic zone of the Banda Sea (Indonesia): A mathematical analysis of algal pigment fingerprints. Neth J Sea Res 22: 123-137

Hofmann E, Lipphardt BL, Smith DA, Locarnini RA (1993) Palmer LTER: Hydrology in the LTER region. Ant J U S 28: 209-211

Holm-Hansen O, Mitchell BG, Hewes CD, Karl DM (1989) Phytoplankton Blooms in the Vicinity of Palmer Station, Antarctica. Polar Biology 10: 49-57

Holm-Hansen O, Mitchell BG (1991) Spatial and temporal distribution of phytoplankton and primary production in the western Bransfield Strait region. Deep-Sea Res 38: 961-980

Horne AJ, Fogg GE, Eagle DJ (1969) Studies *in situ* of the primary production of an area of inshore Antarctic Sea. J Mar Biol Ass UK 49: 393-405

Huntley M, Karl DM, Niiler P, Holm-Hansen O (1991) Research on Antarctic Coastal Ecosystem Rates (RACER): and interdisciplinary field experiment. Deep-Sea Res 38: 911-941

Jeffery SW (1974) Profiles of photosynthetic pigments in the central North Pacific Ocean. Mar Bio 37: 33-37

Kang S-H, Lee S (1995) Antarctic phytoplankton assemblage in the western Bransfield Strait region, February 1993: composition, biomass, and mesoscale distributions. Mar Ecol Prog Ser 129: 253-267

King JC (1994) Recent climate variability in the vicinity of the Antarctic Peninsula. Inter J Climatology 14: 357-369

Klink JM, Smith DA, Smith RC (1994) Hydrography in the LTER region during August and September 1993. Ant J U S 29: 219-221

Krebs WN (1983) Ecology of neritic marine diatoms, Arthur Harbor, Antarctica. Micropaleontology 29: 267-297

Lancelot C, Billen G, Vet C, Becquevort S, Mathot S (1991a) Modelling carbon cycling through phytoplankton and microbes in the Scotia-Weddell Sea area during sea ice retreat. Mar Chem 35: 305-324

Lancelot C, Veth C, Mathot S (1991b) Modelling ice-edge phytoplankton bloom in the Scotia-Weddell sea sector of the Southern Ocean during spring 1988. J Mar Syst 2: 333-346

Lancelot C, Billen G, Veth C, Becquevort S, Mathot S (1993) Factors controlling phytoplankton ice-edge blooms in the

marginal ice-zone of the northwestern Weddell Sea during seas ice retreat 1988: field observations and mathematical modelling. Polar Biology 13: 377-387

Lizotte MP, Priscu JC (1992) Photosynthesis-irradiance relationships in phytoplankton from the physically stable water column of a perennially ice-covered lake (Lake Bonney, Antarctica). J Phycol 28: 179-185

Mathot S, Dandois J-M, Lancelot C (1992) Gross and net primary production in the Scotia-Weddell Sea sector of the Southern Ocean during spring 1988. Polar Biology 12: 321-322

McMinn A, Hodgson D (1993) Summer phytoplankton succession in Ellis Fjord, eastern Antarctica. J Plank Res 15: 925-938

Mitchell BG, Holm-Hansen O (1991) Observations and modeling of the Antarctic phytoplankton crop in relation to mixing depth. Deep-Sea Res 38: 981-1007

Mitchell BG, Brody EA, Holm-Hansen O, McClain C, Bishop J (1991) Light limitation of phytoplankton biomass and macronutrient utilization in the Southern Ocean. Limnol Oceanogr 36: 1662-1677

Moline MA, Prézelin BB (1994) Palmer LTER: Impact of a large diatom bloom on macronutrient distribution in Arthur

Harbor during austral summer 1991-1992. Ant J U S. 29(5): 217-219

Moline MA, Prézelin BB (1996) High-Resolution Time-Series Data for Primary Production and Related Parameters at a Palmer LTER Coastal Site: Implications for Modeling Carbon Fixation in the Southern Ocean. Polar Biology. In press

Moline MA, Prézelin BB, Schofield O, Smith RC (1996) Temporal dynamics of coastal Antarctic phytoplankton: Environmental driving forces and impact of a 1991-1992 summer diatom bloom on the nutrient regimes. In: Battaglia B, Valencia J, Walton DWH (eds) Antarctic Communities. Cambridge University Press. In press

Mura MP, Satta MP, Agusti S (1995) Water-mass influences on summer Antarctic phytoplankton biomass and community structure. Polar Biology 15: 15-20

Murphy EJ, Clarke A, Symon C, Priddle J (1995) Temporal variation in Antarctic sea-ice: analysis of a long term fast-ice record from the South Orkney Islands. Deep-Sea Res 42: 1045-1062

Neale PJ, Richerson PJ (1987) Photoinhibition and the diurnal variation of phytoplankton photosynthesis, I,

Development of a photosynthesis-irradiance model from studies of *in situ* responses. J Plank Res 9: 167-193

Nelson DM, Smith WOJ (1991) Sverdrup Revisited: Critical Depths, Maximum Chlorophyll Levels, and the Control of Southern Ocean Productivity by the Irradiance-Mixing Regime. Limnol Oceanogr 36: 1650-1661

Prézelin BB, Bozcar B (1986) Molecular bases of cell absorption and fluorescence in phytoplankton: potential applications to studies in optical oceanography. In: Round F, Chapman D (eds) Progress in Phycological Research. Biopress Ltd. , Bristol. 4: 349-465.

Prézelin BB, Glover HE, VerHoven B, Steinberg DK, Matlick HA, Schofield O, Nelson NB, Wyman M, Campbell L (1989) Blue-green light effects on light-limited rates of photosynthesis: relationship to pigmentation and productivity estimates from the Sargasso Sea. Mar Ecol Prog Ser 54: 121-136

Prézelin BB, Glover HE (1991) Variability in time/space estimates of phytoplankton biomass and productivity in the Sargasso Sea. J Plankton Res 13S: 45-67

Rivkin RB (1991) Seasonal patterns of planktonic production in McMurdo Sound, Antarctica. Amer Zool 31: 5-16

Ross RM, Quetin LB (1992) Palmer long-term ecological research (LTER): An overview of the 1991-1992 season. Ant J U S 27: 235-236

Ryther JH, Hulbert EM (1960) On Winter Mixing and the Vertical Distribution of Phytoplankton. Limnol Oceanogr 5: 337-338

Sakshaug E, Slagstad D, Holm-Hansen O (1991) Factors controlling the development of phytoplankton blooms in the Antarctic Ocean-A mathematical model. Mar Chem 35: 259-271

Sakshaug E, Slagstad D (1992) Sea ice and wind: Effects on primary productivity in the Barents Sea. Atmosphere-Ocean 30: 579-591

Satoh H, Wantanabe K, Kanda H, Takahashi E (1986) Seasonal changes of chlorophyll a standing stocks and oceanographic conditions under fast ice near Syowa Station, Antarctica 1983/84. Antarc Rec 30: 19-32

Scharek R, Smetacek V, Fahrbach E, Gordon LI, Rohardt G, Moore S (1994) The transition from winter to early spring in the eastern Weddell Sea, Antarctica: Plankton biomass and composition in relation to hydrography and nutrients. Deep-Sea Res 41:1231-1250

Schofield O, Prézelin BB, Smith RC, Stegmann PM, Nelson NB, Lewis MR, Baker KS (1991) Variability in spectral and nonspectral measurements of photosynthetic light utilization efficiencies. Mar Ecol Prog Ser 78: 253-271

Schofield O, Moline MA, Prézelin BB (1994) Photoadaptation in a coastal phytoplankton bloom and impact on the radiation utilization efficiency for carbon fixation. Ant J U S 29: 214-216

Schofield O, Moline MA, Prézelin BB (1996) Variability of the maximum quantum yield for carbon fixation in Antarctic coastal waters. Limnol Oceanogr. Submitted

Shabica SV, Hedgpeth JW, Park PK (1977) Dissolved oxygen and pH increases by primary production in the surface water of Arthur Harbor, Antarctica, 1970-1971. In: Llano GA (ed) Adaptations Within Antarctic Ecosystems. Gulf, Houston pp 83-97

Smetacek, V; Scharek, R; Gordon, LI; Eicken, H; Fahrbach, E; Rohardt, G; Moore, S (1992) Early spring phytoplankton blooms in ice platelet layers of the southern Weddell Sea, Antarctica. Deep-Sea Res 39: 153-168

Smith RC, Baker KS, Handley P, Newberger T (1992) Palmer LTER program: Hydrography and optics within the

peninsula grid, zodiac sampling grid during the 1991-1992 field season. Ant J U S 27: 253-255

Smith RC, Baker KS, Fraser WR, Hofmann EE, Karl DM, Klink JM, Quetin LB, Prézelin BB, Rorr RM, Trivelpiece WZ, Vernet M (1995) The Palmer LTER: A long-term ecological research program at Palmer Station, Antarctica. Oceanography 8: 77-86

Smith WOJ, Nelson DM (1985) Phytoplankton bloom produced by a receding ice edge in the Ross Sea: Spatial coherence with the density field. Science 277: 163-166

Sommer U, Stabel H-H (1986) Near surface nutrient and phytoplankton distribution in the Drake Passage during early December. Polar Biology 6: 107-110

Stark P (1994) Climate warming in the central Antarctic Peninsula area. Weather 49: 215-220

Townsend DW, Keller MD, Sieracki ME, Ackleson SG (1992) Spring phytoplankton blooms in the absence of vertical water column stratification. Nature 360: 59-62

Tréguer P, Lindner L, Bennekom AJ, van Panouse M, Leynaert A, Jacques G (1991) The production of biogenic silica in the Weddell-Scotia Seas measured by using radiotracer 32 Si. Limnol Oceanogr 36: 1217-1227

Turner D, Owens NJP (1995) A biogeochemical study in the Bellingshausen Sea: Overview of the STERNA 1992 expedition. Deep-Sea Res 42: 907-932

Vaulot D, Birrein J-L, Marie D, Casotti R, Veldhuis MJW, Kraay GW, Chrétiennot-Dinet M-J (1994) Morphology, ploidy, pigment compoistion, and genome size of cultured strains of *Phaeocystis* (Prymnesiophyceae). J Phycol 30: 1022-1035

Vernet M (1992) RACER: predominance of cryptomonads and diatoms in the Gerlache Strait. Ant J U S 27: 157-158

Villafañe VE, Helbling EW, Holm-Hansen O (1995) Spatial and temporal varability of phytoplankton biomass and taxanomic composition around Elephant Island, Antarctica, during the summers of 1990-1993. Mar Bio 123: 677-686

Waters KJ, Smith RC (1992) Palmer LTER: A sampling grid for the Palmer LTER program. Ant J U S 27: 236-239

Weatherly, JW; Walsh, JE; Zwally, HJ (1991) Antarctic sea ice variations and seasonal air temperature. J Geophys Res 96: 15119-15130

Whitaker TM (1982) Primary production of phytoplankton off Signy Island, South Orkneys, the Antarctic. Proc R Soc Lond 214: 169-189

Wright SW, Jeffery SW (1987) Fucoxanthin pigment markers of marine phytoplankton analysed by HPLC and HPTLC. Mar Ecol Prog Ser 38: 259-266

Wright SW, Jeffery SW, Mantoura RFC, Llewellyn CA, Bjørnland T, Repeta D, Welschmeyer N (1991) Improved HPLC method for analysis of chlorophylls and caroteniods from marine phytoplankon. Mar Eco Prog Ser 77: 183-196

Zimmerman RC, SooHoo JB, Kremer JN, D'Argenio DZ (1987) Evaluation of variance approximation techniques of non-linear photosynthesis-irradiance models. Mar Biol 95: 209-215

Table 1. Monthly mean biomass and total primary production for LTER stations B and E from 1991-1994. Mean values are ± 1 SD.

		Station B		Station E	
Year/ Month	$Q_{par}(0^+)$ mol m^{-2} d^{-1}	Chl *a* mg Chl a m^{-2}	PP g C m^{-2}	Chl *a* mg Chl a m^{-2}	PP g C m^{-2}
1991-92					
December	48.6 ± 12.7	183.4 ± 119.2	78.12 †	178.9 ± 71.1	71.61
January	28.9 ± 11.4	115.7 ± 89.4	40.61 †	74.9 ± 29.9	18.91
February	28.0 ± 11.5	49.4 ± 19.2	20.72 †	89.2 ± 31.8	25.76
1992-93					
November	27.5 ± 8.7	37.9 ± 8.9	34.80	31.8 ± 6.8	21.90
December	33.3 ± 9.7	48.4 ± 15.3	20.15	61.6 ± 33.3	28.83
January	39.6 ± 13.7	28.1 ± 5.8	12.09	41.7 ± 12.1	14.26
1993-94					
August ‡	6.1 ± 3.1	7.6 ± 0.2	0.62	–	–
September	11.4 ± 5.6	14.5 ± 7.0	3.30	12.5 ± 1.0	2.70
October	27.3 ± 7.0	18.1 ± 12.7	5.97	11.2 ± 2.5	1.55
November	31.4 ± 14.0	18.7 ± 11.0	10.20	22.4 ± 12.9	12.60
December	38.8 ± 10.7	51.0 ± 13.9	20.77	51.6 ± 12.6	24.18
January	30.0 ± 9.9	25.8 ± 7.0	10.85	21.6 ± 2.1	9.92

† Values vary slightly from those in Moline and Prézelin (1996; Chapter 3) due to improvements in the interprolation methods. See text.

‡ Monthly means and totals are estimated from the last 13 days of the month.

Figure 1. Location of LTER sampling station B (64° 46.45' S, 64° 03.27' W) and E (64° 48.90' S, 64° 02.43' W) with respect to Palmer Station and the Antarctic Peninsula (inset). The distance between stations B and E is ~3 km.

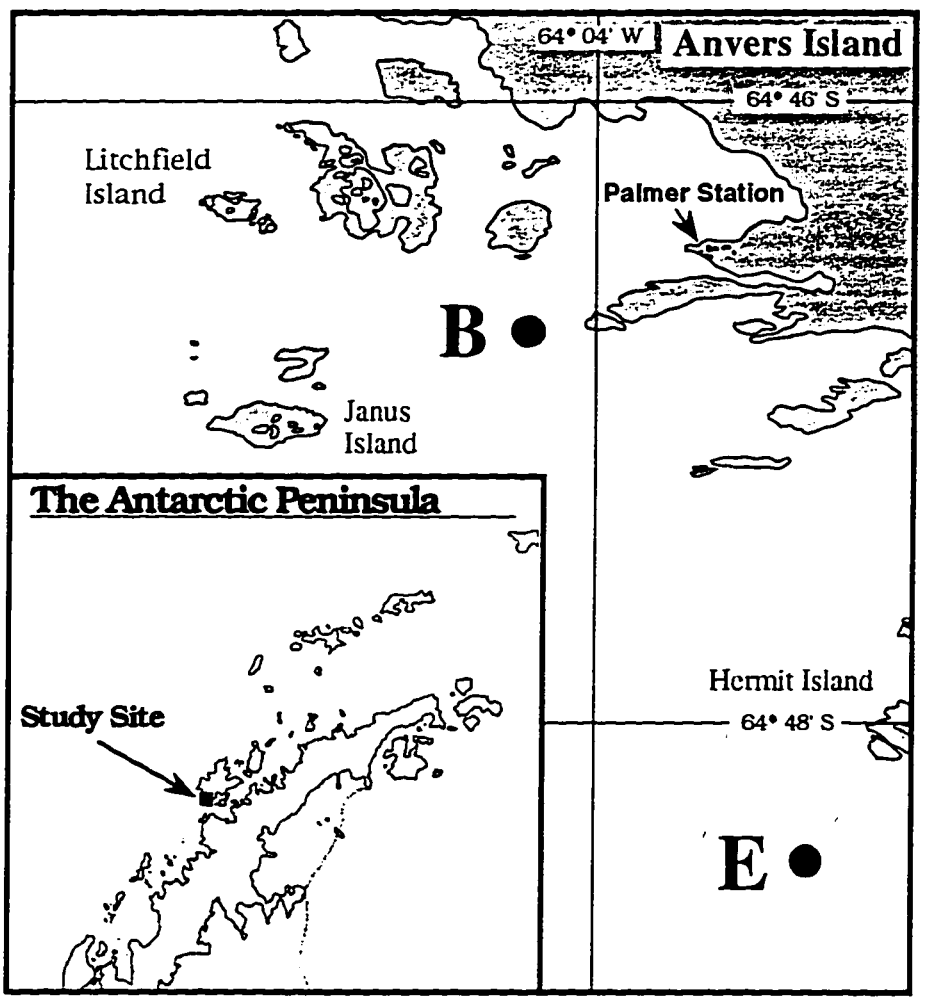
64° 04' W
Anvers Island
64° 46' S
Litchfield Island
Palmer Station
B
Janus Island
The Antarctic Peninsula
Study Site
Hermit Island
64° 48' S
E

Figure 2A. Seasonal change at station B in the depth distribution of chlorophyll a (mg Chl a m^{-3}) over the three field seasons from 1991-1994. Discrete samples are shown as filled circles; 1991-92 n=215, 1992-93 n=232, 1993-94 n=182. The upper contour (1991-92) is overlaid with the seasonal change in the depth of the upper mixed layer (white line). The presence of significant pack ice (>50% coverage) is indicated by hatch bars. Contours are shown with a maximum of 3 mg Chl a m^{-3} for comparative purposes between years. Chl a concentrations within the phytoplankton bloom during the 1991-92 season were typically in excess of 10 mg m^{-3} (see text). Arrow indicate the initiation of glacial meltwater input into the region. Note the difference in the depth scales.

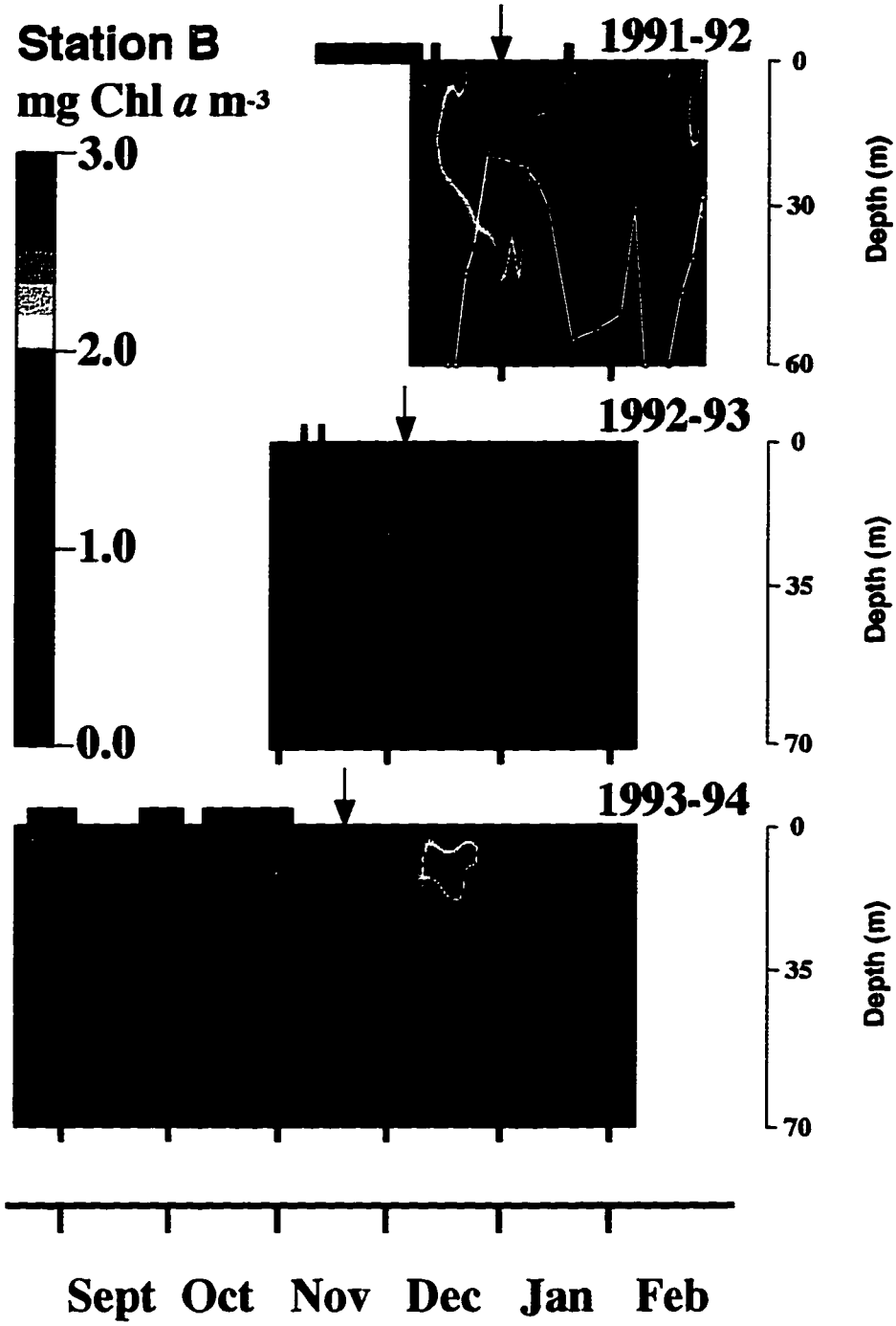
Station B
mg Chl a m-3
3.0
2.0
1.0
0.0
1991-92
1992-93
1993-94
0
30
60
35
70
Depth (m)
Sept
Oct
Nov
Dec
Jan
Feb

Figure 2B. Seasonal change at station E in the depth distribution of chlorophyll a (mg Chl a m^{-3}) over the three field seasons from 1991-1994. Discrete samples are shown as filled circles; 1991-92 n=134, 1992-93 n=207, 1993-94 n=170. The upper contour (1991-92) is overlaid with the seasonal change in the depth of the upper mixed layer (white line). Contours are shown with a maximum of 3 mg Chl a m^{-3} for comparative purposes between years. Chl a concentrations within the phytoplankton bloom during the 1991-92 season were typically in excess of 8 mg m^{-3} (see text). Arrows are same as Fig. 2A.

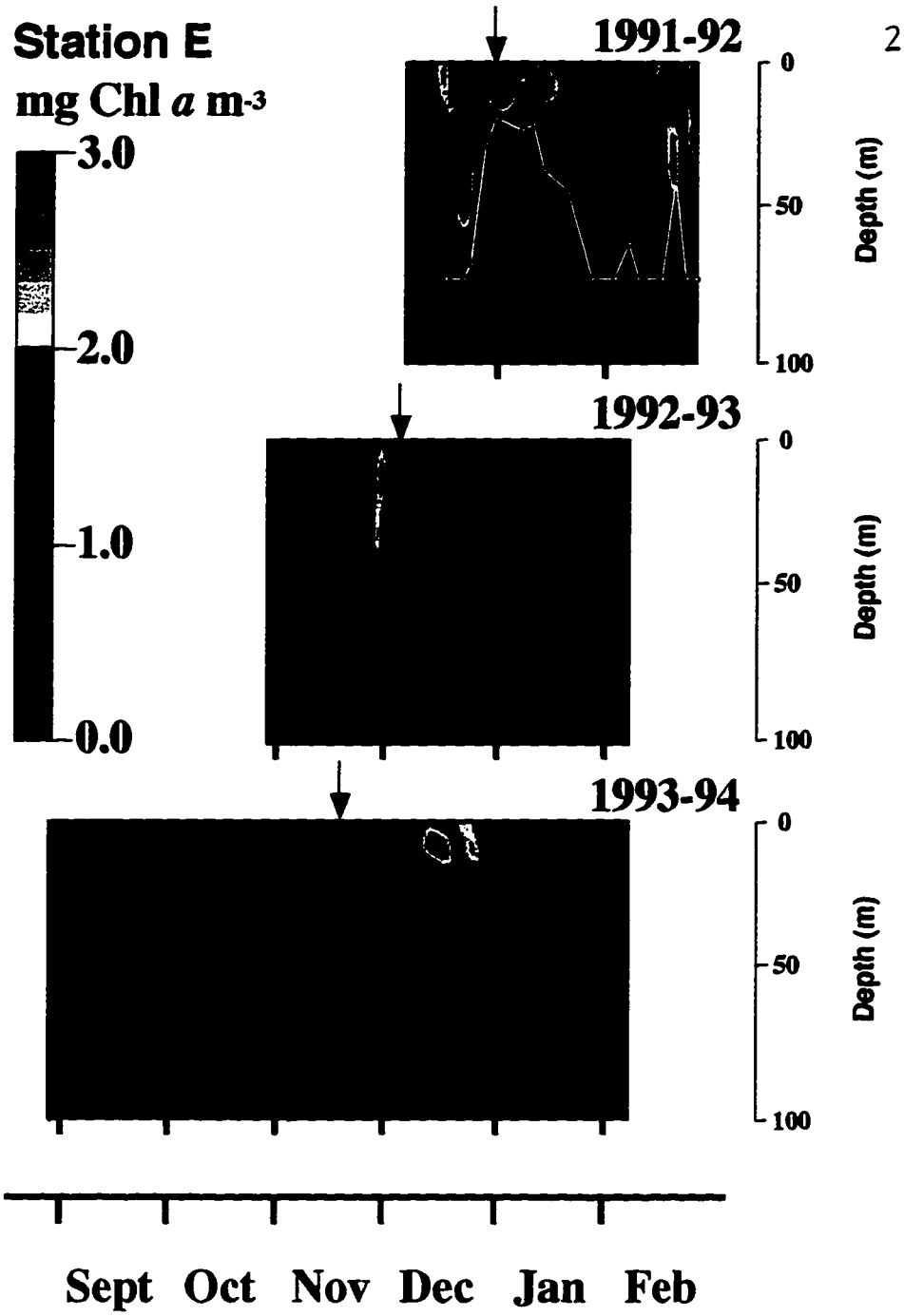
Station E
mg Chl a m-3
3.0
2.0
1.0
0.0
1991-92
1992-93
1993-94
0
50
100
Depth (m)
Sept
Oct
Nov
Dec
Jan
Feb

Figure 3. Station B comparison between average daily wind speed (m s^{-1}) and integrated (0-20 m) Chl a (mg m^{-2}) during the austral summer period from 1991-1994. The horizontal dotted line has been added to each year at 10 m s^{-1} (~5 knots) for comparative purposes. Note the different scales for Chl *a* over the three years. The presence of significant pack ice (>50% coverage) is indicated by hatch bars.

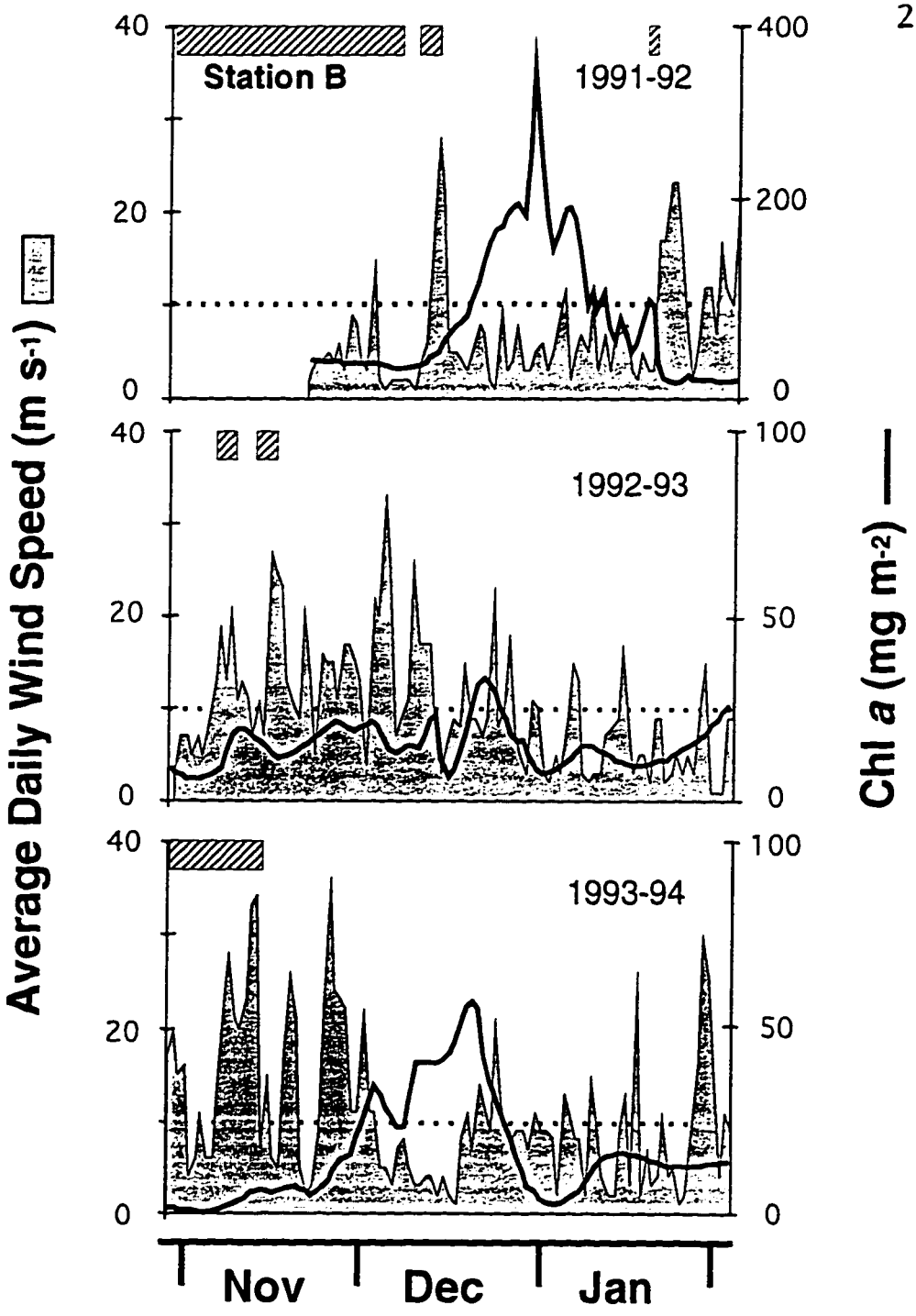
Station B
1991-92
1992-93
1993-94
40
20
0
400
200
100
50
Nov
Dec
Jan
Average Daily Wind Speed (m s-1)
Chl a (mg m-2)

Figure 4. Tidal height (m) measured at Palmer Station from December 10 to December 31, 1991 (upper). Maximum tide differential (m) derived from upper panel is shown with the percent difference in the integrated (0-20m) Chl a between station B and E (1-E/B) (middle). Directions of tidal flow are shown for solar noon (time of sampling). (lower) The difference between the average temperatures in the upper 10m at station B and E from December, 1991 to January, 1992.

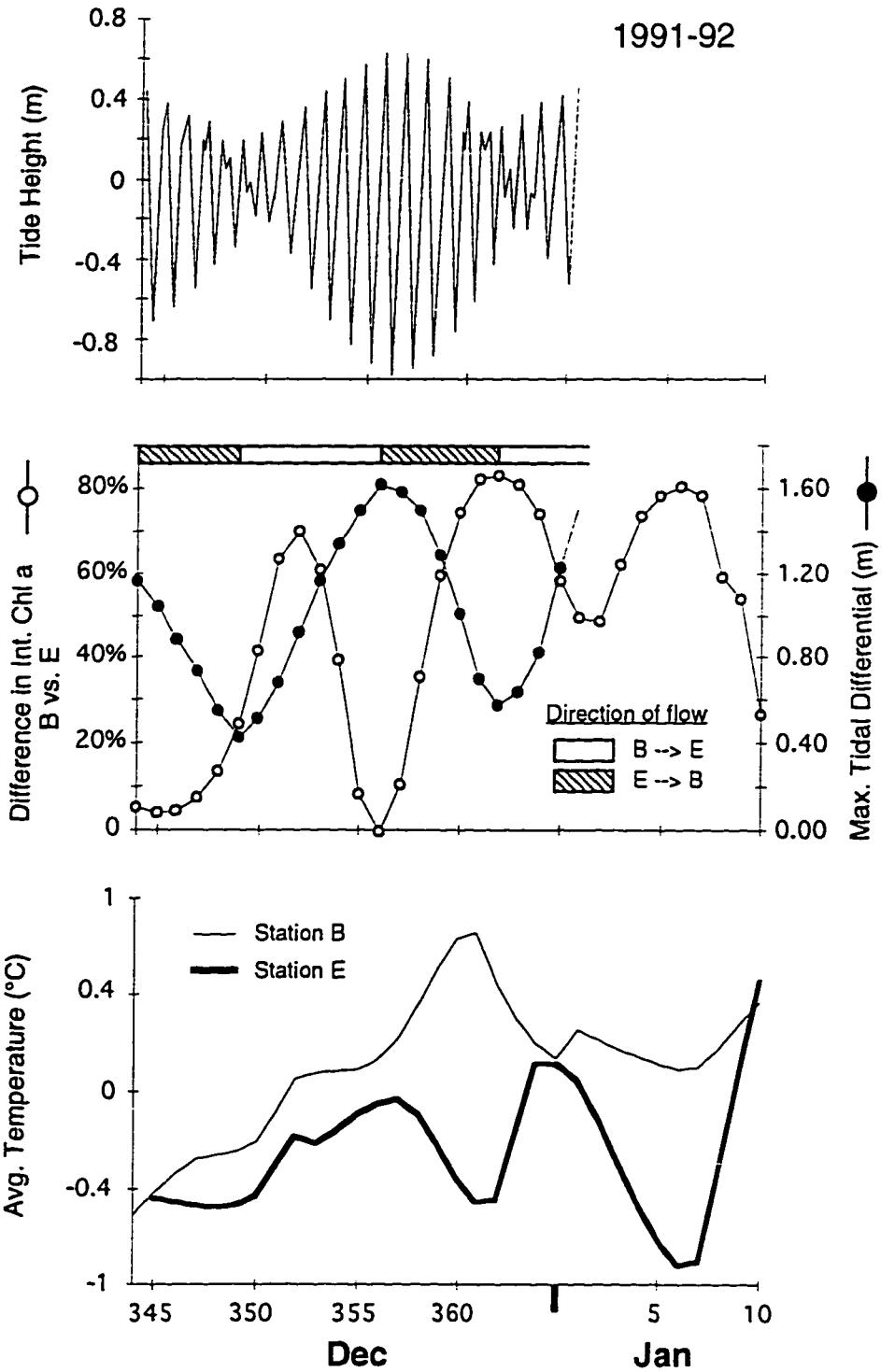
1991-92
Tide Height (m)
0.8
0.4
0
-0.4
-0.8
Difference in Int. Chl a B vs. E
80%
60%
40%
20%
0
Direction of flow
B --> E
E --> B
1.60
1.20
0.80
0.40
0.00
Max. Tidal Differential (m)
Avg. Temperature (°C)
Station B
Station E
1
0.4
0
-0.4
-1
345
350
355
360
5
10
Dec
Jan

Figure 5A. Seasonal change at station B in the depth distribution of temperature (° C) over the three field seasons from 1991-1994. The presence of significant pack ice (>50% coverage) is indicated by hatch bars. Contours are shown for temperatures ranging from +1.2 to - 1.4° C for comparative purposes between years. Arrows are same as Fig. 2A. Note the difference in the depth scales.

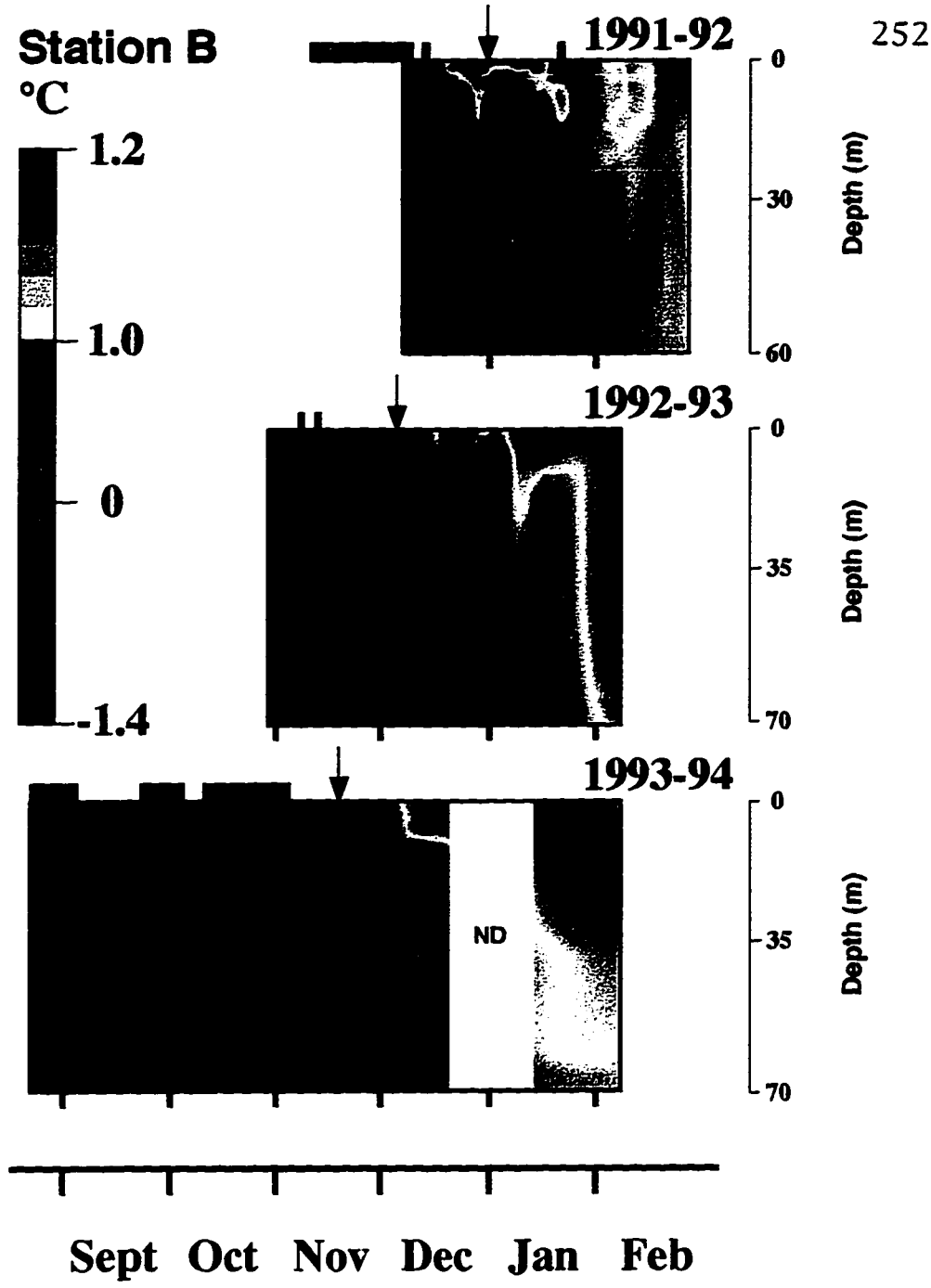
Station B
°C
1.2
1.0
0
-1.4
1991-92
1992-93
1993-94
ND
0
30
60
35
70
Depth (m)
Sept
Oct
Nov
Dec
Jan
Feb

Figure 5B. Seasonal change at station E in the depth distribution of temperature (° C) over the three field seasons from 1991-1994. Contours are shown for temperatures ranging from + 1.2 to -1.4 ° C for comparative purposes between years. Arrows are same as Fig. 2A.

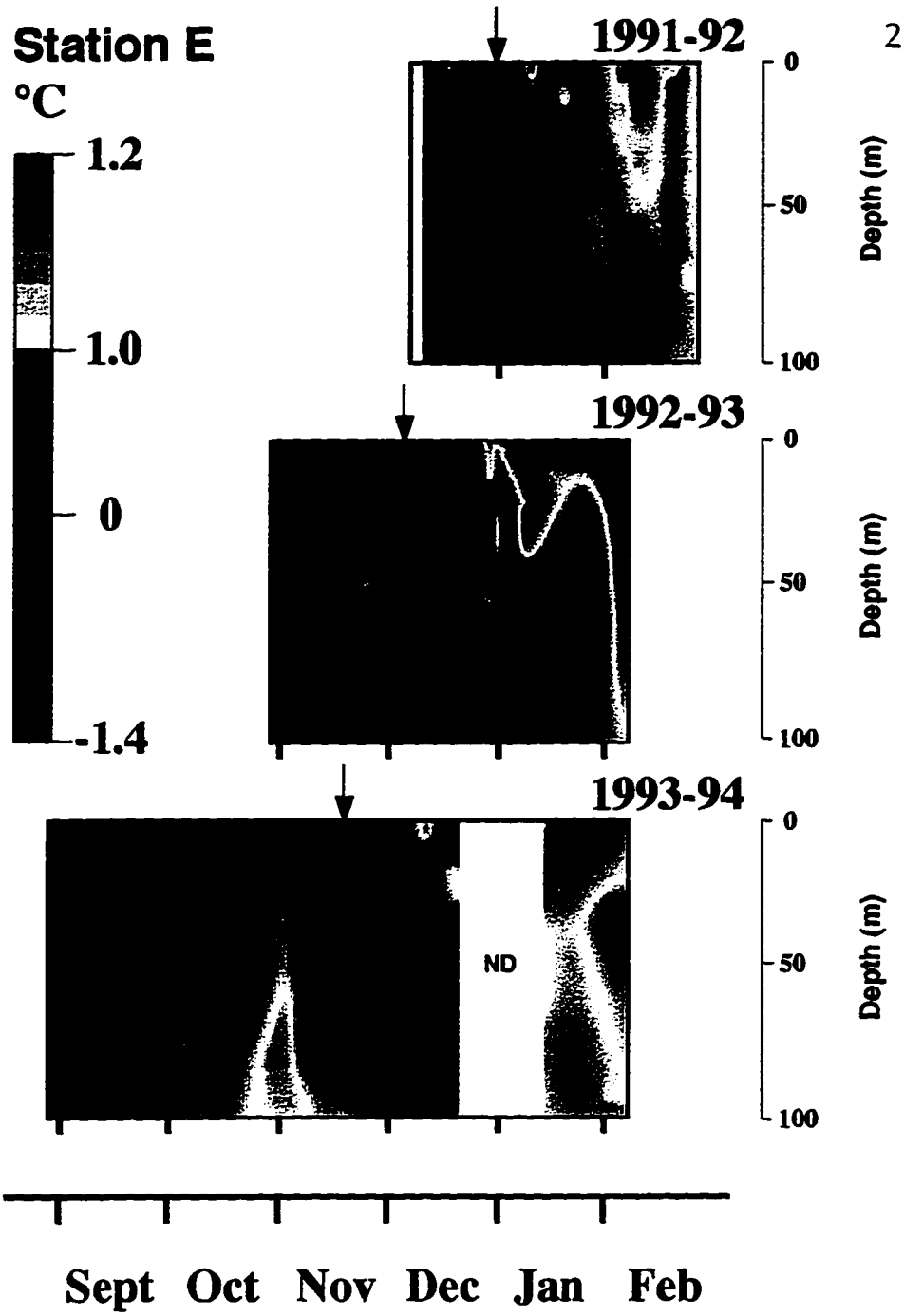
Station E
°C
1.2
1.0
0
-1.4
1991-92
1992-93
1993-94
ND
0
50
100
Depth (m)
Sept
Oct
Nov
Dec
Jan
Feb

Figure 6A. Depth and time distribution of daily simulated in situ production (mg C m^{-3} d^{-1}) at station B over the three field seasons from 1991-1994. Discrete samples are shown in Fig. 2A. Contours are shown with a maximum of 100 mg C m^{-3} d^{-1} for comparative purposes between years. Daily simulated in situ production within the phytoplankton bloom during the 1991-92 season were typically in excess of 400 mg C m^{-3} d^{-1} (see text). Contour are overlaid with the seasonal change in the depth of the 0.1% Q_{par} (white line). The presence of significant pack ice (>50% coverage) is indicated by hatch bars. Arrows are same as Fig. 2A. Note the difference in the depth scales.

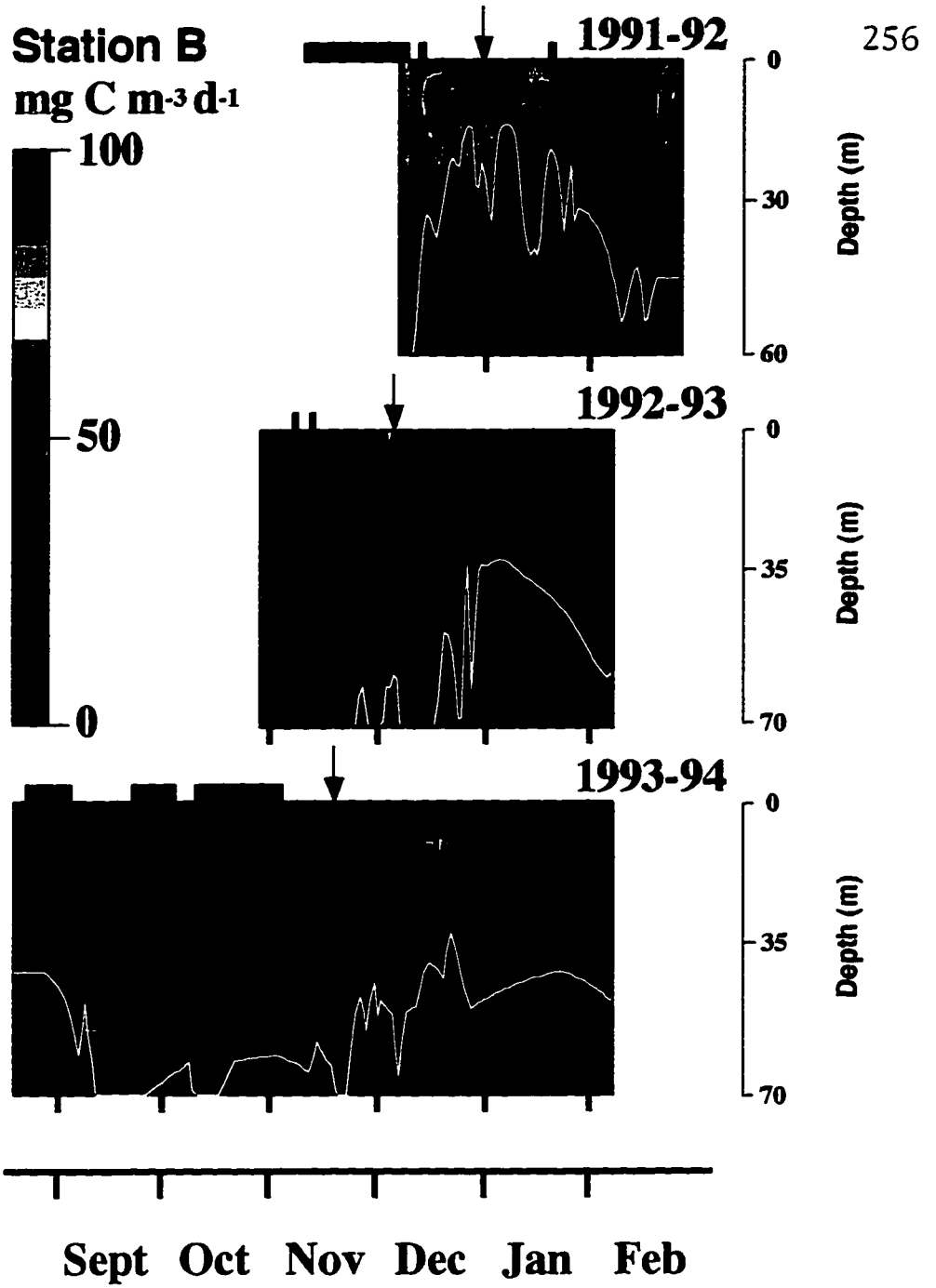
Station B
mg C m-3 d-1
100
50
0
1991-92
1992-93
1993-94
0
30
60
35
70
Depth (m)
Sept
Oct
Nov
Dec
Jan
Feb

Figure 6B. Depth and time distribution of daily simulated in situ production (mg C m^{-3} d^{-1}) at station E over the three field seasons from 1991-1994. Discrete samples are shown in Fig. 2B. Contours are shown with a maximum of 100 mg C m^{-3} d^{-1} for comparative purposes between years. Daily simulated in situ production within the phytoplankton bloom during the 1991-92 season were typically in excess of 300 mg C m^{-3} d^{-1} (see text). Contour are overlaid with the seasonal change in the depth of the 0.1% Q_{par} (white line). Arrows are same as Fig. 2A.

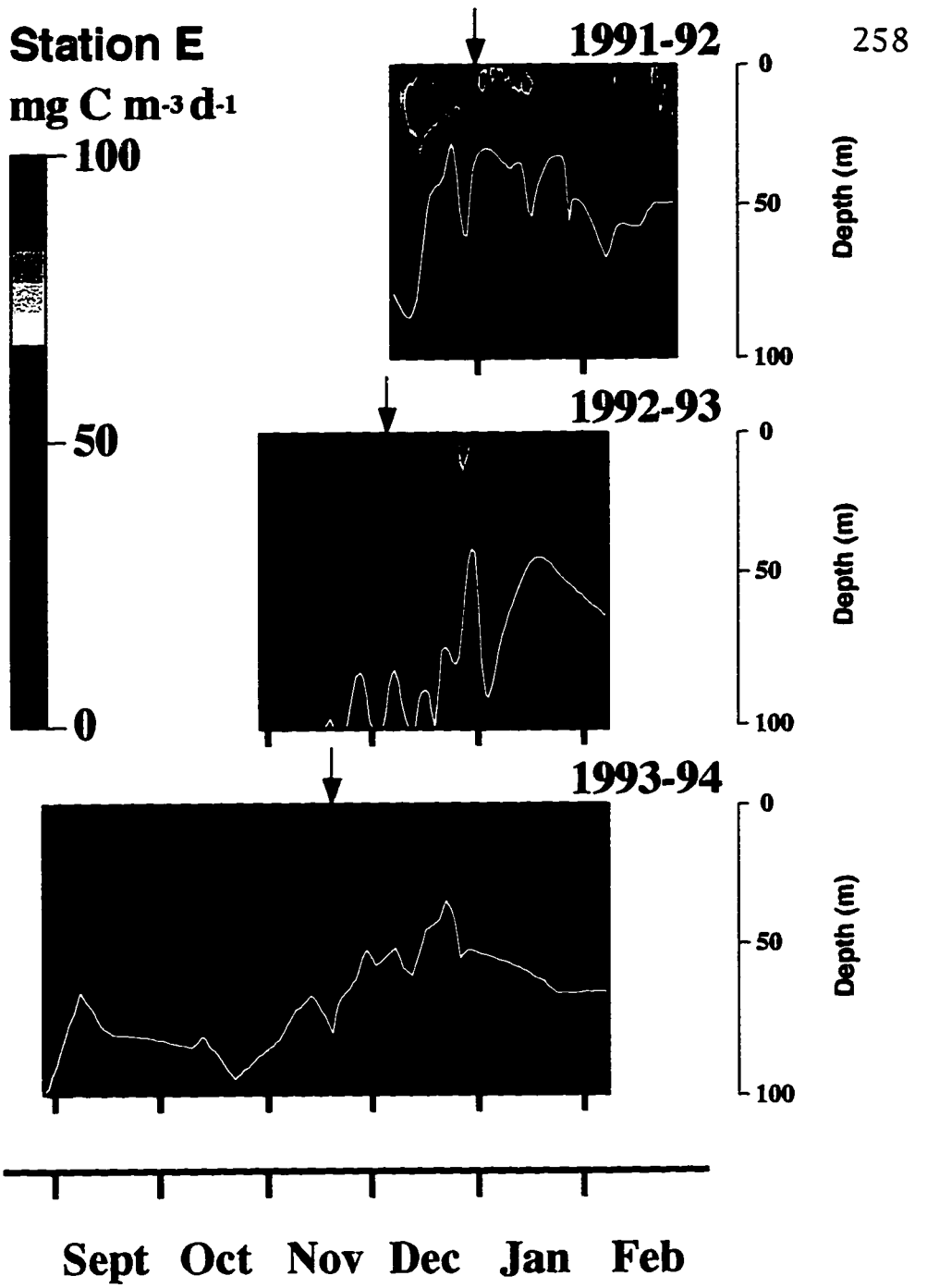
Station E
mg C m-3 d-1
100
50
0
1991-92
1992-93
1993-94
0
50
100
Depth (m)
Sept
Oct
Nov
Dec
Jan
Feb

Figure 7. Total integrated Chl a (mg m^{-2}) and daily simulated in situ production (g C m^{-2} d^{-1}) for stations B and E over the three field seasons from 1991-1994. Station B was integrated to 60 m for 1991-92 and 70 m for 1992-1994. The depth of integration for station E was 100 m.

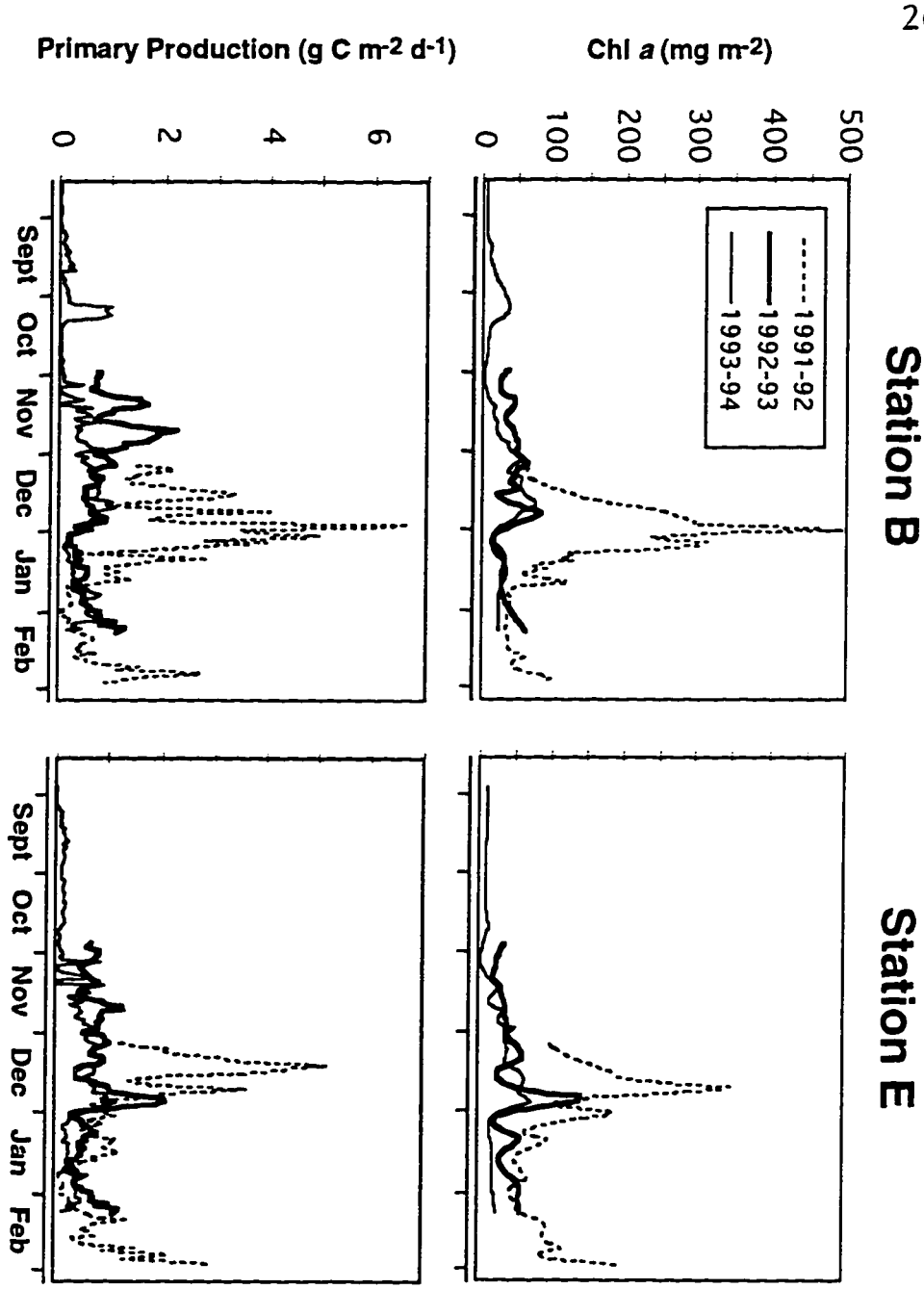
Station B
Station E
Chl a (mg m-2)
Primary Production (g C m-2 d-1)
1991-92
1992-93
1993-94
0
100
200
300
400
500
0
2
4
6
Sept
Oct
Nov
Dec
Jan
Feb

Figure 8. Total integrated Chl *a* (mg m^{-2}) in the euphotic zone (0.1% Q_{par} isolume) versus the daily simulated *in situ* production (g C m^{-2} d^{-1}) for stations B and E over the three field seasons from 1991-1994. The best-fit linear regression is included (P=0.025*[Chl *a*]+0.015, r^2=0.80, n=156).

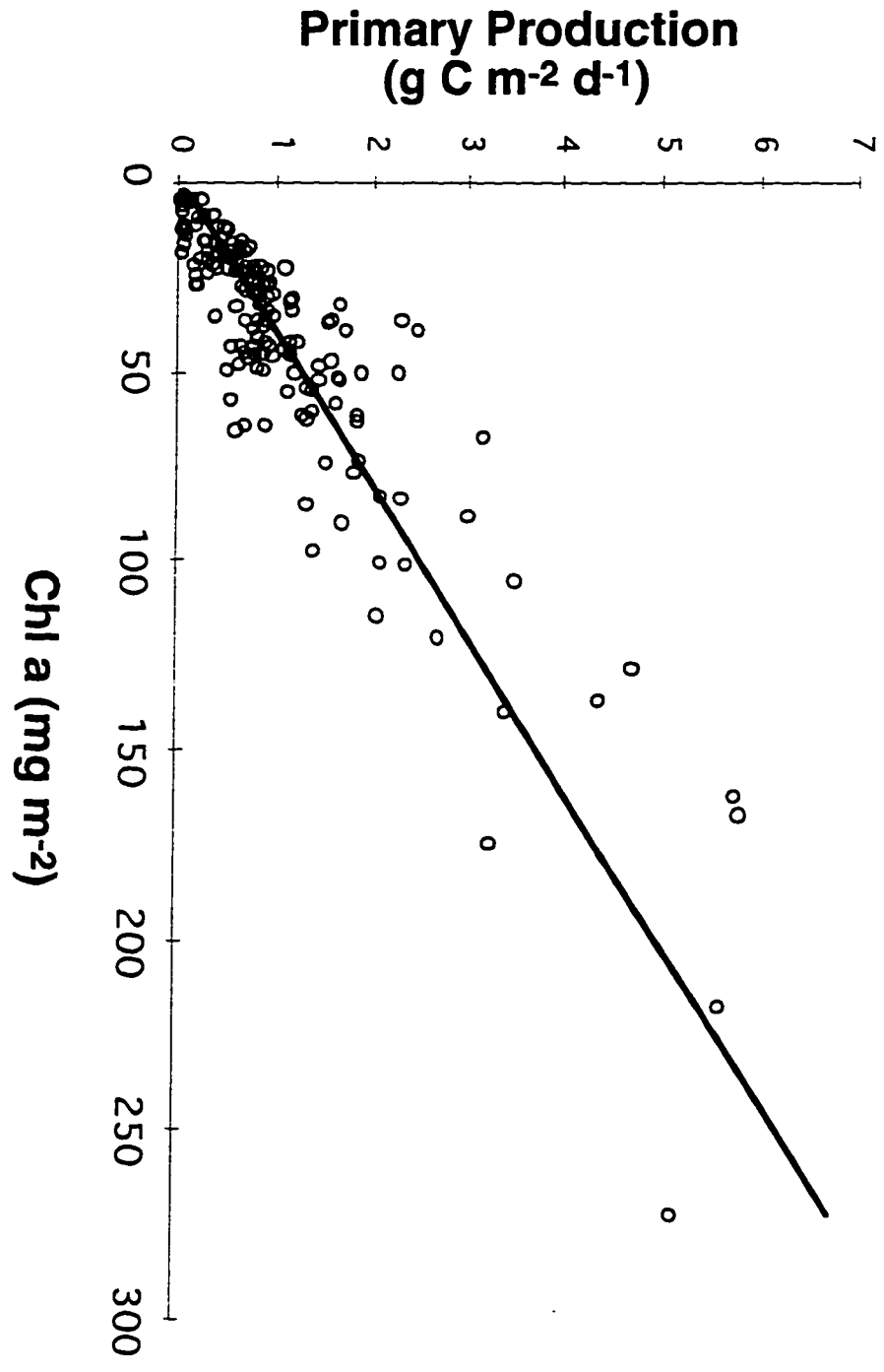
Primary Production
(g C m-2 d-1)
0
1
2
3
4
5
6
7
Chl a (mg m-2)
0
50
100
150
200
250
300

Figure 9A. Seasonal change in the depth integrated percent composition of the four different phytoplantkon groups represented at station B over the three field seasons from 1991-1994. Overlaid on the 1991-92 panel is the change in the average water column density (σt) in the upper 50 m. See text for explaination of the arrows. The presence of significant fast/pack ice (>50% coverage) is indicated by hatch bars. As in Fig. 2A, arrows indicate the initiation of glacial meltwater input into the region. Note the difference in scales for depth.

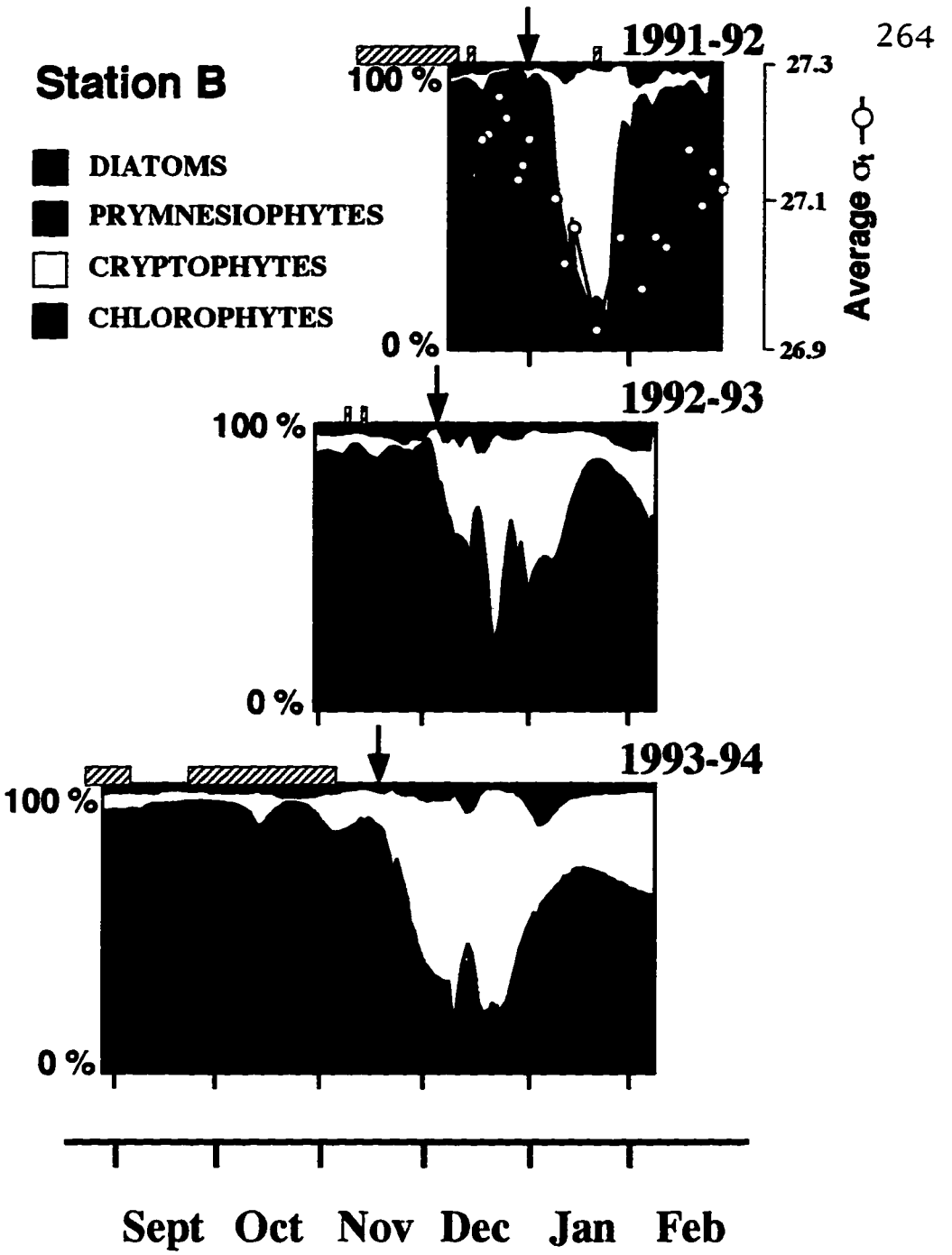
Station B
DIATOMS
PRYMNESIOPHYTES
CRYPTOPHYTES
CHLOROPHYTES
1991-92
1992-93
1993-94
100 %
0 %
27.3
27.1
26.9
Average σt
Sept
Oct
Nov
Dec
Jan
Feb

Figure 9B. Seasonal change in the depth integrated percent composition of the four different phytoplantkon groups represented at station E over the three field seasons from 1991-1994. Overlaid on the 1991-92 panel is the change in the average water column density (σt) in the upper 50 m. Arrows are same as Fig. 8A.

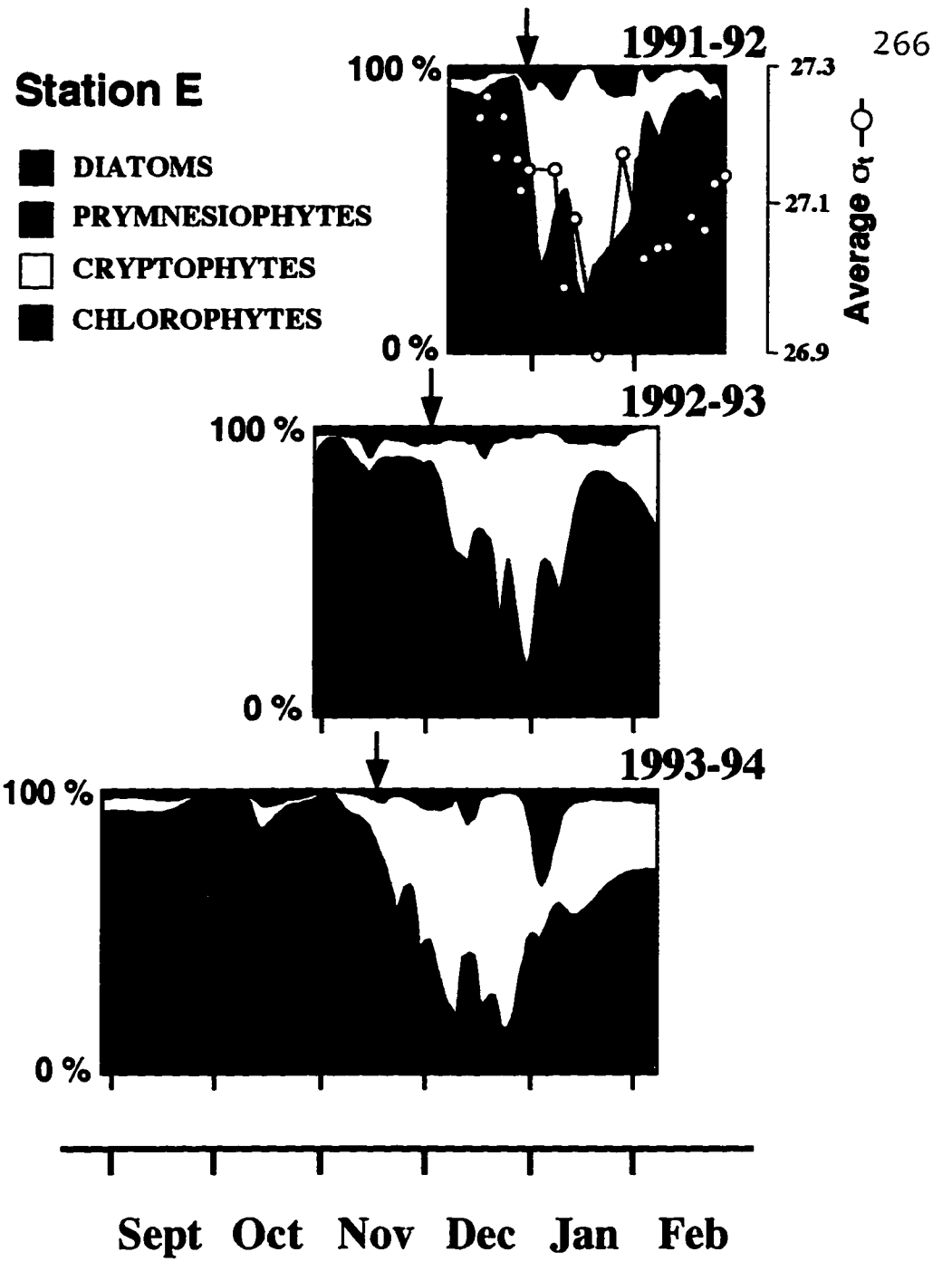
Station E
DIATOMS
PRYMNESIOPHYTES
CRYPTOPHYTES
CHLOROPHYTES
1991-92
100 %
0 %
27.3
27.1
26.9
Average σt
1992-93
100 %
0 %
1993-94
100 %
0 %
Sept Oct Nov Dec Jan Feb

Figure 10. Variability in the range of (A) intraannual and (B) peak interannual biomass (mg Chl a m^{-2}) for this study and other temporal studies in coastal Antarctic regions.

A

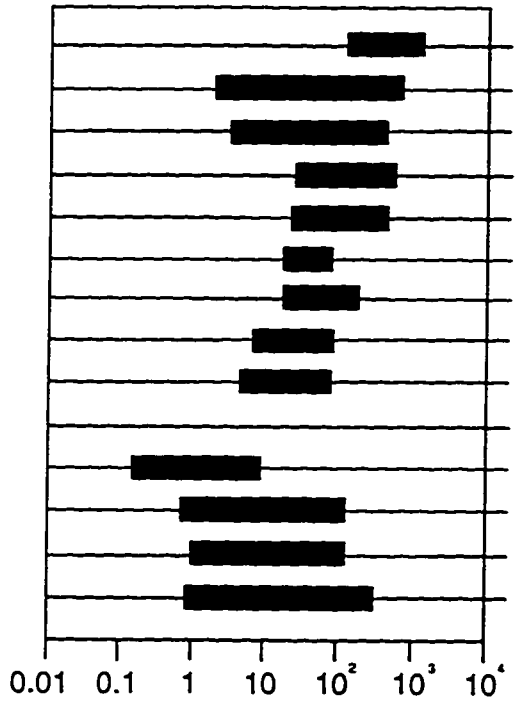

Location	Year	Study
Antarctic Peninsula		
S. Orkney Is.	1966-67 Dec-May	Horne et al., 1969
S. Orkney Is.	1972-73 Jun-Jun	Whitaker, 1982
S. Orkney Is.	1973-74 Jun-Feb	Whitaker, 1982
Anvers Is. (Sta B)	1991-92 Nov-Feb	This Study
Anvers Is. (Sta E)	1991-92 Nov-Feb	This Study
Anvers Is. (Sta B)	1992-93 Nov-Jan	This Study
Anvers Is. (Sta E)	1992-93 Nov-Jan	This Study
Anvers Is. (Sta B)	1993-94 Aug-Jan	This Study
Anvers Is. (Sta E)	1993-94 Aug-Jan	This Study
Continental Margin		
Ongul Is.(shallow)	1983-84 Jan-Jan	Satoh et al., 1986
Ongul Is.	1983-84 Jan-Jan	Satoh et al., 1986
Ongul Is.	1983-84 Jan-Jan	Satoh et al., 1986
McMurdo Sound	1984-86 Sept-Jan	Rivkin, 1991

B

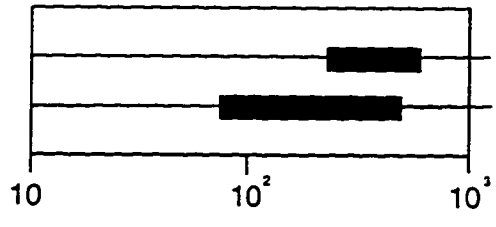

S. Orkney Is.	1972-74	Whitaker, 1982
Anvers Is.	1991-94	This Study

Chl *a* (mg m-2)

Figure 11. Seasonal change in the mean percent contribution of cryptophytes to the total integrated biomass at station B and E from 1991-1994. Shaded area represents one standard deviation from the mean. The mean air temperature at Palmer Station for the study period is also shown. The vertical arrow indicates the summer solstice.

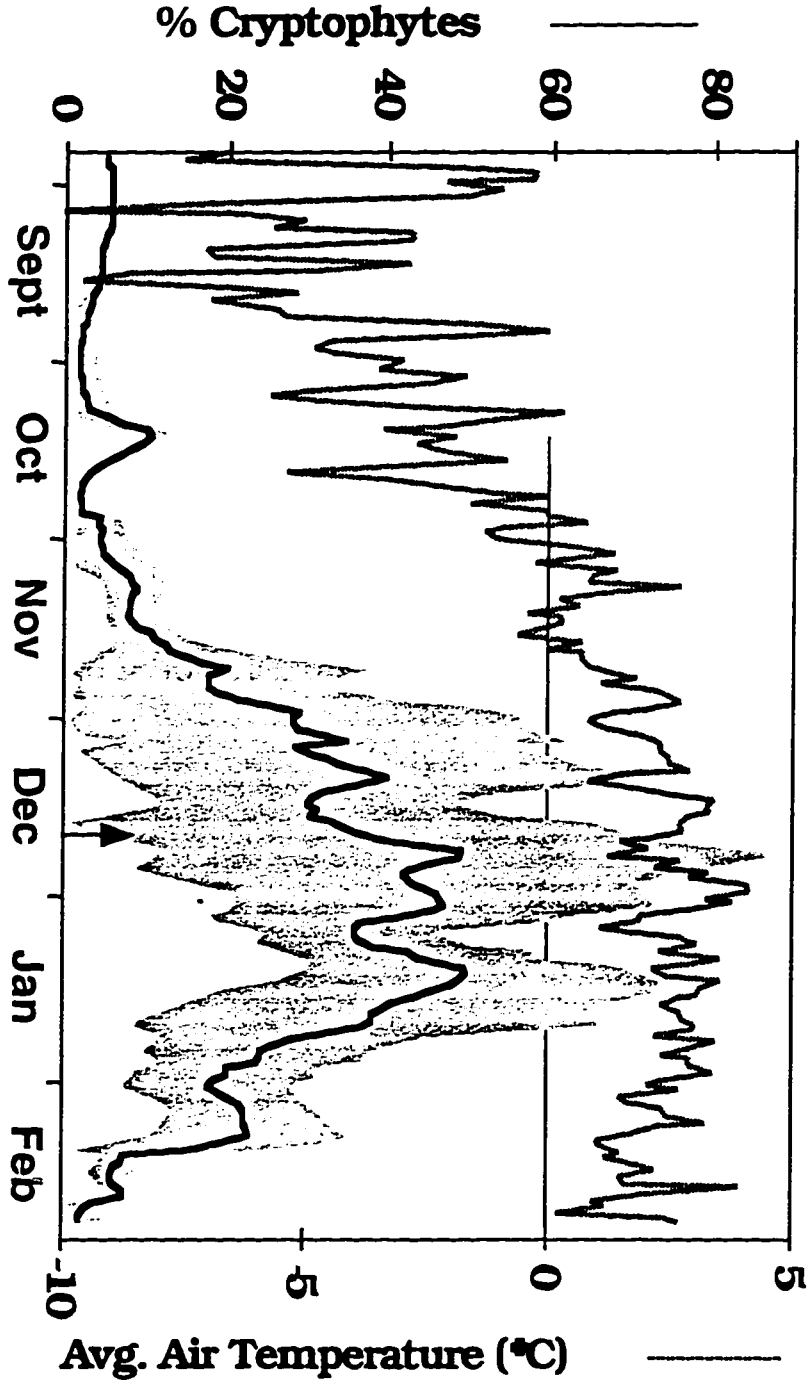
% Cryptophytes
0
20
40
60
80
Sept
Oct
Nov
Dec
Jan
Feb
-10
-5
0
5
Avg. Air Temperature (°C)

CHAPTER V

Variability of inorganic macronutrients in an Antarctic coastal region (1991-1994)

ABSTRACT

As part of the Long Term Ecological Research (LTER) program, a high resolution temporal data base was collected during the austral spring/summer seasons of 1991-1994 in shelf waters adjacent to Palmer Station, Antarctica to examine the temporal distribution of inorganic nutrients and utilization by phytoplankton. During two periods of low wind stress and stratification of the water column resulted in development of large blooms with biomass approaching 30 mg Chl a m^{-3} and maximum integrated concentrations of 494 mg Chl a m^{-2}. Macronutrient during these events rapidly decreased to very low concentrations (18.5 μM Si, 0.72 μM N, 0.04 μM P). Seasonal mean N:P:Si ratios agreed well with previous studies, however, at times over the sampling seasons, ratios indicated disproportionate uptake by phytoplankton and were found to partially depend on the taxonomic composition in the water column. Primary production determined by nutrient depletion in the water column was found to correspond well to measure in situ primary productivity for the large 1991-92 bloom. However, determining primary production by nutrient loss can deviate from measured results by an order of magnitude during times of high meltwater input. The maximum potential

for photosynthesis per unit Chl a decreased with decreasing nutrient, although was highly variable depending location in the water column and the extent of vertical mixing. Increased synthesis of light harvesting pigmentation occurred during low ambient nutrient concentrations in response to increasing biomass and self-shading. Despite the periods of extremely low nutrient conditions, daily in situ growth rates remained high, suggesting phytoplankton during this study were not nutrient limited.

INTRODUCTION

The Southern Ocean is characterized by high macronutrient concentrations resulting from upwelling of deep North Atlantic water to the surface at the Antarctic Divergence (Jones et al. 1990; Dower et al. 1996). Surface nutrient levels generally show a seasonal decrease (Whitaker 1982; Lancelot et al. 1993; Priddle et al. 1994), however, only rarely to the degree that restricts phytoplankton growth (see Holm-Hansen et al. 1994). Areas where severe depletion has been documented are restricted to ice edge zones (Nelson and Treguer 1992), coastal areas (Perrin et al. 1987; Holm-Hansen et al. 1989) and embayments (McMinn et al. 1995), where significant stratification, in terms of intensity and duration, provides conditions suitable to stimulate growth of large blooms (Smetacek and Passow 1990; Mitchell and Holm-Hansen 1991a; Mitchell et al. 1991; Nelson and Smith 1991; Sakshaug and Slagstad 1991; Sakshaug et al. 1991).

A high-resolution temporal data base was collected in shelf waters adjacent to Palmer Station, Antarctica as part of the Palmer Long-Term Ecological Research (LTER) program (see Introduction) for concurrent determinations of physical, biological and chemical parameters related to phytoplankton

ecosystem dynamics. Here, data from the austral spring/summer period of 1991-1994 is used to 1) quantify the distribution of inorganic nutrients; 2) identify physical and biological processes that alter water column nutrient concentrations and nutrient ratios; 3) compare productivity estimates derived from nutrient loss with measured in situ primary productivity (Moline and Prézelin 1996b; Chapter 4); and 4) examine possible impact of changing ambient nutrient concentrations on phytoplankton physiology.

METHODS

Sampling

Over the austral spring/summer period from November, 1991, through February, 1994, a total of 1,382 discrete water samples were collected at five Palmer Long-Term Ecological Research (LTER) stations (Sta A, B, C, D, and E; Fig. 1) for concurrent determinations of optical, biological and chemical parameters. Sta A is shallowest of the five stations (~45 m), adjacent to Palmer Station. The depth of each subsequent station increases to a maximal depth of ~ 280 m at Sta E, located on the northern edge of the Bismarck Strait.

Water column sampling was conducted from a Mark V Zodiac® using 5-liter GoFlo® sampling bottles. Whenever possible, samples were collected with in a few hours of solar noon. Daily average wind speed/direction, precipitation and snow height measurements were made at Palmer Station during the study period as part of a long term database collected by the U. S. National Science Foundation.

Inorganic and Particulate Organic Nutrient Determination

Subsamples of whole water for nutrient determination were filtered within an hour of collection through a 0.2 μm Nuclepore® membrane, and the 20 ml filtrate for each sample was stored in polycarbonate scintillation vials (acid washed) at -70 °C. Samples were later transported at -20°C to the Marine Science Analytical Laboratories, University of California, Santa Barbara for nutrient analyses. Methods for determination of the dissolved inorganic NO_3^- (N), PO_4^{3-} (P), and $Si(OH)_4$ (Si) concentrations were those of Johnson et al. (1985).

Subsamples for particulate organic carbon (POC) and nitrogen (PON) analyses were filtered onto precombusted Whatman® GF/F glass fiber filters and transported in desiccated conditions to the Marine Science Analytical

Laboratories, University of California, Santa Barbara. POC and PON concentrations were quantified for each sample using a Control Equipment Corp. 240XA CHN analyzer.

Phytoplankton Pigmentation

Aliquots of all whole water samples were analyzed for the algal pigments using reverse-phase HPLC procedures detailed in Moline and Prézelin (1996a) for the 1991-92 season and Wright et al. (1991) for the following two years. One liter samples were filtered on 0.4 μm nylon 47 mm Nuclepore® filters and extracted in 3 ml 90% acetone for 24 hr in the dark at -20 °C. Pigment separation was achieved with the aid of an Hitachi® L-6200A pump and an L-4250 UV/VIS variable wavelength detector (436 nm) equipped with a Waters® Radial-PAK C_{18} column (8 x 100 mm; 5 μm) during the 1991/92 season and a Waters® Resolve C_{18} column (3.9 x 300 mm; 5 μm) for the following two seasons. Peak identities of algal extracts were determined by comparing their retention times with pure pigment standards. Calibration studies comparing methods of Bidigare et al. (1989) and Wright et al. (1991), showed no significant quantitative differences for any of the pigments of interest. For the purposes of the present study, temporal/spatial patterns are presented for chlorophyll a (Chl

a), an indicator of total phytoplankton biomass, and the phytoplankton group-specific pigments Chlorophyll b (Chl b) for chlorophytes (Jeffrey 1974), fucoxanthin (Fuco) for diatoms (Wright and Jeffery 1987) alloxanthin (Allo) for cryptophytes (Gieskes 1983) and the sum of 19'-hexanoyloxyfucoxanthin (Hex) and 19'-butanoyloxyfucoxanthin (But) as a marker for chromophytes-nanoflagellates (in the Antarctic primarily *Phaeocystis pouchetii*) (Vaulot et al. 1994; Wright and Jeffrey 1987). In order to estimate the respective contribution of each taxonomic groups, multiple regression analyses were performed on concentrations of the taxonomic pigments quantified for each discrete sample against Chl a (Gieskes et al. 1988; Everitt et al. 1990; Bustillos et al. 1995). The regression analyses for each year yielded the following results:

1991-92: Chl a = 1.93 Fuco + 2.84 Allo + 1.59 (Hex + But) + 0.50 Chl b (r^2 = 0.99, $p<0.001$)

1992-93: Chl a = 1.63 Fuco + 2.79 Allo + 1.81 (Hex + But) + 0.45 Chl b (r^2 = 0.94, $p<0.001$)

1993-94: Chl a = 0.96 Fuco + 3.56 Allo + 1.68 (Hex + But) + 0.80 Chl b (r^2 = 0.96, $p<0.001$)

For additional details of the regression analyses, see Claustre et al. (1996).

Surface and In-Water Q_{par} Measurements

Surface and in-water Q_{par} (400-700 nm) measurements made during the 1991-92 season are detailed in Moline and Prézelin (1996a) (Chapter 3). For the 1992-93 and 1993-94 seasons, Q_{par} measurements were performed using an in-water Li-Cor® LI-190SA quantum scalar irradiance sensor and a Li-Cor® LI-190SA reference sensor. In addition to irradiance profiles taken during sampling, incident Q_{par} was recorded continuously every 5 min over the 3 yr period using a Li-Cor® LI-190SA. A comparison between data collected from the sensors at Palmer Station and those collected from the Zodiac® sampling platform showed that Q_{par} readings differed < 5 %. Intercalibration of the sensors between years showed a difference of < 1 %. In-water and reference light data were used to calculate the percent Q_{par} at each sampling depth, which was assumed not to change over the course of a day. Percent Q_{par} data were interpolated (linear interpolation of log-transformed data) vertically in the water column over one meter intervals for primary production calculations.

Photosynthesis-Irradiance Relationships and Growth Rate Calculations

Estimates of daily in situ growth rates were derived from primary production rates, which were, in turn, derived from photosynthesis-irradiance (P-I) relationships measured for 756 discrete water samples. The P-I procedures, detailed for the 1991-92 season in Moline and Prézelin (1996a) (Chapter 3), were the same methods used for the following two seasons.

Freshly collected field samples were incubated in laboratory blue-green light Q_{par} photosynthetrons, using established radiolabelled $H^{14}CO_3$ uptake procedures (Prézelin et al. 1989; Prézelin and Glover 1991). Blue-green light fields more closely mimic in-water spectral conditions in clear ocean waters and tend to release cells from artificial white light (or far-red) effects, which can reduce carbon uptake rates and photosynthetic quantum efficiencies (Prézelin et al. 1989; Schofield et al. 1991). Incubations times were kept to 90 min and incubation temperatures were controlled to within 0.2 °C of in situ temperatures.

Non-linear curve fits for P-I data were calculated using the Simplex method of Caceci and Cacheris (1984). Curve fitting provided the photosynthetic parameters P_{max} (mg C mg

Chl $\underline{a}^{-1}$ h^{-1}), the light-saturated photosynthetic potential, Ik (μEin m^{-2} s^{-1}), an estimate of the minimum irradiance required to saturate photosynthesis, α [mg C mg Chl $\underline{a}^{-1}$ h^{-1} (μEin m^{-2} s^{-1})$^{-1}$], the light limited photosynthetic efficiency, β [(mg C mg Chl $\underline{a}^{-1}$ h^{-1} (μEin m^{-2} s^{-1}) $^{-1}$], the efficiency of photoinhibition and It (μEin m^{-2} s^{-1}), the irradiance threshold for the onset of photoinhibition. Estimates of the standard deviations for the P-I parameters were calculated using the procedures described by Zimmerman et al. (1987). Discrete P-I relationships with estimated standard deviations of > 25 % for P_{max} and/or 30 % for α were eliminated from this study. The effect was to reduce the size of the productivity data base by less than 10%.

In addition to measuring the 'instantaneous' P-I parameters, weekly determinations of the diel periodicity (3 hr resolution) for each P-I parameter were performed at the surface and Chl a maximum over the 3 yr study in order to time-correct the instantaneous measurements and accurately determine daily rates of in situ primary production. The methods of determining diel periodicities of P-I parameters and integrating these measurements into the daily rate calculations have been thoroughly detailed in Moline and Prézelin (1996a) (Chapter 3). The resulting P-I parameters determined for every 2 hr interval over the day were linearly

interpolated at 1 m intervals with depth and combined with Qpar for each meter (see Chapter 4) for calculating primary production.

In situ primary production at each meter for every 2 hr intervals over the day [P (z, t)] was calculated, using the hyperbolic tangent model of Neale and Richerson (1987), such that

$$P(z,t) = P_{\max}(z,t) \bullet \tanh\left(\frac{Q_{par}(z,t)}{I_k(z,t)}\right) \qquad \text{Eq. 1}$$

when Qpar (z, t), the measured integrated in situ irradiance for each 2 hr interval, was less than I_t (z, t) and

$$P(z,t) = P_{\max}(z,t) \bullet \tanh\left(\frac{Q_{par}(z,t)}{I_k(z,t)}\right) \bullet \exp\left[-\beta\left(Q_{par}(z,t) - I_t(z,t)\right)\right] \qquad \text{Eq. 2}$$

when Qpar (z, t) was greater than I_t (z, t). Daily rates of production [P (d^{-1}; z)] were computed as the sum of the twelve daily 2 hr intervals.

Daily in situ carbon-specific growth rates [μ(z)] at each depth were calculated from Holm-Hansen et al. (1977) as

$$\mu(z) = \ln\left(\frac{\frac{C(z)}{Chl(z)} + P^B(z)}{\frac{C(z)}{Chl(z)}}\right) \qquad \text{Eq. 3}$$

where C(z) and Chl(z) are the phytoplankton carbon and Chl a at a given depth and $P^B(z)$ is the daily in situ production per unit Chl a or daily increase in phytoplankton carbon per unit Chl a. C(z) was assumed to be primarily phytoplankton carbon, which is reasonable for these Antarctic coastal waters where the contribution of detrital matter is low (Mitchell and Holm-Hansen 1991b; Claustre et al. 1996). This is a refinement of the growth models of Cullen (1990) and Sakshaug et al. (1989) in that the productivity calculations include diel variations in the in situ light field and photosynthetic parameters.

Contour plots in this study were generates using exponential kriging methods (Spyglass® Transform, Champaign, IL).

RESULTS and DISCUSSION

Interannual and Subseasonal Variability in Standing Stock and Inorganic Nutrient Fields

Water column stability in the study area resulted primarily from low wind stress (Moline et al. 1996). Two extended periods during the spring/summer seasons from 1991-1994 had uninterrupted low wind speeds, below 11 m s^{-1}. (Fig. 2A; arrows). The first period, starting in December, 1991, lasted ca. one month with stability during the latter part of the interval being further enhanced by stratification from glacial meltwater input. It was during this period that a large diatom bloom developed (Fig. 2B), significantly reducing average water column inorganic nutrients (Fig. 2C). The entire 1992-1993 season was characterized by high intermittent wind speeds. Correspondingly, integrated biomass was low throughout the season with little impact of the water column nutrient field. A second period of low wind stress occurred in December, 1993, with similar responses in biomass accumulation and nutrient depletion (Fig. 2). The duration of this event, however, was significantly shorter (ca. 10 days) and the magnitude of the biological responses were similarly reduced. The subseasonal dynamics in inorganic nutrients in relation to Chl a biomass

distributions, for both LTER stations B and E from 1991-1994 are shown in figures 3, 4 and 5.

The 1991-1992 field season was characterized by a large phytoplankton bloom immediately following the break-up of the local fast ice at Sta B (Fig. 2A & B, top). Peak Chl a concentrations reached 29.21 mg Chl a m^{-3} at Sta B and 10.89 mg Chl a m^{-3} at Sta E, with concentrations from 3-5 mg Chl a m^{-3} extended down to a depth of ca. 50 m at both stations. For additional details of the Chl a biomass distributions related to physical forcing mechanisms for all three field seasons, see Moline and Prézelin (1996ab; Chapters 3 and 4). Associated with the bloom was the reduction of N and P to levels below detection ($P < 0.1$ μM, $N < 0.5$ μM). As might be expected, there was also a significant reduction of the Si concentration (> 40 μM to < 25 μM) during the diatom bloom, however, this nutrient did not show a similar decrease. The simplest explanation was that an essential nutrient, other than Si, was limiting cell growth rates. An alternate possibility is the half-saturation constant, Ks, for Si uptake was exceptionally high for this *Coscinodiscus* diatom. Previous studies have found Ks values for Si in diatoms as high as 89.4 μM for Antarctic diatoms (Sommer and Stabel, 1986).

Although water column biomass was significantly higher at Sta B than at Sta E during the 1991-1992 bloom, there were pulsed events at Sta E found to be a result of tidal washing between waters from Sta B and waters from the Bismarck Strait (Moline and Prézelin 1996b; Chapter 4). The nutrient contours also display these temporal changes, further indicating this bloom was isolated to the coast with lower biomass and higher nutrients associated with the Bismarck Strait. After the bloom was advected from the area, there was an increase in P and N concentrations to pre-bloom levels, while measuring an abrupt decrease in the Si concentration throughout the water column from 30 μM to 20 μM (Fig. 3). Temperature-salinity profiles indicated that these rapid changes in water column nutrients resulted from the advection of a different watermass, low in phytoplankton biomass into the area (data not shown). The P rich, N rich, and Si poor watermass observed the later half of this study could have been a result of Southern Ocean surface water (usually high P, N and Si concentrations) mixing with coastal glacial meltwater (high P and N concentrations and no Si). Such common mixing processes would have a diluting effect with Si while not effecting the P and N concentrations. This is supported by the differences in Si concentrations between Sta B and E during this

period, with Sta B closer to the meltwater source and showing a decrease in Si to 60m, while the influence at Sta E were limited to the upper 15m and corresponded to periods of high precipitation (Moline et al. 1996). This dilution effect has been documented for other Antarctic coastal (McMinn et al. 1995) and pelagic regions (Kang and Lee 1995). Runoff from penguin rookeries on nearby Torgerson Island and Litchfield Island has been shown have a similar effect of enhancing concentrations of P and N, yet diluting the Si (Dawson et al. 1985).

During the 1992-93 field season, the region around the LTER nearshore stations was ice free and had been so for most of the year with the exception of two days in November at Sta B (Fig. 4). In 1992-1993, spring or summer phytoplankton blooms were absent. Biomass concentrations at were relatively low over the entire season with peak concentrations at Sta B in late December and early February of 2.25 and 2.12 mg Chl a m^{-3}, respectively. Peak standing crop at Sta E occurred in late November and was generally less coupled with Sta B than during the 1991-92 season. Vertical profiles routinely indicated uniform depth distributions of Chl a concentrations at both Sta B and E, suggestive of high vertical mixing. Rapid 4-5 day increases and decreases in water column biomass also

suggest significant advection of watermasses in and out of the region.

Contours of N, P and Si during the 1992-93 season also show rapid increases in concentrations with decreasing biomass and visa versa (Fig. 4). This is most evident during December, 1992 at Sta B. Concentrations of N, P and Si only decreased to 15, 1.2 and 35 μM, respectively, as a result of low biomass. Decreased concentrations in all nutrients at Sta B and E in mid January, 1993, during a period of very low phytoplankton biomass, may have resulted from dilution by the high precipitation.

During the 1993-94 season, sampling began in late August when heavy land-fast ice was a dominant feature at Sta B (Fig. 5A). During the late winter and early spring, biomass remained low, averaging 0.17 mg Chl a m^{-3}. There was an increase in Chl a measured at Sta B during the beginning of October that was not recorded at Sta E. This may have been the result of release of ice algal communities during the break-up of the land-fast ice. After the break-up of the third ice event in early November, biomass steadily increased at Sta B to a maximum of 4.91 mg Chl a m^{-3} at the end of December. Sta E showed similar temporal biomass distribution to Sta B,

however, the overall concentrations at Sta E were lower than at Sta B (Fig. 5).

High biomass associated with the ice algal communities in late August and early September, 1993 had a measurable effect on the surface inorganic nutrient concentrations (Fig. 5A). McMinn et al. (1995) found similar results in Ellis Fjord during ice algal mat formation, however, their results showed much higher depletion, as the sea-ice remained throughout the summer season. A nutrient pulse (> 35 μM N, > 2.5 μM P and> 80 μM Si), recorded after the break-up of the third ice event and may have been a result of advection of a different watermass into the area or release of ice brine, found to have high concentrations of nutrients (95 μM N, 9 μM P, and 225 μM Si; Dieckmann et al. 1991). With the development of the bloom in early December, 1993, nutrient concentrations were significantly decreased at Sta B and E to < 5 μM N, < 0.6 μM P and < 10 μM Si (Fig. 5). Similar to the 1991-92 season, there were periodic fluctuations in biomass and nutrient concentrations at both stations resulting from tidal forcing. In conjunction with the disappearance of the bloom, was an increase in water column nutrient concentrations to pre-bloom concentrations.

Inorganic Nutrient Ratios

Mean macronutrient ratios for all stations and depths were found to be quite similar between years (Table 1). The ratios of Si: N and Si: P deviate from Redfield ratios of N: P: Si = 16:1:15 (Redfield et al. 1963), however, are comparable to ratios found by Jennings et al. (1984) (11:1:24) for the Southern Ocean and McMinn et al. (1995) for a coastal region (13.8:1:25.5). Dissolved Si: N here range from 1.5-2.0, which are high for non-Southern Ocean blooms, suggesting a high Si demand, but within the reported range Antarctic coastal areas (Perrin et al. 1987; McMinn et al. 1995) and ice edge regions (Jennings et al. 1984). Si: N uptake ratios of 0.8-1.2 have been recorded for cultured diatoms, however changes in light, temperature, nutrient limitation, and species differences have been found to vary Si: N ratios two to three fold (Brzezinski 1985).

Although the mean nutrient ratios were found to be similar between years, there was significant variability (Fig. 6). The N: P ratio for the 1991-92 season showed a significant difference between the non-bloom and bloom conditions (14.14 $\mu M \pm 2.99$ vs. 48.65 $\mu M \pm 28.66$ respectively, $p<0.01$) (Fig. 6A). The increased N : P ratio was due to the disproportionate

depletion of P over N. The linear regression for the combined pre/post bloom N : P data gives values [LTER 91-92: P= 0.054 N + 0.359, n = 291, r^2 = 0.69] nearly identical to those reported by Kamykowski and Zentara (1989) for the Southern Ocean using the NODC dataset [NODC: P= 0.059 N + 0.312, n = 38,282, r^2 = 0.73]. During the bloom, however, there was significant deviation from this line with N:P ratios > 80 (Fig. 3A), suggesting possible P limitation. Harrison et al. (1982), similarly found disproportionate uptake rates of P over N in phytoplankton populations in the eastern Arctic in Baffin Bay, resulting in high ambient N: P ratios compared to temperate and tropical areas. Supporting evidence that P limitation may be an episodic event that limits plant growth along the Palmer Peninsula is from a study by Holm-Hansen et al. (1989). During a summer diatom (*Rhizosolenia* sp.) bloom in 1985 near Palmer Station, high POC/ATP (average=665) and Chl a/ATP (average=7.6) ratios were found in the presence of extremely low P concentrations (< 0.1 μM). This combination of observations may have been the result of the onset of P limitation inducing high cellular levels of both POC and Chl a and relatively low cellular ATP concentrations.

Because Si concentrations did not show large range and possible dilution effects by glacial runoff and precipitation (see

above), it is difficult to interpret the Si: N ratio for the 1991-92 season. Low Chl a concentrations over the 1992-93 season resulted in a limited range of nutrient utilization (Fig. 6C, D). The general relationship between N and P was similar to the non-bloom conditions seen during the 1991-92 season. Significant deviation from this relationship occurred during the end of the season when both P and Si were high while the N concentration remained near 20 μM (Fig. 6C, D), indicating high N utilization. In mid January, 1993 (Fig. 4A) there was a disproportionate decrease in the concentration Si, seen as a cluster of points below the regression line in figure 6D. This appears similar to the N: Si ratio during the 1991-92 season and may be a result of dilution by glacial meltwater and/or precipitation. Interesting to note is that even though the N: Si ratio shifted during this event, the relative nutrient utilization (the slope) did not change over a range of Si and N concentrations. This suggest that the process of nutrient dilution (in this case) was not significant in determining the uptake rates of the phytoplankters.

For the 1993-94 season, N: P ratios again were similar to the NODC dataset for the Southern Ocean with less variability than the prior two seasons. According to a model proposed by Kamykowski and Zentara (1989), the dissolved N: Si ratio for

the 1993-94 season indicate a phytoplankton Si: N uptake ratio of <1.8, assuming NO_3^- was the primary nitrogen source, which is equivalent to previously reported values (see McMinn et al. 1995).

The depth distribution of the N: P and Si: N ratios over the two bloom seasons at Sta B (1991-92 and 1993-94) highlight the variability shown in figure 6 (Fig. 7). The N: P ratios for both seasons show significant changes correlating with the timing and depth distributions of the blooms (Fig. 7A & C). High N: P ratios (> 75) were measure throughout the water column in December, 1991, however abruptly changed after the first week of January, 1992. The Si: N also showed a significant increase during the bloom as a result of higher uptake of N over Si. The fact that the N: P was also high illustrates the preferential uptake of P over N during the diatom bloom shown in figure 6A. The bloom in 1993-94 showed a different nutrient signature with decreasing N: P and a slight increase in the Si: N ratio. This ratio combination indicates high uptake of N relative to both P and Si.

As previously mentioned, nutrient ratios have been found to vary significantly with changes in light, temperature, and taxonomic composition. Both light and temperature conditions during the two blooms were not found to be

significantly different (Claustre et al. 1996; Moline and Prézelin 1996b), therefore, the temporal patterns of taxonomic changes were examined as the source of variability in nutrient utilization between the two blooms.

The inorganic nutrients and Chl a sampled during the 1991-92 season, show a significant ($p<0.001$) log-linear relationship decrease in N and P with increasing Chl a (Fig. 8A&B). A similar relationship was found using the diatom-specific pigment, fucoxanthin, indicating that the primary drawdown of nutrients during the bloom resulted from diatoms (Fig. 8C&D). During the 1991-92 season, diatoms dominated the large bloom (Fig. 3A) until the first week in January at which time a rapid transition from diatom to cryptophytes occurred (Fig. 9A). The timing of this transition corresponded to the shift in the nutrient ratios (Fig. 7A&B). Mixed populations of nanoflagellates, diatoms and chlorophytes were present for the remainder of the season, when there was little change in the nutrient ratios. (Fig. 9A).

Similarly for the inorganic nutrients and Chl a sampled during the 1993-94 season, a log-linear relationship decrease in N and P with increasing Chl a was found (Fig. 10A&B). Because biomass during 1993-94 was an order of magnitude lower than 1991-92, the relationship was not as robust,

however still significant ($p<0.001$). A similar relationship was found using the taxon-specific pigment, alloxanthin, indicating that the primary drawdown of nutrients during the 1993-94 bloom was by cryptophytes (Fig. 10C&D). During the 1993-94 season, the cryptophyte bloom (Fig. 5A) was isolated to the near surface waters, while a mixed population was found below 30 m (Fig. 9B). The timing and depth distribution of the cryptophyte bloom was tightly coupled to the N:P decrease in the water column (Fig. 7C). Interestingly, the disappearance of the ice earlier in 1993 corresponded with a transition from diatoms to nanoflagellates (Fig 9B) and a dramatic increase in the N:P ratio and decrease in the Si:N ratio (Fig. 7 C & D).

Nutrient ratios and chemical characteristics for cryptophyte dominated waters where significantly different than those for other taxonomic groups or mixed populations during the two bloom years (Table 2). This is similar to results by Sommer and Stabel (1986) and Sommer (1988) which showed correlations between regional differences in community composition and Si:N ratios along the west coast of the Antarctic Peninsula and Drake Passage. This finding was attributed to resource competition theory (Tilman 1977), which competes with physical forces, control by higher trophic levels, allelopathic interactions, and other forces in determining the

specific patterns of species at any given time and place. Competitive nutrient interactions between species has been shown to occur in culture experiments (Tilman et al. 1986; Sommer 1991), however field examples are rare. Results from the LTER sampling region have suggested that salinity changes resulting from glacial meltwater runoff stimulate the growth these cryptophyte populations (Moline and Prézelin 1996b; Chapter 4). Likewise, it may be the change in the nutrient signatures of the water column brought on during these runoff periods that creates a competitive advantage for cryptophytes. Previous results have also shown the water column photosynthetic cross section for these cryptophyte populations to be significantly less than for other groups, suggesting physiological differences and possibly altered nutrient requirements (Claustre et al. 1996).

Primary Production

The 1991-92 diatom bloom and the 1993-94 cryptophyte bloom occurred during periods of low wind stress and stratified conditions (Fig. 2). Density profiles from 1991-92 show that the mixed layer depth shallowed during the development of the bloom from 60m to 20m (Moline et al. 1996; Chapter 1). Under these conditions, phytoplankton were isolated in the

near surface water, well past the critical period for growth (Smetacek and Passow 1990), resulting in bloom formation. Uptake of nutrients was high during the two blooms with average N depletion of 475.4 (1991-92) and 737.6 mmol m^{-2} (1993-94); P depletion rates of 40.8 (1991-92) and 35.5 (1993-94) mmol m^{-2}; and Si depletion rates of 1623.5 mmol m^{-2} (1993-94) between stations. These translate to mean daily uptake of 20.6 mmol N m^{-2} d^{-1} (1991-92) and 72.2 mmol Si m^{-2} d^{-1} (1993-94). These estimates are high compared to open ocean measurements (Jones et al. 1990), however are within the range for nitrate uptake (7-35 mmol N m^{-2} d^{-1}; Waldron et al. 1995) and biogenic silicate production (7-93 mmol Si m^{-2} d^{-1}; Nelson and Smith 1986) measured for bloom conditions along ice-edge zones.

Using the C:N:P:Si ratio of 62:11:1:24.8 (Jennings et al. 1984; Barry 1988), carbon primary productivity was estimated from the measured nutrient depletion. These calculations were restricted to the bloom periods where the water column was known to be stable, reducing the influence of advection, which has been shown to be prevalent phenomena in this regions during periods of high winds. Compared to the measured primary productivity, estimates based on nutrient depletion during the 1991-92 bloom were significantly lower (Table 2).

Primary productivity measurements were short (1.5 hr) incubations and thus good estimates of *gross* rather than *net* production. Because of possible regeneration of nutrients within the upper water column during this 23 day period and any upward nutrient flux through the pycnocline, primary productivity based on nutrient loss are estimates of *net* nutrient availability (Olson 1980). Mathot et al. (1992) conducted a thorough study quantifying the differences of gross *versus* net primary production during the EPOS cruises in the Weddell Sea. Across many environmental conditions (with and without sea ice), net productivity was found to be 44-67% of total carbon fixation with an average of 64% in ice-edge zones and open ocean regions. If this percentage is applied to the measurements at Sta B and E in 1991, *net* primary production is estimated at 40.96 and 24.32 g C m^{-2}, respectively, corresponding well to estimates based on nutrient depletion. As mentioned above, tidal flushing was a measured physical force at station E. Over the 23 days of the 1991-92 bloom, this would have the effect of both periodically increasing the water column nutrients (from the Bismarck Strait) and decreasing measured productivity. This resulted in lower measured productivity and estimates compared to Sta B (Table 3).

Results from the 1993-94 bloom were different, with measured primary productivity an order of magnitude lower than that estimated by nutrient depletion (Table 3). With biomass 10-fold lower than the 1991-92 season and comparable nutrient loss during both blooms, a mechanism for nutrient loss other than phytoplankton uptake was operating in this region over the 1993-94 summer season. Advection of an already nutrient depleted water column into the area could explain a sharp drop in nutrient concentration, but not the steady decline that was measure in the LTER sampling region. Precipitation and snow height data, taken over the same period, strongly suggest that the decrease in nutrients was a result of dilution (Fig. 11). The timing of the nutrient 'loss' corresponds well with the period, at the end of November 1993, of rapid snow melt and heavy precipitation (both rain and snow). This result has serious implications for estimating primary productivity from nutrient loss in areas of high freshwater input. As stated above, the input of freshwater during the 1991-92 season occurred after the diatom bloom and during a transition period to cryptophyte dominance, therefore, productivity estimates from that season are believed to be robust. While estimates of productivity from nutrient loss may not be affected from meltwater during the early

portion of the growing season (Whitehouse et al. 1995), the question still remains for other coastal (Barry 1988; McMinn et al. 1995) and ice-edge studies (Jennings 1984) where similar estimates have been made during warmer months.

Physiological Response to Changes in Inorganic Nutrients

Many studies have demonstrated the effect of nutrient concentrations on the physiological status of phytoplankton in cultures and natural populations (see Platt 1981; Cleveland et al. 1989; Schofield et al. 1993). Given the range of biomass and *in situ* nutrients concentrations measured in the LTER region from 1991-1994, the physiological responses of phytoplankton to changing nutrients were examined.

The relationship between the maximum photosynthetic rate (P^B_{max}; mg C mg Chl a^{-1} h^{-1}) and the concentrations of N and P are shown for all stations, depth and sampling days in figure 12. A general trend of decreasing P^B_{max} with decreasing nutrient concentration is evident. The variability at any given nutrient concentration is high, but that is to be expected given that at any nutrient concentration, phytoplankton can be distributed throughout the water column in either mixing or stable conditions. Phytoplankton at the base of the euphotic

zone will generally have a lower P^B_{max} than those at the near surface under similar nutrient conditions (Schofield et al. 1993). Both N and P concentrations had a similar effect on α^B, the light-limited rate of photosynthesis (data not shown). Given that > 70% of the water column productivity was light saturated for the three year period (Claustre et al. 1996), figure 12 is a good measure of the impact of nutrients on *the upper limit* of photosynthetic production in this region.

Moreover, the ratio of Chl a to POC showed a dependence on the in situ nutrient concentration (Fig. 13). As concentrations of both N and P decreased, Chl a:POC exponentially increased. This could be a combination of decreasing carbon content as a result of decreased photosynthesis (Fig. 12) and/or the utilization of nutrients in increasing the phytoplankton absorption cross-section in response to the high light attenuation measured during the blooms (Moline and Prézelin 1996b).

Given the impact of changing nutrient concentrations on photosynthetic production, in situ specific growth rates would also likely be dependent on the nutrient field. In situ specific growth rates were high (0.1 - 1.0 d^{-1}; see Furnas 1991) across the range of nutrient concentrations, however, showed significantly more variability toward higher concentrations

(Fig. 14). This relationship held true for all years and also for light saturated maximum hourly growth rates (data not shown). These results contradict findings by Vernet et al. (1991), which showed decreasing growth rate with decreasing nutrient concentration under light saturating conditions. The relationships in figure 14 are bound by maximum growth rates reported for Antarctic phytoplankton (Sakshaug and Holm-Hansen 1986) and maximum nutrient concentrations for the Southern Ocean (Kamykowski and Zentara 1989), however the question of why low growth rates (equivalent to those at high nutrient concentrations) were not measured at low nutrient conditions still remains. Highest growth rates in this study occurred during the initiation of the two summer blooms (data not shown). Nutrient concentrations over these periods decreased, at times approaching detection levels (Fig. 6), yet growth remained high. Half saturation constants, Ks, of Antarctic phytoplankton for Si have been found to be extremely high, with means of 12-22 μM (Jacques 1983) and 36.9 μM (Sommer 1986) depending on species. Ks values for N, however, have been shown to be as low as 0.3 μM for Antarctic diatoms (Sommer 1986). These phytoplankton, therefore, may have the ability to take up nutrients from ambient concentrations (> 70 μM Si, > 35 μM N, > 2.5 μM P) to the

minimal levels measured in this study (18.5 μM Si, 0.72 μM N, 0.04 μM P) and still maintain maximum uptake and growth. Phytoplankton have the ability to store nutrients as lipids, carbohydrates, and proteins for later use as environmental conditions changes. Additionally, the Chl a:POC ratios were found to increase with increasing in situ growth rate, evidence suggesting the 'storage' of N, as pigment proteins, during the times of low ambient nutrient concentrations (Fig. 15). As mentioned above, the channeling of nutrients to enhance light harvesting ability may have been a photophysiological response to self-shading, which occurred during both bloom periods (Moline and Prézelin 1996b). Interestingly, results here, on the time scales ranging from days to years, support classical work by Droop (1986) and Caperon (1968), which found physiological conditions of phytoplankton dependent on the intracellular nutrient pools (cell quotient) and not the surrounding ambient concentrations.

CONCLUDING REMARKS

Results from this intense three year study show that, under certain hydrographic and meteorological conditions (high

stratification and low wind speeds), large coastal blooms develop and considerably decrease macronutrient concentrations. The uptake of N and P were shown to be disproportionate and change depending on taxonomic composition of the water column. Moreover, nutrient ratios were found to significantly deviate over time from Redfield ratios and previously reported ratios from the Antarctic.

Primary production determined by nutrient depletion in the water column was found to correspond well to measure in situ primary productivity for the 1991-92 bloom. However, during times of high freshwater input in coastal regions and possibly along receding ice edges, determining primary production by nutrient loss can deviate from measured results by an order of magnitude. The maximum potential for photosynthesis per unit Chl a decreased with decreasing nutrient concentration, although was highly variable depending location in the water column and the extent of vertical mixing. Increased synthesis of light harvesting pigmentation occurred during low ambient nutrient concentrations in response to increasing biomass and self-shading. The fact that daily in situ growth rates remained high under extremely low nutrient conditions raises doubt that phytoplankton during this study were nutrient limited.

ACKNOWLEDGMENTS

N. Boucher, B. Bozcar, T. Diem, T. Evens, B. Golden, P. Handley, R. Jovine, H. Matlick, T. Newberger, S. Roll, K. Seydel, K. Scheppe, O. Schofield, J. Standish, B. Sullivan, T. Westerberry and the ASA personnel at Palmer Station are acknowledged for their assistance in data collection during the three field seasons. R. Bidigare and M. Ondrusek are thanked for generously providing HPLC training and pigment standards. This study was supported by National Science Foundation grant DPP 90-901127 to B. Prézelin.

LITERATURE CITED

Barry JP (1988) Hydrographic patterns in McMurdo Sound, Antarctica and their relationship to local benthic communities. Polar Biology 8:377-391.

Bidigare RR, Schofield O, Prézelin BB (1989) Influence of zeaxanthin on quantum yield of photosynthesis of *Synechococcus* clone WH7803 (DC2). Mar Ecol Prog Ser 56: 177-188

Brzezinski MA (1985) The Si:C:N ratio of marine diatoms: interspecific variability and the effect of some environmental variabilities. J Phycol 21: 347-357

Bustillos-Guzman J, Claustre H, Marty J-C (1995) Specific phytoplankton signature and their relationship to hydrographic conditions in the coastal northwestern Mediterranean Sea. Mar Ecol Prog Ser 124: 247-258

Caceci MS, Cacheris WP (1984) Fitting curves to data. Byte 9: 340-362

Caperon J (1968) Populations growth of *Isochrysis galbana* to nitrate variation at limiting concentrations. Ecology 49: 715-721

Claustre H, Moline MA, Prézelin BB (1996) Sources of Variability in the Light Utilization Index for Antarctic Coastal Waters. J Geophys Res, in press

Cleveland JS, Perry MJ, Kiefer DA, Talbot MC (1989) Maximal quantum yield of photosynthesis in the northwestern Sargasso Sea. J Mar Res 47: 869-886

Cullen JJ (1990) On models of growth and photosynthesis in phytoplankton. Deep Sea Res 37: 667-683

Dawson R, Schramm W, Bölter M (1985) Factors influencing the production, decomposition and distribution of organic and inorganic matter in Admiralty Bay, King George Island. In: Siegfried WR, Condy PR, Laws RM (eds) Antarctic Nutrient Cycles and Food Webs. Sringer-Verlag. Berlin Heidelberg pp 109-114

Dieckmann GS, Lange MA, Ackley SF, Jennings JC (1991) The nutrient status in sea ice of the Weddell Sea during winter: effects of sea ice texture and algae. Polar Biology 11: 449-456

Dower KM, Lucas MI, Phillips R, Dieckmann G, Robinson DH (1996) Phytoplankton Biomass, P-I relationships and primary production in the Weddell Sea, Antarctica, during the austral autumn. Polar Biology 16: 41-52

Droop MR (1968) Viatamin B12 and marine ecology. IV. The kinetics of uptake, growth and inhibition in *Monochrysis lutheri*. J Mar Bio Assoc UK 48: 689-733

Everitt DA, Wright SW, Volkman JK, Thomas DP, Lindstrom EJ (1990) Phytoplankton community compositions in the western equatorial Pacific determined from chlorophyll and carotenoid pigment distribution. Deep-Sea Res 37: 975-997

Furnas MJ (1990) *In situ* growth rates of marine phytoplankton: approaches to measurement, community and species growth rates. J Plank Res 12:1117-1151

Gieskes WWC (1983) Dominance of cryptophyceae during the phytoplankton spring bloom in the central North Sea detected by HPLC analysis of pigments. Mar Bio 75: 179-185

Gieskes WWC, Kraay GW, Nontji A, Setiapermana D, Sutomo (1988) Monsoonal alteration of a mised and a layered structure in the phytoplankton of the euphotic zone of the Banda Sea (Indonesia): A mathematical analysis of algal pigment fingerprints. Neth J Sea Res 22: 123-137

Harrison WG, Platt T, Irwin B (1982) Primary production and nutrient assimilation by natural phytoplankton populations of the Eastern Canadian Arctic. Can J Fish Aquat Sci 39: 335-345

Holm-Hansen O, El-Sayed SZ, Franceschini GA, Cuhel RL (1977) Primary productivity and the factors controlling

phytoplankton growth in the Southern Ocean. In: Llano GA (ed) Adaptations Within Antarctic Ecosystems. Gulf, Houston pp 11-50

Holm-Hansen O, Mitchell BG, Hewes CD, Karl DM (1989) Phytoplankton Blooms in the Vicinity of Palmer Station, Antarctica. Polar Biology 10: 49-57

Holm-Hansen O, Amos AF, Silva N, Villafañe V, Helbling EW (1994) *In situ* evidence for a nutrient limitation of phytoplankton growth in pelagic Antarctic waters. Ant Science 6: 315-324

Jacques G (1983) Some ecophysiological aspects of Antarctic phytoplankton. Polar Biology 2: 27-33

Jeffery SW (1974) Profiles of photosynthetic pigments in the central North Pacific Ocean. Mar Bio 37: 33-37

Jennings JCJr, Gordon LI, Nelson DM (1984) Nutrient depletion indicates high primary productivity in the Weddell Sea. Nature 308: 51-54

Johnson KS, Petty RL, Thomsen J (1985) Flow injection analysis for seawater micronutrients. In: A. Zirino (ed) Mapping Strategies in Chemical Oceanography. Advances in Chemistry Series 209: 7-30

Jones EP, Nelson DM, Treguer P (1990) Chemical Oceanography. In: Smith WOJ (ed) Polar Oceanography: Part A: Physical

Science, Part B: Chemistry, Biology, Geology. Academic Press, Inc. San Diego. pp 407-476

Kamykowski D, Zentara S-J (1989) Circumpolar plant nutrient covariation in the Southern Ocean: patterns and processes. Mar Ecol Prog Ser 58: 101-111

Kang S-H, Lee S (1995) Antarctic phytoplankton assemblage in the western Bransfield Strait region, February 1993: composition, biomass, and mesoscale distributions. Mar Ecol Prog Ser 129: 253-267

Lancelot C, Billen G, Veth C, Becquevort S, Mathot S (1993) Factors controlling phytoplankton ice-edge blooms in the marginal ice-zone of the northwestern Weddell Sea during seas ice retreat 1988: field observations and mathematical modelling. Polar Biology 13: 377-387

Mathot S, Dandois J-M, Lancelot C (1992) Gross and net primary production in the Scotia-Weddell Sea sector of the Southern Ocean during spring 1988. Polar Biology 12: 321-322

McMinn A, Gibson J, Hodgson D, Aschman J (1995) Nutrient limitation in Ellis Fjord, eastern Antarctica. Polar Biology 15: 269-276

Mitchell BG, Holm-Hansen O (1991a) Observations and modeling of the Antarctic phytoplankton crop in relation to mixing depth. Deep-Sea Res 38: 981-1007

Mitchell BG, Holm-Hansen O (1991b) Bio-optical properties of Antarctic Peninsula waters: differentiation from temperate ocean models. Deep-Sea Res 38: 1009-1028

Mitchell BG, Brody EA, Holm-Hansen O, McClain C, Bishop J (1991) Light limitation of phytoplankton biomass and macronutrient utilization in the Southern Ocean. Limnol Oceanogr 36: 1662-1677

Moline MA, Prézelin BB (1996a) High-Resolution Time-Series Data for Primary Production and Related Parameters at a Palmer LTER Coastal Site: Implications for Modeling Carbon Fixation in the Southern Ocean. Polar Biology. In press

Moline MA, Prézelin BB (1996b) Long-term monitoring and analyses of physical factors regulating variability in coastal Antarctic phytoplankton biomass, *in situ* productivity and taxonomic composition over subseasonal, seasonal and interannual time scales. Mar Ecol Prog Ser. Submitted

Moline MA, Prézelin BB, Schofield O, Smith RC (1996) Temporal dynamics of coastal Antarctic phytoplankton:

Environmental driving forces and impact of a 1991-1992 summer diatom bloom on the nutrient regimes. In: Battaglia B, Valencia J, Walton DWH (eds) Antarctic Communities. Cambridge University Press. In press

Neale PJ, Richerson PJ (1987) Photoinhibition and the diurnal variation of phytoplankton photosynthesis, I, Development of a photosynthesis-irradiance model from studies of *in situ* responses. J Plank Res 9: 167-193

Nelson DM, Smith WO (1986) Phytoplankton bloom dynamics of the Ross Sea ice edge. II. Mesoscale cycling of nitrogen and silicon. Deep Sea Res 33: 1389-1412

Nelson DM, Smith WO (1991) Sverdrup revisited: Critical depths, maximum chlorophyll levels, and the control of Southern Ocean productivity by the irradiance-mixing regime. Limnol Oceanogr 36: 1650-1661

Nelson DM, Treguer P (1992) Role of silicon as a limiting nutrient to Antarctic diatoms: evidence from kinetic studies in the Ross Sea ice-edge zone. Mar Ecol Prog Ser 80: 225-264

Olson RJ (1980) Nitrate and ammonium uptake in Antarctic waters. Limnol Oceanogr 25: 1064-1074

Perrin RA, Lu P, Marchant HJ (1987) Seasonal variation in marine phytoplankton and ice algae at a shallow Antarctic coastal site. Hydrobiol 146: 33-46

Platt T (ed) (1981) Physiological bases of phytoplankton ecology. Can Bull Fish Aquat Sci Vol 210

Prézelin BB, Glover HE (1991) Variability in time/space estimates of phytoplankton biomass and productivity in the Sargasso Sea. J Plankton Res 13S: 45-67

Prézelin BB, Glover HE, VerHoven B, Steinberg DK, Matlick HA, Schofield O, Nelson NB, Wyman M, Campbell L (1989) Blue-green light effects on light-limited rates of photosynthesis: relationship to pigmentation and productivity estimates from the Sargasso Sea. Mar Ecol Prog Ser 54: 121-136

Priddle J, Brandini F, Lipski M, Thorley MR (1994) Pattern and variability of phytoplankton biomass in the Antarctic Peninsula region: an assessment of the BIOMASS cruises. In: El-Sayed SZ (ed) Southern Ocean Ecology: the BIOMASS Perspective. Cambridge Press, Cambridge pp 49-61

Redfield AC, Ketchum B, Richards FA (1963) The influence of organisms on the composition of seawater. In: Hill MN (ed) The Sea, vol. 2. Wiley-Interscience, New York pp26-77

Sakshaug E, Holm-Hansen O (1986) Photoadaptation in Antarctic phytoplankton: variations in growth rate, chemical composition and P versus I curves. J Plank Res 8: 459-473

Sakshaug E, Kiefer DA, Andresen K (1989) A steady state description of growth and light absorption in the marine diatom *Skeletonema costatum.* Limnol Oceanogr 34: 198-205

Sakshaug E, Slagstad D (1991) Light and productivity of phytoplankton in polar marine ecosystems: a physiological view. In: Sakshaug E, Hopkins CCE, Øritsland NA (eds) Proceedings of the Pro Mare Symposium on Polar Marine Ecology, Trondheim, 12-16 May 1990. Polar Res 10: 69-85

Sakshaug E, Slagstad D, Holm-Hansen O (1991) Factors controlling the development of phytoplankton blooms in the Antarctic Ocean-A mathematical model. Mar Chem 35: 259-271

Schofield O, Prézelin BB, Smith RC, Stegmann PM, Nelson NB, Lewis MR, Baker KS (1991) Variability in spectral and nonspectral measurements of photosynthetic light utilization efficiencies. Mar Ecol Prog Ser 78: 253-271

Schofield O, Prézelin BB, Bidigare RR, Smith RC (1993) *In situ* photosynthetic quantum yield. Correspondence to hydographic and optical variability within the Southern California Bight. Mar Ecol Prog Ser 93: 25-37

Smetacek V, Passow U (1990) Spring bloom initiation and Sverdrup's critical-depth model. Limnol Oceanogr 35: 228-234

Sommer U (1986) Nitrate- and silicate-competition among antarctic phytoplankton. Mar Bio 91: 345-351

Sommer U (1988) The species composition of Antarctic phytoplankton interpreted in terms of Tilman's competition theory. Oecologia 77: 464-467

Sommer U (1991) Comparative nutrient status and competitive interactions of two antarctic diatoms (*Corethron criophilum* and *Thalassiosira antarctica*). J Plank Res 13: 61-75

Sommer U, Stabel H-H (1986) Near surface nutrient and phytoplankton distribution in the Drake Passage during early December. Polar Biology 6: 107-110

Tilman D (1977) Resource competition between planktonic algae: an experimental and theoretical approach. Ecology 58: 338-348

Tilman D, Kiesling R, Sterner R, Kilham SS, Johnson FA (1986) Green, bluegreen and diatom algae: taxonomic difference in cometative ability for phosphorus, silicon and nitrogen. Arch Hydrobiol 106: 473-485

Vaulot D, Birrein J-L, Marie D, Casotti R, Veldhuis MJW, Kraay GW, Chrétiennot-Dinet M-J (1994) Morphology, ploidy, pigment compoistion, and genome size of cultured strains of *Phaeocystis* (Prymnesiophyceae). J Phycol 30: 1022-1035

Vernet M, Letelier R, Karl DM (1991) RACER: Phytoplankton growth rates in the northern Gerlache Strait during the spring bloom of 1989. Ant J U S 26: 154-156

Waldron HN, Attwood CG, Probyn TA, Lucas MI (1995) Nitrogen dynamics in the Bellingshausen Sea during the Austral spring of 1992. Deep Sea Res 42: 1253-1276

Whitaker TM (1982) Primary production of phytoplankton off Signy Island, South Orkneys, the Antarctic. Proc R Soc Lond 214: 169-189

Whitehouse MJ, Priddle J, Woodward EMS (1995) Spatial variability in inorganic nutrients in the marginal ice zone of the Bellingshausen Sea during the Austral spring. Deep Sea Res 42: 1047-1058

Wright SW, Jeffery SW (1987) Fucoxanthin pigment markers of marine phytoplankton analysed by HPLC and HPTLC. Mar Ecol Prog Ser 38: 259-266

Wright SW, Jeffery SW, Mantoura RFC, Llewellyn CA, Bjørnland T, Repeta D, Welschmeyer N (1991) Improved HPLC method for analysis of chlorophylls and caroteniods from marine phytoplankon. Mar Eco Prog Ser 77: 183-196

Zimmerman RC, SooHoo JB, Kremer JN, D'Argenio DZ (1987) Evaluation of variance approximation techniques of non-linear photosynthesis-irradiance models. Mar Biol 95: 209-215

Table 1: Mean macronutrient ratios at Stations A-E from 1991-1994.

	N	P	Si	n
1991-92	16.49	1	25.44	404
1992-93	12.37	1	25.61	378
1993-94	14.53	1	24.01	326

Table 2. Ratios of inorganic nutrient concentrations and chemical charateristics for samples collected when cryptophytes contributed >40% of phytoplankton biomass compared with samples of other/mixed communities for 1991 and 1993 at Stations A-E. Mean values with standard errors are shown.

	Ratio	Cryptophytes	n	Other/Mixed	n
1991	**N:P**	14.09±0.52	79	26.88±1.41	309
	Si:P	- - -		- - -	
	Si:N	- - -		- - -	
	C:N	5.14±0.28	53	5.19±0.21	198
	Chl a:C	0.0117±0.0020	57	0.0064±0.0004	173
1993	**N:P**	11.59±0.24	89	15.14±0.19	237
	Si:P	22.54±0.53	89	24.20±0.41	238
	Si:N	1.97±0.04	89	1.63±0.03	237
	C:N	6.15±0.13	85	7.10±0.10	182
	Chl a:C	0.0044±0.0002	85	0.0036±0.0003	182

Table 3. Comparison of measured primary production and estimates based on nutrient depletion at Stations B and E in 1991 and 1993.

	1991 Total ($g\ C\ m^{-2}$)	Daily avg ($g\ C\ m^{-2}d^{-1}$)	min ($g\ C\ m^{-2}d^{-1}$)	max ($g\ C\ m^{-2}d^{-1}$)	1993 Total ($g\ C\ m^{-2}$)	Daily avg ($g\ C\ m^{-2}d^{-1}$)	min ($g\ C\ m^{-2}d^{-1}$)	max ($g\ C\ m^{-2}d^{-1}$)
Sta B								
Measured	64.58	2.81	1.09	6.46	4.46	0.20	0.02	0.46
NO3	38.70	1.68	0.33	3.86	49.74	2.26	0.06	6.13
PO4	30.79	1.34	0.02	4.23	26.78	1.22	0.12	2.88
Si	- - -	- - -	- - -	- - -	51.91	2.36	0.79	3.44
Sta E								
Measured	38.12	1.73	0.47	3.49	6.83	0.30	0.03	0.56
NO3	24.11	1.10	0.61	5.02	49.51	2.15	0.16	6.23
PO4	29.89	1.36	0.11	5.69	26.06	1.13	0.17	1.90
Si	- - -	- - -	- - -	- - -	43.29	1.88	0.50	5.06

Figure 1. Location of Palmer LTER sampling stations A-E with respect to Palmer Station and the Antarctic Peninsula (inset).

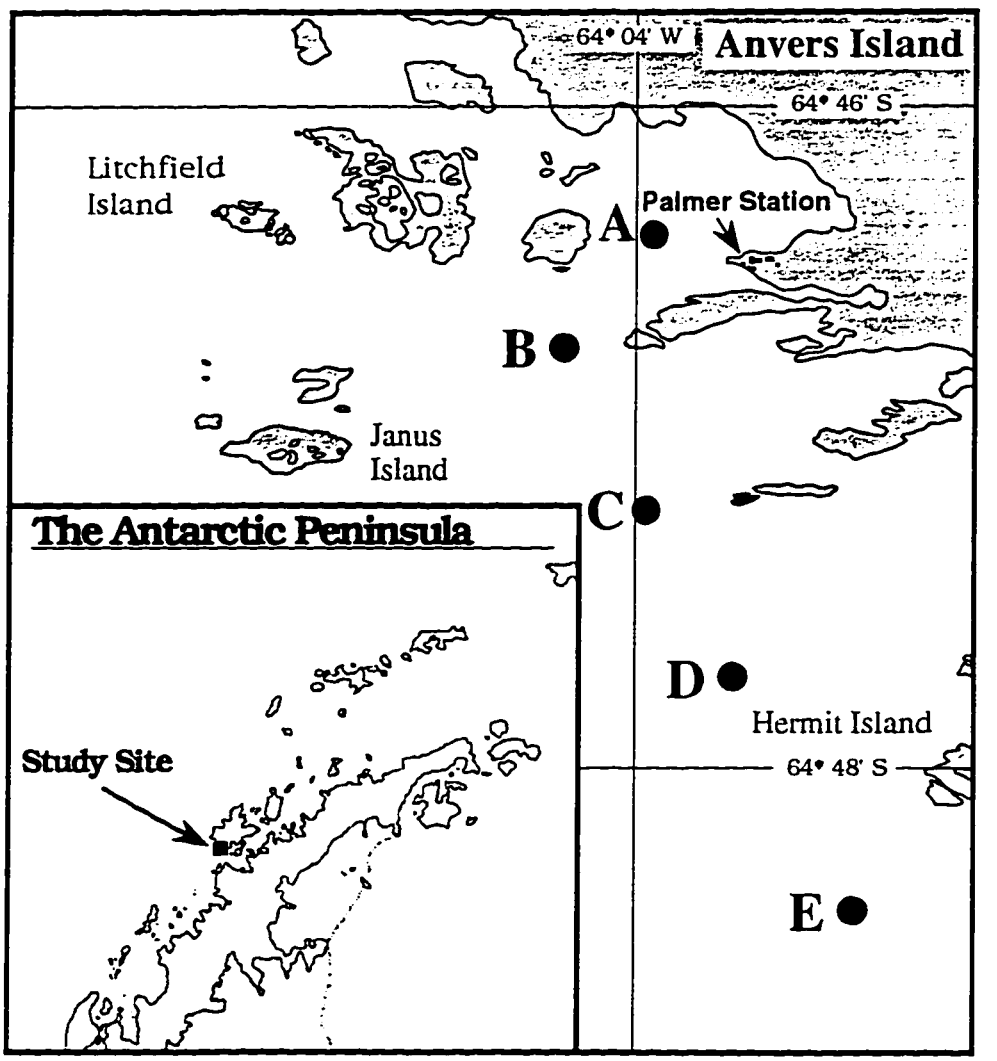
64° 04' W
Anvers Island
64° 46' S
Litchfield
Island
Palmer Station
A
B
Janus
Island
C
The Antarctic Peninsula
D
Hermit Island
Study Site
64° 48' S
E

Figure 2. Temporal change in the (A) daily average wind speed, (B) 20 m depth integrated chlorophyll a, and (C) 20 m average water column N and P concentrations at station B over the three spring/summer seasons from 1991-1994. The wind speed of 11 m s^{-1}, found to threshold for water column stability and biomass accumulation (Moline and Prézelin, submitted), has been marked horizontal line in (A). Arrows indicate the two periods when the daily average wind speeds were below this threshold for an extended interval.

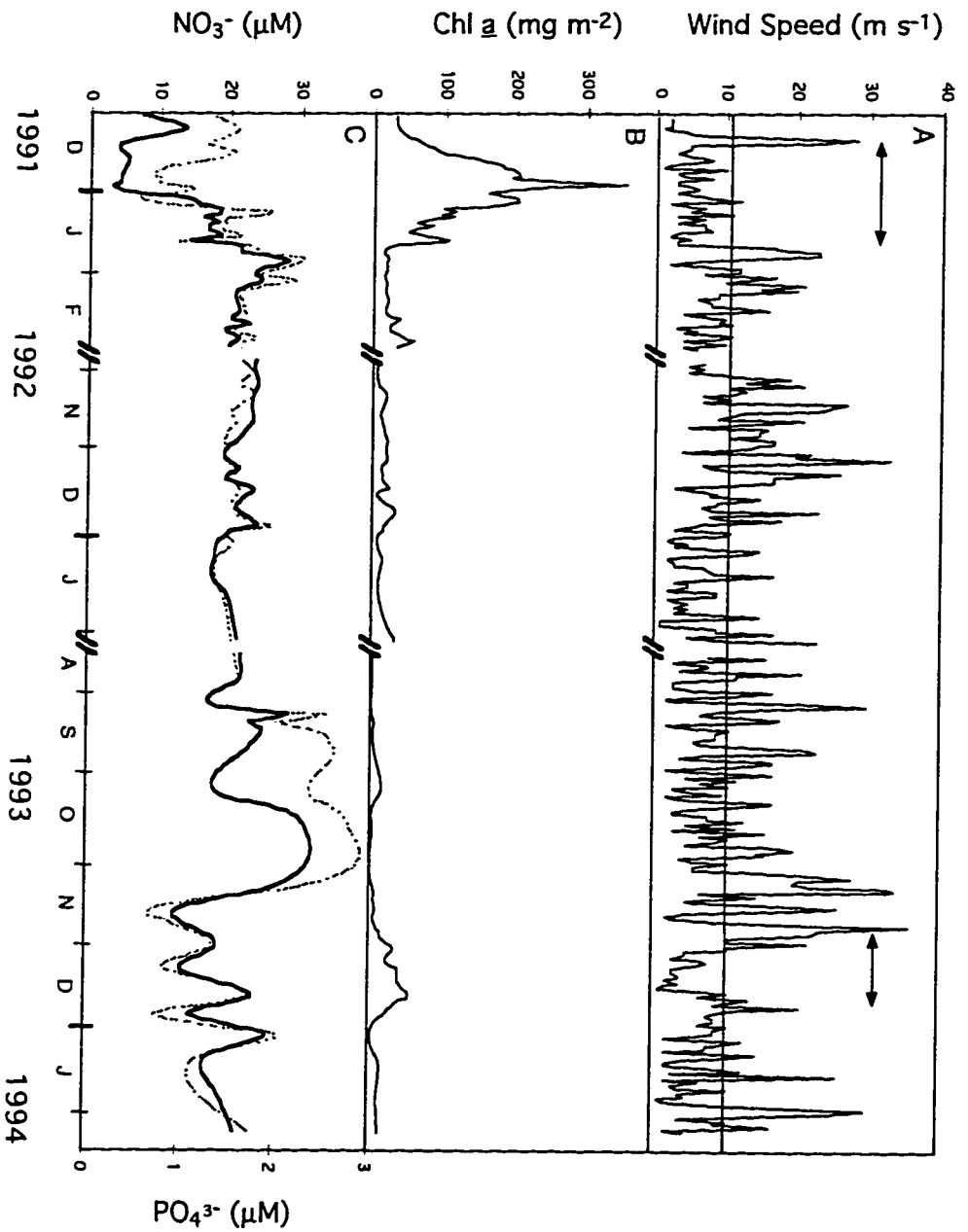
NO3- (μM)
Chl a (mg m-2)
Wind Speed (m s-1)
A
B
C
1991
1992
1993
1994
PO43- (μM)

Figure 3A. Change in the depth distribution of chlorophyll a (mg Chl a m^{-3}), N, P, and Si at station B over the 1991-1992 spring/summer season. Discrete samples are shown as filled circles; n=215.

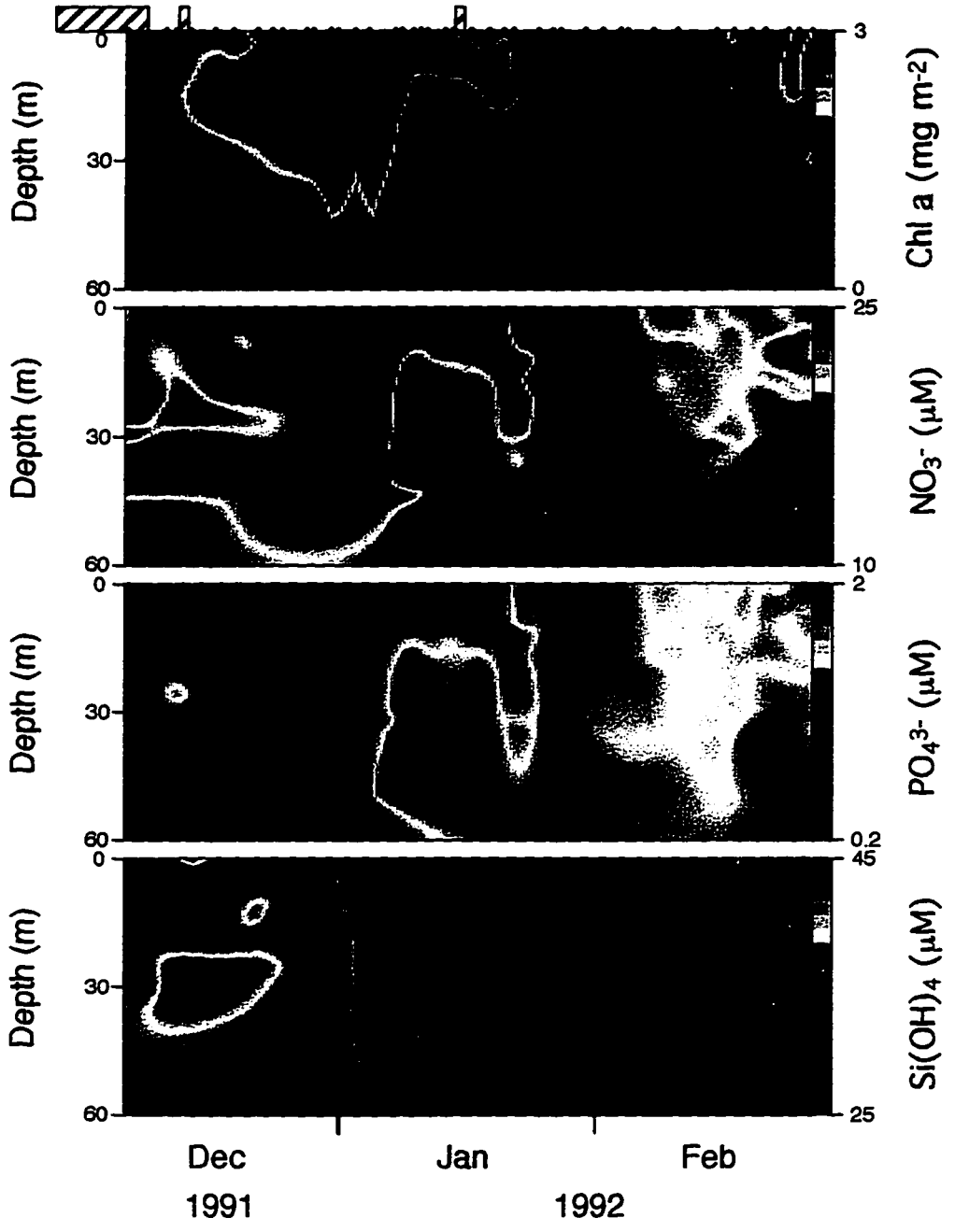
Depth (m)
0
30
60
3
0
Chl a (mg m-2)
25
10
NO3- (µM)
2
0.2
PO43- (µM)
45
25
Si(OH)4 (µM)
Dec
1991
Jan
Feb
1992

Figure 3B. Same as figure 3A except for station E. Discrete samples are shown as filled circles; n=134.

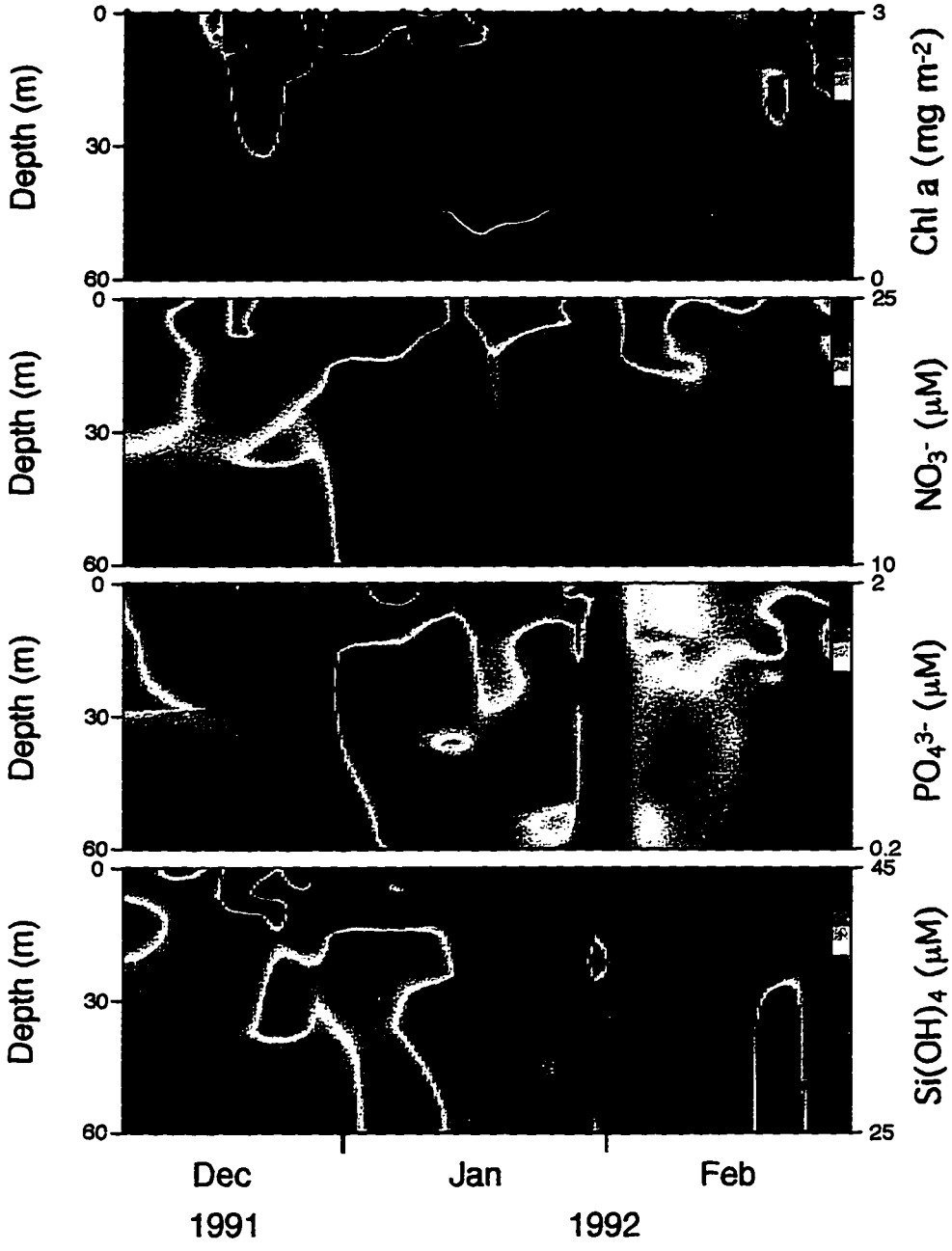
Depth (m)
0
30
60
3
0
Chl a (mg m-2)
25
10
NO3- (μM)
2
0.2
PO43- (μM)
45
25
Si(OH)4 (μM)
Dec
1991
Jan
Feb
1992

Figure 4A. Change in the depth distribution of chlorophyll a (mg Chl a m^{-3}), N, P, and Si at station B over the 1992-1993 spring/summer season. Discrete samples are shown as filled circles; n=232.

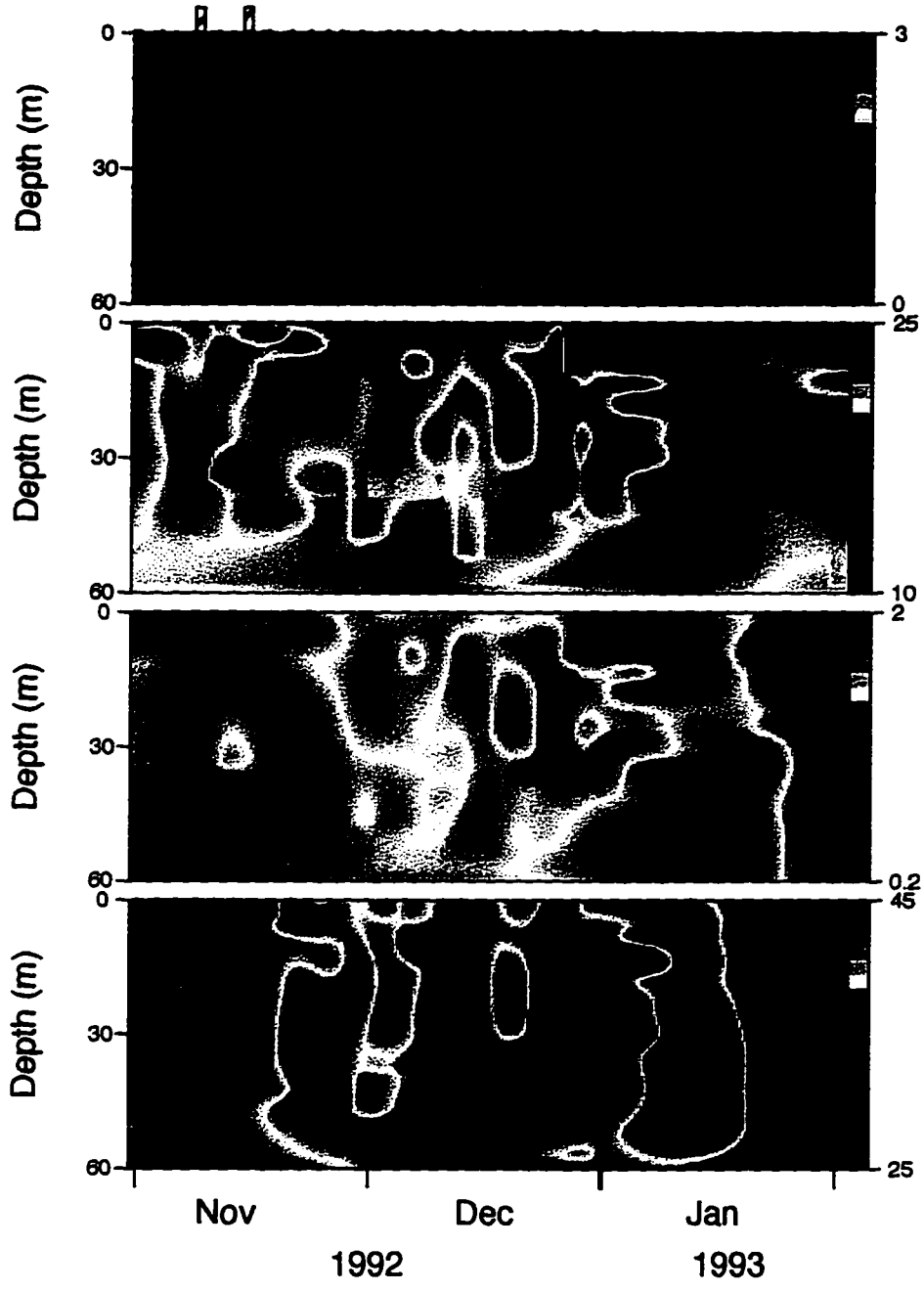
Depth (m)
0
30
60
3
0
Chl a (mg m-2)
Depth (m)
0
30
60
25
10
NO3- (μM)
Depth (m)
0
30
60
2
0.2
PO43- (μM)
Depth (m)
0
30
60
45
25
Si(OH)4 (μM)
Nov
Dec
Jan
1992
1993

Figure 4B. Same as figure 4A except for station E. Discrete samples are shown as filled circles; n=207.

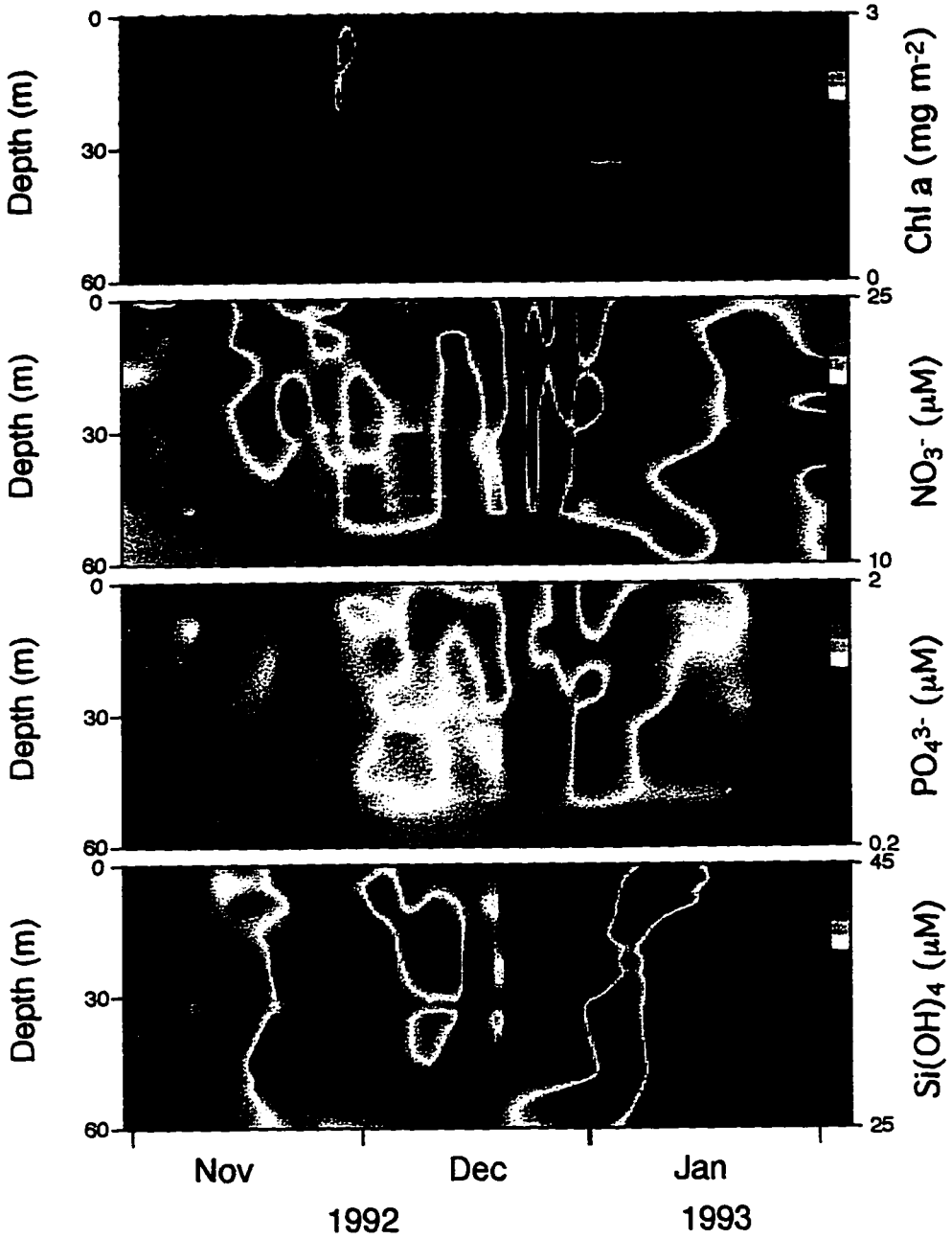
Depth (m)
0
30
60
Chl a (mg m-2)
3
0
NO3- (μM)
25
10
PO43- (μM)
2
0.2
Si(OH)4 (μM)
45
25
Nov
Dec
Jan
1992
1993

Figure 5A. Change in the depth distribution of chlorophyll a (mg Chl a m^{-3}), N, P, and Si at station B over the 1993-1994 spring/summer season. Discrete samples are shown as filled circles; n=182.

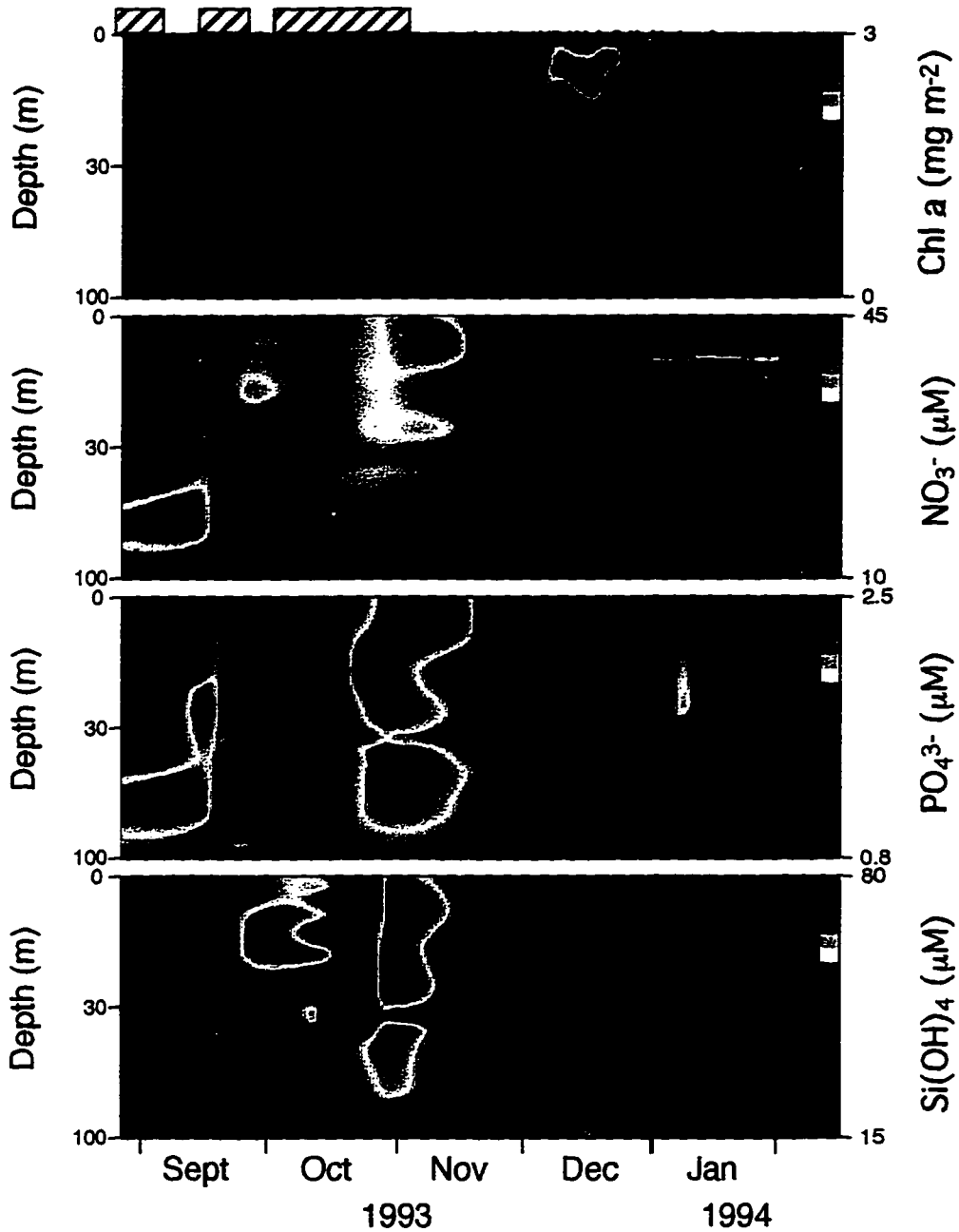
Depth (m)
0
30
100
3
0
Chl a (mg m-2)
45
10
NO3- (µM)
2.5
0.8
PO43- (µM)
80
15
Si(OH)4 (µM)
Sept
Oct
Nov
Dec
Jan
1993
1994

Figure 5B. Same as figure 5A except for station E. Discrete samples are shown as filled circles; n=170.

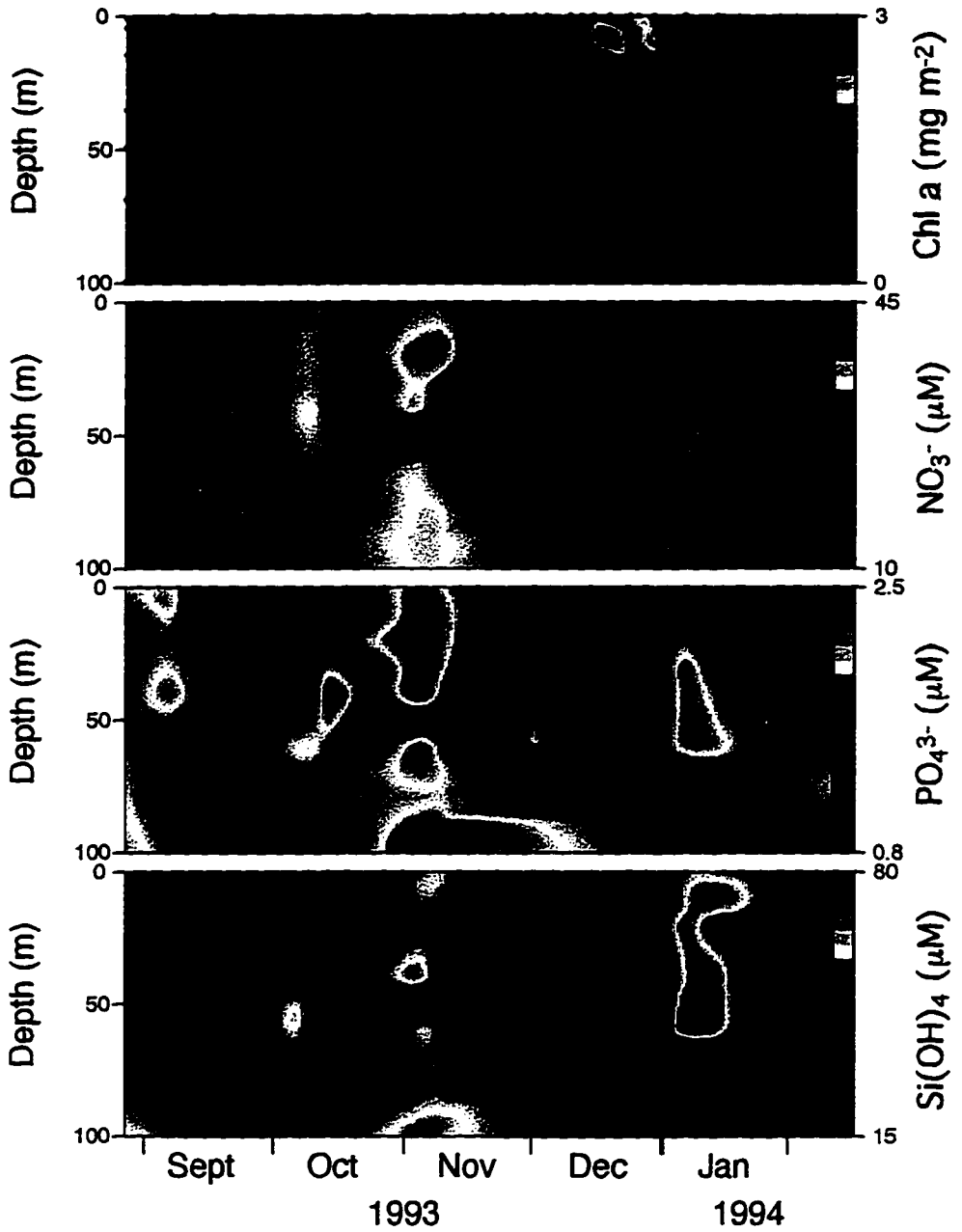
Depth (m)
0
50
100
Chl a (mg m-2)
3
0
NO3- (μM)
45
10
PO43- (μM)
2.5
0.8
Si(OH)4 (μM)
80
15
Sept
Oct
Nov
Dec
Jan
1993
1994

Figure 6. Nutrient ratios in Palmer LTER area from 1991-1994. (A) P: N and (B) Si: N for all stations, depths and dates from 12/2/91-2/27/92. (C) P: N and (D) Si: N for all stations, depths and dates from 10/28/92-2/7/93. (E) P: N and (F) Si: N for all stations, depths and dates from 8/19/93-2/5/95. Open squares in (A) represent samples taken during the diatom bloom from 12/10/91-1/7/92 (see text).

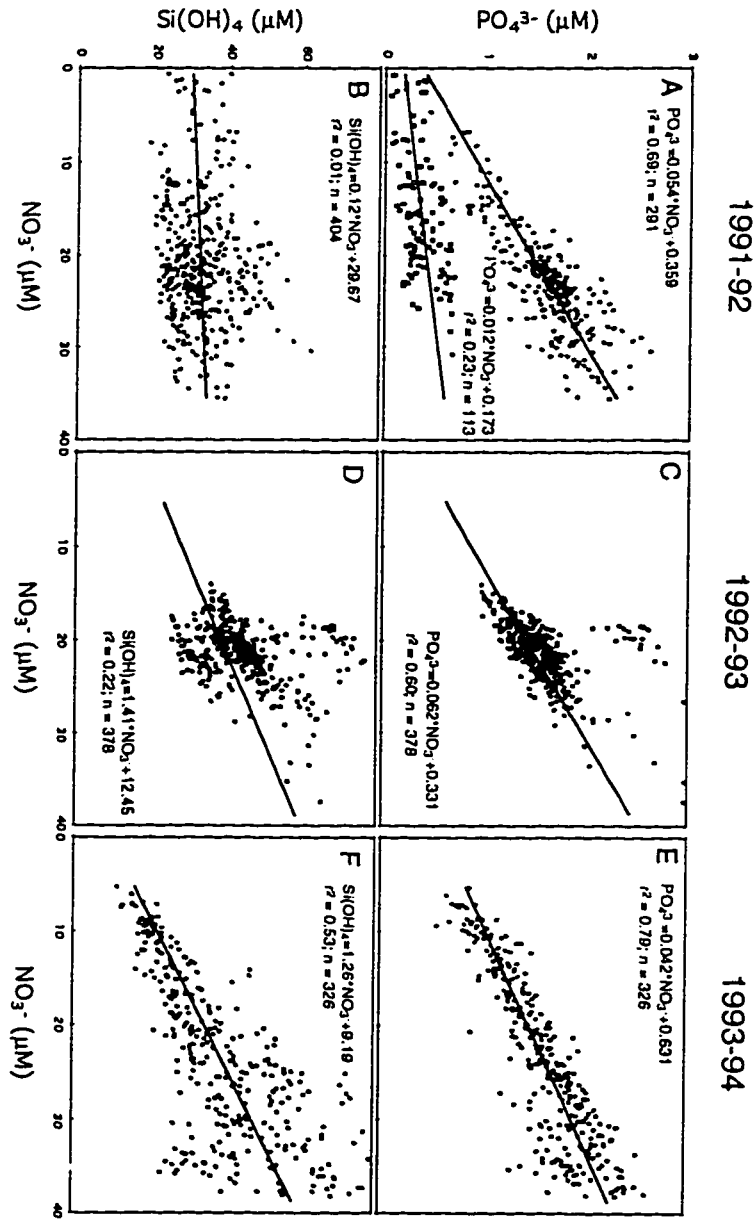
1991-92
1992-93
1993-94
PO4 3- (µM)
Si(OH)4 (µM)
NO3- (µM)
A PO4 3-=0.054*NO3-+0.359
r2 = 0.69; n = 291
PO4 3-=0.012*NO3-+0.173
r2 = 0.23; n = 113
B Si(OH)4=0.12*NO3-+29.67
r2 = 0.01; n = 404
C PO4 3-=0.062*NO3-+0.331
r2 = 0.60; n = 378
D Si(OH)4=1.41*NO3-+12.45
r2 = 0.22; n = 378
E PO4 3-=0.042*NO3-+0.631
r2 = 0.78; n = 326
F Si(OH)4=1.26*NO3-+9.19
r2 = 0.53; n = 326

Figure 7. Seasonal change in the depth distribution of (A) N: P and (B) Si: N for the 1991-1992 spring/summer season and the (C) N: P and (D) Si: N for the 1993-1994 spring/summer season. Contour scales apply to both years. Note difference in depths between the two seasons.

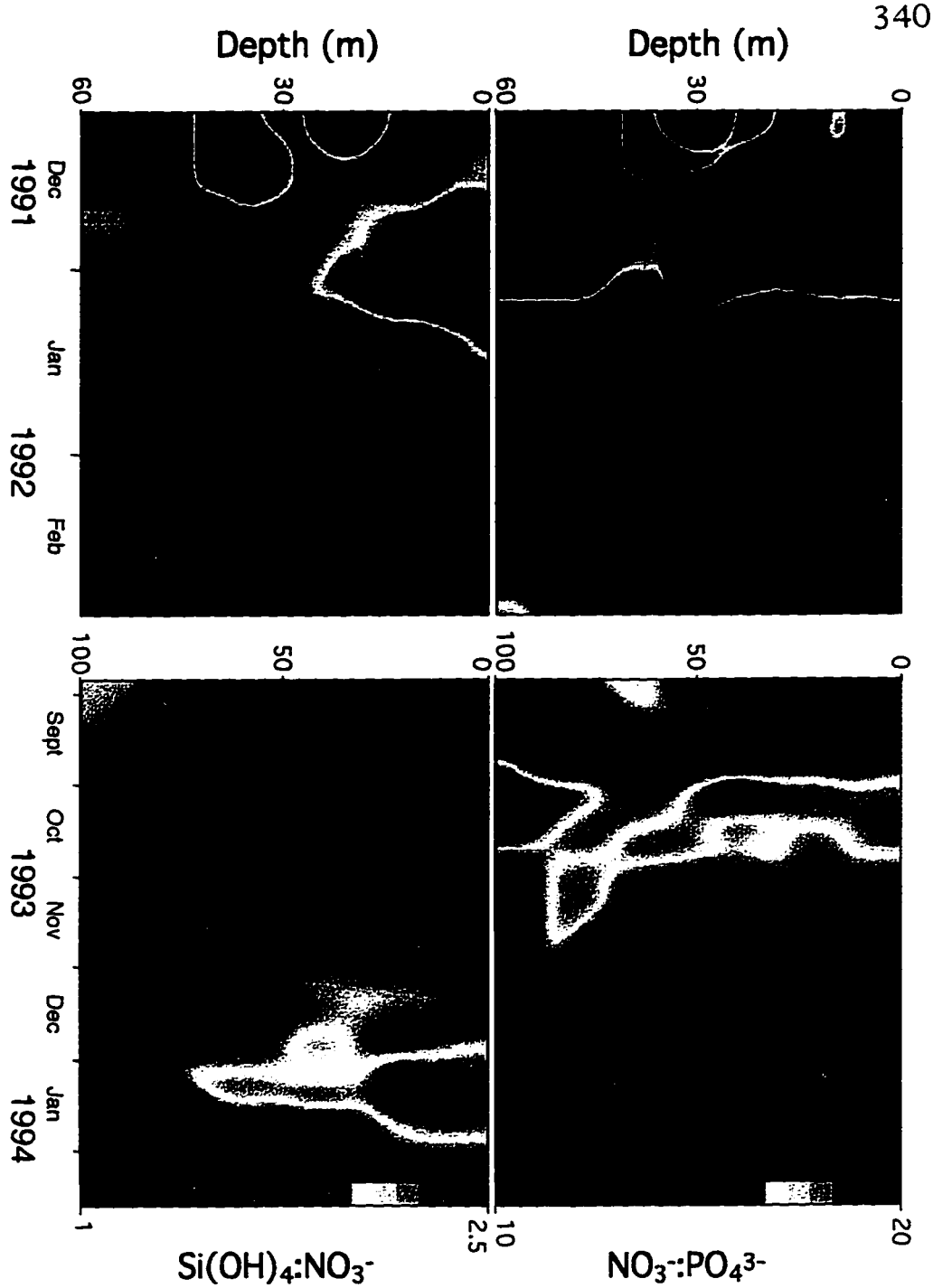
Depth (m)
Depth (m)
60
30
0
60
30
0
1991
Dec
Jan
1992
Feb
100
50
0
100
50
0
1993
Sept
Oct
Nov
Dec
1994
Jan
1
2.5
10
20
Si(OH)4:NO3-
NO3-:PO43-

Figure 8. Seasonal change in the depth distribution of four different phytoplankton groups represented at station B over (A) 1991-1992 and (B) 1993-1994. Contours are based on the percent contribution to the total chlorophyll a concentration; >50% for diatoms, >50% for cryptophytes, >25% for nanoflagellates, and >20% for chlorophytes.

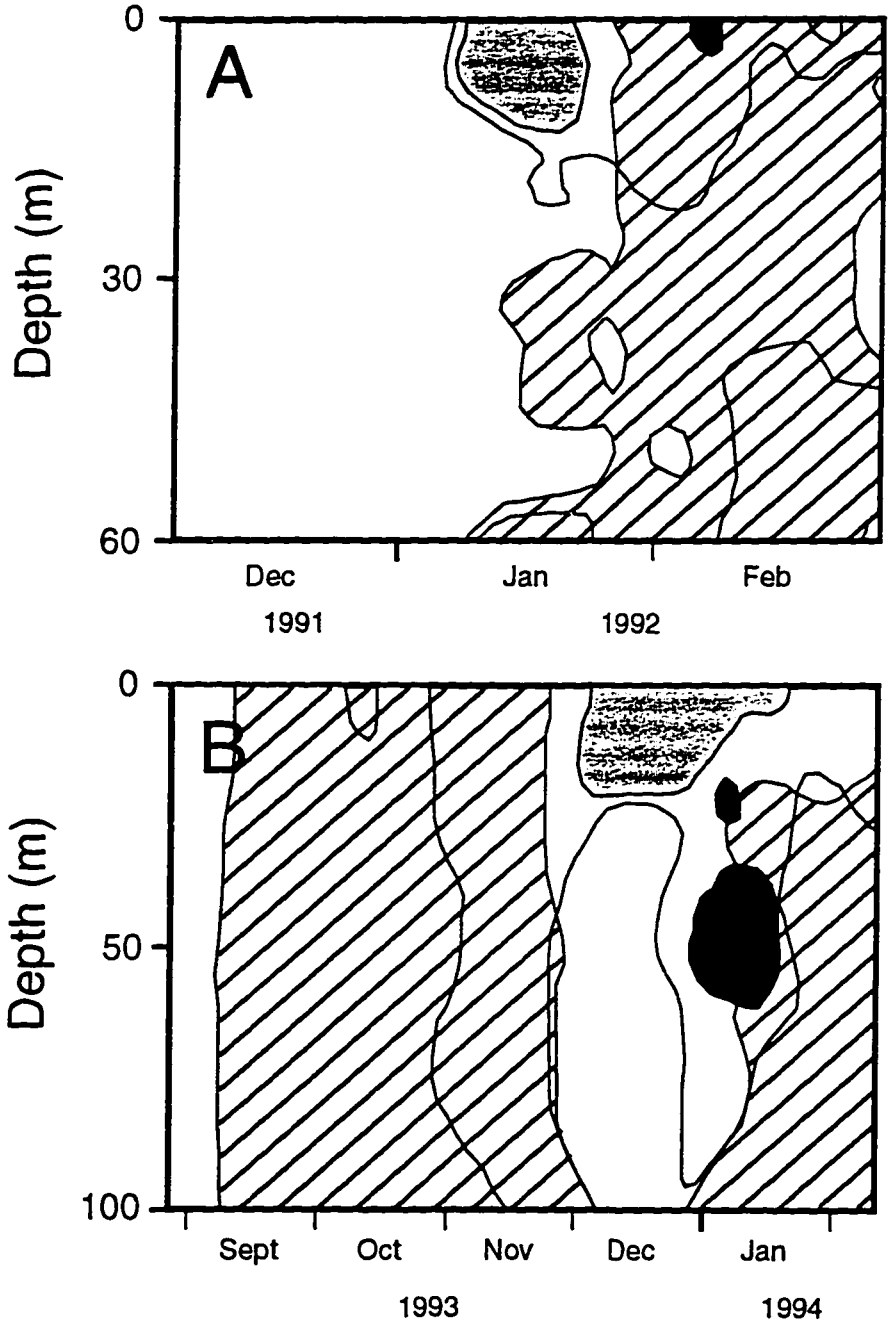
A
Depth (m)
0
30
60
Dec
Jan
Feb
1991
1992
B
Depth (m)
0
50
100
Sept
Oct
Nov
Dec
Jan
1993
1994

Figure 9. Relationships between the concentration of chlorophyll a and (A) N and (B) P and fucoxanthin (the primary accessory pigment in diatoms) and (C) N and (D) P for all stations and depths during the 1991-1992 spring/summer season. Best-fit log-linear regressions are included.

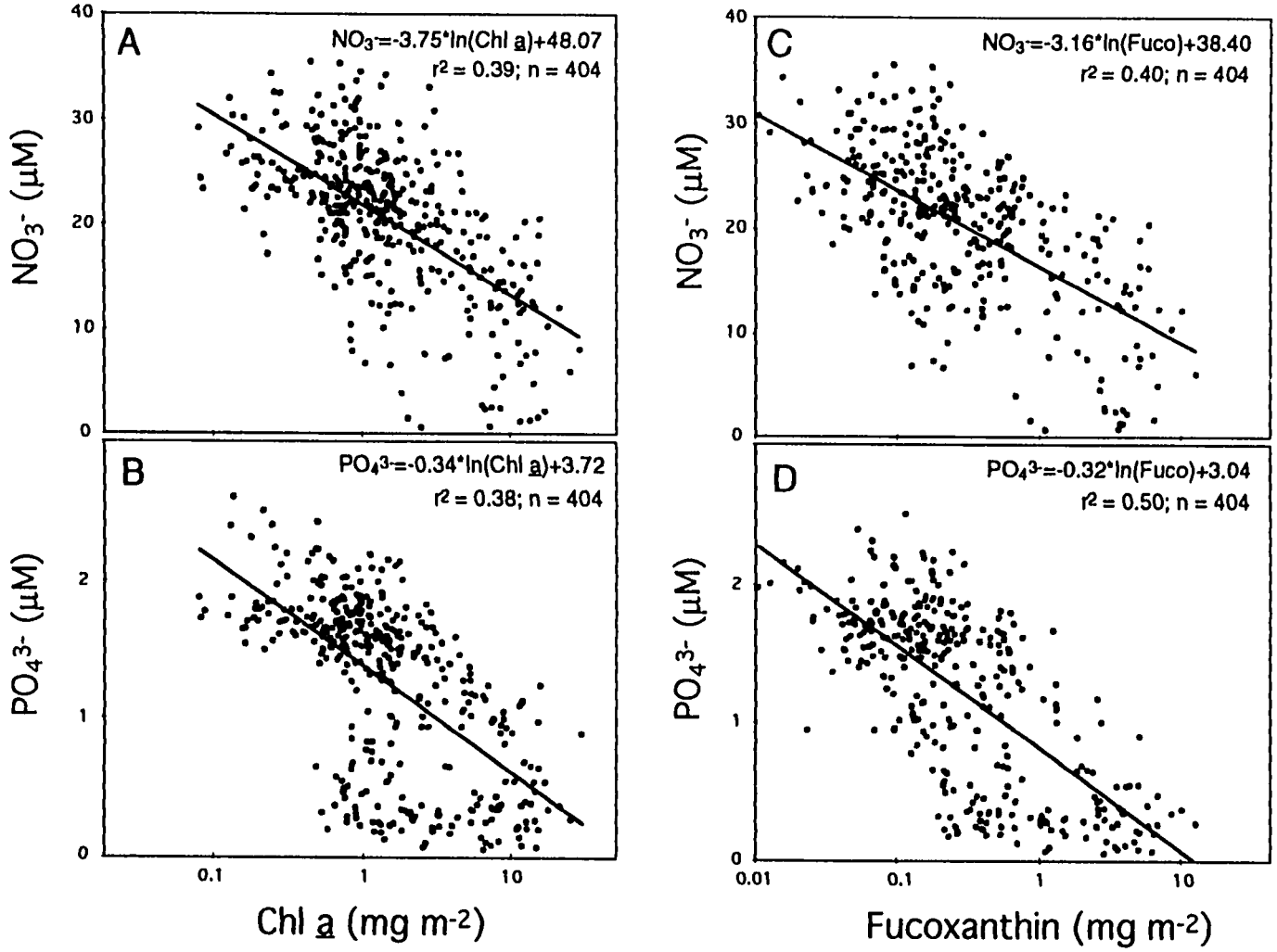
A
NO_3^-=-3.75*ln(Chl a)+48.07
r^2 = 0.39; n = 404
B
PO_4^{3-}=-0.34*ln(Chl a)+3.72
r^2 = 0.38; n = 404
C
NO_3^-=-3.16*ln(Fuco)+38.40
r^2 = 0.40; n = 404
D
PO_4^{3-}=-0.32*ln(Fuco)+3.04
r^2 = 0.50; n = 404
NO_3^- (µM)
PO_4^{3-} (µM)
Chl a (mg m^{-2})
Fucoxanthin (mg m^{-2})

Figure 10. Relationships between the concentration of chlorophyll a and (A) N and (B) P and alloxanthin (the primary accessory pigment in cryptophytes) and (C) N and (D) P for all stations and depths during the 1993-1994 spring/summer season. Best-fit log-linear regressions are included.

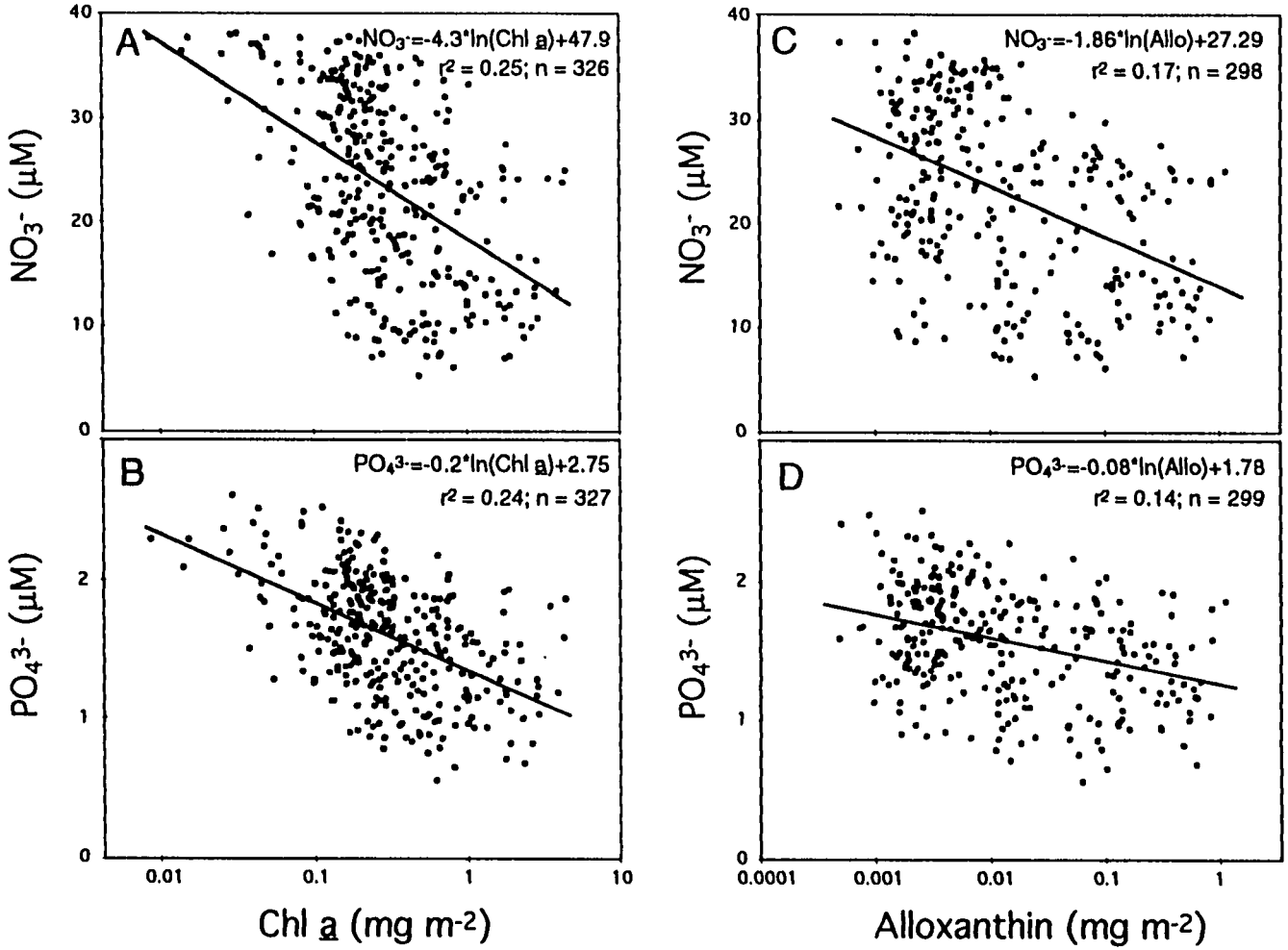
A
NO_3^-=-4.3*ln(Chl a)+47.9
r^2 = 0.25; n = 326
B
PO_4^{3-}=-0.2*ln(Chl a)+2.75
r^2 = 0.24; n = 327
C
NO_3^-=-1.86*ln(Allo)+27.29
r^2 = 0.17; n = 298
D
PO_4^{3-}=-0.08*ln(Allo)+1.78
r^2 = 0.14; n = 299
NO_3^- (µM)
PO_4^{3-} (µM)
Chl a (mg m^{-2})
Alloxanthin (mg m^{-2})

Figure 11. (A) Daily precipitation and snow height recorded at Palmer Station during the 1993-94 summer season and the (B) water column NO3- concentration at station B over the same period.

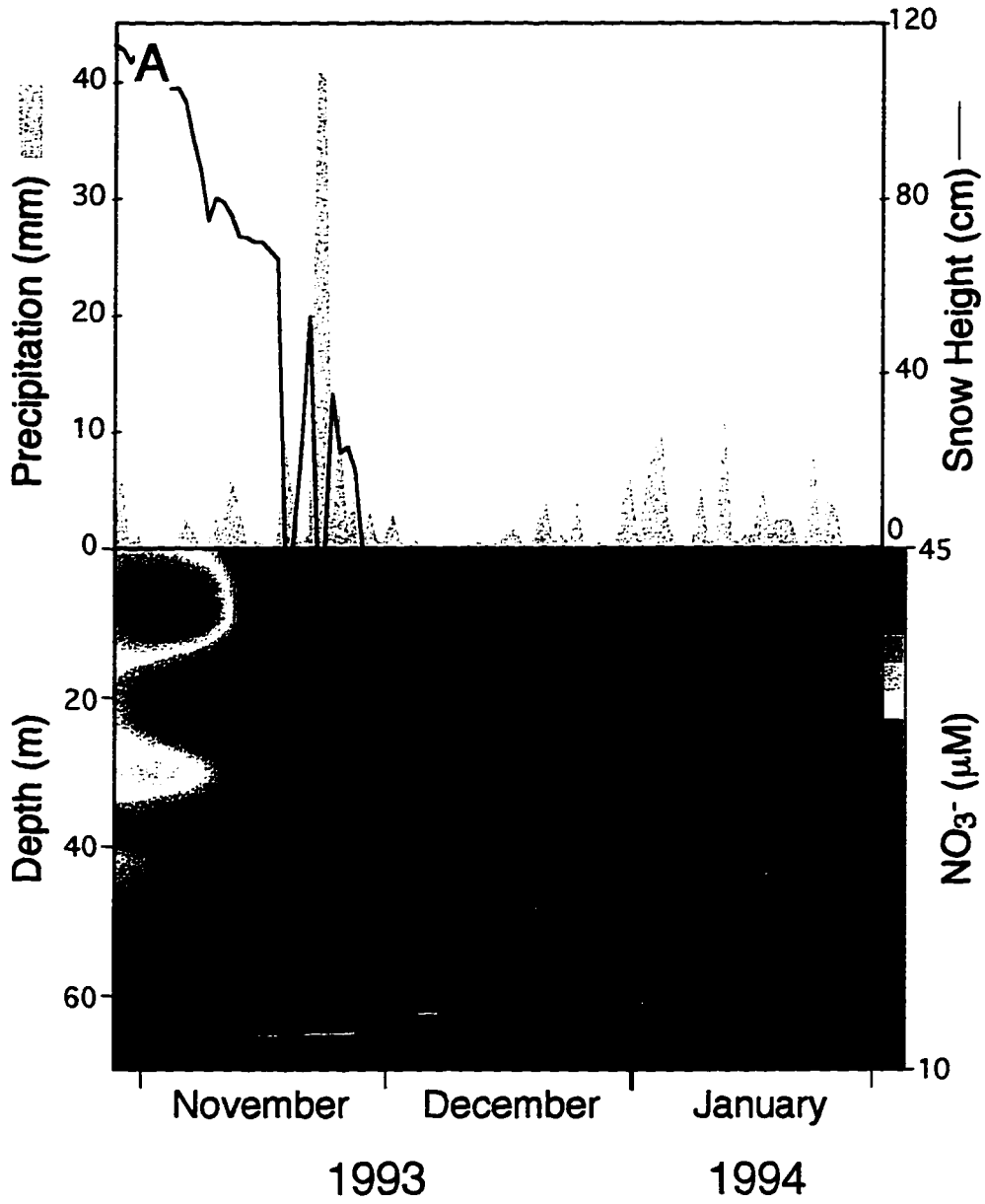
A
Precipitation (mm)
40
30
20
10
0
120
80
40
0
Snow Height (cm)
45
Depth (m)
20
40
60
10
NO_3^- (μM)
November
December
January
1993
1994

Figure 12. Relationships between (A) N and (B) P concentrations and maximum rate of carbon uptake per unit chlorophyll a (mg C mg Chl a h^{-1}) for all stations and depths during the 1991-92 (filled circles), 1992-93 (X's), and 1993-94 (open squares) spring/summer seasons.

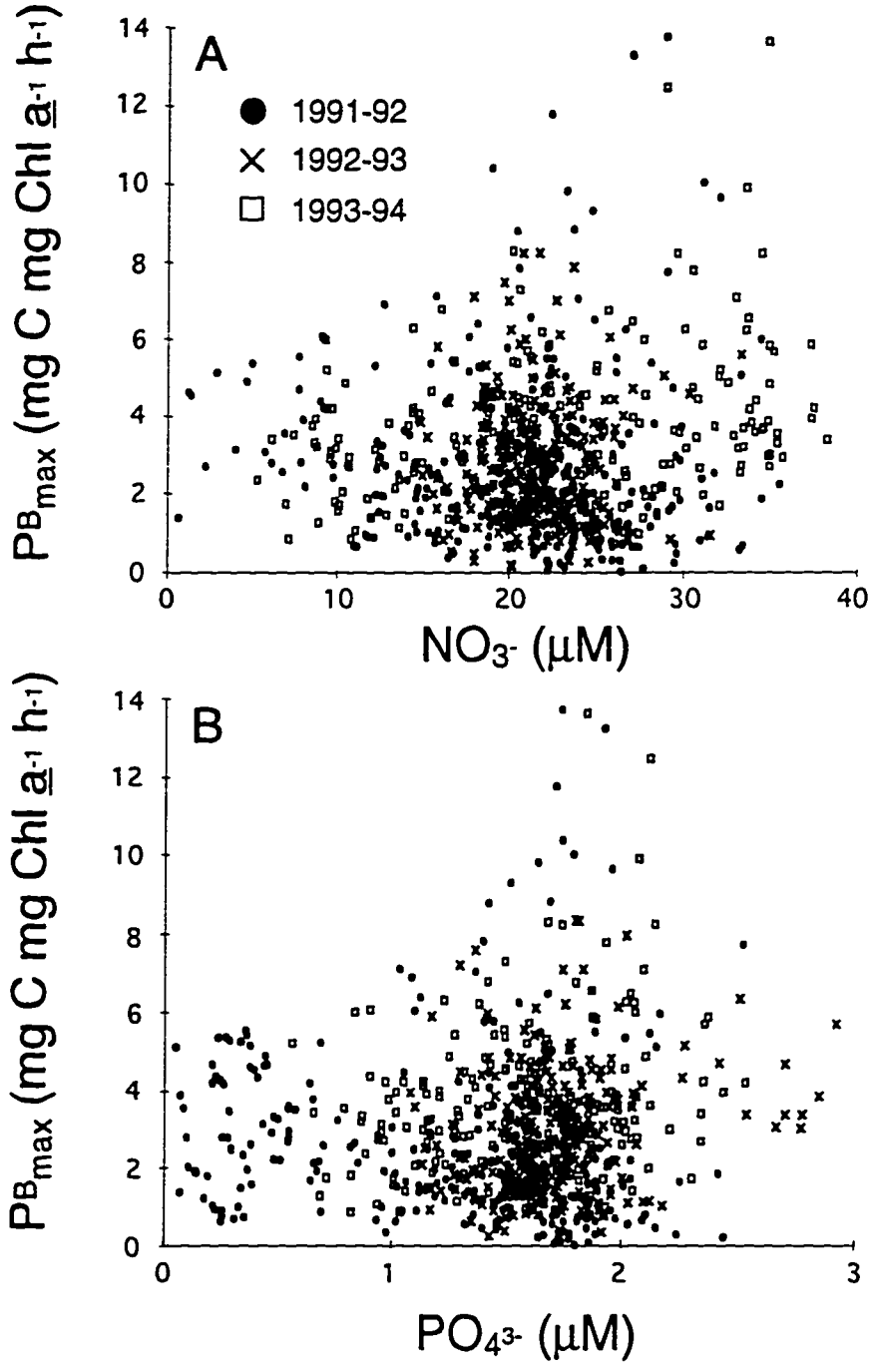
A
1991-92
1992-93
1993-94
PB_{max} (mg C mg Chl a^{-1} h^{-1})
NO_3- (µM)
B
PB_{max} (mg C mg Chl a^{-1} h^{-1})
$PO_4$3- (µM)

Figure 13. Relationships between (A) N and (B) P concentrations and the ratio of chlorophyll a to particulate organic carbon (wt:wt) for all stations and depths during the 1991-92 (filled circles), 1992-93 (X's), and 1993-94 (open squares) spring/summer seasons.

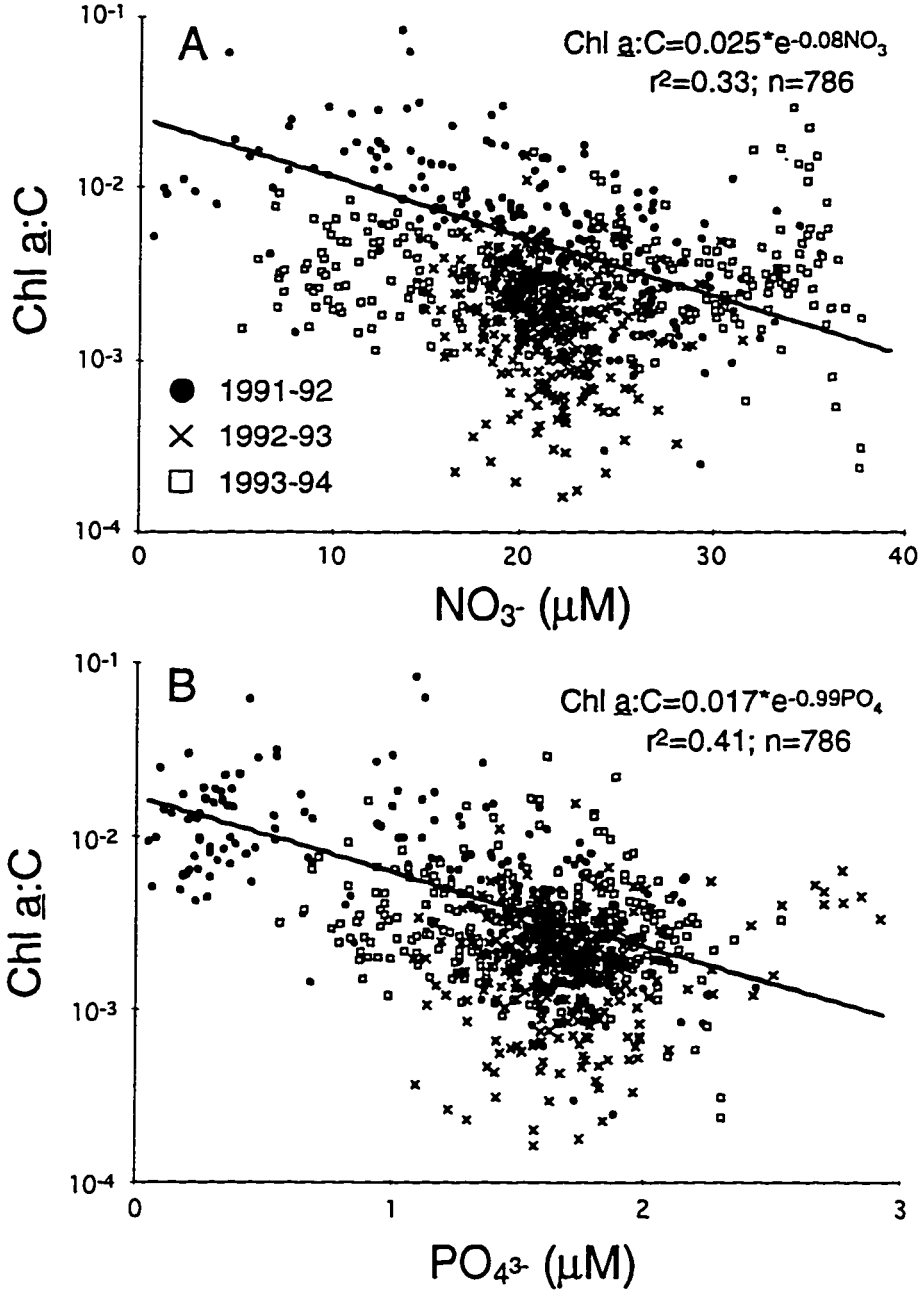
A
Chl a:C=0.025*e-0.08NO3
r2=0.33; n=786
1991-92
1992-93
1993-94
Chl a:C
NO3- (µM)
B
Chl a:C=0.017*e-0.99PO4
r2=0.41; n=786
Chl a:C
PO43- (µM)

Figure 14. Relationships between (A) N and (B) P concentrations and the measured daily in situ growth rates for all stations and depths during the 1991-92 (filled circles), 1992-93 (X's), and 1993-94 (open squares) spring/summer seasons. Maximum growth rates (dashed gray lines; Sakshaug and Holm-Hansen 1986) and maximum inorganic nutrient concentrations (solid gray lines; Kamykowski and Zentara 1989) for the Southern Ocean are included. A 'minimum envelope' for parameters has been drawn for the measured data (see text).

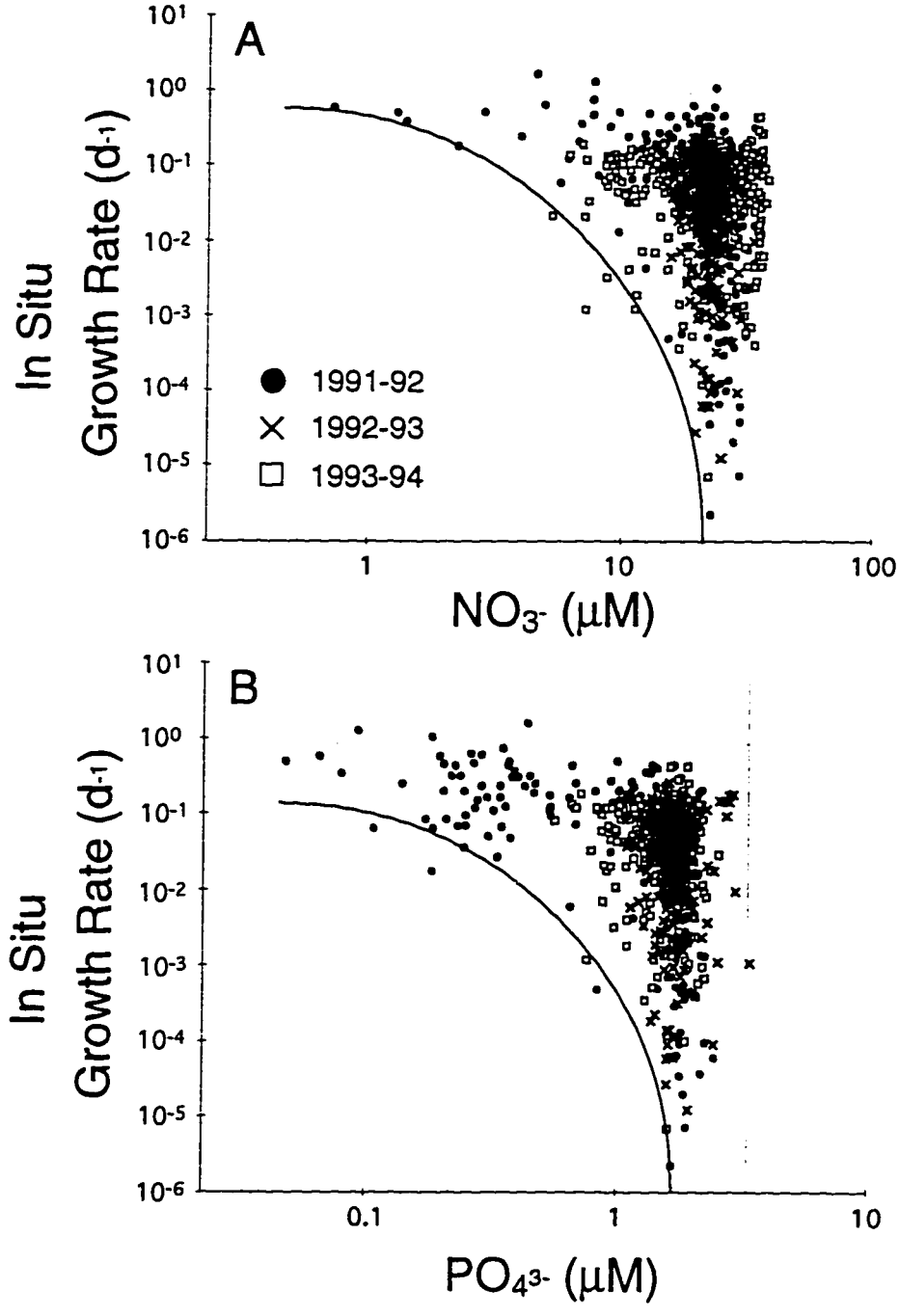
A
In Situ Growth Rate (d-1)
101
100
10-1
10-2
10-3
10-4
10-5
10-6
1991-92
1992-93
1993-94
1
10
100
NO3- (µM)
B
In Situ Growth Rate (d-1)
0.1
1
10
PO43- (µM)

Figure 15. Relationships between the measured daily in situ growth rate and the ratio of chlorophyll a to particulate organic carbon for all stations and depths during the 1991-92 (filled circles), 1992-93 (X's), and 1993-94 (open squares) spring/ summer seasons. The best-fit power function has been included.

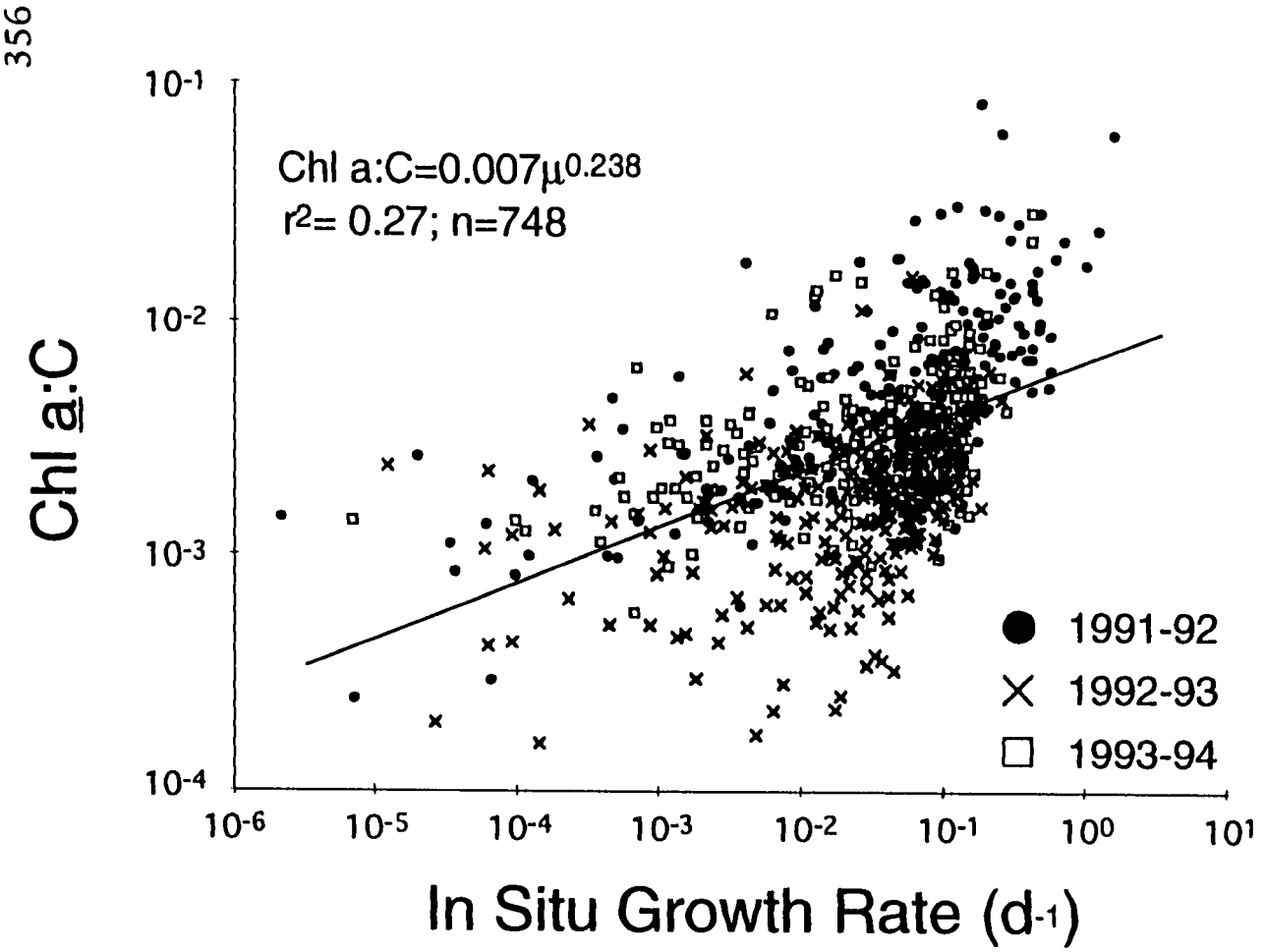
Chl a:C=0.007μ^0.238
r²= 0.27; n=748
Chl a:C
10-1
10-2
10-3
10-4
10-6
10-5
10-4
10-3
10-2
10-1
100
101
1991-92
1992-93
1993-94
In Situ Growth Rate (d-1)